Institut für Allgemeine Pathologie und Pathologische Anatomie

Development and application of methods for mass spectrometric analysis of acute myeloid leukemia derived cell lines to identify receptor tyrosine kinase inhibitor resistance mechanisms and serum biomarkers

Alperen Cagatay Serdaroglu

Vollständiger Abdruck der von der

Fakultät für Medizin

der Technischen Universität München zur Erlangung des akademischen Grades eines Doktors der Naturwissenschaften genehmigten Dissertation.

Vorsitzende/-r: Prof. Dr. Jürgen Ruland

Prüfende/-r der Dissertation:

1. TUM Junior Fellow Dr. Peer-Hendrik Kuhn, Ph.D.
2. Prof. Dr. Kathrin Lang

Die Dissertation wurde am 18.05.2017 bei der Technischen Universität München eingereicht und durch die Fakultät für Medizin am 18.10.2017 angenommen.

Development and application of methods for mass spectrometric analysis of acute myeloid leukemia derived cell lines to identify receptor tyrosine kinase inhibitor resistance mechanisms and serum biomarkers

Alperen Cagatay Serdaroglu

Content

Zusammenfassung

Das Sekretom umfasst lösliche Proteine und kleine Moleküle, die entweder sezerniert oder proteolytisch aus Zellen freigesetzt werden. Diese löslichen Faktoren sind entscheidend für die interzelluläre Kommunikation und die Homöostase physiologischer Prozesse im Gewebe. Veränderungen im Sekretom können zu Krankheitszuständen wie Krebs, neurodegenerativen Erkrankungen oder Autoimmunerkrankungen beitragen. Daher kann die Analyse des Sekretoms und Oberflächenproteoms uns Informationen über krankheitsbedingte Störungen in der interzellulären Kommunikation geben, woraus neue Behandlungsstrategien und diagnostische Biomarker resultieren könnten. Secretome protein enrichment with click sugars (SPECS) ist eine neuartige Technologie, die die massenspektrometrische Analyse von Sekretomen verschiedener Zelltypen in vitro auch in Gegenwart von fötalem Kälberserum ermöglicht. Ein Aspekt meiner Arbeit beschäftigte sich mit der Entwicklung einer verbesserten SPECS-Methode, die letztendlich das alte Protokoll in Bezug auf die Anzahl der identifizierten Glykoproteine, die Sequenzabdeckung und die Intensitäten der identifizierten Glykoproteine übertraf. Dies wird höchstwahrscheinlich in der Zukunft eine Verringerung des benötigten Materials für die MS-Analyse um mehr als die Hälfte ermöglichen.

Neben der Optimierung der SPECS-Methode habe ich SPECS zur Untersuchung von Rezeptortyrosinkinasesignalwegen im Rahmen der akuten myeloischen Leukämie (AML) angewendet. AML ist eine Neoplasie des hämatopoetischen Systems mit aggressiven und heterogenen Eigenschaften, die aufgrund des Auftretens von Chemoresistenzen mit Chemotherapie nur schwer zu heilen ist. Daher wurden neben der Chemotherapie, unter Berücksichtigung häufiger Mutationen in den Rezeptortyrosinkinasen FLT3 und c-kit bei AML, gezielte Therapien wie die pharmakologischen Inhibition von FLT3 mittels Sorafenib entwickelt. Jedoch leiden sowohl Monotherapie als auch Kombinationstherapien von Rezeptortyrosinkinase-Inhibitoren mit Chemotherapie an einer schnellen Resistenzbildung und einem Wiederauftreten der Erkrankung. Daher erfordert die AML ein besseres Verständnis ihrer Biologie und bessere Biomarker für die Krankheitsüberwachung. Zu diesem Zweck habe ich zuerst das Sekretom und Oberflächenproteom von 6 FAB-Subtyp-verwandten AML-Zelllinien, einschließlich der Rezeptortyrosinkinaseexpression analysiert. Diese Daten enthalten zahlreiche Biomarkerkandidaten, die im Serum von AML Patienten getestet werden könnten, um die AML-Krankheitslast zu überwachen und den AML-Subtyp zu identifizieren. Zweitens, um mehr über Resistenzentwicklungen auf eine gezielte Therapie mit dem Inhibitor Sorafenib zu erfahren, habe ich das Sekretom und Oberflächenproteom von Sorafenib behandelten und unbehandelten, die FLT3-Mutation tragenden MV4-11-Zellen unter Verwendung von SPECS und Massenspektrometrie analysiert und verglichen. Die MS-Daten zeigen, dass Überlebens- und Proliferations-assoziierte Rezeptoren wie FLT3, ICAM3, CD84 und CSFR1 in Sorafenib behandelten MV4-11 Zellen signifikant erhöht waren, während negative Modulatoren des Rezeptortyrosinkinase-Signalwegs wie PTPRJ-, PTPRC- und Apoptose-induzierende Faktoren wie FAS signifikant verringert waren. Dies zeigt, dass das AML-Oberflächenproteom sehr dynamisch reagieren kann, um den Verlust der FLT3-Signalisierung zu kompensieren.

Da die Sekretom-Analyse eine Menge neuer potentieller Biomarker ergab, habe ich eine erste Methode entwickelt, um das Serum von AML-Patienten zu analysieren. Der Vergleich des Serums von zwei Patienten vor und nach Chemotherapie mit vollständiger Remission zeigte, dass die Proteine CD44 und MPO gut mit der Krankheitslast korrelieren. Beide Proteine sind etablierte Marker in der Leukämie-FACS-Analyse. Schließlich habe ich die CRISPR-Cas9-Genmodifikationstechnik in AML-Zelllinien etabliert, um einen exklusiven Verlust von FLT3- oder c-kit-Signalisierung zu untersuchen und die Gal4-VP16-getriebene Expression und Reinigung von Rezeptortyrosinkinase-Liganden in

unserem Labor wie FLT3L und c-Kit Ligand etabliert. Beide Werkzeuge sind für zukünftige Studien zu FLT3 und c-kit unerlässlich.

ABSTRACT

The secretome comprises soluble proteins and small molecules that either are secreted or proteolytically released from cells. These soluble factors are crucial for intercellular communication and tissue homeostasis. Perturbations in the secretome can lead to diseases such as cancer, neurodegenerative or autoimmune disorders. Therefore, the analysis of secretomes could help to learn more about disease-associated perturbations in intercellular communication and thereof derived treatment strategies and diagnostic biomarkers. Secretome protein enrichment with click sugars (SPECS) is a novel technology that enables the mass spectrometric (MS) analysis of secretomes in various cell types in vitro even in the presence of fetal calf serum. One aspect of my thesis dealt with the development of an improved SPECS method that finally outperformed the old protocol in terms of number, intensity and sequence coverage of identified glycoproteins. This most likely will allow a reduction of required input material for MS analysis in the future.

Besides optimizing the SPECS method, I applied SPECS to study receptor tyrosine kinase (RTK) signalling in acute myeloid leukemia (AML). AML is a neoplasia of the hematopoietic system with aggressive and heterogeneous characteristics difficult to cure with chemotherapy due to the occurrence of chemo resistance. Therefore, after chemotherapy, targeted inhibition of RTKs such as FLT3 has been developed considering frequent mutations of FLT3 and c-kit in AML. However, both monotherapy and combinations of RTK inhibitors with chemotherapy suffer from fast resistance formation and disease recurrence. Hence, AML requires a better understanding of its molecular biology and better biomarkers for disease monitoring. To this aim, I first analysed the secretome and surface proteome of 6 FAB subtype-related AML cell lines including RTK expression. These data provide a rich resource to be tested as serum biomarkers to monitor AML disease load and AML subtype identification. Second, to learn more about resistance development towards a targeted therapy with the FLT3 inhibiting TKI Sorafenib, I analysed the secretome and surface proteome of the FLT3 mutation carrying MV4-11 cell line in response to Sorafenib using SPECS and mass spectrometry. The MS data demonstrate that in Sorafenib treated cells survival and proliferation related receptors such as FLT3 itself, ICAM3, CD84 and CSFR1 were significantly increased while negative modulators of RTK signalling like PTPRJ, PTPRC and apoptosis inducing factors such as FAS were significantly decreased demonstrating that the AML surface proteome can react very dynamic to compensate FLT3 signalling.

As secretome analysis provides a rich resource of biomarkers, I established a first MS method for serum anlaysis of AML patients. Comparing the serum of two patients before and after chemotherapy with complete remission showed that the proteins CD44 and MPO correlate well with disease load, being both established markers in leukemic blast FACS analysis. Finally, I established CRISPR-Cas9 gene editing in AML cell lines to study an exclusive loss of FLT3 or c-kit signalling and established the Gal4-VP16 driven expression and purification of RTK ligands in our lab such as FLT3L and c-Kit ligand. Both tools will be essential for future studies on FLT3 and c-kit.

1 Introduction

1.1 Mass Spectrometry Based Proteomics

The eukaryotic proteome is a complex mixture of proteins that have synergistic or independent activities that all contribute to physiological cell function. While the cellular genome remains identical in most cells of multicellular organism such as mice and men, the proteome can change giving rise to different cell types that in the end contribute to organ formation. Hence, understanding either the physiological or the pathological state of a cell and therewith-linked changes in protein expression can be best investigated via whole proteome analysis. Mass spectrometry (MS) based protein analysis is an elegant technology to study proteomes in a qualitative and quantitative manner. Protein expression, protein interactions and post-translational modification profiles can be identified by mass spectrometry (1, 2).

The working principle of mass spectrometry is based on measuring the mass to charge ratio (m/z) of ions. Basically, the ion source unit of a given mass spectrometer converts molecules into gas phase ions. The mass analyser separates the ions according to their m/z ratio and number of ions at each m/z value recorded by a detector. Peptide and protein ionization can be achieved by electrospray ionization (ESI) (3) and matrix-assisted laser desorption/ionization (MALDI) (4) while their analysis can be achieved with different mass analysers such as a quadrupole (Q), linear ion traps (QIT, LTQ), time of flight (TOF) and Fourier-transform ion cyclotron resonance (FTICR). Afterwards, hybrid applications were generated with combination of different mass analysers such as Q-Q-TOF, Q-Q-LTQ, Q-TOF (5) . In 1999, a new type of analyser was invented called orbitrap (6). Ions are trapped and oscillate harmonically around a spindle-like electrode with a frequency of their m/z values. This movement causes a current in the electrode that is Fourier-transformed into time domain resolved mass spectra (7).

For fragmentation of molecules such as peptides, Collision induced dissociation (CID) technique has been widely used in MS (8). This method fragments peptide cation backbones with rare gas atoms in the gas phase. This method is not suitable for large peptides. In the following years, more fragmentations methods were established such as Electron capture dissociation (ECD) (9, 10), Electro transfer dissociation (ETD) (11, 12) and High-energy collisional dissociation (HCD) (13).

Nowadays, combination of these techniques are used for the design of new MS machines with different accuracy and measuring strategies for analysing the proteome such as LTQ-Velos-Orbitrap (14). This hybrid machines combines robustness, MS/MS capability, sensitivity and high mass accuracy and resolution capabilities.

For MS analysis, there are two main strategies called top-down (whole protein analysis) proteomics and shotgun (bottom-up) proteomics for MS analysis (15, 16). Shotgun proteomics is the analysis of complex peptide mixtures of protein digestion with specific enzymes. Shotgun proteomics is a simple approach and complex mixtures can be analysed with this strategy but conversion of protein mixtures into peptide mixtures increases complexity and thus requires efficient separation. Furthermore, this technique detects only

the most abundant peptides and post-translational modifications can be lost. In top-down proteomics, proteins are directly fragmented during the MS analysis. This strategy is suitable for whole protein detection of post-translational modifications, sequence variabilities but samples should have a low complexity or just the protein of interest.

Changes in the proteome level can be one of the reason for disease state and progression. Hence, monitoring changes in proteins level and their individual modifications or mutations can give an idea about the disease status. In recent years, quantitative proteomics has been introduced to mass spectrometry by the development of labelling strategies such as isotope-coded affinity tags (ICAT) (17) or Stable isotope labelling with amino acids in cell culture (SILAC) (18). Isotopically distinct tags are used in both strategies, cysteine labelling for ICAT and lysine and arginine labelling for SILAC (17, 18). Mass-spectrum intensities are used for quantifications. However, stable isotope-based labelling protocols requires extra steps and time whereas label-free quantification is the easiest and most economical approach. Label-free quantification comprises two different strategies. One strategy is measuring and comparing the signal intensity of peptide precursor ions. Another strategy is counting and comparing the number of fragment spectra identifying peptides of a given protein (19). Furthermore, label-free quantification can be applicable to a variety of samples including clinical samples (20, 21). Using label-free quantification, many samples can be measured and compared in parallel while stable isotope labelling techniques are typically limited to fewer experiments due to time and economical perspectives. Furthermore Label free methods provide a higher dynamic range of quantification (19).

Different mass spectrometry data analysis programmes are available online like MaxQuant, MASCOT or SEQUEST (22-24). These programmes are applicable with reference databases and provide protein identification searching peptides with similar spectra in the MS measurements.

Shotgun analysis of protein lysates allows analysis of only the most abundant proteins. Hence, enrichment strategies are necessary to analyse less abundant proteins such as extracellular proteins. Nowadays, there are new methods that comprises different labelling strategies or immobilization to get better MS analysis and quantification of low abundant proteins or litte input material such as SPECS, sp3, TAILS or lectin magnetic bead arrays (25-28). In my thesis, I used a novel method called secretome protein enrichment with click sugar (SPECS) and surface-click method for detection of glycoproteins(27, 29, 30).

1.2 Secretome Protein Enrichment with Click sugars and Surface-Click

1.2.1 The secretome a mean to intercellular communication in multicellular organisms

The secretome comprises the entirety of all proteins and small molecules released from a given cell type into the extracellular space. These soluble factors are important for intercellular communication in multicellular organisms. Perturbations in the secretome or the surface proteome of a given cell can lead to disease conditions such as cancer, neurodegenerative disease, autoimmune disorders or cardiovascular disease (31-34). Specific cases like, HER2 overexpression is observed in 15-20% of the breast cancer cases and connected to survival signalling pathways. HER2 cleavage by metalloproteases and

accumulation leads to resistance towards treatment (35-38). In Acute myeloid leukemia, 13%-22% of c-kit mutation are linked to t(8;21) chromosomal translocation and c-kit expression is highly upregulated in AML1/ETO positive AML (39-41). Furthermore, mutations in the receptor tyrosine kinase FLT3 are the most common mutation (30%) in acute myeloid leukemia and lead to a poor prognosis of patients (42-45). Hence, studying the secretome and the surface proteome in AML is of great importance for our understanding of pathogenic processes. The protein component of the secretome comprises either soluble proteins that can be readily secreted or membrane-tethered proteins whose ectodomain can be released by ectodomain shedding catalysed by various extracellular protease families. Therefore, new biomarkers for classification and status monitoring of AML might be identified from analysis of the AML secretome and surface proteome.

1.2.2 Technical issues that impair secretome analysis with mass spectrometry

However, an unbiased analysis of the secretome with mass spectrometry from cell culture media with mass spectrometry has been nearly impossible due to fundamental limitations. The contribution to the total protein content in serum- supplemented media by the secretome comprised of secreted and proteolytically liberated proteins is very low. Most cell culture media are supplemented with serum of fetal calf origin (FCS) to maintain survival of many cell types in *in vitro* cultures. However, serum contains high concentrations of serum proteins such as albumin, immunoglobulins or other serum proteins. These supplemented proteins exceed the secretome proteins by several orders of magnitude (46). In addition, apoptotic cells release highly abundant intracellular proteins (Fig 1.). Therefore, as current state-of-the-art mass spectrometers with a typical shotgun method measure only the most abundant peptide ions resulting from the most abundant proteins in a mixture only serum proteins but not cell-derived proteins of the secretome are measured and identified. One strategy to solve this problem is the use of serum-free medium (47). However, most cell types are not suitable for this strategy due to their dependence on serum factors for cell survival. Further, serum free conditions can change cell physiology leading to incorrect results. Another strategy is the overexpression of specific proteins or proteases to increase the secretome or shedded proteins itself but this strategy in the case of could lead to false positive results (48)

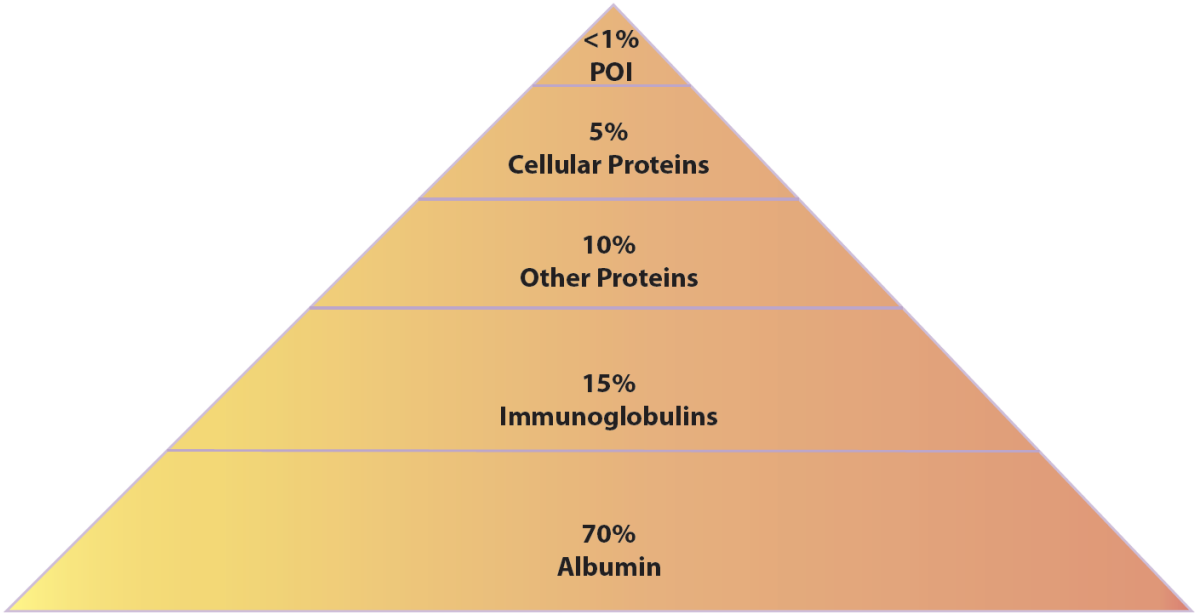

Figure 1. Conditioned cell media composition. Media comprises albumin, immunoglobulins, other proteins, cellular proteins and protein of interest.

1.2.3 The secretome protein enrichment with click sugars (SPECS) method enables secretome analysis with mass spectrometry

The Secretome Protein Enrichment with Click Sugars (SPECS) method is an eligible strategy to overcome problems during mass spectrometry aided analysis of the secretome in serum containing media. According to UNIPROT, the majority of extracellular proteins (%87) are glycoproteins. SPECS facilitates the enrichment of glycoproteins, the majority of secretome proteins by taking advantage of this feature. To this aim, SPECS combines metabolic glycoprotein labelling with azido group containing sugars and subsequent click chemistry catalysed biotinylation of prior metabolically labelled glycoproteins (27). First, glycoproteins are metabolically labelled with azido sugars such as Tetraacetyl-N-azidoacetyl-mannosamine (ManNAZ) sugar being converted into sialic acid analogues which are incorporated in the glycoprotein during their synthesis (49). Second, prior metabolically labelled glycoproteins are biotinylated via copper-free strain-promoted click chemistry between the strained alkyne of DBCO-Biotin and the azide group of ManNAZ forming a triazole heterocycle while hardly reacting with any other chemical moieties which is hence termed as a biorthogonal reaction (50). Alternative sugars such as N-azidoacetylgalactosamine tetraacylated (GalNAZ) or N-azidoacetylglucosamine tetraacylated (GlcNAZ) sugars can be used instead of ManNAZ to label O-glycosylated extracellular proteins or in the latter case O-GlcNAc modified intracellular proteins. These are suitable for metabolic labelling of glycoproteins but predominantly incorporate into O-linked glycans (51). Biotinylation of proteins allows their subsequent enrichment with a streptavidin pull down. Purified proteins are finally subjected to in-gel digestion and mass spectrometric analysis. (Fig.2)

1.2.4 Surface-Click method enables cell surface proteome analysis with mass spectrometry

The surface-click protocol is based on the same strategies as the SPECS protocol comprising metabolic labelling of cellular glycoproteins with azido sugars (ManNAZ) during their synthesis and click chemistry assisted biotinylation here directly applied to the cell pellet (29, 30). Afterwards, cells are lysed with a suitable lysis buffer and glycoproteins can be enriched with a streptavidin pulldown. Eluted proteins are loaded on a SDS gel for separation and proteins are subjected to tryptic digestion. Afterwards, peptides are ready for MS analysis (Fig.3)

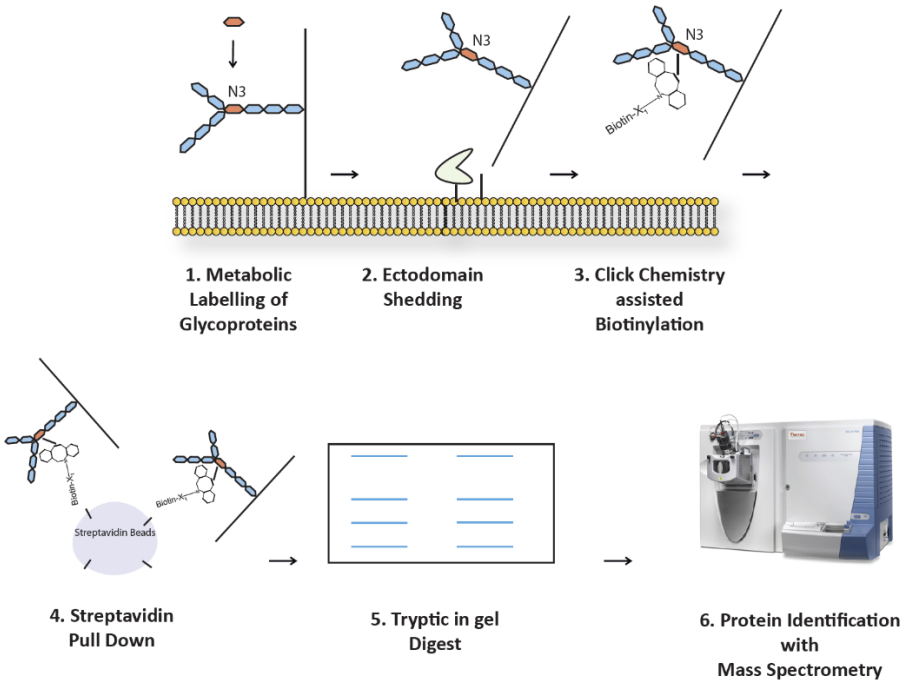

Figure2. Main workflow of the SPECS protocol. SPECS comprises metabolic glycoprotein labelling with azido sugars, their click chemistry assisted biotinylation and streptavidin pull-down. Eluted enriched glycoproteins are subjected to SDS-PAGE and tryptic digestion. Afterwards, resulting peptides are ready for MS measurements.

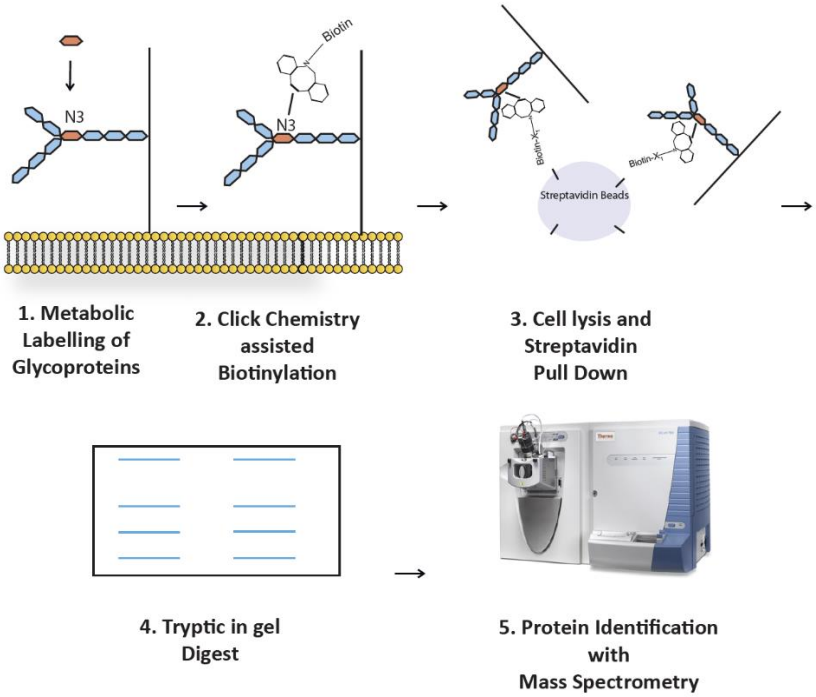

Figure3. Main workflow of Surface-click protocol. Surface-click procedure comprises metabolic glycoprotein labelling with azido sugars, click chemistry assisted biotinylation, cell lysis and streptavidin pull down of labelled glycoproteins. Eluted enriched glycoproteins are subjected to SDS-PAGE and tryptic digestion. Afterwards, resulting peptides are ready for MS measurements.

1.2.5 SPECS Optimizations and Objectives

The SPECS method has already enabled us to identify the protease substrates of BACE1 (27), SPPL3 (52), and ADAM10 (29). These studies indicated that SPECS is a powerful tool to analyze the secretome and the physiological function of extracellular acting enzymes such as proteases. Hence, in the first part of my thesis, I tried to optimize different aspects of the SPECS protocol to reduce the required input material and increase the number of quantifiable glycoproteins. Therefore, I tried to optimize the SPECS protocol with different biotin conjugates, different reaction buffers, conditions and pH.

1.3 Acute Myeloid Leukemia (AML)

1.3.1 Hematopoiesis in the human body

All corpuscular blood components are produced by hematopoietic stem cells via a complex differentiation and replication program**.** Firstly, hematopoietic stem cells differentiate into a common lymphoid progenitor and a common myeloid progenitor cell. (53) Secondly, differentiation of lymphoid progenitor cells gives rise to natural killer cells, B- and T-lymphocytes while differentiation of common myeloid progenitor cells results in the generation of myeloblasts, megakaryoblasts, proerythroblast that subsequently give rise to mature blood elements such as different types of granulocytes, thrombocytes and erythrocytes (Fig.4). All of these blood elements play specific roles in the human body.

Erythrocytes act as oxygene carriers to tissues, thrombocytes take part in coagulation, monocytes act in inflammatory response and B- and T- lyphocytes and granulocytes are involved in the immune defense (54, 55).

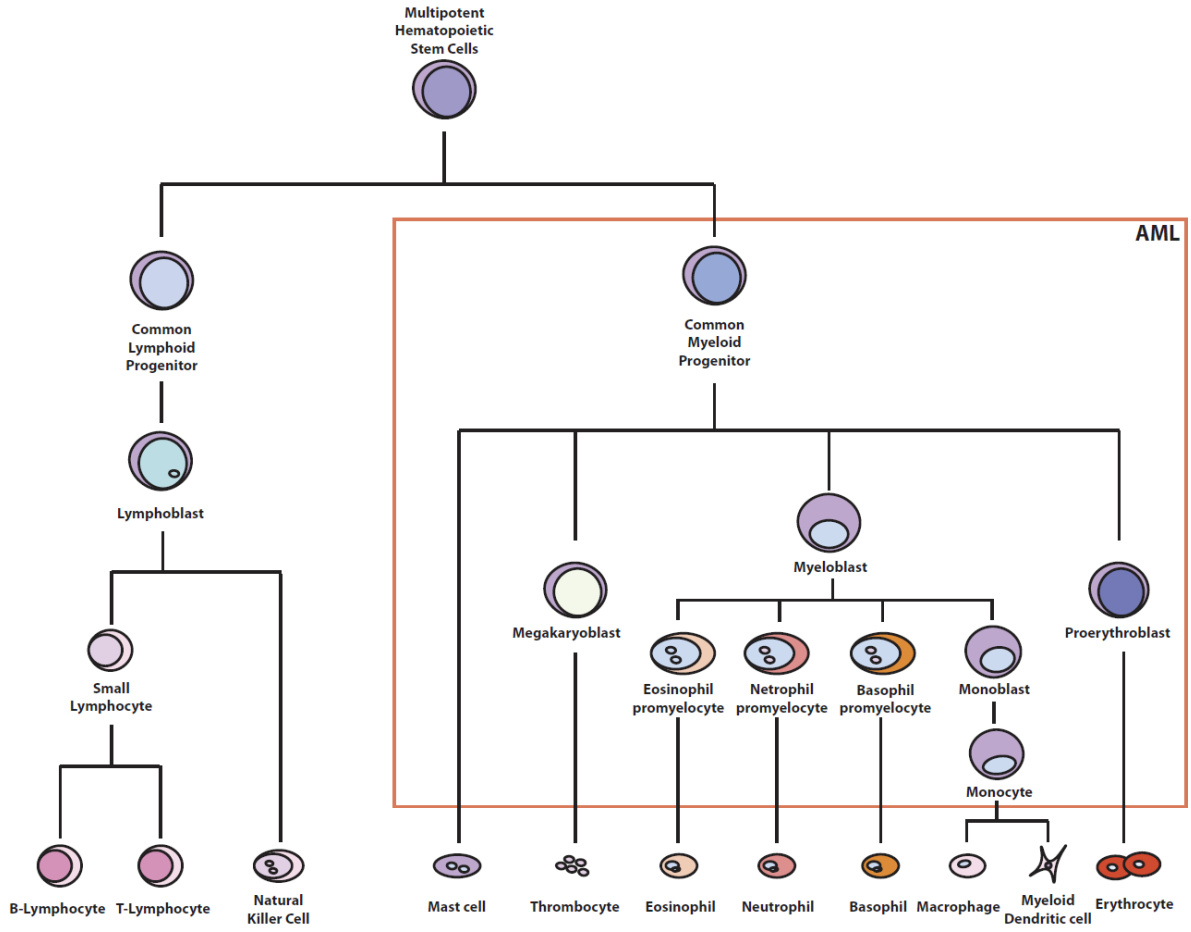

Figure 4. Hematopoiesis in the human body. Red box includes potential AML cells. (Figure adapted from (55))

Recent studies indicate that oncogenic mutations in early differentiation steps of hematopoietic cells can lead to leukemia (56). There are four major types of leukemia defined as Acute myeloid leukemia (AML), Chronic myeloid leukemia (CML), Acute lymphocytic leukemia (ALL) and Chronic lymphocytic leukemia (CLL) (57). The definition of chronic or acute depends on the maturity of leukemic cells. Leukemias are defined as acute if disease related leukemic cells stop differentiation at an early stage of differentiation and have a high proliferation rate both contributing to an aggressive disease progression (58). On the other hand, leukemias are defined as chronic if the disease related leukemic cells are partially mature and have a low proliferation rate leading to a slow disease progression. Among all leukemia types, the 5-year survival rate of acute myeloid leukemia (AML) patients is about 26% and AML causes most of leukemia related deaths according to the American Cancer Society report (59). Survival rates already indicate the aggressive nature of AML. Acute Myeloid Leukemia (AML) begins with the expansion of early myeloid progenitors with aggressive, heterogeneous characteristics leading to the accumulation of immature and

nonfunctional myeloid cells in the bone marrow and blood (Fig.4- red box). In this manner, myeloid cells invasively (blasts) outcompete normal blood elements. This results in various consequences and severe symptoms such as anemia, thrombocytopenia, increase of non-functional white blood cells. These imbalances in the blood elements cause severe symptoms such as bruising and bleeding, headache, fever, pain and weakness.

1.3.2 Symptoms of Acute Myeloid Leukemia

Bone marrow invasion by leukemic cells can impair physiological production of blood elements. Therefore, this may cause different symptoms. Low erythropiesis causes anemia. In the case of anemia, body tissues are not supplied with sufficient oxygen and leading to fatigue, weakness, headache and dizzinesss (60). Other risks may arise from low thrombocytopoiesis, which can lead to uncontrolled bleeding even for example on nose and gums (61). Furthermore, a low number of mature white blood cell leads to increased risk of infection. On the other hand, increased leukemic cells in the bloodstream can lead to organ defects in the long term.

Because of the aggressive nature of AML, these symptoms may suddenly appear and there is currently no early screening test available. However, blood counts and genetic analysis may be useful for early diagnosis.

1.3.3 Current diagnosistics

For current treatment options a correct diagnosis of AML is important. Mainly, a complete blood count (CBC) measuring the number of white blood cells, red blood cells and platelets is the first diagnostic tool to identify blood abnormalities as it is the case in AML. Most AML patients suffer from anemia and too many immature white blood cells in the blood. After CBC, the cellular composition of the bone marrow is analyzed histologically and by FACS from bone marrow biopsies or aspirates. If blast cells represent more than 20-30 % of all blood forming elements in the bone marrow, patients are diagnosed with AML (normal blast count should be around 5% or less). However, CBC, histological and cytological analysis of bone marrow biopsies or aspirates are not sufficient, as AML is a heterogeneous disease with different subtypes with differing biology and response to therapy modalities (62). To define the correct subtype additional diagnostic methods such as cytochemistry, cytogenetic and molecular genetic analyses are necessary. Aberrant or increased expression of cell surface and secreted proteins in AML can be detected via cytochemistry. For example, overexpression of myeloperoxidase (MPO), CD34 and/or KIT can be observed in certain AML subtypes. Cytogenetic analyses detect chromosomal abnormalities in leukemic cells from bone marrow samples (63). There are four types of chromosomal aberrations. Chromosomal translocations describes breakage of two different chromosomes and subsequent exchange of the break products between both chromosomes t(8;21). An inversion describes that part of a chromosome which is still at its original place but with inversed orientation such as inv (16). A deletion indicates deletion on a specific chromosome such as del(7) . Addition or duplication means that part of or the complete chromosome are duplicated or present as many copies such as +8. Cytogenetical tests take time and require bone marrow aspirates that are painful for the patient and always bear a risk of infection and bleeding. However, the current AML

subtype classification and subtype specific treatment options depend on cytogenetic and molecular genetic diagnostic methods of bone marrow aspirates.

1.3.4 French-American-British (FAB) and World health organization (WHO) Classification of AML

The first categorization system of AML was defined as French-American-British (FAB) classification system in 1976 (64). FAB mainly relies on microscopic examination and routine staining to determine blast cells and their myeloid types. FAB classification comprised mainly eight subtypes (M0 through M7). These subtypes were defined according the type and maturation grade of leukemic cells. (Table 1)

FAB subtypes	Morphological Classification
AML-M0	Undifferentiated acute myeloblastic leukemia
AML-M1	Acute myeloblastic leukemia with minimal differentiation
AML-M2	Acute myeloblastic leukemia with maturation
AML-M3	Acute promyelocytic leukemia
AML-M4	Acute myelomonocytic leukemia
AML-M5	Acute monocytic leukemia
AML-M6	Acute erytroid leukemia
AML-M7	Acute megakaryocytic leukemia

Table1. FAB classification of Acute Myeloid Leukemia.

The FAB subtypes are a useful and practical system for general classification but it does not take into account many factors that contribute to the prognosis of an individual patient. The FAB classification did not include genetic abnormalities, new immunological features and morphological similarities between different syndromes. Therefore, the World health organization (WHO) set up a new system for AML subtype classification that additionally considers the genetic basis and new immunological features of leukemia. The WHO classification firstly depends on the major lineages such as myeloid, lymphoid, histiocytic and mast cells. In addition to the major lineage, morphology, immunophenotypes, genetic abnormalities and syndrome types define the disease subtypes. As these features and especially the genetic basis of leukemiogenesis are not fully defined, WHO classification system still mainly depends on morphological clustering (Table 2) (57).

AML with recurrent genetic abnormalities
AML with t(8:21)(q22;q22.1); RUNX1-RUNX1T1
AML with inv(16)(p13.1q22) or t(16;16)(p13.1;q22); CBFB-MYH11
APL with PML-RARA
AML with t(9;11)(p21.3;q23.3);MLLT3-KMT2A
AML with t(6;9)(p23;q34.1); DEK-NUP214
AML with inv(3)(q21.3q26.2) or t(3;3)(q21.3;q26.2); GATA2, MECOM
AML (megakaryoblastic) with t(1;22)(p13.3;q13.3); RBM15-MKL1
AML with BCR-ABL1 (provisional entity)

AML with mutated NPM1
AML with biallelic mutations of CEBPA
AML with mutated RUNX1 (provisional entity)
AML and myelodysplastic syndrome,
Therapy-related myeloid neoplasm
AML, NOS
AML with minimal differentiation
AML without maturation
AML with maturation
Acute myelomonocytic leukemia
Acute monoblastic/monocytic leukemia
Pure erythroid leukemia
Acute megakaryoblastic leukemia
Acute basophilic leukemia
Acute panmyelosis with myelofibrosis
Myeloid Sarcoma
Myeloid proliferations related to Down Syndrome
Transient Abnormal myelopoiesis (TAM)
Myeloid leukemia associated with Down syndrome

Table2. WHO classification of Acute Myeloid Leukemia

Once the AML subtype is defined for a given patient, a specific treatment modality adapted to the AML subtype can be applied.

1.3.5 Current Treatment Options

Currently, there are mainly two treatment options in clinics that are based on chemotherapy or targeted drug therapies. Chemotherapy is based on the inhibition of DNA replication. For example, Cytarabine inhibits DNA polymerase (65, 66) and Daunorubicin or Idarubicin block topoisomerase II activity (67). Chemotherapy includes two main steps. The first step called remission induction is an intensive chemotherapy administered to AML patients to cause a complete remission of AML. This would end up with cure or refractory situations. In case of refractory AML an additional high dose chemotherapy is administered to the patient. In case of a complete remission, low dose of chemotherapy is given called post-remission. These steps are necessary to prevent the formation of resistant cells**.** Therewithal according to the mutation type, additional targeted drug therapies can be applied which is mainly related to receptor tyrosine kinases (68).

Receptor tyrosine kinases are a family of membrane bound receptors with a tyrosine kinase domain in their cytoplasmic domain that activates survival and proliferation promoting pathways upon ligand binding such as PI3K, RAS and AKT (69). Mutations or amplification of receptor tyrosine kinases in malignant cells can lead to increased activation of these pathways and thus contribute to disease progression in cancer. Receptor tyrosine kinase inhibitors are successfully applied to various cancer types (70). In AML, recurrent mutations in the receptor tyrosine kinase FLT3 have been identified in up to 30% of patients with *de novo* AML (44, 45). FLT3 mutations comprise the more frequent in length varying internal tandem duplication (FLT3-ITD) of the juxtamembrane region and less frequent activating point mutations in the

cytoplasmic FLT3 kinase domain (FLT3-TKD) both leading to a constitutive activation of FLT3 (71, 72).

Chemotherapy drugs hit proliferating cells thus not only killing or suppressing cancer cell growth but also affecting or killing healthy cells which leads to severe side effects such as increase risk of infection, easy bruising or bleeding, weakness, hair loss and diarrhea. Therefore, in cancer therapy, targeted therapies become increasingly important. Targeted therapy focuses on specific targets that are changed particularly in specific cancer types. Overexpression of receptor tyrosine kinases and mutations are in the focus of targeted therapies. There are different applications of targeted therapies such as small molecular inhibitors, monoclonal antibodies coupled with specific chemicals or immunotoxins (73). Targeted therapy for FLT3 mutated cases is based on the inhibition of constitutive FLT3 receptor tyrosine kinase activity. Midostaurin, Quizartinib, Gilteritinib, Crenolanib and Sorafenib are used in clinic trials for targeted therapies in FLT3 wildtype and FLT3 mutated AML patients (42, 71). Sorafenib inhibits FLT3, c-KIT, VEGFR, RAF and PDGFR activity. In phase I clinical trials Sorafenib reduced leukemic cells and achieved complete remission in many patients (74-77). In a phase II clinical trial, patients with FLT3-ITD mutation with a Sorafenib dose of 200-400 mg twice daily showed strong complete remission with some side-effects but patients relapsed on average within 72 days upon remission. Resistance towards Sorafenib can in part be caused by the mutations D835Y and D835H in the FLT3 receptor tyrosine kinase domain (78-80). In the beginning of Sorafenib treatment, patients are in remission for a short term period but develop a relapse during long term treatment with Sorafenib (71).

Midostaurin, Quizartinib, Gilteritinib and Crenolanib are FLT3 tyrosine kinase related drugs that in combination with chemotherapy reagents are still in trial. The RATIFY study investigates whether the combination of FLT3 inhibitors with chemotherapy improves survival or not (42, 71, 81).

The initial results of targeted FLT3 inhibition with small molecule drugs are promising. However, they are not of long duration. As there currently is no successful treatment option for FLT3 mutated AML cases, it is important to understand the underlying biology of Sorafenib resistance in AML. Understanding the biology of Sorafenib resistance will be important for determining AML progression under Sorafenib treatment and the development of new treatment strategies.

1.3.6 Prognosis and possible resistance mechanisms of AML

AML prognosis and treatment strategy is mainly releated to patient age. Patients below 60 years generally have a 35-40% of survival, patients older than 60 generally has 5-15% chance of survival for 3-5 years (82, 83). Older patients cannot tolarate high doses of chemotherapy and additional diseases increase the risk of death. These obstacles make it difficult to reach complete remission and high survival rates.

AML resistance mechanisms are generally linked to defects in antiapoptotic signaling and aberrant activation of survival and proliferation pathways. This basically can be caused by mutations in specific genes, overexpression of specific receptor and/or autocrine signaling of the cells (42).

For instance, frequently mutated FLT3 is linked to PI3K, RAS downstream signaling units that are part of proliferation and survival promoting pathways (71, 84). Additionally, highly activated AKT, STAT, ERK downstream signaling units can lead to the formation of aberrant FLT3 transcripts (85). FLT3-ITD mutation presence forms resistant cells to FLT3 inhibitors (84).

c-kit gene is another frequently mutated gene in AML. c-kit gain of function mutations are frequently found in AML patients with a chromosomal t(8;21) translocation which leads to higher relapse risk and poor prognosis (39-41).

1.4 Investigation of FLT3 and c-kit with the genome editing technology CRISPR-Cas9

Genome editing tools are helpful for understanding gene function in the cellular, tissue or full organism context. Knock out or knock in strategies can provide a deeper understanding of gene function. Different gene editing technologies were established in recent years like zinc finger nucleases (ZFNs), transcription activator-like effector nucleases (TALENs) and the youngest technology called CRISPR-Cas9 (86-95). Clustered regularly interspaced short palindromic repeats (CRISPR) in combination with the bacterial nuclease Cas9 are a state-of-the-art technology for genome editing which aids the generation of targeted gene knockouts. The system comprises of the bacterial endonuclease Cas9, single guided RNAs (sgRNAs) that together create a DNA double strand break (96, 97) (Fig.5).

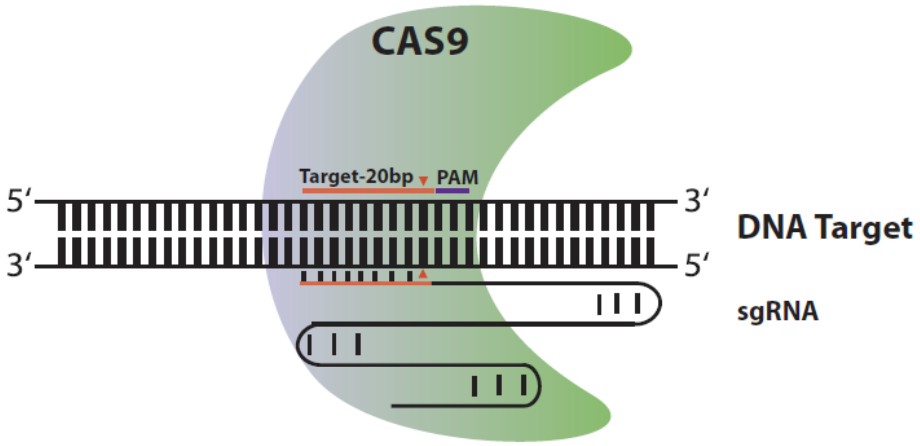

Figure5. CRISPR-CAS9 nuclease. DNA sequence is targeted by Cas9 nuclease, 20 nucleotides guide sequence (red) and scaffold forms sgRNA. PAM sequence shown in purple. Cas9 mediated break shown in red triangle.

In particular, streptococcus pyogenes based CRISPR-Cas9 system cleavage is dependent on the protospacer adjacent motif (PAM) sequence that should immediately follow the target sequence 5`NGG (98). Different PAM motifs are required for different Cas9 types such as 5`-NNAGAA for S. termophilus based Cas9 or 5`NNNNGATT for Neisseria meningiditis based Cas9 (99, 100). These PAM sequences are important for generation of double strand breaks. Another important aspect for CrispR-Cas9 to work is a 20 nucleotide long target sequence which needs to be designed according the targeted DNA exon. There are different databases that provide sgRNA in silico designs (101). Other technologies like ZFNs and TALENs are dependent on DNA binding proteins and catalytic action of nucleases while the CRISPR-Cas9

system is only based on a small RNA guiding Cas9 to achieve Double stranded breaks (97). These double strand breaks can be repaired by the non-homologous end joining (NHEJ) pathway or homology directed repair (HDR) pathways. NHEJ pathway is activated generally in the absence of a repair template and this process results in insertion/deletion (indel) mutations (86, 87, 97). These indel mutations could lead to premature stop codons or frameshift mutations (102). On the other hand, HDR pathway uses a repair template to repair the double strand break site. This process can be exploited to make defined modification of the target sites (103, 104). The CRISPR-Cas9 system has several advantages over the previous genome editing tools like simplicity and speed of design. Guide RNAs can easily be designed and CRISPR action depends on ribonucleotide complex formation and not protein-DNA recognition. Furthermore, the CRISPR system has a more efficient action and allows simultaneous multiple gene editing (97). The main risk of CRISPR system is that guide RNAs can bind to off-target sequences and thus lead to unspecific double strand breaks at off-target exon sites. In order to minimize the risk of off-target cleavage, in silico based prediction algorithms for sgRNA designs are in use (101).

Receptor tyrosine kinase drugs generally inhibit multiple kinases. Hence, these experiments do not fully indicate the specific receptor activity. Therefore, CRISPR-Cas9 technology could provide us with specific receptor tyrosine kinase knockouts to understand the biological role of a single receptor and thus support the identification of AML resistance mechanisms. To this aim, I plan to generate knock outs on exon sites of FLT3 and c-KIT receptor in AML cell lines.

1.5 Receptor tyrosine kinase ligand production with the Gal4/VP16-UAS system

Gal4 is a modular protein from Saccharomyces cerevisiae that works as a transcriptional activator via binding to upstream activating sequences (UAS) (105). This complex activates transcription of target genes in yeast (105). The Gal4-UAS system can be operated in various animal cells such as xenopus, zebrafish, mice and drosophila (106-109). In the next years,for stronger activation of directed gene expression, Gal4-VP16 system was started to use (110). The Gal4-VP16 system comprises the DNA binding Gal4 protein from S. cerevisiae and a transcriptional activation domain-VP16 from herpes simplex virus (111). The Gal4V-P16 fusion protein can promote much stronger expression of desired genes in eukaryotic cells than the Gal4 protein alone (110). For gene expression, one plasmid carrying the UAS element with a minimal promoter followed by the desired recombinant gene coding sequence and a second plasmidcoding forh the Gal4/VP16 sequence are coexpressed in a cell.

To study receptor tyrosine kinase activation upon binding of a receptor tyrosine kinase specific ligand (RTKL), I plan to produce different recombinant receptor tyrosine kinase ligands in the mammalian cell line HEK293T. Therefore, bipartite lentiviral vector expression system based on Gal4/VP16-UAS system is used for the production. This system comprises three plasmids. First plasmid has the upstream 5xUAS site and desired recombinant ligands sequence can be clone downstream of UAS. After the recombinant ligand sequence HIS-tag and biotin acceptor proteins are placed (112, 113). Second plasmid comprises the Gal4/Vp16 activator sequence and third plasmid comprises the E.coli derived biotin ligase (secBirA-KDEL) sequence that can biotinylate RTKL during maturation (112, 113). After the production, ligands can be purified with HIS-tag (poly histidine-tag) purification (114, 115). Afterwards

streptavidin-HRP detection can be applied to detect recombinant ligands. After the production of specific receptor tyrosine kinase ligands, RTKs will be stimulated with specific RTKL and proteomics changes can be observed.

1.6 AML Research Objectives

Receptor tyrosine kinase profiles of different AML cell lines and identification of resistance mechanism could give an idea about treatment strategies and biomarkers for early diagnosis of AML. Hence, during my thesis, I focused on:

1. Secretome and surface-proteome profile analysis of 6 different AML cell lines reflecting different FAB classifications. This study could provide novel diagnostic biomarkers.
2. Sorafenib inhibition of specific cell lines to understand how cells become resistant to treatment via analyzing their secretome and surface proteome.
3. Generating CRISPR-Cas9 mediated knock-outs on FLT3 and KIT receptors to understand more deeply the RTK related biology of AML via analyzing their secretome and surface proteome.
4. Production of recombinant FLT3 and KIT ligands and designing a stimulation experiments on specific cell lines**.**

2 Materials and Methods

2.1 Cell Culture

2.1.1 Cell culture media and supplements

Dulbecco's Modified Eagle Medium	(61965-026,	GIBCO)
RPMI-1640- L-Glutamine media	(21875-034,	GIBCO)
Fetal Bovine Serum	(10270-106,	GIBCO)
Penicillin-Streptomycin	(15140-122,	GIBCO)
Non-essential amino acids (NEAA)	(1140-035,	GIBCO)

2.1.2 Cell lines

KG1α	(M0-M1, Acute Myeloblastic leukemia with minimal differentiation, DSMZ No: ACC421)
Kasumi-1	(M2, Acute Myeloblastic leukemia with maturation, DSMZ No: ACC220)
NB-4	(M3, Acute promyelocytic leukemia, DSMZ No: ACC207)
OCI-AML5	(M4, Acute myelomonocytic leukemia, DSMZ No: ACC247)
MV4-11	(M5, Acute monocytic leukemia, DSMZ No: ACC102)
CMK	(M7, Acute megakaryocytic leukemia, DSMZ No: ACC392)
HEK 293T cells	(Embryonal kidney cells, DSMZ No: ACC635)

All AML cell lines are obtained from DSMZ (German collection of Microorganism and Cell cultures, Germany) or kindly provided by PD Dr. Fiegl, Grosshadern Hematology department.

2.1.3 Cell Culture Conditions

Sterile Hood	(Heraeus)

Incubator	(Thermo Scientific or Heraeus)
T75 Flasks	(658170, Cellstar)
6 well plates	(657160, Cellstar)
10 cm dishes	(83.1802, Sarstedt)
Centrifuge	(4K15, Sigma)
Light Microscope	(TS100, Nikon Eclipse)

AML cell lines are cultured in RPMI-1640- L-Glutamine media supplemented with 10% Fetal Bovine Serum and 1% Penicillin-streptomycin. HEK293T cells are cultured in Dulbecco's Modified Eagle Medium with 10% Fetal Bovine Serum, 1 % Penicillin-streptomycin. Cells are cultured in 6 well plates, 10 cm dishes or in t75 flasks 20 ml medium 37°C and 5% CO_2. Sterile hood is used for manipulation and passaging of the cells.

2.1.4 AML patient Material

AML patient serums are obtained as frozen stock (-80°C) from our collaboration Hematology department of Technical University of Munich.

2.1.5 Sorafenib Treatment

MV4-11	(M5, Acute monocytic leukemia, DSMZ No: ACC102)
Sorafenib	(8705, Cell Signalling)

$2x10^6$ Mv4-11 cells are cultured in RPMI medium supplemented with 5nM or 10 nM of Sorafenib for 2 weeks. Every 3 days cell culture medium is exchanged for fresh medium supplemented with corresponding amounts (5 nM, 10 nM) of Sorafenib. DMSO is used as control. When cell number reached the $40x10^6$ SPECS protocol is applied.

2.2 Protein Analysis

2.2.1 Cell lysis

NaCl	(S7653, Sigma Aldrich)
KCl	(P9333, Sigma Aldrich)
Na_2HPO4	(255793, Sigma Aldrich)
KH_2PO_4	(1551139, Sigma Aldrich)
Tris	(93362, Sigma Aldrich)
Triton X	(108603, Merck)
PBS	(136mM NaCl, 12mM Na_2HPO_4, 1 mM KH_2PO_4, 2mM KCl, pH7.4)
STET lysis buffer	(50 Mm Tris pH7.5, 150mM NaCl, 2mM EDTA, 1% Triton X)
Table top centrifuge	(5417R, Eppendorf)

2.2.2 Cell Lysis protocol for AML cell lines and HEK293T cells

AML cell lines are collected and centrifuged at 800rpm to get rid of dead cells and particles. Media are either transferred to new tubes or discarded. Cell pellets are washed with ice cold PBS and lysed with a plate type adapted lysis buffer volume.

For HEK293T cells, media are collected with serological pipettes or removed with a vacuum pump attached to a glass needle. Afterwards cells are washed with ice cold PBS. Healthy HEK293T cells remain attached to the plate surface. Afterwards ice-cold lysis buffer is directly added to the cells. Cells are detached in re-suspended using a P1000 pipette.

Type of Dishes	Amount of Lysis Buffer
24 well plate	300 µl
6 well plate	500 µl
10 cm dishes	1000 µl

Table3. Lysis volume per type of dishes.

After a 15 min incubation on ice, cell lysates are centrifuged at 14.000g at 4°C for 5 min in a precool table top centrifuge. After the clarification, supernatants are transferred to fresh tubes and protein concentrations are measured with Pierce BCA assays.

2.2.3 Protein concentration quantification assays

Pierce BCA Assay	(23225, Pierce BCA Protein, 562nm).
Red 660 Protein Assay	(015R, G Bioscience, 660nm)
Elisa Reader	(Infinite F200 Pro, Tecan)
96 well Plates	(144895, Thermo Scientific)

BCA Assay:

10 µl of lysate are placed into one well of a 96 well plate.

Pierce BCA assay components A and B are mixed in a 50:1 ratio. 200 µl of the AB mixture are added to 10 µl of cell lysate or BSA standard and incubated for 30 min at 37°C until the purple dye occurs.

Red 660 protein assay:

Or 150 µl Red 660 Protein assay buffer is added to 10 µl cell lysate or BSA standard and incubated for 5 min at room temperature.

Absorbance measurement:

Absorbance is measured with an ELISA plate reader at 562 nm for the BCA assay or 660 nm for the RED 660 protein assay according to the instructions of the manufacturer. Bovine Serum Albumin is used as a reference standard to determine the absolute protein concentration of the samples.

2.2.4 SDS PAGE

Lower Tris Buffer	(1.5 M Tris pH8.8, 0.4% SDS)
Upper Tris Buffer	(0.5 M Tris pH 6.8, 0.4% SDS)
Acrylamide	(T802.1, 40%, ROTH)
TEMED	(2367.3, ROTH)
APS	(Ammoniumpersulfate, A3678, Sigma Aldrich)

Protein SB Laemmli, reducing 4x	(8% SDS, 40% Glycerol, 10% Mercaptoethanol, 125mM Tris pH 6.8, 0.025% Bromophenol Blue)
Protein SB non-reducing 4x	(8% SDS, 40% Glycerol, 125mM Tris pH 6.8, 0.025% Bromophenol Blue)
Urea Sample Buffer 1X	(3.125 ml 1M Tris pH6.8, 1g SDS, 3.75 ml Glycerol, 1.25ml Mercaptoethanol, 24,024g Urea total in 50 ml)
SDS Running Buffer 1x	(25mM Tris, 192mM Glycin, 0.1% SDS)
Gel running system	(Mini-Protean system, Biorad)
Power supply	(Powerpac 300, Biorad)
Gel cast equipment	(Plates and gel racks, Biorad)
MW marker	(See blue plus 2, Invitrogen)

Separation Gel	**8% Gel**	**10% Gel**	**12% Gel**	**15% Gel**
Acrylamid 40%	7.8 ml	4 ml	6 ml	4 ml
ddH_2O	4.2 ml	8 ml	6 ml	8ml
4X Lower Tris	4 ml	4 ml	4 ml	4 ml
APS	30µl	30µl	30µl	30µl
TEMED	30µl	30µl	30µl	30µl
Total	16 ml	16 ml	16 ml	16 ml

Stacking Gel	
Acrylamid 40%	1.3 ml
ddH_2O	6.5 ml
4X Upper Tris	2.5 ml
APS	30µl
TEMED	30µl
Total	10.3 ml

Table 4. Different Tris-Glycine polyacrylamide gel composition.

Thick and thin glass plates are placed into gel casting gaskets for SDS page gel preparation. 7.5 ml of separation gel solution are poured with a serological pipette between the glass plates. Afterwards 250µl of Isopropanol are thoroughly layered above the separation gel solution to remove bubbles and seal the gel from air. Upon gel polymerization, isopropanol is removed with tissue paper while tilting the gels and, 2.5 ml stacking gel are layered above the polymerized separation gel. Finally, spacers with different well sizes are placed inside the stacking gel solution. After stacking gel polymerization, spacers are removed and gels are placed into an electrophoresis chamber and covered with running buffer. Depending on further processing of the gel and particularities such as antibody characteristics, proteins are mixed with either 4x Laemmli buffer or non-reducing Laemmli buffer and cooked for 5 min at 95°C or incubated at 45°C. According the protein concentration, proteins are loaded on the gel. Gels are run with 80V until the sample front is focused and reaches the separation gel. When the molecular weight marker becomes visible on the separation gel, voltage is adjusted to 120V and samples are run through the gel until the bromophenol blue front leaves the gel.

2.2.5 Schägger Gels for proteins with low molecular weight

Anode Buffer	(200mM Tris/HCL pH8.9)
Cathode Buffer	(0.1M Tris/HCL, 0.1M Tricine, 0.1% SDS(w/v)

Gel buffer	(3M Tris/HCL pH8.4, 0.3% SDS (w/v)
Acrylamide Solution	(49.5% Acrylamide, 3% Bis-Acrylamide in ddH_2O (w/v))
Glycerol	(32% Glycerol in ddH_2O)

Schägger Gels	**Sep. Gel (2 Phase)**	**Sep Gel (1. Phase)**	**Stacking Gel**
Acrylamide Solution	3.5 ml	1.5 ml	0.5 ml
Gel Buffer	3.5 ml	2.5 ml	1.55 ml
ddH_2O	-	3.5 ml	4.2 ml
Glycerine	3.5 ml	-	-
APS	32.5 µl	35 µl	25 µl
TEMED	3.25 µl	4 µl	5 µl
Total	10.5 ml	7.5 ml	6.7 ml

Table 5. Different Tris-Tricine polyacrylamide gel composition.

The Schägger gel system is a discontinuous gradient gel system for separation of low molecular weight proteins. The solutions are prepared as indicated in the table and poured into the gel gasket while tilting the gel gasket holder in a 45° angle in the following order: Separation gel 2 solution, - separation gel 1 solution. Afterwards, 250 µl of isopropanol are layered above the separation gel. After separation gel solidification, the stacking gel solution is layered above the solidified separation gel. Proteins are run through the gels mentioned under Tris-Glycine SDS page gels.

2.2.6 Coomassie Brilliant Blue Staining of Gels

Coomassie Brilliant Blue R	(6104-59-2, Sigma Aldrich)
Acetic Acid	(100063, Merck)
Glass Plates	
Horizontal Shaker	(Edmund Bühler)

For preparation of a Coomassie brilliant blue staining solution 50 ml of Acetic acid are added to a 500 ml glass bottle. 125 mg of Brilliant Blue R are solved in acetic acid and stirred for 30 minute. Afterwards ddH_2O is added to a final volume of 500 ml and the mixture is subsequently stirred for 1 hour.

For Coomassie staining of proteins, SDS page gels with separated proteins are carefully transferred to clean glass tanks, covered with Coomassie staining solution and afterwards they are incubated on horizontal shaker for 30 minutes. For destaining of the background, SDS page gels are repeatedly incubated in fresh 10% (v/v) acetic acid solution until the background staining vanished and protein bands are visible.

2.2.7 Western Blot

Mini Protean Blotting System	(Biorad)
PVDF membranes 0.45µm	(10600023, GE Healthcare)
Nitrocellulose membranes 0.45µm	(1228243, GVS North America)
Filter Papers	(A. Hartenstein)
Sponges and Transfer Cassettes	(Biorad)
Transfer Buffer 1x	(25mM Tris, 240 mM Glycin)
Tween20	(P1379, Sigma Aldrich))

PBS-Tween	(136mM NaCl, 12mM Na_2PO_4, 1 mM KH_2PO_4, 2mM KCl, pH7.4 + 1% Tween20)
Blocking Buffer	(5% Skim milk powder (70166, Sigma Aldrich) dissolved in PBS-Tween)
I-Block	(1g I-Block powder is dissolved in 500ml of PBS-Tween solution. Heat the buffer until I Block is completely dissolved. Avoid boiling -Store at 4°C)
Horizontal Shaker	(Edmund Bühler)
ECL	(RPN2106, GE Bioscience)
ECL prime	(RPN2232, GE Bioscience)
Medical X-ray film	(47410, Fujifilm)
Western Blot Developer	(ImageQuant)

After SDS-PAGE, the stacking gel is removed from the separation gel. The transfer sandwich is prepared in the following order: black plastic of the cassette, sponge, 2 filter papers, separation gel, transfer membrane, 2 filter papers, sponge and white plastic of the cassette inside the transfer buffer. Every layer, make sure to remove the bubbles. Then transfer sandwich is placed into the transfer chamber and ice block is placed inside with transfer buffer. Than the transfer is run at 0.40 ampere for 1:05 hours. After this procedure, proteins are transferred and immobilize in the membrane. Afterwards membranes are transferred to plastic dishes and subjected to blocking with blocking buffer for 30 min 250-300 rpm on horizontal shaker. Then blocking buffer is removed and membranes are washed with PBS-Tween for 15 min. Then 10 ml of primary antibody solution is prepared according to data sheet of the antibody and incubated for 2 hours at room temperature or 4°C overnight shaking. (If no primary antibody is needed directly skip to secondary antibody incubation step for example biotinylated proteins detected by Streptavidin-HRP.) In the next day membranes are washed with PBS-Tween for 15 min. Then, secondary antibody is applied for 1 hour at room temperature. Then the membranes are washed for 30-45 min with PBS-Tween. Afterwards, membranes are incubated with mixture of ECL or ECL prime (1:1) for 1 min and proteins are detected with medical x-ray films or directly with Western Blot developer.

2.2.8 Densitometry and statistical Analysis of Western Blots and Coomassie gels

Protein specific bands and background intensities are measured by ImageJ-version 1.50g 64-bit. Background intensities are subtracted from the protein specific band intensities. Corrected values are divided by the control value to get the relative intensities. The average fold change and standard error are calculated from the relative intensity values of all technical replicates of a given experiment. Heteroscedastic, two sided t-test is performed on log2 transformed relative intensity values control and treatment conditions to obtain statistical significance. Coomassie gels are analysed in the same way.

2.2.9 Antibody List

Tween20	(P1379, Sigma Aldrich)
PBS-Tween	(136mM NaCl, 12mM Na_2PO_4, 1 mMKH_2PO_4, 2mM KCl, pH 7.4 + 1% Tween20)
5% BSA	(Bovine Serum Albumin is dissolved in PBS-Tween)
Sodium Azide	(5% Sodium Azide Stock)

Antibodies are prepared and applied according to instruction of the manufacturer. In general protocol, primary antibodies are diluted in 10 ml PBS Tween + 0.5% BSA + 50µl of Sodium Azide Stock (0.05%).

Following primary antibodies are used in our experiments:

Antibody	Epitope	Dilution	Host	Source
FLT3-FLK2 Antibody	Human-FLT3 extracellular	1-500	mouse	sc19635-SantaCruz
Phospho-FLT3 (Tyr589/591)	Human-FLT3 Tyr589/591	1-1000	rabbit	3464-Cell Signalling
Phospho-Flt3 (Tyr969)	Human-FLT3 Tyr 969	1-1000	rabbit	3463-Cell Signalling
FLT3 (8F2)	Human-FLT3- Ser740	1-500	rabbit	3462-Cell Signalling
c-KIT (D13A2)	Human-c-KIT-Tyr703	1-500	rabbit	3074-Cell Signalling
Phospho c-KIT (Tyr719)	Mouse-c-KIT-Tyr719	1-1000	rabbit	3391-Cell Signalling
Phospho c-Kit (Tyr703)	Human-c-KIT-Tyr703	1-1000	rabbit	3073-Cell Signalling
c-KIT(Ab81)	Human-c-KIT	1-500	mouse	sc13508- Santa Cruz
Anti-Beta-Actin	Beta-Actin	1-10000	mouse	5316-Sigma Aldrich
Anti-Calnexin	Calnexin	1-5000	rabbit	4731-Sigma Aldrich
Anti-sAPP -1D1	Human-APP	1-100	rat	Elizabeth Krammer
Anti-sAPP-7H6	Human-APP	1-100	rat	Elizabeth Krammer
Anti-Human-IgG	Human-IgG	1-1000	rabbit	109489, Abcam
Cas9 (7A9-3A3)	S.Pyogenes- Cas9	1-1000	mouse	14697,Cell Signalling
Anti-TNFR2	Human-TNFR2	1-1000	Mouse	BM4054, Acris

Table 6. Antibody List

Following HRP-conjugates are used in our experiments:

HRP-Conjugates	Dilution	Source
Anti-Mouse-HRP	1-10000	W402B-Promega
Anti-Rabbit-HRP	1-10000	W401B-Promega
Anti-Rat-HRP	1-10000	Sc2065-SantaCruz
Streptavidin-Peroxidase	1-5000	S2438-250G, Sigma life sciences

Table 7. HRP-conjugates

2.2.10 Optimization of SPECS reaction parameters in small-scale format

DBCO-PEG12-Biotin (Click Chemistry Tools)
DBCO-Sulfo-Biotin (CLKA116-10, Jena Bioscience)
Vivaspin 500 filter Columns (VS0122, Sartorius)
PBS pH6.0 (13.2% 0.1 M Na_2HPO_4, 86.8% 0.1 M KH_2PO_4, 133 mM NaCl, 2 mM KCl)
PBS pH 7.0 (61.5% 0.1 M Na_2HPO_4 ,38.5% 0.1 M KH_2PO_4, 133 mM NaCl, 2 mM KCl)

PBS pH 8.0	(94% 0.1 M Na_2HPO_4 ,6% 0.1 M KH_2PO_4, 133 mM NaCl, 2 mM KCl)
PBS pH 9.0	(99.5% 0.1M Na_2HPO_4 ,0.5% 0.1 M KH_2PO_4 ,133 mM NaCl, 2 mM KCl)
0.1 M Tris-HCl	(93362, Sigma Aldrich) buffer pH 6.0, pH7.0, pH 8.0 and pH 9.0)
Iodoactemide 30 nmol,60nmol,120nmol	(I6125-256, Sigma Aldrich)

For optimization experiments $20x10^6$ HEK cells are metabolically labelled with 100µM of ManNAZ sugar for 2 days or DMSO is used as solvent control. Afterwards conditioned media are collected and divided into 400 µl aliquots. 400 µl aliquots are concentrated using 30 KDa Vivaspin 500 filter columns at 14.000g and 4°C for 20 min. This procedure is repeated three times adding 400µl of distilled water to the sample and discarding the flow through after each centrifugation step to remove non-metabolized ManNAZ sugars. Concentrated media (around 25µl) is biotinylated using either DBCO-Peg12-Biotin conjugate or DBCO-Sulfo-Biotin conjugate. The reaction is run in either water pH7.2 or PBS pH6.0, pH7.0, pH8.0 or pH9.0 or 0.1 M Tris-HCL buffer pH 6.0, pH7.0, pH8.0 and pH9.0. 2µl of 50mM DBCO-Biotin stocks are diluted with 500 µl of the respective buffers. 25 µl of the respective buffers (5nmol-Biotin containing) are added to concentrated samples for biotinylation reaction and incubated at 4°C overnight. On the second day, columns are subjected to three diafiltration steps with 400µl water at 14.000g and 4°C to remove non-reacted biotin conjugates. The retentate is diluted to a final volume of 400µl with water, transferred to Eppendorf tubes and frozen down at -20°C for further usage. For SDS-page, samples are diluted 20-fold with distilled water and cooked with 4x protein sample buffer. Streptavidin-Peroxidase is used in western blot to detect the biotinylated proteins.

2.2.11 Old Secretome Protein Enrichment with Click Sugars (SPECS) protocol

ManNAZ sugar	(Provided by Stefan Brase)
PVDF Filters 0.45 µm	(SLHV033RS, Millex)
Ultrafiltration columns- 30KDa-Vivaspin20	(VS2022, Sartorius)
DBCO-PEG12-Biotin	(Click Chemistry Tools)
High capacity streptavidin agarose beads	(20361, ThermoFisher)
Polyprep Columns	(731-1550, BioRad)
Washing Buffer	(PBS+2%SDS)
Urea Sample Buffer 1X	(3.125 ml 1M Tris pH6.8, 1g SDS, 3.75 ml Glycerol, 1.25ml Mercaptoethanol, 24,024g Urea total in 50 ml)
Biotin Stock	(100mM Biotin (B4501, Sigma Aldrich) solved in DMSO (A994.2, Roth))

Cells are seeded into T75 flasks. For metabolic labelling, 20 ml of appropriate media are grown in the presence of 100µM ManNAZ sugar (40µl of 50mM ManNAZ stock is diluted in 20 ml of medium). Two days later media are collected in 50 ml falcon tubes and centrifuged at 800rpm to clarify media fromcells and debris. Cells pellets are placed on ice during the

consecutive steps of the surface-click procedure. Media are filtered through 0.45µm filters into 30kDa MWCO ultrafiltration columns. Columns are subjected to three centrifugation steps at 4000g, and 4°C discarding the flow through and adding 20 ml of distilled water after each centrifugation step. These steps are necessary for removing the non-metabolized ManNAZ sugars. After these steps, 500 µl concentrated retentate are inside the column. 100 nmol DBCO-PEG12-Biotin are diluted in ddH_2O. (2µl of 50mM DBCO-PEG12-Biotin stock are diluted in 500µl of ddH_2O). 500µl respective buffer with DBCO-PEG12-Biotin is added to retentate and incubated overnight at 4°C. At the next day, samples are subjected to three centrifugation steps at 4000g and 4°C discarding the flow through and adding 20 ml of distilled water after each centrifugation step. These centrifugations steps are necessary for removing non-reacted Peg12-DBCO-Biotin conjugates. The final retentate is diluted with 9.5 ml PBS with 2%(w/v) SDS and loaded on a polyprep column packed with 300 µl of high capacity streptavidin agarose beads. Samples are loaded on the polyprep column twice to increase binding of biotinylated glycoproteins to streptavidin beads. Afterwards, streptavidin beads are washed three times with 10 ml PBS with 2%SDS (w/v). Then, streptavidin beads are collected to Eppendorf tubes and cooked with 150µl of urea sample buffer containing 3mM Biotin (33µl of 100mM Biotin Stock is diluted in 1ml of Urea Sample Buffer) for elution of the glycoproteins. Eluted proteins are separated with 10% Tris/Glycine gel. After SDS-page, gels are subjected to coomassie staining followed by a tryptic in-gel digestion procedure for MS measurements.

2.2.12 New Secretome Protein Enrichment with Click Sugars (SPECS) protocol

ManNAZ sugar	(Provided by Stefan Brase)
PVDF Filters 0.45 µm	(SLHV033RS, Millex)
Ultrafiltration columns- 30KDa-Vivaspin20	(VS2022, Sartorius)
PBS pH7.0	(61.5% 0.1 M Na_2HPO_4 ,38.5% 0.1 M KH_2PO_4, 133 mM NaCl, 2 mM KCl)
Biotin click reagent- Sulfo-DBCO-Biotin	(CLKA116-10, Jena Bioscience)
High capacity streptavidin agarose beads	(20361, ThermoFisher)
Polyprep Columns	(731-1550, BioRad)
Washing Buffer	(PBS+2%SDS)
Urea Sample Buffer 1X	(3.125 ml 1M Tris pH6.8, 1g SDS, 3.75 ml Glycerol, 1.25ml Mercaptoethanol, 24,024g Urea total in 50 ml)
Biotin Stock	(100mM Biotin (B4501, Sigma Aldrich) solved in DMSO (A994.2, Roth))

Cells are seeded into T75 flasks. For metabolic labelling, 20 ml of appropriate media are grown in the presence of 100µM ManNAZ sugar (40µl of 50mM ManNAZ stock is diluted in 20 ml of medium). Two days later media are collected in 50 ml falcon tubes and centrifuged at 800rpm to clarify media fromcells and debris. Cells pellets are placed on ice during the consecutive steps of the surface-click procedure. Media are filtered through 0.45µm filters into 30kDa MWCO ultrafiltration columns. Columns are subjected to three centrifugation steps at 4000g, and 4°C discarding the flow through and adding 20 ml of distilled water after

each centrifugation step. These steps are necessary for removing the non-metabolized ManNAZ sugars. After these steps, 500 µl of concentrated retentate are inside the column. 100 nmol Sulfo-DBCO-Biotin is diluted in PBS pH 7.0. (2µl of 50mM DBCO-Sulfo-Biotin stock diluted in 500µl of PBS pH7.0). 500µl of respective buffer with DBCO-Sulfo-Biotin is added to the retentate and incubated overnight at 4°C. At the next day, samples are subjected to three centrifugation steps at 4000g and 4°C discarding the flow through and adding 20 ml of distilled water after each centrifugation step. These centrifugations steps are necessary for removing non-reacted Peg12-DBCO-Biotin conjugates. The final retentate is diluted with 9.5 ml PBS with 2%(w/v) SDS and loaded on a polyprep column packed with 300 µl of high capacity streptavidin agarose beads. Samples are loaded on the polyprep column twice to increase binding of biotinylated glycoproteins to streptavidin beads. Afterwards, streptavidin beads are washed three times with 10 ml PBS with 2%SDS (w/v). Then, streptavidin beads are collected to Eppendorf tubes and cooked with 150µl of urea sample buffer containing 3mM Biotin (33µl of 100mM Biotin Stock is diluted in 1ml of Urea Sample Buffer) for elution of the glycoproteins. Eluted proteins are separated with 10% Tris/Glycine gel. After SDS-page, gels are subjected to coomassie staining followed by a tryptic in-gel digestion procedure for MS measurements.

2.2.13 Surface-Click Protocol

Peg12-DBCO-Biotin	(Click Chemistry Tools)
STET lysis buffer	(50mM Tris pH7.5, 150mM NaCl, 2mM EDTA, 1% Triton X)
PVDF Filters 0.45 µm	(SLHV033RS, Millex)
High capacity streptavidin agarose beads	(20361, ThermoFisher)
Polyprep Columns	(731-1550, BioRad)
Washing Buffer	(PBS+2%SDS)
Urea Sample Buffer 1X	(3.125 ml 1M Tris pH6.8, 1g SDS, 3.75 ml Glycerol, 1.25ml Mercaptoethanol, 24,024g Urea total in 50 ml)
Biotin Stock	(100mM Biotin (B4501, Sigma Aldrich) solved in DMSO (A994.2, Roth)

In parallel to media preparation, cell pellets are subjected to a biotinylation step with 100 nmol of DBCO-PEG12-Biotin (2µl of 50 mM DBCO-PEG12-Biotin stock are diluted in 1ml of PBS). Cells are incubated with 1ml PBS containing 100 nmol of Biotin conjugates for 2 hours on ice. Afterwards cells are subjected to centrifugation and washed with 1ml PBS to get rid of unreacted DBCO-Biotin conjugates. Afterwards, cells are lysed with 5ml STET lysis buffer for 15 min on ice. Next, lysates are subjected to a clarifying spin at 4000g for 5 min. Clarified lysatesare filtered with 0.45µm PVDF filters into new 15 ml Falcon tubes. From 5ml lysate, 50 µl are collected for measuring the protein concentration. The remaining lysate are mixed with 5ml of PBS+2% (w/v) SDS and mixed well. Next, each lysate is loaded on a polyprep column packed with 300 µl of high capacity streptavidin agarose beads. Samples are loaded on the polyprep columns two times to increase binding efficiency of biotinylated glycoproteins to streptavidin beads. Afterwards, streptavidin beads are washed three times with 10 ml PBS +2%SDS (w/v). Washed Streptavidin beads with bound glycoproteins are transferred to a 1.5 ml Eppendorf tube and cooked at 95°C with 150µl of urea sample buffer containing 3mM

Biotin (33µl of 100mM Biotin Stock is diluted in 1ml Urea Buffer) for elution of the glycoproteins. Eluted glycoproteins are separated with a 10% Tris/Glycine gel. After separation of glycoproteins with SDS-page, gels are subjected to coomassie staining followed by a tryptic in-gel digestion procedure for MS measurements.

2.2.14 Preparation of AML patient serum for MS measurements

G sepharose 4 fast flow	(17061801, GE healthcare)
PVDF Filters 0.45 µm	(SLHV033RS, Millex)
Vivaspin 500 filter columns	(VS0122, Sartorius)
EZ-Link Alkoxyamine-Peg4-Biotin	(26137, Thermo Scientific)
m-Phenylenediamine	(23954, Sigma Aldrich)
Sodium Periodate	(311448, Sigma Aldrich)
Labeling Buffer	(1ml PBS buffer pH 6.7 + 2,5µmol Aminooxybiotin (10µl) + 20 mM Phenylenediamine + 1mM Sodium Periodate)

Human serums are treated with G sepharose for 2 hours at 4°C on a rotary shaker. Afterwards, patient serums are centrifuged and filtered through 0.45µm PVDF filters to a fresh eppendorf tube. Afterwards samples can be subjected to western blot with Anti-human IgG antibody to detect the depletion of IgG proteins. Next, serum samples are concentrated with 30 KDa Vivaspin 500 filter columns and treated with 100µl of labelling buffer at 4°C for 1 hour. Afterwards, samples can be subjected to western blot with streptavidin-HRP to detect biotinylation reaction efficiency. Next, serum samples are incubated with 150 µl of streptavidin agarose beads on a rotary shaker for 2 hours at 4°C to catch up biotinylated glycoproteins. Afterwards, beads are washed with 500µl of PBS+2% SDS three times and cooked at 95°C with 100µl of urea sample buffer containing 3mM Biotin for elution of captured glycoproteins. Eluted proteins are separated with 10% Tris/Glycine gels and subjected to Coomassie Brilliant Blue R Staining for half an hour at room temperature. Thereafter, gels are washed with 10% acetic acid to get rid of background staining until proteins become visible on the gels. Afterwards, gels are cut into 8 gel slices excluding albumin band at around 60kDa. Every gel slices are further cut into smaller cubes around $1mm^3$ and transferred into suitable plates and tryptic gel digestion procedure is applied.

2.2.15 Tryptic in-gel Digestion (Adapted from Shevchenko et al. Nat Protoc. 2006)

96 well sterile plates	(249946, Thermo Scientific)
Ammonium Bicarbonate	(09830, Sigma Aldrich)
Chromasolv water	(39253, Sigma Aldrich)
Ammonium Bicarbonate - ABC Buffer	(100mM ABC-395mg of ABC dissolved in 50 ml Chromasolv water)
Acetonitrile-ACN	(34967, Sigma Aldrich)
Wash Solution	(50mM ABC, 40% ACN)
Dithiothreitol (DTT) buffer	(10mM DTT/100mM ABC buffer- 100µl of 1M DTT mixed in 10 ml of ABC Buffer)

Iodoacetemide (IAA) buffer	(55mM IAA/100mM ABC buffer- 102mg of IAA dissolved in 10 ml of ABC buffer)
Trypsin	(V511A, Promega)
Trypsin Buffer	(1ml of ACN, 1ml of ABC buffer and 9 ml of chromasolv water)
Extraction Buffer	(1:2, 5% Formic Acid in chromasolv water and ACN)

After coomassie staining gels are cut into 14 gel slices excluding the albumin band at around 60kDa. Then, every gel slice is cut into smaller cubes around $1mm^3$ and transferred into sterile 96 well plates. Gel cubes are subjected to 3 to 4 washing steps with wash solution until coomassie staining has vanished. Afterwards, 150µl of pure ACN are applied to gel cubes for 10 min until the become white and small. ACN is removed and50µl DTT buffer are added to shrunken gel cubes and incubated at 55°C for 30 minute. Next, samples are chilled down to room temperature and 150µl of ACN are added and incubated for 10 min to shrink the gel cubes. Solvents are removed andgel pieces are covered with IAA buffer and incubated in the dark for 20 minute at room temperature. Afterwards gel pieces are consecutively incubated with 150 µl ACN for 10 min,150 µl ABC buffer for 10 min and 150 µl ACN for 10 min removing all liquids after each incubation step to get rid of remaining DTT and IAA buffer. Finally, gel cubes are subjected to trypsination. To each sample, 150 ng of trypsin in 100 µl trypsin buffer are added in two consecutive 50 µl portions on ice waiting 30 min and 1 hour for the first and for the second portion to be absorbed by the gel cubes. Before addition of the second portion, wait until the first portion is fully absorbed by the gel cubes Finally enough ABC buffer is added to cover the gel pieces andsamples are incubated overnight at 37°C. At the next morning extraction buffer is prepared freshly. Gel pieces are incubated with 100µl of extraction buffer for 15 min and peptides are transferred to respective vials. These extraction steps are repeated until the gels pieces are completely shrunken. Afterwards peptides are dried with a speed vac and stored at -20°C until MS measurements.

2.2.16 Mass Spectrometric Measurements

LTQ-Velos Pro Orbitrap	(Thermo Fisher Scientific)
Liquid Chromatography	(UHPLC, Proxeon)
30 cm Columns	(New objective, FS360-75-8-N-S-C30, Woburn, MA, US)
C18 Resin	(ReproSil-Pur 120 C18-AQ, 1.9µm, Dr. Maisch, Germany)
Nanoflex Ionsource	(Thermo Fisher Scientific, US)
Column Oven	(PRSO-V1, Sonation, Germany)

Samples are analysed with an LTQ-Velos Pro Orbitrap coupled to an Easy nLC 100 nano ultrahigh performance liquid chromatography system equipped with a 30 cm column packed with C18 resin for reverse phase separation of peptides. A 75 min binary gradient of water (A) and acetonitrile (B) supplemented with 0.1% formic acid heated to 50°C by a column oven is used (0 min., 8% B; 50 min., 25% B; 70 min., 42% B; 71 min., 95% B; 75 min., 95% B). A Nanoflex ionsource equipped is used for peptide ionization. The MS acquisition method consisted of an initial FTMS scan recorded in profile mode with a resolution of 60,000, a mass range from

300 to 1400 m/z and a target value of 1,000,000. Subsequently, the 10 most intense peptide ions per Full MS scan are chosen for collision-induced dissociation (CID) within the ion trap. An isolation width of 2 m/z and a normalized collision energy of 35% with 10 ms activation time as well as wide band activation is used. A dynamic exclusion of 60 s is applied.

2.2.17 Data analysis and Statistical Analysis of MS results

Max Quant version 1.5.3.12 is used for analysing acquired data. A UniProt database of Homo sapiens released at 2016/01/12 is used for protein identification. The following settings are used in MaxQuant: Trypsin/P digestion mode, the number of missed cleavages is set to 2. Peptide modification is set to maximum of 5. N- terminal acetylation and oxidation of methionines are set as variable modifications. Label-free quantification (LFQ) and intensity based absolute quantification (iBAQ) algorithms are used for quantification between and within samples respectively. For LFQ quantification at least 2 ratio counts of razor and unique peptides are set. Peptide and protein false discovery rate is set to 0.01. The first search option peptide tolerance is set to 20 ppm. The main search peptide tolerances is set to 4.5 ppm. The proteingroup output file is processed for data analysis with Perseus version 1.5.3.1. Missing values are imputed with standard distribution. P-values are calculated from $\log_2$ transformed LFQ intensities. For statistical significance analysis a two-sided heteroscedastic t-test is applied. Threshold for significance is determined as p-value of 0.05.

For SPECS optimizations experiments, in the Max Quant analysis normalization is skipped to get LFQ intensities that depend on non-normalized peptide intensities.

For AML cell line profile analysis, after the Max Quant analysis, the proteingroup output file is processed for data analysis. LFQ intensities are averaged from 6 technical replicates of each protein present in each cell line. Afterwards, every corrected LFQ value is divided by the present maximum value to get a heat map. Maximum expression is shown in red and value 1 while minimum expression is shown in blue and value 0. Perseus vesion 1.5.3.1 is used for cluster analysis.

2.3 Methods for DNA Preparations

2.3.1 Oligonucleotides

Oligonucleotides are obtained from Sigma Aldrich. Oligonucleotides are solubilized in ddH_2O to a concentration of 100µM and stored at -20°C for further usage. Following oligonucleotides are used in the experiments.:

Oligonucleotide Name	Sequence	#
FLT3 genomic sgRNA01/02 seq fw	TTCAGTCGGCAACGTGTTCT	1
FLT3 genomic sgRNA01/02 seq rev	AGGGAGCTGTGCTTAAAGACC	2
FLT3 genomic sgRNA03 seq fw	TGGACAGCCCTGCTCTAAGTA	3
FLT3_genomic sgRNA03 seq rev	AGCCAAAGTTTCCTGTTTAAATGA	4
FLT3 genomic sgRNA04 seq fw	TGGACAGCCCTGCTCTAAGTA	5
FLT3 genomic sgRNA04 seq rev	TTGAAGGAATGGAGTGCCAGG	6
sgRNA-FLT3-1-f	CGCGGAGCGCACACCCGAGGTCTTCCG	7
sgRNA-FLT3-1-r	CTCGCGTGTGGGCTCCAGAAGGCCAAA	8
sgRNA-FLT3-2-f	CGCGGAGGGGGTCTCAACGCACACCCG	9
sgRNA-FLT3-2-r	CTCCCCCAGAGTTGCGTGTGGGCCAAA	10

sgRNA-FLT3-3-f	CGCGGAGGAGCGTTCCAGAGCCGATCG	11
sgRNA-FLT3-3-r	CTCCTCGCAAGGTCTCGGCTAGCCAAA	12
sgRNA-FLT3-4-f	CGCGGAGAGAACAATGATTCATCAGTG	13
sgRNA-FLT3-4-r	CTCTCTTGTTACTAAGTAGTCACCAAA	14
sgRNA-KIT-1-f	GCGGAGGCTTTGGACACAGACACAAC	15
sgRNA-KIT-1-r	CTCCGAAACCTGTGTCTGTGTTGCAAA	16
sgRNA-KIT-2-f	CGCGGAGGCAAGCTATCTTCTTAGGGA	17
sgRNA-KIT-2-r	CTCCGTTCGATAGAAGAATCCCTCAAA	18
sgRNA-KIT-3-f	CGCGGAGGTCACTTCTGGGTCTGTGAG	19
sgRNA-KIT-3-r	CTCCAGTGAAGACCCAGACACTCCAAA	20
sgRNA-KIT-4-f	CGCGGAGGCCTAATCTCGTCGCCCACG	21
sgRNA-KIT-4-r	CTCCGGATTAGAGCAGCGGGTGCCAAA	22
c-kit genomic sgRNA01/02 seq fw	GAGGGGCCACATTTCTTTTCA	23
c-kitgenmoic sgRNA01/02 seq rev	GCAATCCCAACACTCTCCCA	24
c-kit genomic sgRNA03 seq fw	GTCACTTTAGGAGGGTTGCTTTT	25
c-kit genomic sgRNA03 seq rev	CTCAACTCCCAGAGGCAGAT	26
c-kit genomic sgRNA04 seq fw	CATTCAGCACATCCTGGCTTG	27
KITLG_LHA_fw_primer	TCAGGAGCAGGAGGATCATCGGATGAAGGGATCTGCAGGAAT	28
KITLG_RHA_rev_primer	CAAGCCTAACGAGGAGGAGAGGATGGCTGCAACAGGGGGTAA	29
FLT3L_fw_LHA_primer	TCAGGAGCAGGAGGATCATCGGATACCCAGGACTGCTCCTTCC	30
FLT3L_rev_RHA_primer	CAAGCCTAACGAGGAGGAGAGGATGGGCTGCGGGGCTGTCGGGGC	31
VEGFA_LHA_fw_primer	TCAGGAGCAGGAGGATCATCGGATGCACCCATGGCAGAAGGAGGAGGGCAGAATCATC	32
VEGFA_RHA_rev_primer	CAAGCCTAACGAGGAGGAGAGGATCCGCCTCGGCTTGTCACATCTGCAAGTACGTTCGTTTAA	33
IGF1_LHA_fw_primer	TCAGGAGCAGGAGGATCATCGGATGGACCGGAGACGCTCTGCGGG	34
IGF1_RHA_rev_primer	CAAGCCTAACGAGGAGGAGAGGATAGCTGACTTGGCAGGCTTGAG	35
IGF2_LHA_fw_primer	TCAGGAGCAGGAGGATCATCGGATGCTTACCGCCCCAGTGAGACC	36
IGF2_RHA_rev_primer	CAAGCCTAACGAGGAGGAGAGGATCTCGGACTTGGCGGGGGTAGC	37
EGF_fw_LHA_ primer	TCAGGAGCAGGAGGATCATCGGATAATAGTGACTCTGAATGTCCCCTGTC	38
EGF_rw_RHA_ primer	CAAGCCTAACGAGGAGGAGAGGATGCGCAGTTCCCACCACTTCAG	39
FGF_LHA_fw_primer	TCAGGAGCAGGAGGATCATCGGATCCCGCCTTGCCCGAGG	40
FGF_RHA_rev_primer	CAAGCCTAACGAGGAGGAGAGGATGCTCTTAGCAGACATTGGAAGAAAAAGTATAGCTTTCTGCCCAGG	41
VEGFC_LHA_fw_primer	TCAGGAGCAGGAGGATCATCGGATGCACATTATAATACAGAGATC	42
VEGFC_RHA_rev_primer	CAAGCCTAACGAGGAGGAGAGGATACGTCTAATAATGGAATGAAC	43
VEGFD_LHA_fw_primer	TCAGGAGCAGGAGGATCATCGGATTTTGCGGCAACTTTCTATGAC	44
VEGFD_RHA_rev_primer	CAAGCCTAACGAGGAGGAGAGGATTCTTCTGATAATTGAGTATGG	45
WPRE_rev_primer	GGCATTAAAGCAGCGTATCC	46
U6_fw_Kuhn	CCTTCACCGAGGGCCTATTTCC	47

Table 8. Oligonucleotides

2.3.2 Plasmid Constructs

Commercial Plasmids used in this thesis:

pAL119-FLT3L	(21910, Addgene)
pFLCIII-Fm-VEGFA	(H05D018B04, Source Bioscience)
pFLCI-Fm-KITLG	(H023063I15, Source Bioscience)
pENTR22B.1-IGF1	(IOH58981, Source Bioscience)
pENTR221-IGF2	(IOH13185, Source Bioscience)
pcR4-TOPO-EGF	(7939576, Source Bioscience)
pWD1SPb-FGF	(25812, Addgene)
pCMV-Sport6-VEGFC	(3901717, Source Bioscience)
pCMV-Sport6-VEGFD	(5202065, Source Bioscience)

lentiCas9-blast (52962, Addgene)

2.3.3 In-Slico Design and Manipulations

Vector NTI Advance 11 is used for designing and manipulations of the plasmids and PCR products in silico.

2.3.4 Polymerase Chain Reaction (PCR)

Taq DNA polymerase (M0267L, NEB)
10x ThermoPol Reaction Buffer (M0267L, NEB)
Primers (100µM)
Tamplate DNA (100-200ng)
dNTPs (13412421, Roche)
Thermocycler (Eppendorf)
For amplification of DNA fragments, standard PCR set up is used as follows:

Thermo Pol Reaction Buffer	5µl
Taq DNA Polymerase	0.5µl
Forward Primer	0.4µl
Reverse Primer	0.4µl
dNTPs	1µl
Tamplate (100ng-200ng/µl)	1µl
Total	50µl

Table 9. PCR reaction set-up.

Tubes are placed to thermocycler and typical programme is used as following:

3min at 95°C	for initial denaturing
30 sec at 95°C	for denaturing the DNA in the cycle (x30)
30 sec at 52-60°C	for annealing of the primers in the cycle (x30)
15 sec 300 sec at 72°C	for extension of the products in the cycle (x30)
2-5 min at 72°C	for final extension

Table 10. PCR scheme with thermo-cycler.

Annealing temperature is adjusted according to calculated annealing temperature using Primer 3 plus. Extension step is depending on the PCR product length and polymerase fidelity (1000bp per 60 sec for Taq DNA Polymerase, 750 bp per 60 sec for PWO DNA Polymerase)

2.3.5 Restriction Digest

Restriction enzymes are provided from New England Biolabs (NEB). For selection of the optimal buffer for digests with two restriction enzymes, double digest finder on NEB website is used. Standard set up for restriction digest is designed as follows:

Plasmid or PCR fragments (1µg/µl)	1µl
Restriction enzyme 1 (10U/µl)	0.5µl
Restriction enzyme 2 (10U/µl)	0.5µl
Restriction enzyme buffer (10x)	1µl
ddH_2O	17µl

Total	20µl

Table 11. Set-up of a restriction digest.

Restriction digest tubes are generally incubated at 37°C for 1 hour. Different restriction enzymes require different optimal expression temperature and incubation times. Hence, enzymes should be used according the instructions of the manufacturer.

2.3.6 DNA agarose gel electrophoresis

DNA sample buffer 4x	(30% Glycerol, 10mM EDTA (EDS, Sigma), 0.05% Orange G (3756, Sigma Aldrich), water =50ml)
TAE buffer	(40mM Tris, 20mM Acetic Acid, 1mM EDTA)
Agarose	(840004, Biozyme)
Gel Red	(S420, Biotium)
DNA size marker	(D3937, Sigma Aldrich)
Power Supply	(Pac300, Biorad)
Chamber	(Biorad)
Fluorescence Imaging	(Vilber)
Printer	(P95, Mitsubishi)

Separation of DNA is performed with TAE agarose gel electrophoresis. According to the DNA size, proper agarose (0.5-1.5%) amounts are cooked with TAE buffer. Typically, if the DNA fragment is shorter than 500 bp, agarose gel concentration is set to 1.5% for better separation. Agarose powder iscooked in TAE buffer until the agarose is completely dissolved. Hot agarose gel solution is transferred to a running chamber and gel red is mixed at a ratio of 1/10000. Aftergel solidification, DNA samples are diluted with 4X DNA sample buffer and loaded into the gel wells. DNA sample buffer assists sample loading and visualization. Afterwards, DNA samples are separated at 100V for 30-45 min. After electrophoresis, DNA bands are visualized under UV light, photos and digital picture are taken for documentation and desired DNA bands are cut out for further processing.

2.3.7 DNA Extraction from the Gel

After gel electrophoresis, desired DNA bands are cut with asterile scalpel and collected in a corresponding Eppendorf tube. Afterwards, the gel and PCR clean up kit (740609.240c, Macherey-Nagel) is used according the instruction of the manufacturer. Typical, clean-up process is applied as follows:

400-500µl of the binding buffer are added to the gel piece and incubated at 50°C for 5-10 min. Dissolved samples are loaded on a spin column and centrifuged at 14.000g for 1 min. Flow through is discarded and 600µl wash solution are added and centrifuged at 14.000 g for 1min. Next, the flow through is discarded and spin columns are centrifuged at 2min for drying the membranes. Than 30-50µl of the elution buffer are added directly to the filter and and the filter column is transferred to a fresh 1.5ml Eppendorf tube. Afterwards samples are centrifuged at 10.000g for 2 min. Finally, samples can be stored at -20°C until further processing.

2.3.8 DNA ligation

T4 DNA ligase enzyme is used for ligation of PCR fragments or designed oligos into suitable plasmids. Critical part of the ligation is vector length and DNA fragment length ratio which should be considered for the ligation reaction. Molar ratio between vector and backbone should be around 1 to 5. Typical calculations and DNA ligation mixture is done as follows:

$Mass_{fragment}$ [ng] = 5x mass vector [ng] x $length_{fragment}$ [bp]/ $length_{vector}$ [bp]

Vector- Plasmid digested with restriction enzymes	Cal
Insert- PCR fragments or digested DNA	Cal
T4 DNA ligase buffer x10	2 µl
T4 DNA ligase (NEB)	1µl
ddH_2O	Final 20µl

Table 12. Set-up of a DNA ligation reaction.

2.3.9 Gibson Assembly (adapted from New England Biolab Protocol)

Nicotine Amide Adenine Dinucleotide-NAD (N7004-1G, Sigma Aldrich)
Phusion DNA polymerase (M0530S, NEB)
T5 exonuclease (M0363S, NEB)
Taq DNA ligase (M0208L, NEB)

5x Final Isothermal rxn Buffer	Amount	Stock Concentrations
25% PEG-8000	0.75 g	Powder
500 mM Tris/HCL pH7.5	1500 µl	1M
50 mM $MgCl_2$	75 µl	2M
50 mM DTT	150 µl	1M
4mM (dNTP mix)	120 µl	100mM
5mM NAD	300 µl	50 mM
ddH_2O	Take up to 3 ml total volume	

Final 2X Gibson Master Mix	250 µl Volume	1000 µl Volume
5X Isothermal Buffer	100 µl	400µl
T5 Exonuclease 1.0 U/µl	2 µl	8 µl
Phusion DNA polymerase 2U/µl	6.25 µl	25 µl
Taq DNA ligase 40U/µl	50 µl	200 µl
ddH_2O	141.75 µl	367 µl

Set up the following reactions on ice:

	Recommended Amount of Fragments	
	2-3 Fragment Assembly	4-6 Fragment Assembly
Total Amount of Fragments	0.02-0.5 pmols	0.2-1 pmols
Gibson Assembly Master Mix 2X	10µl	10 µl
ddH_2O	total 20 µl	total 20 µl

Table 13. Gibson assembly mix and reaction set-up.

Optimized cloning efficiency is achieved with 50-100ng of vectors with 2-3-fold excess of insert. Use 5 times more of insert if the insert size is less than 200 bps.

Incubate the samples in a thermocycler at 50°C for 15 minutes for 2 or 3 fragments. Afterwards transform NEB 5-alpha component E.coli cells with 2µl of the assembly reaction, following the transformation protocol.

Plasmid #11 is subjected to an EcoRV restriction digest. Linearized vector is loaded on a TAE agarose gel and extracted from the gel. According to plasmid backbone size and insert size gibson assembly reaction is set up according to the instructions of the NEB protocol.

2.3.10 Transformation of the Plasmids

Luria Broth	(L3397, Sigma Aldrich)
Luria Broth-Agar	(L3272, Sigma Aldrich)
Incubator Shaker	(Infors HT or Innova40)
Thermoshaker	(Thermomixer C, Eppendorf)

Within the context of this thesis the following bacterial strains are used for transformation procedure: 5-alpha Component E. coli -High Efficiency (C2987, NEB), DH5-alpha bacteria. Component bacteria are thawed on ice for 10 minutes. 20µl-60µl of component bacteria are transferred to fresh tube and 10-100 ng of plasmid are added and component bacteria are incubated on ice for 30 min. Afterwards, a 30 second heat shock is applied at 42°C. Next, transformed bacteria are placed on ice for 5 minutes. 950 µl of SOC medium or luria broth without antibiotics are added to the transformed bacteria and incubated at 37°C and 250 rpm on a thermoshaker. 150µl of bacteria solution are evenly distributed on a Luria Broth agar plate with the necessary antibiotic (such as ampicillin 100µg/ml) for selection. Afterwards, plates are incubated at 37°C overnight. The following day different single colonies are picked and subjected to small scale production at 37°C and extraction of the plasmids (mini-prep)

2.3.11 Mini Prep- Small Scale Plasmid Production

Luria Broth	(L3397, Sigma Aldrich)
Incubator Shaker	(Infors HT or Innova40)
Ampicillin	(9393, Sigma Aldrich)
Mini-Prep Kit	(740588.250, Macherey-Nagel)

A single bacterial colony is transferred to a 15 ml falcon tube with 5 ml of Luria Broth (LB) supplemented with a suitable antibiotic adapted to the plasmid coded resistance (e.g. 100 µg/ml of ampicillin). The falcon tube is incubated at 37°C and 300 rpm in a shaker incubator overnight. The next day, bacterial cultures are centrifuged down at 4600 rpm for 10 min. LB media are discarded and plasmid DNA is extracted from the bacteria mini-prep kit according to the instructions of the manufacturer. A typical small-scale plasmid extraction procedure comprises of the following steps:

250 µl of resuspension buffer (includes RNase) are applied to the bacterial pallet. Then 250 µl of lysis buffer are added and incubated for 5 min at room temperature until the bacteria are

lysed. Afterwards 300µl of neutralizing buffer are added and mixed until a white precipitate forms in the solution. Samples are centrifuged at 11.000g for 5 minutes to clarify the sample from the white precipitate. Next clarified supernatants are loaded on a silica membrane DNA trap column and centrifuged at 11.000g for 1 min. The resulting flow through is discarded, 600 µl of wash solution are added to the DNA trap column and centrifuged at 11.000g for 1 min. After discarding the wash buffer flow through, the silica membranes of the DNA trap column are dried centrifuging the columns at 11.000 g for 2 min. Finally, 35-50 µl of elution buffer are carefully added to the silica membrane, incubated for 1 min at room temperature and finally centrifuged at 11.000g for 1 minute. Eluted plasmids are stored at 4°C for short term storage and at -20°C for long term storage.

2.3.12 Sequence Verifications

After the mini-prep, 1 µg of the DNA is send to a company such as GATC, Konstanz for sequencing. Sequences are provided by the company within 2-3 working days. Sequencing data are compared to in silico generated data with Vector NTI Advance 11 programme with the alignment function.

2.3.13 Midi Prep- Large Scale Plasmid Production

Luria Broth	(L3397, Sigma Aldrich)
Incubator Shaker	(Infors HT or Innova40)
Ampicillin	(9393, Sigma Aldrich)
Midi-prep kit	(740412.50, Macherey- Nagel)

After sequence verification, correct clones of plasmids are subjected to large scale production. Plasmids are again transformed to DH5alpha bacteria and propagated in 250 ml of Luria broth (LB) medium supplemented with a suitable antibiotic adapted to the plasmid coded resistance (e.g. 100 µg/ml of ampicillin) at 37°C and 300 rpm shaking overnight. The next day, the bacterial solution is transferred to big falcon tubes and centrifuged at 6000 rpm. Afterwards media are discarded and the bacterial pellet is processed according the midi-prep plasmid extraction protocol of the manufacturer. Typical midi prep plasmid extraction procedure comprises of the following steps:

The bacterial pellet is resuspended in 8 ml of resuspension buffer (includes RNase) using a serological pipet. Then 8 ml of lysis buffer are added incubated for 5 minutes at room temperature. During lysis incubation time, DNA trap column with a filter inset is placed into a suitable midi-prep rack to be equilibrated by the addition of 12 ml equilibration buffer into the filter inset. 8 ml of neutralizing buffer are added to the lysed bacteria sample and mixed until a white precipitate forms. Next, samples are loaded onto the equilibrated filter inset DNA trap column combination. After passage of the sample through the DNA trap column, 5 ml of equilibration buffer are loaded onto the filter inset to elute remaining DNA. Next, the filter inset is discarded and 8 ml wash buffer are applied to the DNA trap column. Next, a 50 ml of falcon tube is placed under the DNA trap column and 5 ml of elution buffer are filled into the column to elute trapped DNA. After flow through of elution buffer, the DNA trap column is discarded and 3.5 ml of isopropanol are applied to the DNA containing flow through

and centrifuged at 4000g for 30 min. After centrifugation a whitish DNA pellet should be visible at the bottom of the falcon. Elution buffer with isopropanol is discarded without disturbing the DNA pellet, 2 ml of 70% Ethanol are added to wash the pellet. The pellet is carefully transferred to a fresh 2 ml eppendorf tube and centrifuged at14.000g for 5 min to pellet the DNA. Afterwards, ethanol is removed and the pellet is dried until it becomes slightly translucent. For reconstitution of the DNA, 500µl of ddH_2O are added and incubated for 2 hours at 4°C to be resuspended. Afterwards, purified plasmid DNA is stored at -20°C.

2.3.14 Plasmids are cloned and used

Plasmid Name	#	Insert	Backbone	RE	Template	Oligo1	Oligo2
pAL119-FLT3L	1	-	-	-	-	-	-
pFLCI-Fm-KITLG	2	-	-	-	-	-	-
pFLCIII-Fm-VEGFA	3	-	-	-	-	-	-
pCMV-Sport6-VEGFC	4	-	-	-	-	-	-
pCMV-Sport6-VEGFD	5	-	-	-	-	-	-
pENTR22B.1-IGF1	6	-	-	-	-	-	-
pENTR221-IGF2	7	-	-	-	-	-	-
pcR4-TOPO-EGF	8	-	-	-	-	-	-
pWD1SPb-FGF	9	-	-	-	-	-	-
lentiCas9-blast	10	-	-	-	-	-	-
F2KP-5XUAS-E1B-CD5-SLIC-BAP-HIS	11	-	-	-	-	-	-
F2KP-5XUAS-E1B-CD5-SLIC-BAP-HIS-FLT3L	12	FLT3	11	EcoRV	1	30	31
F2KP-5XUAS-E1B-CD5-SLIC-BAP-HIS-KITLG	13	KITLG	11	EcoRV	2	28	29
F2KP-5XUAS-E1B-CD5-SLIC-BAP-HIS-VEGFA	14	VEGFA	11	EcoRV	3	32	33
F2KP-5XUAS-E1B-CD5-SLIC-BAP-HIS-VEGFC	15	VEGFC	11	EcoRV	4	42	43
F2KP-5XUAS-E1B-CD5-SLIC-BAP-HIS-VEGFD	16	VEGFD	11	EcoRV	5	44	45
F2KP-5XUAS-E1B-CD5-SLIC-BAP-HIS-IGF1	17	IGF1	11	EcoRV	6	34	35
F2KP-5XUAS-E1B-CD5-SLIC-BAP-HIS-IGF2	18	IGF2	11	EcoRV	7	36	37
F2KP-5XUAS-E1B-CD5-SLIC-BAP-HIS-EGF	19	EGF	11	EcoRV	8	38	39
F2KP-5XUAS-E1B-CD5-SLIC-BAP-HIS-FGF	20	FGF	11	EcoRV	9	40	41
pLKO2mod-EGFP-WPRE-CRISPR-sgRNA	21	-	-	-	-	-	-
pLKO2mod-EGFP-WPRE-CRISPR-sgRNA-FLT3-I	22	sgrna-FLT3-I	21	BspMI	-	7	8
pLKO2mod-EGFP-WPRE-CRISPR-sgRNA-FLT3-II	23	sgrna-FLT3-II	21	BspMI	-	9	10
pLKO2mod-EGFP-WPRE-CRISPR-sgRNA-FLT3-III	24	sgrna-FLT3-III	21	BspMI	-	11	12
pLKO2mod-EGFP-WPRE-CRISPR-sgRNA-FLT3-IV	25	sgrna-FLT3-IV	21	BspMI	-	13	14
pLKO2mod-EGFP-WPRE-CRISPR-sgRNA-KIT-I	26	sgrna-KIT-I	21	BspMI	-	15	16
pLKO2mod-EGFP-WPRE-CRISPR-sgRNA-KIT-II	27	sgrna-KIT-II	21	BspMI	-	17	18
pLKO2mod-EGFP-WPRE-CRISPR-sgRNA-KIT-III	28	sgrna-KIT-III	21	BspMI	-	19	20
pLKO2mod-EGFP-WPRE-CRISPR-sgRNA-KIT-IV	29	sgrna-KIT-IV	21	BspMI	-	21	22

Table 14. Plasmids are cloned and used.

2.3.15 Liposomal plasmid transfection of eukaryotic cells

Lipofectamine 2000	(52887, Invitrogen)
Optimem	(51985, Gibco)
DNA	(Plasmid Vector)

Lipofectamine 2000 and DNA are mixed in a 3:1 ratio (e.g. 1,5 µl Lipofectamine for 0.5 µg DNA, see table) Lipofectamine 2000 is diluted in Optimem without antibiotics and incubated for 5 min. In parallel, DNA is diluted in an equal amount of Optimem and incubated for 5 min. Afterwards, lipofectamine containing medium and DNA containing medium are mixed and incubated for 15 minutes. Finally, the mixture is added to 70% confluent cells without any antibiotics. Generally, after 1-2 day, cells are ready for further processing.

Component	96-well	24-well	6-well
Final DNA per well	100ng	500ng	2500ng
Lipo2000 per well	0.2-0.5 µl	1-2.5 µl	5-12.5µl
Optimem per well	125µl	250µl	700µl

Table 15. Liposomal transfection set-up.

2.3.16 Small scale lentivirus production

Lipofectamine 2000	(52887, Invitrogen)
Plasmid Vectors	(pCMV/psPAX2, pcDNA3.1/VSV-G and transfer vector)
Transfection Medium	(Optimem, 10% FCS)
Packaging Medium	(DMEM, 10%FCS, NEAA, Pyruvate)
PVDF Filters 0.45 µm	(SLHV033RS, Millex)
5 ml, 50 ml syringes	(Terumo)

HEK 293T cells with a low passage number and 70% confluency are optimal for transfection. 1.9 million of HEK cells are added into a 6 well dishe. Transfer vector (1.3µg), psPAX2 (0.83µg) and VSV-G (0.45 µg) are diluted in 125µl of optimem. In parallel, 6.3µl of Lipofectamine 2000 are diluted in 125µl of optimum. Both mixtures are incubated for 5 min at room temperature. Afterwards DNA and Lipofectamine 2000 containing media are mixed gently and incubated for 15 min. Afterwards, the transfection mixture is applied to the HEK cells and incubated overnight. The next day, the transfection medium is discarded and 1.5 ml packaging medium are carefully added to the HEK cells and incubated one day. The following day, the packaging medium contains virus particles. The medium is collected and filtered through a 0.45 µm filter and used for the transduction of the desired target cells.

2.3.17 Large scale lentivirus production

Lipofectamin 2000	(52887, Invitrogen)
Plasmid Vectors	(pCMV/psPAX2, pcDNA3.1/VSV-G and transfer vector)
Transfection Medium	(Optimem, 10% FCS)
Packaging Medium	(DMEM, 10% FCS, 1% NEAA, Pyruvate)
PVDF Filters 0.45 µm	(SLHV033RS, Millex)
5 ml, 50 ml syringes	(Terumo)

9 million HEK cells each are seeded to four 10 cm dish. 31µg of transfer vector, 20µg of psPAX2 and 11µg of VSV-G are diluted in 1.5 ml of optimem. In parallel to that 152µl of lipofectamine 2000 are diluted in 1.5 ml of optimem and incubated for 5 min at room temperature. Afterwards, DNA and lipofectamine containing samples are mixed gently and incubated for 15 min. Afterwards, 750 µl of transfection mixture are added to each of the four 10 cm dishes and incubated overnight. The following day, transfection media are replaced by 8.5 ml of packaging medium per 10 cm dish and incubated one more day. The following day, packaging medium is collected and filtered through a 0.45 µm filter (Millex) into a fresh 50 ml falcon tube. Lentivirus particle containing packaging media can be used for transduction of desired target cells or applied to a lentivirus purification.

2.3.18 Lentivirus purification with PEG precipitation (adapted from US9,005,888 B2)

PEG-8000	(81268, Sigma Aldrich)
PBS buffer	(136mM NaCl, 12mM Na_2PO_4, 1 mM KH_2PO_4, 2mM KCl, pH7.4)
PVDF Filters 0.45 µm	(SLHV033RS, Millex)
TBS-5/BSA buffer	(50mM Tris-HCL pH7.8, 130mM NaCl, 10mM KCl, 5mM $MgCl_2$)

500 mg/ml PEG-8000 is dissolved in PBS buffer and filtered through a 0.45µm PVDF filter to a fresh falcon tube. After large scale lentivirus production, filtered packaging medium is mixed with filtered PEG virus precipitation solution. (1 volume of cold PEG solution to every 4 volumes of lentivector containing supernatant. (e.g.5 ml PEG solution and 20 ml viral supernatant). The mixture is incubated at 4°C overnight. The next morning, supernatant/PEG mixture is centrifuged at 1500g for 30 min at 4°C. After centrifugation, lentivirus particles appear as a white pellet at the bottom of the vessel. Next, supernatant is transferred to a fresh tube and centrifuged at 1500g for 5 min to centrifuge residual virus particles. Supernatants are carefully entirely removed without disturbing the virus pellet and 250 µl TBS5/BSA are added to the virus pellets, incubated for 2 hours in the fridge and afterwards resuspended. Afterwards, lentiviral particle containing buffers are aliquoted into cryogenic vials and stored at -70°C until usage.

2.3.19 Lentiviral transduction of eukaryotic cells

Typically, $0.5x10^6$ of HEK cells or AML cells are placed into a 6-well plate and lentiviral particle containing packaging medium is directly added to the cells for making stable cell lines. Alternatively, purified virus stocks can be directly added to the cells. Potency of the purified virus particles can be tested by the addition of different virus amountsto the same number of cells. The next day, lentivirus containing medium is exchanged for regular growth medium. After 2-3 days later cells are ready for selection (example: Blasticidine) or fluorescent visualizations (example: GFP)

2.4 CRISPR

2.4.1 CRISPR sgRNA Design

sgRNAs are designed from crispr.mit.edu server (Zhang lab). KIT and FLT3 exon regions are uploaded to the server and suitable guides (sgRNA) are designed. Next, 8 sgRNA were sublconed into a lentiviral plasmid under the control of a U6 promoter and with a GFP fluoresecent reporter. Plasmid #21 was cut with BspMI restriction enzyme and with the agarose gel running cut site was separated from the backbone. Afterwards backbone was extracted from the gel. In parallel to that oligonucleotides #7-22, contains guide RNAs and BspMI related flanking were annealed with each other with thermo-cycler. Corresponding oligonucleotides were placed in a PCR tube and starting from the 95°C every second 1°C were decreased and reached 25°C. Afterwards oligonucleotides were ligated to backbone of the Plasmid #21 finally Plasmid #22-29 were generated (Fig.6)

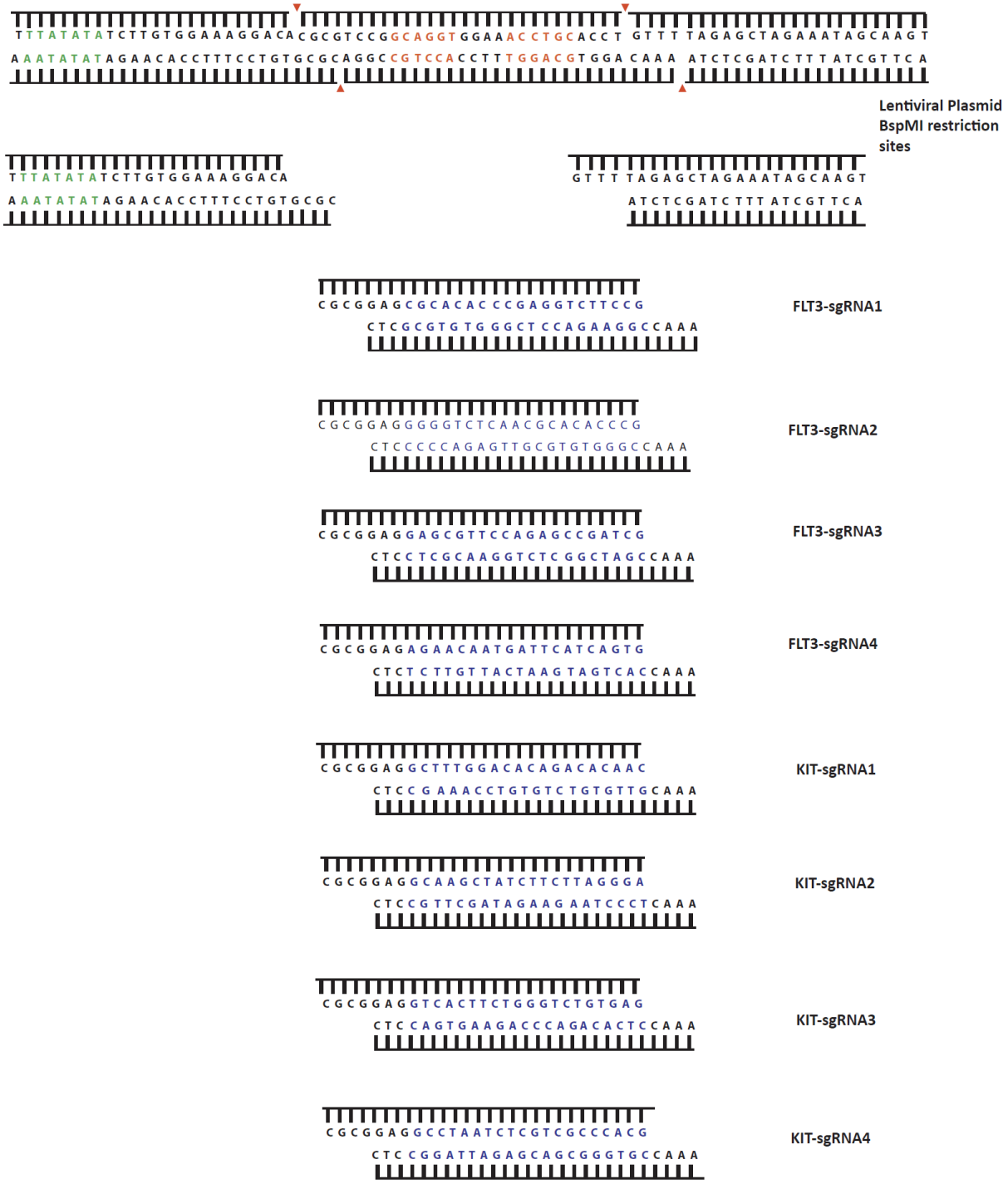

Figure 6. Preparation of lentiviral plasmids that includes sgRNAs for CRISPR-Cas9 system. Recognition site of BspMI shown in red and cut sites shown in red triangles. Guide RNAs for FLT3 and KIT shown in blue colour and placed under the lentiviral plasmid. TATA box shown in green colour.

2.4.2 Genomic DNA isolation

Tail Lysis Buffer	(100mM Tris pH8.5, 5mM EDTA, 0.2% SDS, 200mM NaCl,100µg/ml Proteinase K)
Isopropanol	(818766, Merck)
Ethanol	(818760, Merck)
Thermo Mixer C	(Eppendorf)
Centrifuge	(5417R, Eppendorf)

Equal numbers (e.g. 2-3x10^6) of cells are cultured (WT vs KO) in the six well plate format for 1-2 days. Next, cells are collected and lysed with 500 µl of tail lysis buffer per well. Samples are incubated overnight at 55°C and 650 rpm overnight in a thermocycler. The following day, samples are centrifuged at V_{max} (e.g. 16000 g) for 5 min in an uncooled table top centrifuge. Next, supernatants are transferred to fresh 1.5 ml Eppendorf tubes. 400µl of isopropanol are added to the samples and mixed well until a white DNA precipitate becomes visible. Afterwards, samples are centrifuged 20 min at 14000g and RT. After centrifugation, the supernatant is discarded,500µl of 70% ice-cold ethanol are added to the genomic DNA pellet for washing and the samples are centrifuged for 5 min at 14000g. Afterwards, ethanol is removed and the genomic DNA pellets are dried at 55°C. For reconstitution, 200µl of ddH_2O is used and incubated at 55°C, 750 rpm for 30 min. Samples are stored at -20°C.

2.4.3 T7 Endonuclease Assay (Adapted from Joung's lab)

T7 endonuclease I	(M0302, NEB)
NEBuffer-2	(B7002, NEB)
Thermocycler	(Eppendorf)
DNA sample buffer 4x	(30% Glycerol, 10mM EDTA (EDS, Sigma), 0.05% Orange G (3756, Sigma Aldrich), water =50ml)
Fluorescence Imaging	(Vilber)

Genomic DNA samples are subjected to PCR amplification of the target site. Target sequences are between 300-600 bp long and after the PCR, samples are loaded on an agarose gel run and appropriate bands are cut out and subjected to a gel extraction procedure. After gel extraction of DNA, its concentration is measured with a nanodrop (Thermo Scientific).

400 ng of purified PCR product and 2 µl of NEBuffer-2 and ddH_2O to a total of 19 µl are mixed in a PCR tube. Afterwards, samples are placed in a thermocycler and a hybridization reaction is performed comprising a 95°C incubation step for 5 min followed by chilling at a rate of 2 degree/sec until 85°C and 1 degree/sec until 10°C. Afterwards, 1µl of T7 endonuclease is added to each reaction tubes and incubated at 37°C for 30 min. Sample are mixed with4X DNA sample buffer and loaded on a 1.5% agarose gel. After running of the DNA samples DNA is visualized by a fluorescence imaging system.

2.5 Generated Cell Lines

Cell line	Construct	Target Cell
HEK293T-BAP-HIS-FLT3L	F2KP-5XUAS-E1B-CD5-SLIC-BAP-HIS-FLT3L	HEK293T
HEK293T-BAP-HIS-KITLG	F2KP-5XUAS-E1B-CD5-SLIC-BAP-HIS-KITLG	HEK293T
HEK293T-BAP-HIS-VEGFA	F2KP-5XUAS-E1B-CD5-SLIC-BAP-HIS-VEGFA	HEK293T

HEK293T-BAP-HIS-VEGFC	F2KP-5XUAS-E1B-CD5-SLIC-BAP-HIS-VEGFC	HEK293T
HEK293T-BAP-HIS-VEGFD	F2KP-5XUAS-E1B-CD5-SLIC-BAP-HIS-VEGFD	HEK293T
HEK293T-BAP-HIS-IGF1	F2KP-5XUAS-E1B-CD5-SLIC-BAP-HIS-IGF1	HEK293T
HEK293T-BAP-HIS-IGF2	F2KP-5XUAS-E1B-CD5-SLIC-BAP-HIS-IGF2	HEK293T
HEK293T-BAP-HIS-EGF	F2KP-5XUAS-E1B-CD5-SLIC-BAP-HIS-EGF	HEK293T
HEK293T-BAP-HIS-FGF	F2KP-5XUAS-E1B-CD5-SLIC-BAP-HIS-FGF	HEK293T
HEK293T-CAS9	lentiCas9-blast	HEK293T
MV4-11-CAS9	lentiCas9-blast	MV4-11
Kasumi-CAS9	lentiCas9-blast	Kasumi
NB4-CAS9	lentiCas9-blast	NB4
OCI5-CAS9	lentiCas9-blast	OCI5
HEK293T-CAS9-FLT3-I	pLKO2mod-EGFP-WPRE-CRISPR-sgRNA-FLT3-I	HEK293T-CAS9
HEK293T-CAS9-FLT3-II	pLKO2mod-EGFP-WPRE-CRISPR-sgRNA-FLT3-II	HEK293T-CAS9
HEK293T-CAS9-FLT3-III	pLKO2mod-EGFP-WPRE-CRISPR-sgRNA-FLT3-III	HEK293T-CAS9
HEK293T-CAS9-FLT3-IV	pLKO2mod-EGFP-WPRE-CRISPR-sgRNA-FLT3-IV	HEK293T-CAS9
HEK293T-CAS9-KIT-I	pLKO2mod-EGFP-WPRE-CRISPR-sgRNA-KIT-I	HEK293T-CAS9
HEK293T-CAS9-KIT-II	pLKO2mod-EGFP-WPRE-CRISPR-sgRNA-KIT-II	HEK293T-CAS9
HEK293T-CAS9-KIT-III	pLKO2mod-EGFP-WPRE-CRISPR-sgRNA-KIT-III	HEK293T-CAS9
HEK293T-CAS9-KIT-IV	pLKO2mod-EGFP-WPRE-CRISPR-sgRNA-KIT-IV	HEK293T-CAS9
MV4-11-CAS9-FLT3-I	pLKO2mod-EGFP-WPRE-CRISPR-sgRNA-FLT3-I	MV4-11-CAS9
MV4-11-CAS9-FLT3-II	pLKO2mod-EGFP-WPRE-CRISPR-sgRNA-FLT3-II	MV4-11-CAS9
MV4-11-CAS9-FLT3-III	pLKO2mod-EGFP-WPRE-CRISPR-sgRNA-FLT3-III	MV4-11-CAS9
Kasumi-CAS9-KIT-II	pLKO2mod-EGFP-WPRE-CRISPR-sgRNA-KIT-II	Kasumi-CAS9
Kasumi-CAS9-KIT-III	pLKO2mod-EGFP-WPRE-CRISPR-sgRNA-KIT-III	Kasumi-CAS9
Kasumi-CAS9-KIT-IV	pLKO2mod-EGFP-WPRE-CRISPR-sgRNA-KIT-IV	Kasumi-CAS9
NB4-CAS9-FLT3-II	pLKO2mod-EGFP-WPRE-CRISPR-sgRNA-FLT3-II	NB4-CAS9
NB4-CAS9-FLT3-II	pLKO2mod-EGFP-WPRE-CRISPR-sgRNA-FLT3-II	NB4-CAS9
OCI5-CAS9-KIT-II	pLKO2mod-EGFP-WPRE-CRISPR-sgRNA-KIT-II	OCI5-CAS9
OCI5-CAS9-KIT-II	pLKO2mod-EGFP-WPRE-CRISPR-sgRNA-KIT-II	OCI5-CAS9

Table 16. Generated cell lines.

2.6 Production of recombinant Receptor Tyrosine Kinase Ligands

Lipofectamin 2000	(52887, Invitrogen)
RTKL Vectors	(pCMV/psPAX2, pcDNA3.1/VSV-G and F2KP-5XUAS)
Activator Vectors	(pCMV/psPAX2, pcDNA3.1/VSV-G, FU-ZEO-Gal4-VP16)
Biotin ligase	(pCMV/psPAX2, pcDNA3.1/VSV-G, secBirA-KDEL)
Transfection Medium	(Optimem, 10% FCS)
Packaging Medium	(DMEM, 10%FCS, NEAA, Pyruvate)
PVDF Filters 0.45 µm	(SLHV033RS, Millex)
5 ml, 50 ml syringes	(Terumo)
Sodium Butyrate	(303410, Sigma Aldrich)
Ni-NTA	(30410, Qiagen)
Imidazole	(56750, Sigma Aldrich)

1.9 million of HEK cells are placed to a 6-well dishe. RTKL vector (1.3µg), psPAX2 (0.83µg) and VSV-G (0.45 µg) are diluted in 125µl of optimem. Additionally, for each transfection 0.91µg of activator vector with psPAX2 (0.83µg) and VSV-G (0.45 µg) are diluted in 125µl of optimem. To addition to that 0.91µg of Biotin ligase with psPAX2 (0.83µg) and VSV-G (0.45 µg) are diluted in 125µl of optimem. In parallel to that 6.3µl of lipofectamine is diluted in 125µl of optimem for each transfection and these mixtures are incubated for 5 min at room

temperature. Afterwards DNA and lipofectamine containing mediums are mixed gently and waited for 15 min. Afterwards, transfection mixture is applied on HEK cells for overnight incubation.

Next day, transfection medium is discarded and 1.5 ml packaging medium are added carefully to transfected HEK cells and incubated for one day. Next day, virus particle containing packaging media of respective RTKL vector, activator vector (Gal4VP16) and biotin ligase vector are merged and added to $0.5x10^6$ HEK293T cells to generate a stable cell line. Next day transduction medium is discarded and normal medium is applied to transduced cells. After 3 days, cell media are collected and checked for expression of the specific RTK ligands with western blot. Afterwards, for HIS-tag purification of the specific RTKL, cells are grown in 10-layer flasks for 2-3 days until confluence. Next, cell medium is changed to 6mM sodium butyrate containing medium for boosting expression. After 2 days, cell media are filter through a 0,45 µm filter to a 500 ml bottle and placed on ice. For purification, big columns are packed with 2 ml of Ni-NTA agarose. 5mM imidazole is added to the expression medium which prevents unspecific binding. Afterwards, expression medium is run through the columns at a flow rate of 1 ml/min. 5 column volumes of 10mM imidazole are used for washing the beads. Bound proteins are eluted with 5 times 1 ml elution buffer with 200mM imidazole. 3-30 kDa ultrafiltration columns are used for concentration of RTK ligands (according to ligand size) for 30 min. Afterwards, concentrated ligands are transferred to a fresh Eppendorf tube and 200µl of PBS are used to wash out remaining RTK ligand in the filter tube. Protein concentrations are measured. For preservation glycerol is added 1:1 and ligands are kept at -80°C.

3. Results

3.1 Optimization of SPECS method

3.1.1 Comparison of biotinylation efficiency of DBCO-Sulfo-Biotin and DBCO-PEG12-Biotin reagents

In order to improve the SPECS method, I firstly compared different DBCO labelling reagents in small-scale SPECS experiments. Therefore, HEK 293T cells were cultured with DMEM medium supplemented with ManNAZ or DMSO. After metabolic glycoprotein labelling, ManNAZ labelled glycoproteins were incubated with equal molar quantitites of DBCO-Peg12-Biotin (DPB) or DBCO-Sulfo-Biotin (DSB) under the same conditions to perform a strain promoted, bioorthogonal cycloaddition and thus biotinylation of glycoproteins. In parallel, non-labelled glycoproteins were treated in the same way to reveal DBCO background labelling. Samples were analyzed via Western blot and Streptavidin-HRP to measure biotinylation efficiency of ManNAZ labelled glycoproteins and background labelling of both compounds. At the end, DSB biotinylated ManNAZ labelled glycoproteins 2.5 fold better than DPB. Furthermore, non-specific labelling especially of bovine serum albumin (BSA) was reduced 5-fold in DSB treated samples compared to DPB treated samples. (Fig.7 A-B) The soluble ectodomain of the amyloid precursor protein (sAPP) was used as a loading control. These initial results provided first evidence that DBCO-Sulfo-Biotin (DSB) outperforms DBCO-PEG12-Biotin (DPB) with regard to biotinylation efficiency of ManNAZ labelled glycoproteins while reducing non-specific labelling of non-labelled proteins.

3.1.2 Optimization of buffer compositions and pH for DBCO-PEG12-Biotin and DBCO-Sulfo-Biotin

Next, I compared different pH values and buffer compositions to identify the optimal conditions for strain-promoted glycoprotein biotinylation. Small-scale SPECS experiments were carried out with ManNAZ labelled glycoproteins in conditioned medium and biotinylated proteins were detected by western blot. (Methods-2.2.10). First, I compared different buffer conditions eg. PBS, pH 8.0 and PBS, pH 9.0 with the standard condition water pH 7.2 of the old protocol for both DPB and DSB reagents with regard to biotinylation efficiency of the strain-promoted glycoprotein biotinylation reaction. In all buffer and pH conditions, biotinylation efficiency of DSB was 2.2-fold better than DPB (Fig.8 A-B). Non-specific biotinylation was 2.5 fold higher for DPB compared to DSB (Fig.9 A-B). Furthermore, I observed that both PBS with pH 8.0 and pH 9.0 lead to increased specific and non-specific labelling in comparison to water.

Besides these experiments, DSB was tested with PBS pH 6.0 till pH 9.0 and Tris pH 6.0 till pH 9.0. Non-specific labelling was minimal in PBS pH 6.0, pH 7.0 (Fig.10 A-B) and Tris pH 6.0 (Fig.12 A-B). PBS pH 7.0 and Tris pH 7.0 were the optimum conditions for specific biotinylation of ManNAZ labelled glycoproteins (Fig.11 A-B and Fig.13 A-B). Biotinylation efficiency was increased 1.6 fold with PBS pH 7.0 and 2-fold with Tris pH 7.0 compared to water (Fig.11 B, Fig.13 B). However, unspecific labelling for Tris pH 7.0 increased 1.4-fold compared to water (Fig.12 B)

Finally, I compared PBS pH 7.0 and Tris pH 7.0 with DSB compound with regard to specific and non-specific labelling. Non-specific labelling was almost equal with PBS pH 7.0 and Tris pH 7.0. Specific labelling was increased 1.6-fold with PBS pH7.0 and 1.4-fold for Tris pH 7.0 compared to water. (Fig.14 A-B). Consequently, PBS pH 7.0 with DSB is the optimum condition to obtain the best biotinylation efficiency of ManNAZ labelled glycoproteins with least non-specific labelling.

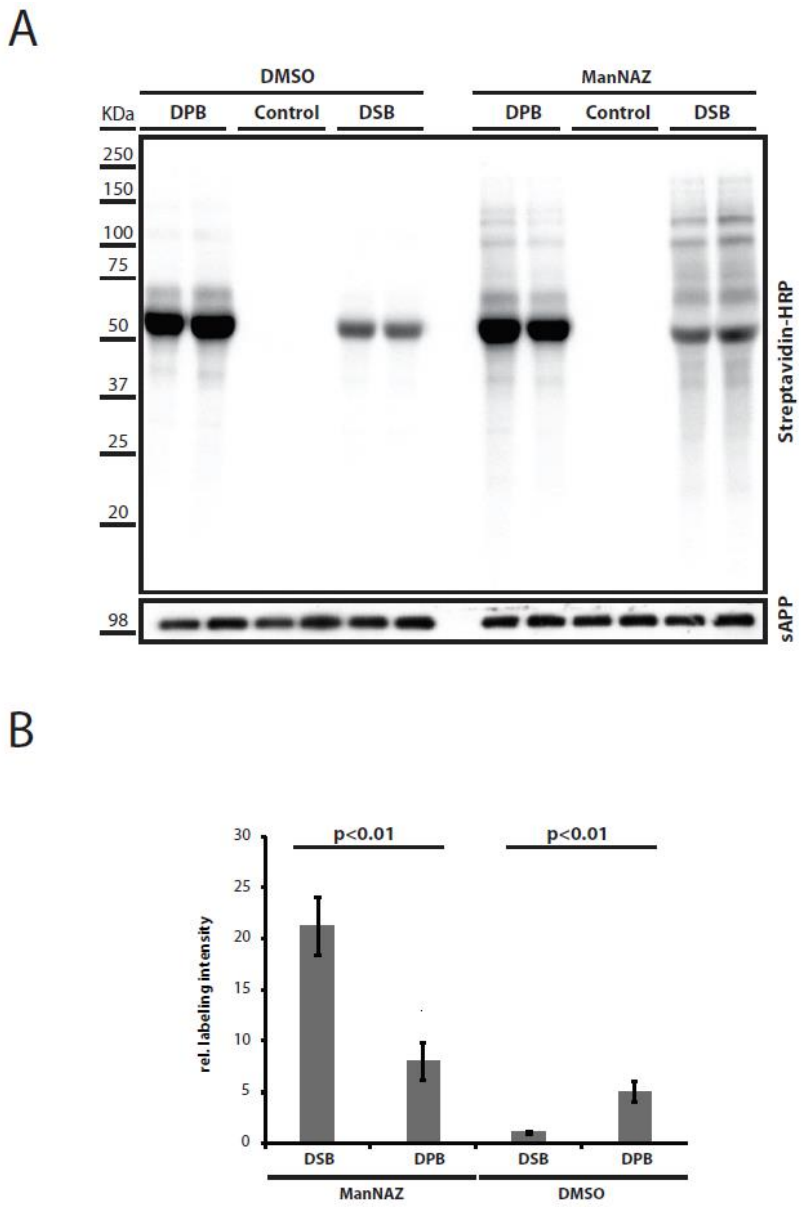

Figure7. Comparison of biotinylation efficiency of DBCO-Sulfo-Biotin (DSB) and DBCO-PEG12-Biotin (DPB) reagents**.** (A) Biotinylated proteins detected with Streptavidin-peroxidase in WB. Cell culture medium was supplemented with 100µM ManNAZ or DMSO as a control and incubated for 48 hours. Afterwards, conditioned media were collected and treated either with DBCO-PEG12-Biotin, DBCO-Sulfo-Biotin or without biotinylation reagent. Detection of soluble Amyloid precursor protein (APP) ectodomain (sAPP) was used as loading control. (B) Quantification of relative labelling intensities of all technical replicates. Quantification of the relative intensities values of DSB and DPB treated replicates in relation to DSB labelled DMSO treated supernatants as reference. (n=6)

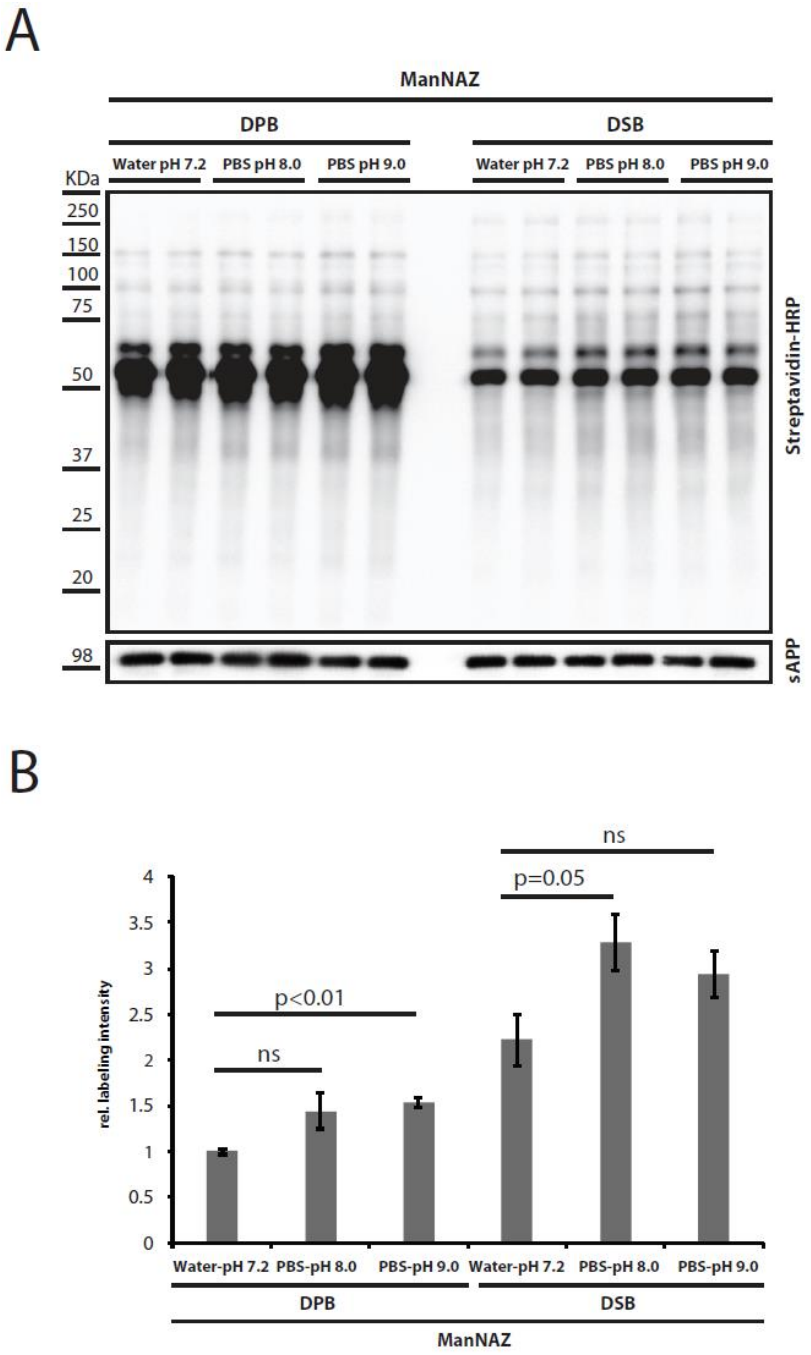

Figure 8. Specific labelling efficiency of DBCO-Sulfo-Biotin (DSB) vs DBCO-PEG12-Biotin (DPB) as a function of buffer composition and pH. (A) Biotinylated proteins detected with Streptavidin-peroxidase in WB. Cell culture medium was supplemented with 100µM of ManNAZ and cells were incubated for 48 hours. Afterwards, conditioned media were collected and treated either with DBCO-PEG12-Biotin or DBCO-Sulfo-Biotin in the buffer conditions water pH7.2, PBS pH 8.0 or PBS pH 9.0. (B) Quantification of the relative labelling intensities of all technical replicates for water pH7.2, PBS pH 8.0 and PBS pH 9.0 (n=4)

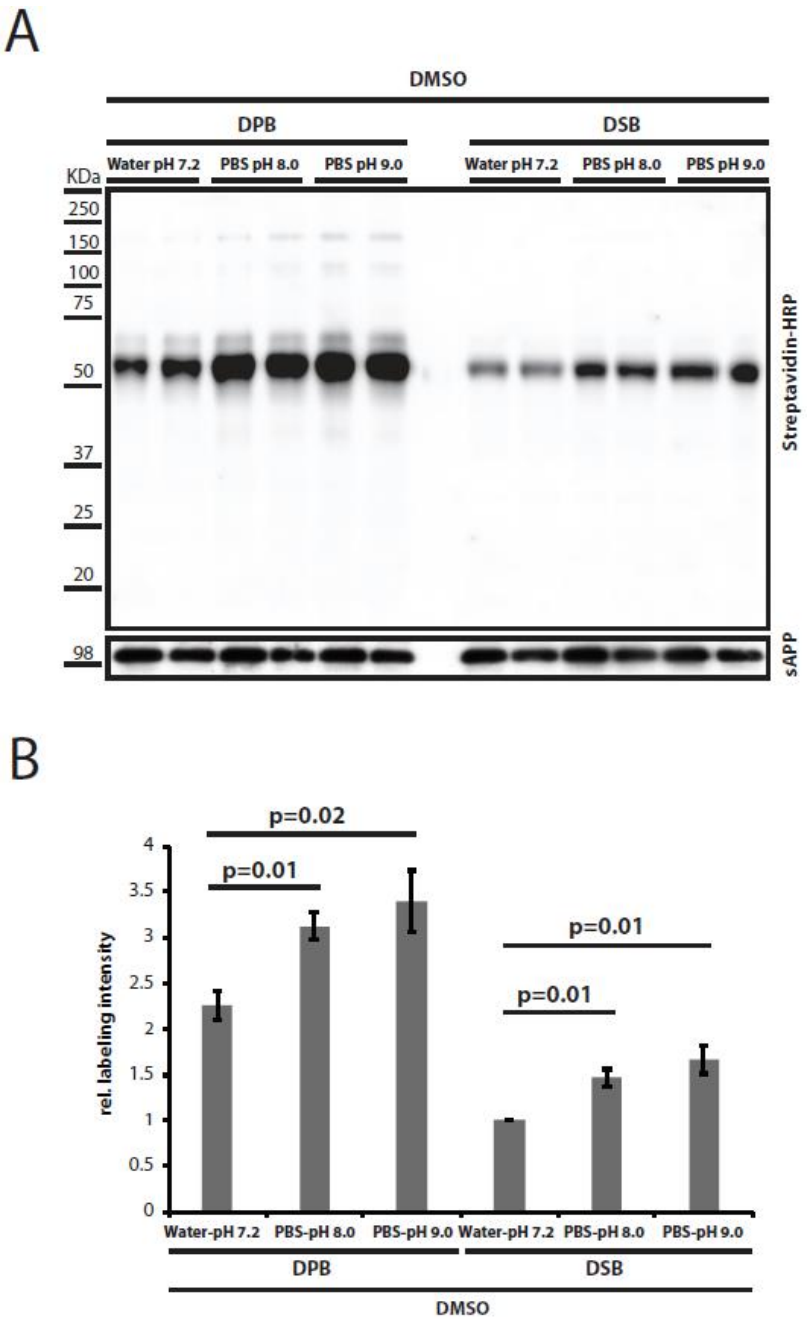

Figure 9. Non-specific labelling efficiency of DBCO-Sulfo-Biotin (DSB) vs DBCO-PEG12-Biotin (DPB) as a function of buffer composition and pH. (A) Biotinylated proteins detected with Streptavidin-peroxidase in WB. Cell culture medium was supplemented with DMSO as solvent control and cells were incubated for 48 hours. Afterwards, media were collected and treated with either DBCO-PEG12-Biotin or DBCO-Sulfo-Biotin each in the buffers water pH 7.2, PBS pH 8.0 in PBS pH 9.0. (B) Quantification of the relative labelling intensities of all technical replicates for water pH 7.2, PBS pH 8.0 and PBS pH 9.0 (n=4)

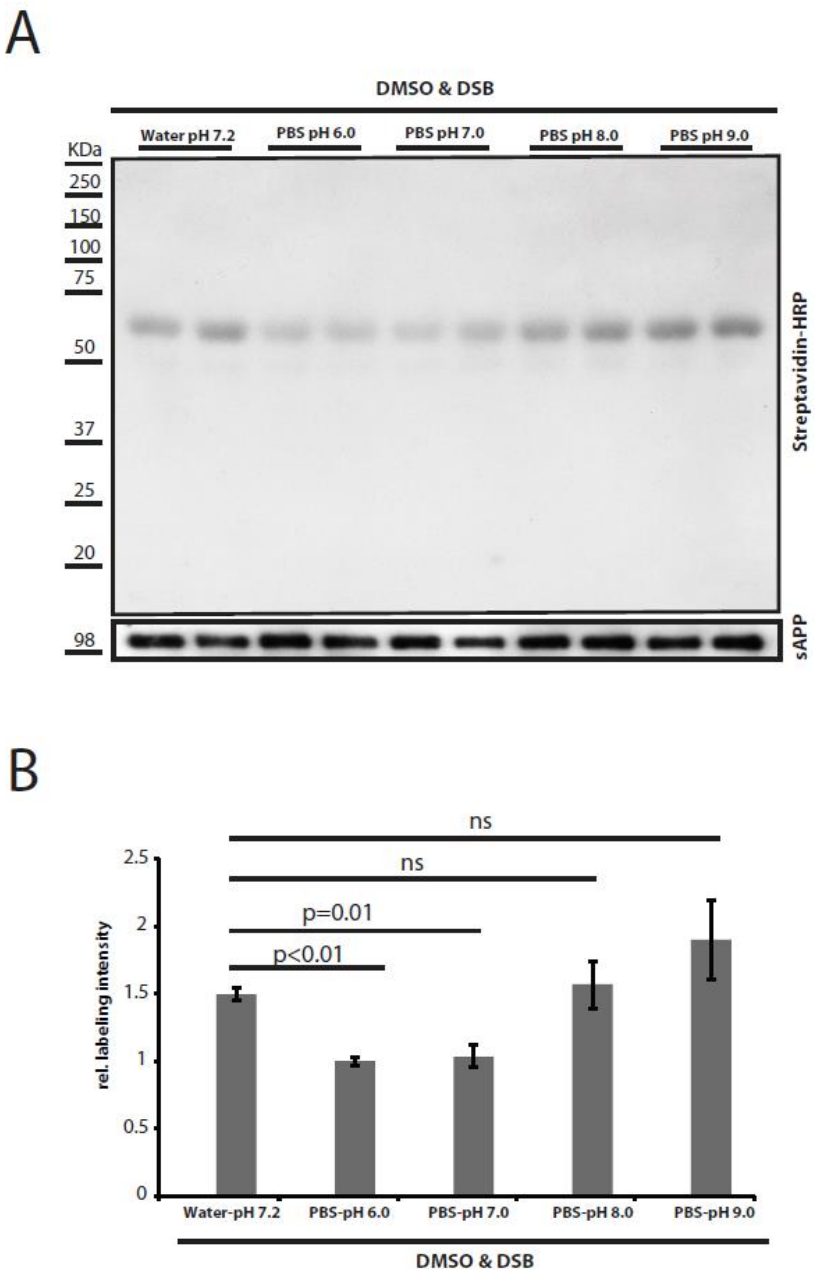

Figure 10. Non-Specific labelling efficiency of DBCO-Sulfo-Biotin (DSB) as a function of buffer composition and pH. (A) Biotinylated proteins detected with Streptavidin-peroxidase in WB. Cell culture medium was supplemented with DMSO as control and cells were incubated for 48 hours. Afterwards, media were collected and treated with DBCO-Sulfo-Biotin with water pH 7.2, PBS pH 6.0, PBS pH 7.0, PBS pH 8.0 or PBS pH 9.0. (B) Quantification of the relative labelling intensities of all technical replicates for water pH 7.2, PBS pH 6.0, PBS pH 7.0, PBS pH 8.0 and PBS pH 9.0 (n=4)

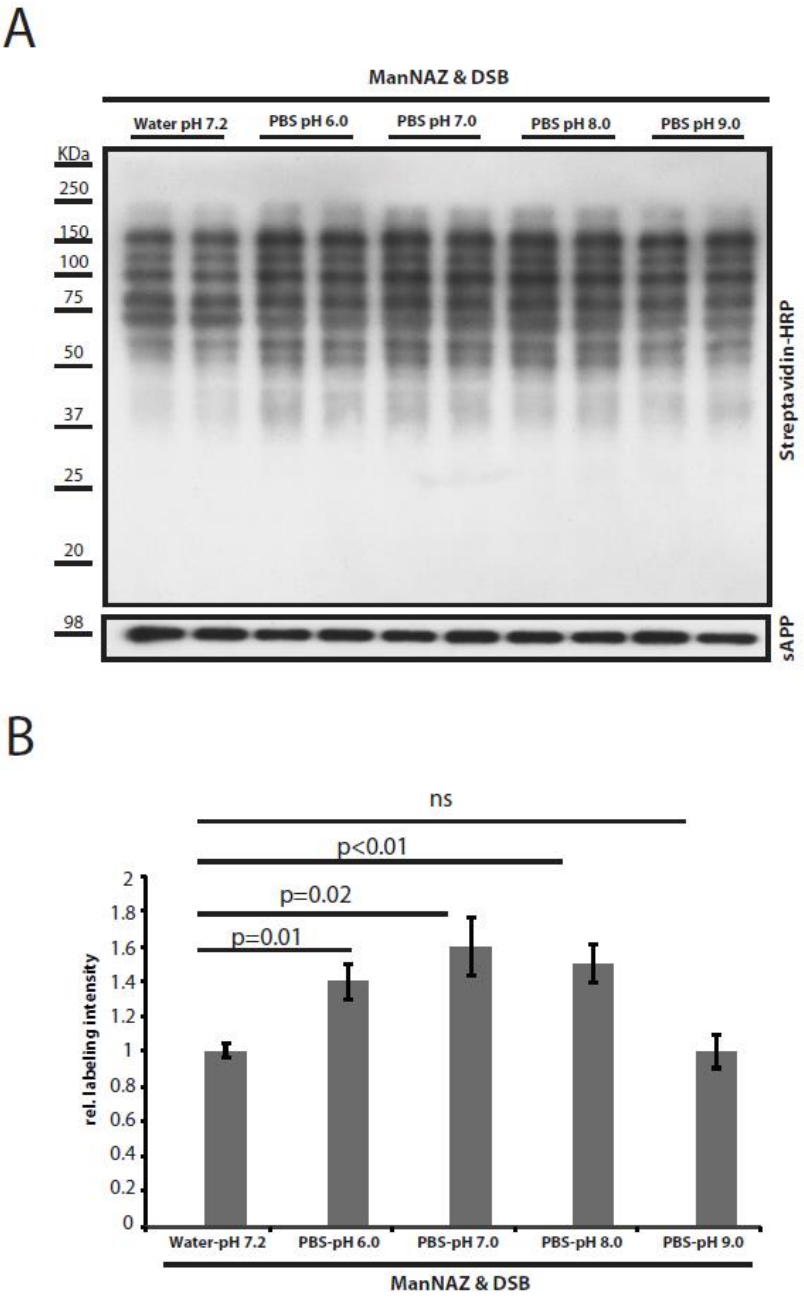

Figure 11. Specific labelling efficiency of DBCO-Sulfo-Biotin (DSB) as a function of buffer composition and pH. (A) Biotinylated proteins detected with Streptavidin-peroxidase in WB. Cell culture medium was supplemented with 100µM of ManNAZ and cells were incubated for 48 hours. Afterwards, media were collected and treated with DBCO-Sulfo-Biotin with water pH 7.2, PBS pH 6.0, PBS pH 7.0, PBS pH 8.0 or PBS pH 9.0. (B) Quantification of the relative labelling intensities of all technical replicates for water pH 7.2, PBS pH 6.0, PBS pH 7.0, PBS pH 8.0 and PBS pH 9.0 (n=4)

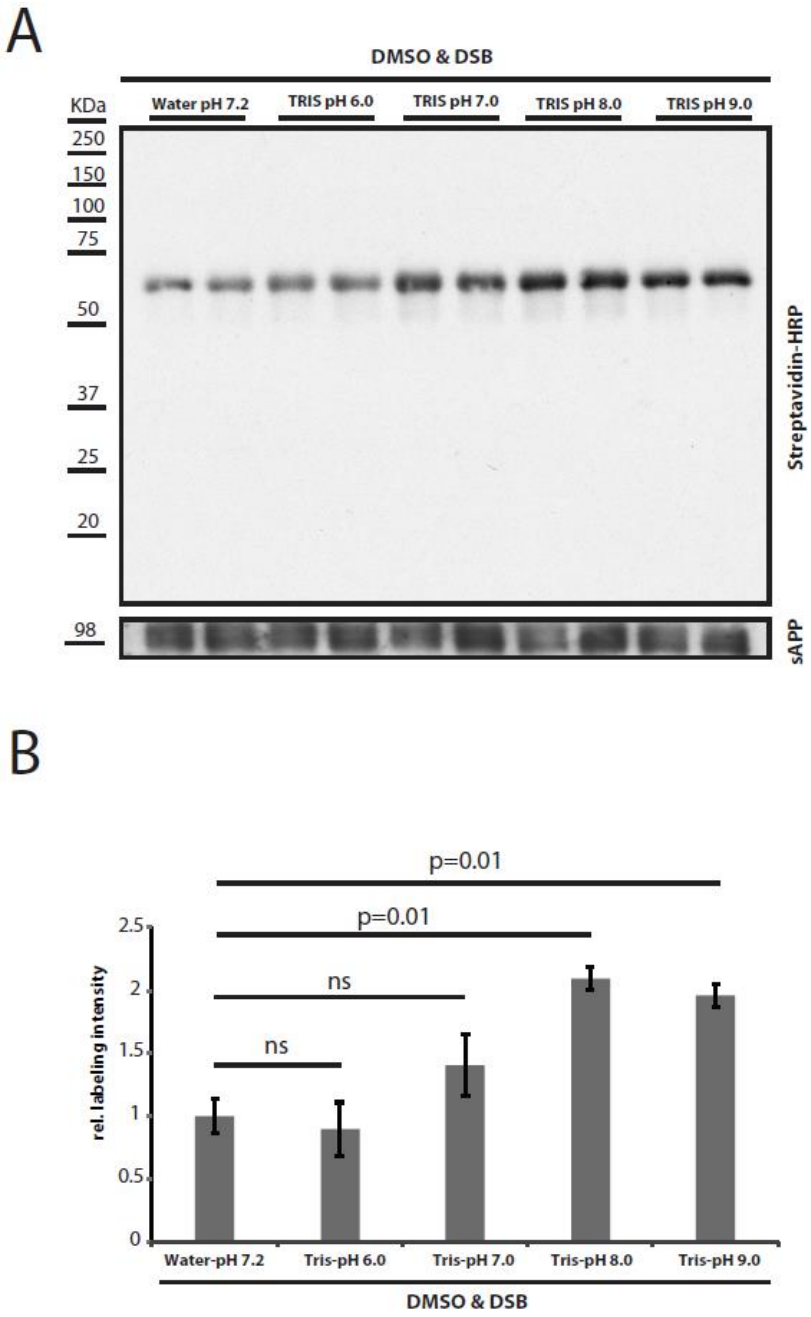

Figure 12. Non-Specific labelling efficiency of DBCO-Sulfo-Biotin (DSB) as a function of buffer composition and pH. (A). Biotinylated proteins detected with Streptavidin-peroxidase in WB. Cell culture medium was supplemented with DMSO as control and cells were incubated for 48 hours. Afterwards, media were collected and treated with DBCO-Sulfo-Biotin with water pH 7.2, Tris pH 6.0, Tris pH 7.0, Tris pH 8.0 or Tris pH 9.0. (B) Quantification of the relative labelling intensities of all technical replicates for water pH 7.2, Tris pH 6.0, Tris pH 7.0, Tris pH 8.0 and Tris pH 9.0 (n=4)

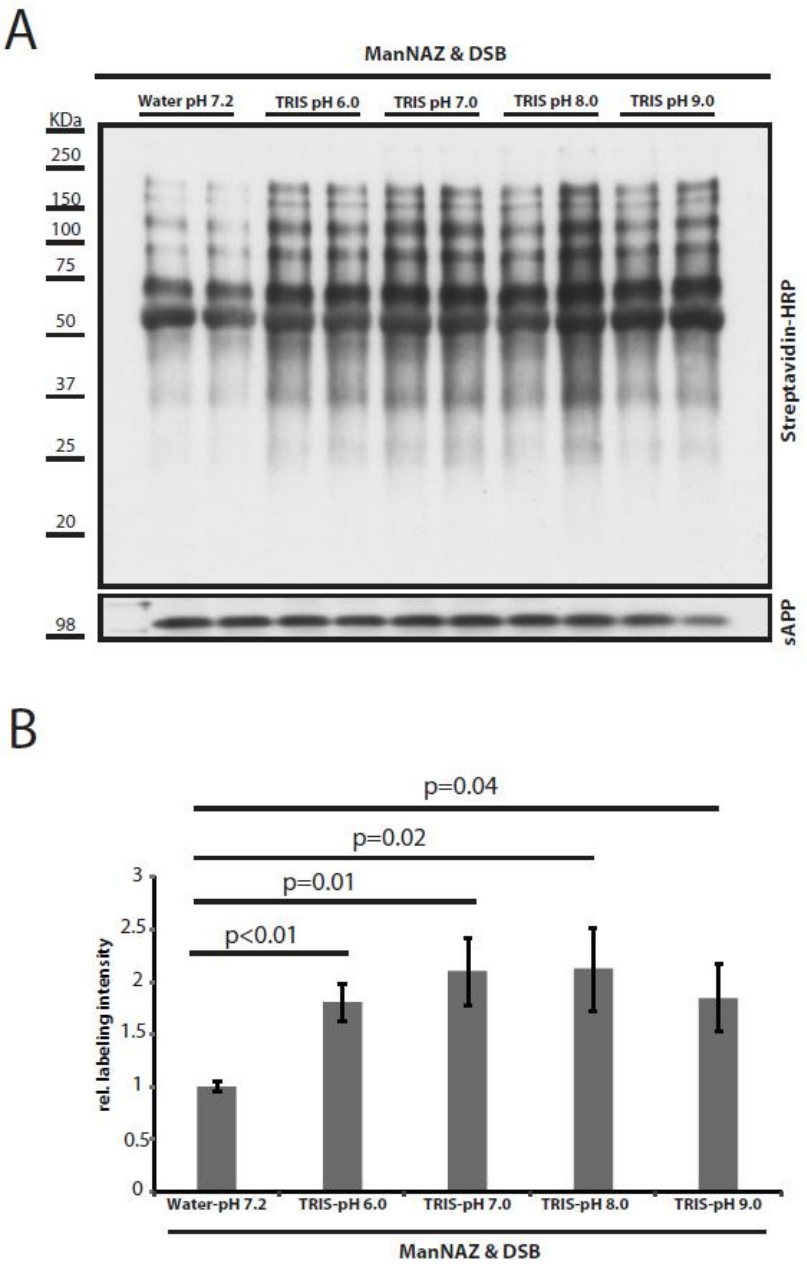

Figure 13. Specific labelling efficiency of DBCO-Sulfo-Biotin (DSB) as a function of buffer composition and pH. (A) Biotinylated proteins detected with Streptavidin-peroxidase in WB. Cell culture medium was supplemented with 100µM of ManNAZ and cells were incubated for 48 hours. Afterwards, media were collected and treated with DBCO-Sulfo-Biotin with water pH 7.2, Tris pH 6.0, Tris pH 7.0, Tris pH 8.0 or Tris pH 9.0. (B) Quantification of the relative labelling intensities of all technical replicates for water pH 7.2, Tris pH 6.0, Tris pH 7.0, Tris pH 8.0 and Tris pH 9.0 (n=4)

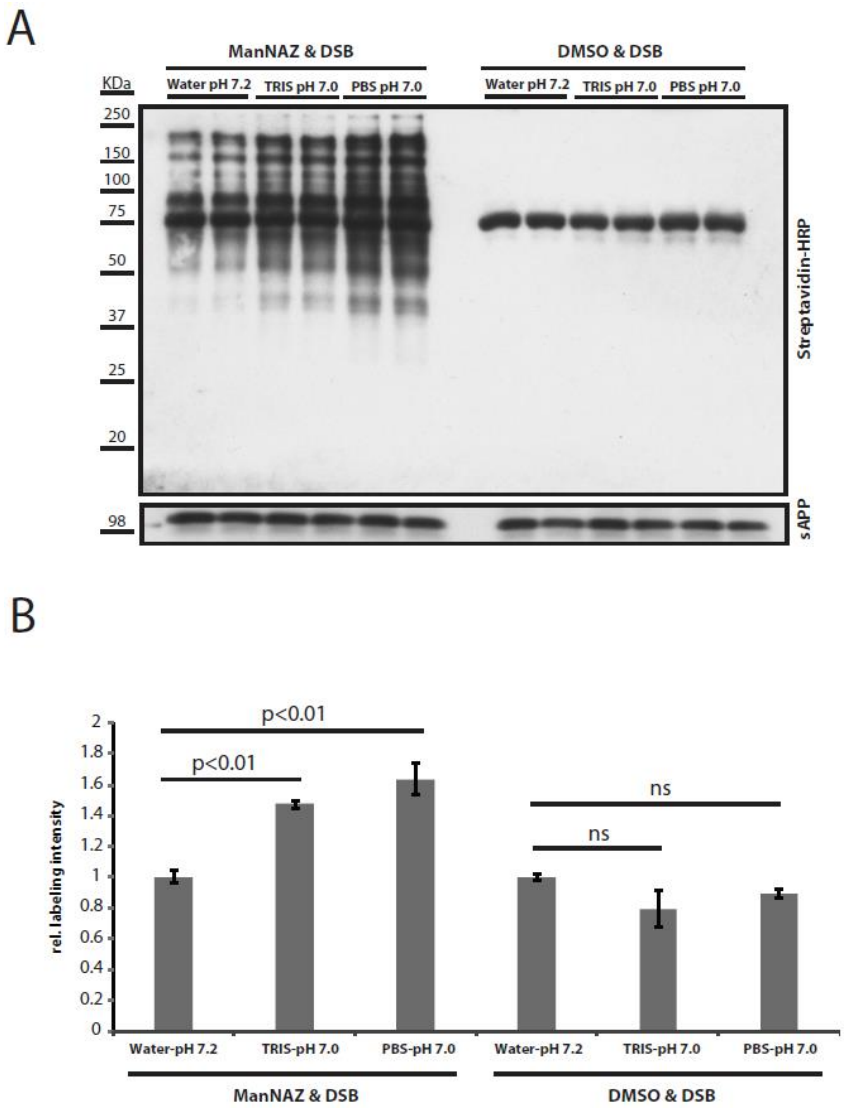

Figure 14. Comparison of specific and non-specific labelling efficiency of DBCO-Sulfo-Biotin (DSB) as a function of buffer composition. (A) Biotinylated proteins detected with Streptavidin-peroxidase in WB. Cell culture medium was supplemented with 100µM of ManNAZ or DMSO as control then cells were incubated for 48 hours. Afterwards, media were collected and treated with DBCO-Sulfo-Biotin with water pH 7.2, Tris pH 7.0 and PBS pH 7.0. (C) Quantification of the relative labelling intensities of the all technical replicates for water pH 7.2, Tris pH 7.0, PBS pH 7.0 (n=4)

3.1.3 Non-specific and specific labelling as a function of iodoacetemide (IAA) alkylation of free thiol groups

To further improve the SPECS protocol, I applied different concentrations of iodoacetamide to block potentially unpaired thiol groups of cysteines that are known to react with strained alkynes in a thiol-yne reaction (116) Especially, the most abundant protein in serum supplements, serum albumin is known to contain an unpaired cysteine at positon 34 (116). Therefore, 30 nmol and 60 nmol of iodoacetemide (IAA) were applied for blocking the free cysteine residues. Concentrated media of ManNAZ or DMSO treated cells were subjected to alkylation reaction in the dark after the first concentration step (Method-2.2.10). Afterwards, samples were reacted with DPB or DSB. Consequently, western blot analysis indicated that

unspecific albumin labelling was not reduced significantly (Fig.15 A-B). On the other hand, biotinylation efficiency of ManNAZ labelled glycoproteins was not significantly changed as well (Fig.16 A-B). Hence, we did not include IAA pre-treatment in further experiments and the final version of the protocol.

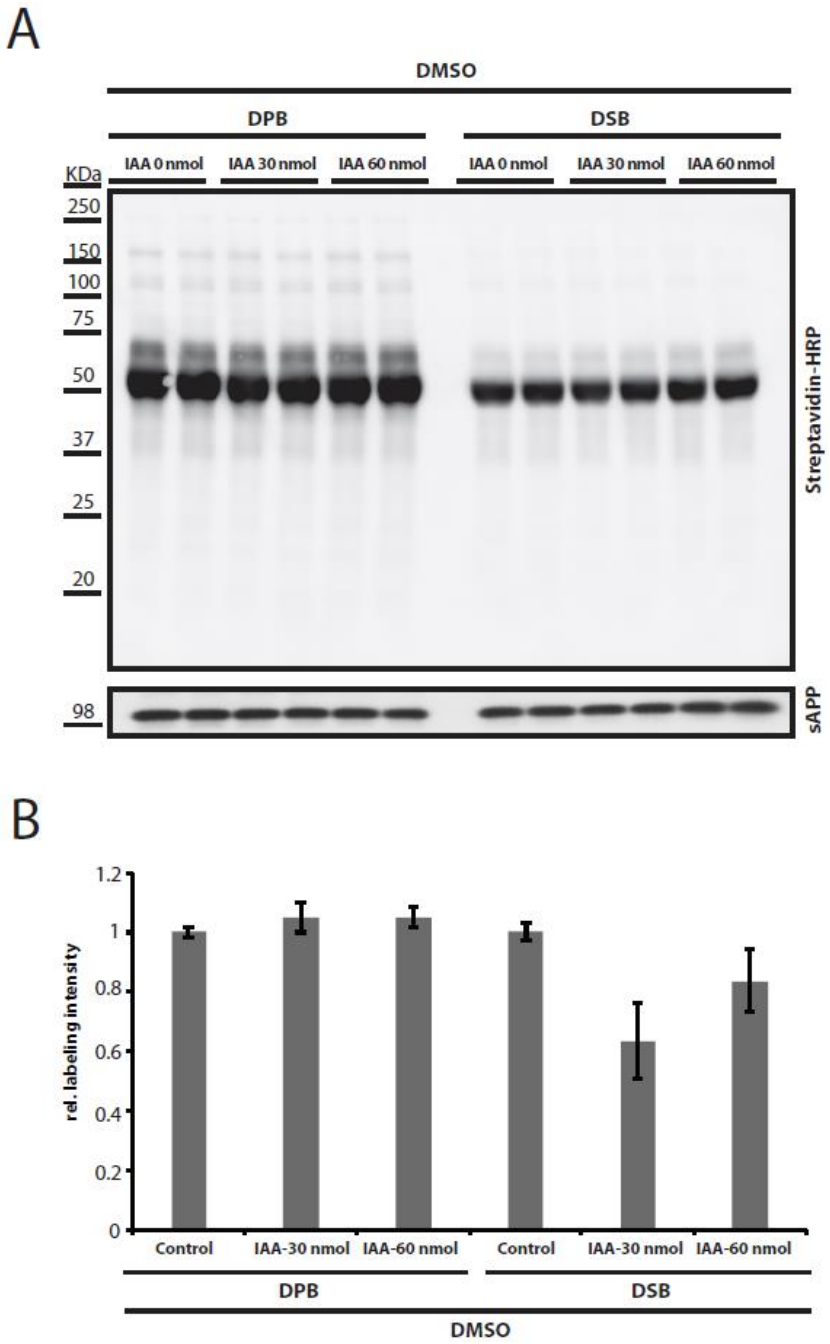

Figure 15. Non-specific labelling efficiency of DBCO-Sulfo-Biotin (DSB) and DBCO-PEG12-Biotin (DPB) as a function of iodoacetemide (IAA) alkylation of free thiol groups. (A) Biotinylated proteins detected with Streptavidin-peroxidasein WB. Cell culture media were supplemented with DMSO as control and cells were incubated with the medium for 48 hours. Afterwards, media were collected and treated with 0-30-60 nmol of IAA. Afterwards, media were treated either with DBCO-Sulfo-Biotin or DBCO-PEG12-Biotin. (B) Quantification of the relative labelling intensities of the all technical replicates for conditions with 0, 30, 60 nmol of IAA and DPB or DSB (n=6).

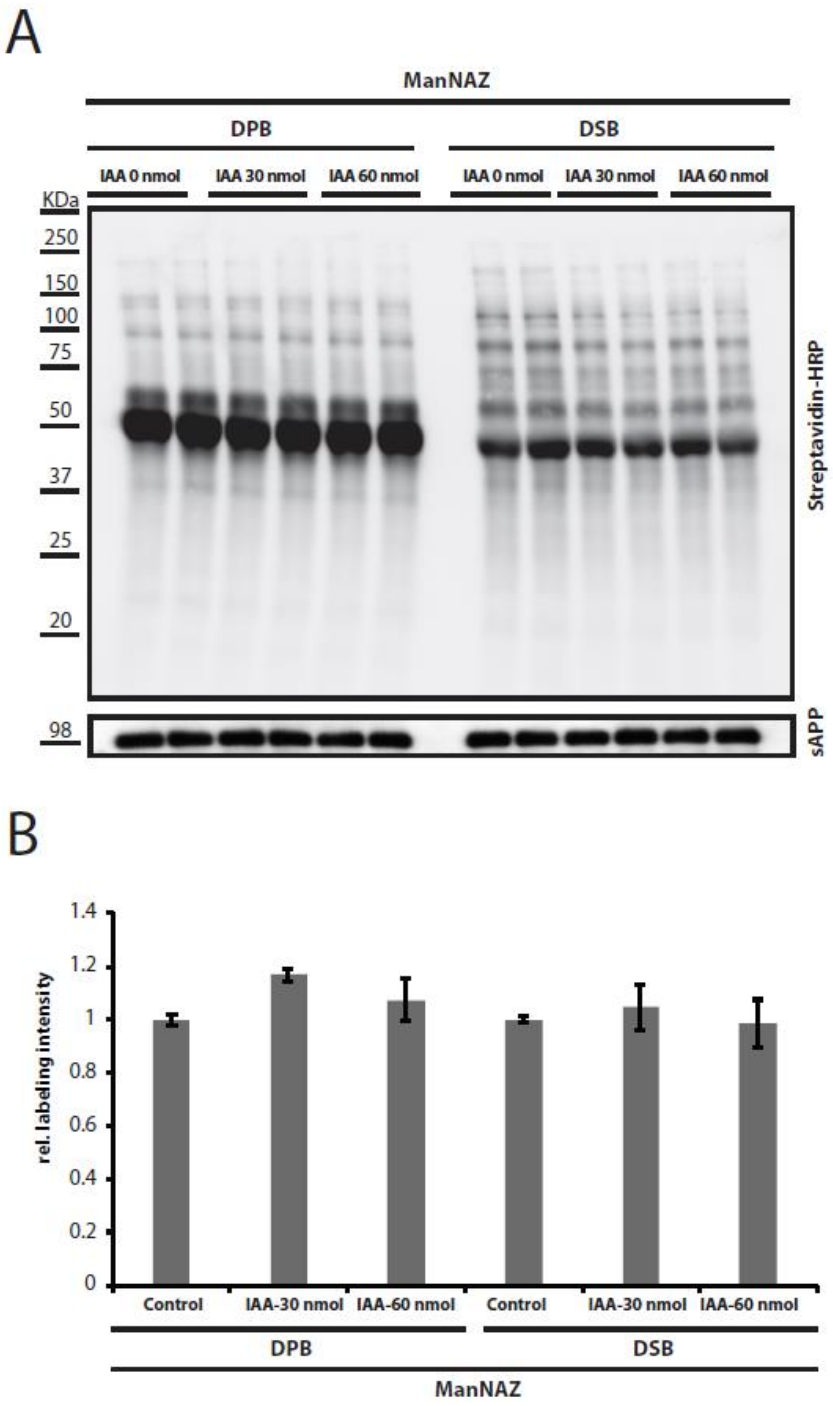

Figure 16. Specific labelling efficiency of DBCO-Sulfo-Biotin (DSB) and DBCO-PEG12-Biotin (DPB) as a function of iodoacetemide (IAA) alkylation of free thiol groups. (A). Biotinylated proteins detected with Streptavidin-peroxidasein WB. Cell culture media were supplemented with 100µM of ManNAZ then cells were incubated for 48 hours. Afterwards, media were collected and treated with 0-30-60 nmol of IAA Afterwards, media treated either with DBCO-Sulfo-Biotin or DBCO-PEG12-Biotin. (B) Quantification of the relative labelling intensities of the all technical replicates for conditions with 0, 30, 60 nmol of IAA and DPB or DSB (n=6).

3.1.4 Comparison of the performance of the old SPECS protocol versus the new SPECS protocol in a mass spectrometry analysis

After optimizing the specificity and efficiency of the SPECS method using the signal intensity of biotinylated proteins in western blot as a read-out, we finally evaluated the performance of the optimized protocol based on protein identifications and sequence coverage using mass spectrometry. Therefore, the optimized protocol (DSB with PBS pH7.0) was compared to the old protocol (DPB with water) with respect to biotinylation of ManNAZ labelled glycoproteins. (Fig.17 A). Four independent replicates were performed with the old and the new SPECS protocol respectively using 20 ml ManNAZ supplemented medium conditioned on $20x10^6$ of HEK cells. (Method 2.2.11, Method 2.2.12) Streptavidin-bead purified biotinylated proteins of the old and the new protocol were compared with Coomassie stained SDS page gels (Method 2.2.6). Cumulative Coomassie staining intensity of the gel lanes of the new protocol showed an average 2.4-fold increase compared to the gel lanes of the old protocol (Fig.17 B-C). Next, gels were subjected to tryptic in-gel digestion (Method 2.2.15) and peptides were analysed by MS (Method 2.2.16). After the Max Quant analysis (Method 2.2.17), only proteins were identified with at least two unique peptides and present in at least 3 out of 4 biological replicates were considered for quantitative analysis.

Using the UniProt database identifier (Glycoprotein, keyword: KW-0325) as a filter, 604 glycoproteins were identified out of 1049 proteins using the new protocol (Table17). On the other hand, using the old protocol 373 glycoproteins were identified out of 646 proteins. (Fig.18 A-C, Table17). Using the new protocol, we detected all proteins that were also detected with the old protocol except for 26 proteins (3 of them glycoproteins) (Fig.18 A) According to the contaminant database of MaxQuant, the new protocol revealed a slightly lower number of 87 contaminating proteins than the old protocol with 90 contaminating proteins. (Fig.18 D). Despite the benefits of the new protocol, 199 additional non-glycosylated proteins were detected (Fig.18 C) Overall, the number of identified glycoproteins was increased by 62% compared to the old protocol (Table 17). On the other hand, the ratio of glycoproteins to non-glycoproteins stayed constant (57% vs 58%). Concerning glycoprotein detection, glycoprotein intensities and protein intensities were significantly increased in the new protocol compared to the old protocol. These results demonstrate that the new protocol outperformed the old protocol (Fig.19) Cumulative glycoprotein intensities were increased 10.4-fold (+945%) in the new protocol (Table 17) while cumulative non-glycoprotein intensities were only 2.4-fold increased in the new protocol. When we plotted log_2-transformed LFQ intensities of glycoproteins and non-glycoproteins versus the number of proteins that fell into a defined intensity groups in a histogram, we observed a much stronger shift for glycoproteins to higher LFQ intensities than for non-glycoproteins (Fig.20 A). Total identified peptides were 14867 for the new protocol and 5912 for the old protocol. This resulted in an enhanced sequence coverage of identified glycoproteins of 9.7% (Table 17). Further calculations showed that the ratio of cumulative glycoprotein intensities over non-glycosylated protein intensities was 1.92 using the old protocol and 8.3 in the new protocol. These results indicated that overall glycoprotein enrichment was improved with the new protocol. Topology of the significantly changed glycoproteins were 173 secreted, 151 type I,

67 type II, 13 GPI, 7 polytopic and 2 Type I/GPI (Fig.20 B). Inter experimental reproducibility was compared with correlation of LFQ values of biological replicates and new protocol demonstrated better results R_{Mean}=0.936 in comparison to old protocol R_{Mean}=0.902. (Fig.20 C). Furthermore, secretome data were analysed with Panther database to identify the components of signalling pathways and important signalling pathways like integrin-, Notch, Wnt or TGF-beta components were identified in our secretome data (Fig.21).
According to overall results, the new protocol outperforms the old protocol in terms of protein intensity, sequence coverage, identified peptides, better inter experimental reproducibility and consequentially quantifiable protein identifications and thus allow reducing the required input material.

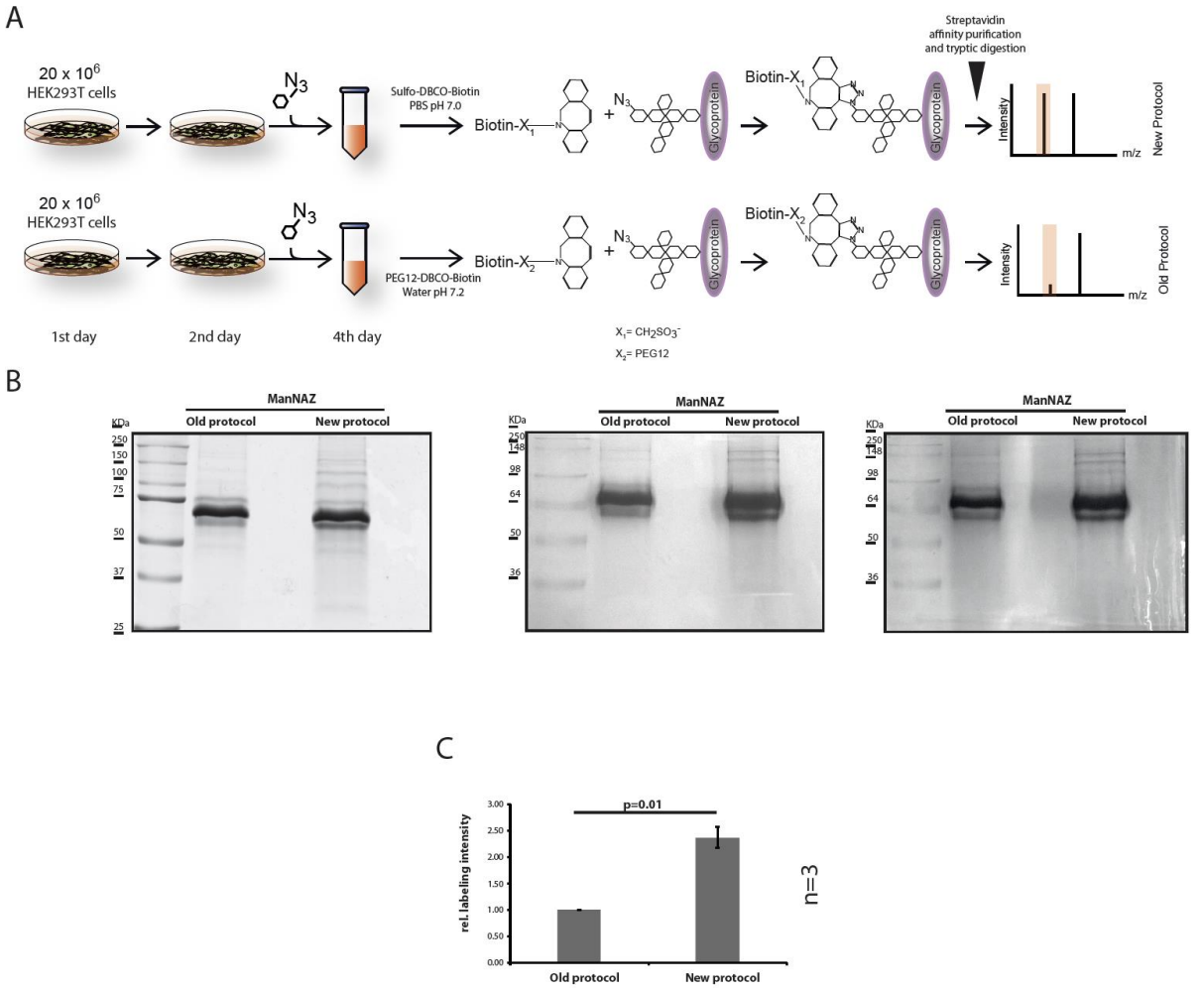

Figure 17. Comparison between work flows and coomassie stainings of old and new SPECS protocol. (A) Workflow of the old and new SPECS protocols comprising of seeding HEK293T cells, metabolic glycan labelling, click chemistry mediated biotinylation, streptavidin pulldown and quantification and identification of captured proteins via mass spectrometry. (B) Coomassie staining of streptavidin-purified biotinylated proteins separated by SDS page using the old and the new SPECS protocol (C) Quantified relative coomassie intensities of the old versus new SPECS protocol considering three biological replicates.

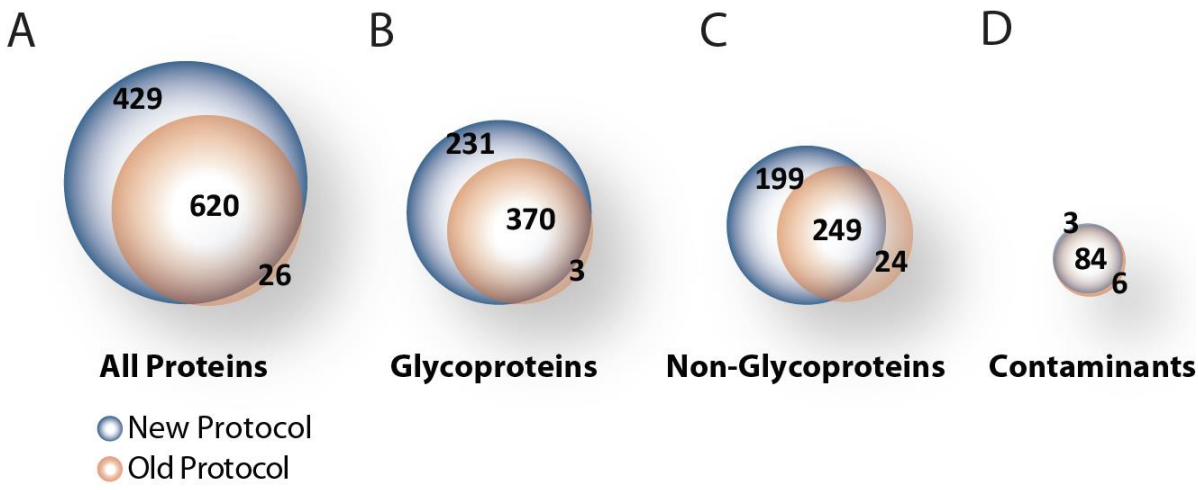

Figure 18. These Venn diagrams show quantitative comparison of detected proteins between old and new SPECS protocol (A) Venn diagram of all identified and quantified proteins and overlap between old and the new SPECS protocol. (B) Venn diagram of identified glycoproteins and overlap between old and the new SPECS protocol. (C) Venn diagram of identified non-glycoproteins and overlap between old and the new SPECS protocol. (D) Overlap between contaminants detected with old and new protocol.

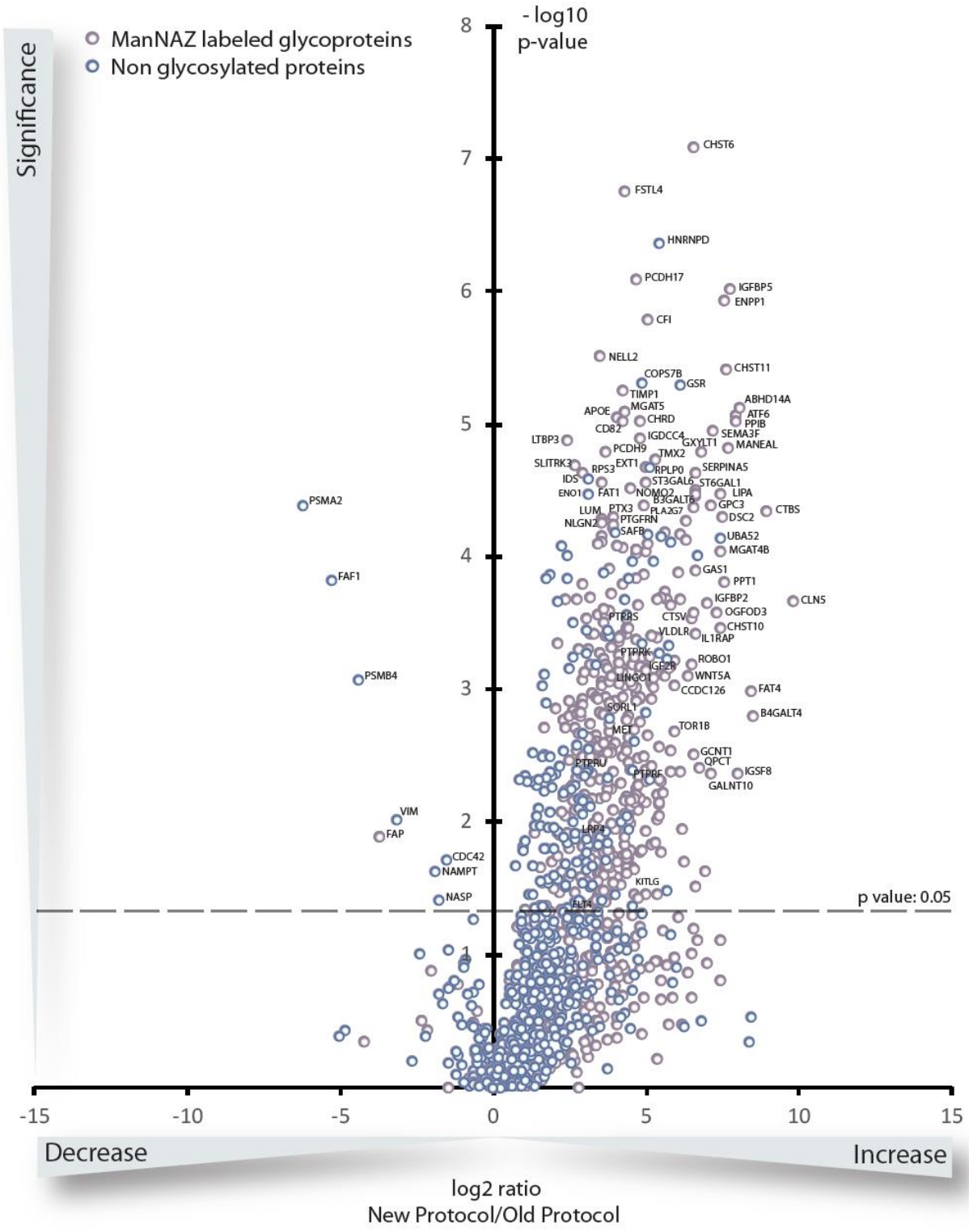

Figure 19. Quantitative comparison between old and the new SPECS protocol with volcano plot. Glycoproteins and non-glycoproteins were identified in 4 biological replicates of old and the new SPECS protocols and p-value is depicted as negative decadic logarithm while the fold change (new protocol/old protocol) is depicted as $\log_2$ value. Significantly changed proteins depicted as: $p \leq 0.05$ ($-\log_{10} \geq 1.3$) Glycoproteins according to Uniprot keywords shown as purple and non-glycosylated proteins shown in blue colour.

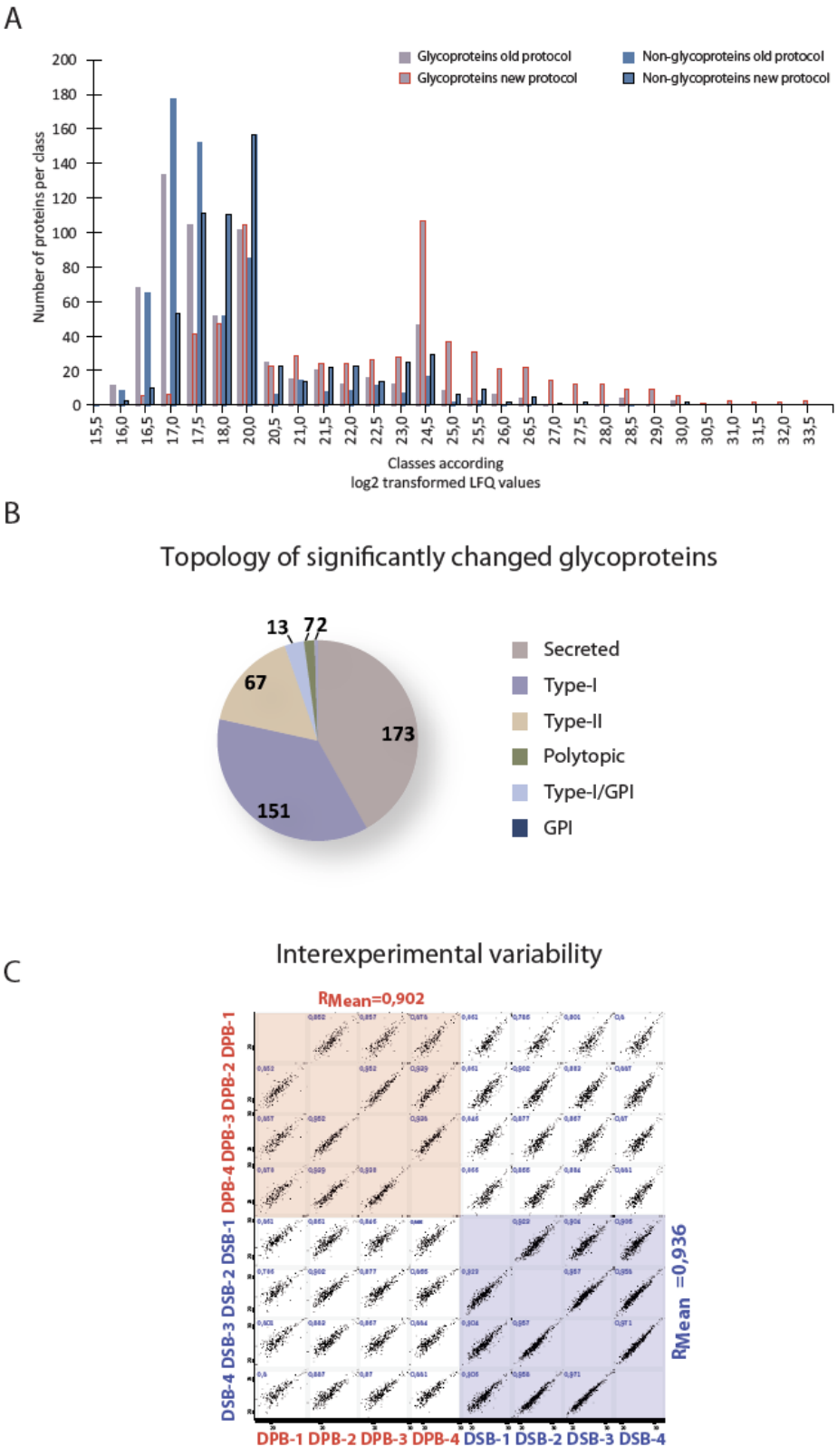

Figure 20. These graphs and histograms show quantitative comparison between old and the new SPECS protocol. (A) Histogram of log_2 transformed LFQ classes for the old and the new protocol. (B) Topology of the significantly changed glycoproteins abundance between old and the new protocol. (C) Interexperimental variability is shown in the multiscatter plot. Old SPECS protocol is shown in light red and new SPECS protocol shown in light blue.

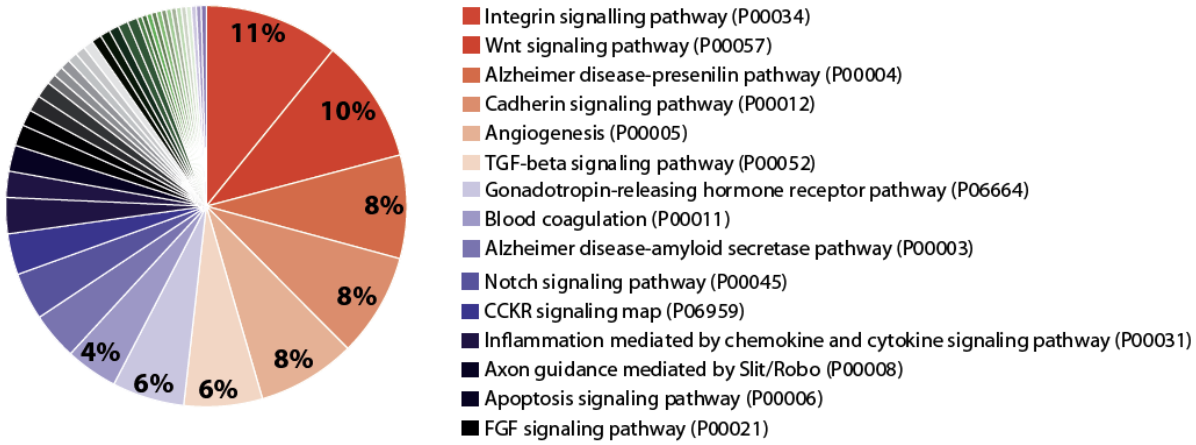

Figure 21. This figure shows GO-Term analysis of glycoproteins to identify pathways covered by secretome analysis.

	New protocol	Old protocol	Increase (%)
Average peptide IDs for all glycoproteins per biological replicate	3824	1537	149
Average peptide IDs per glycoprotein	6.7	2.3	191
Protein IDs (minimum two unique peptides) in ¾	1049	646	62
Quantified glycoproteins in ¾	604	373	62
Average glycoprotein sequence coverage (%)	9.7%	4.0%	143
Average glycoprotein intensity (log2)	22.25	18.86	945
Average non-glycoprotein intensity (log2)	19.19	17.9	142

Table 17. This table comprises overall comparison between old and the new SPECS protocol.

3.2 Optimizations of SPECS for AML cell lines

3.2.1 Investigation of different labelling time periods and concentrations of ManNAZ sugar

First, I wanted to identify the optimum concentration of ManNAZ and optimum incubation time to identify those conditions which yielded the best labelling of the surface proteome. $4x10^6$ NB4 and Kasumi cells were cultured in 2ml of RPMI1640 medium with aforementioned supplements (Method 2.2.1) for optimization experiments. Different concentration of ManNAZ sugar and different incubation periods were tested as described in the table below:

24 hour	24 hour
NB4 2ml $4x10^6$ cell 4µl ManNAZ 50mM stock (100µM)	Kasumi 2ml $4x10^6$ cell 4µl ManNAZ 50mM stock (100µM)
NB4 2ml $4x10^6$ cell 8µl ManNAZ 50mM stock (200µM)	Kasumi 2ml $4x10^6$ cell 8µl ManNAZ 50mM stock (200µM)

48 hour	48 hour
NB4 2ml $4x10^6$ cell 4µl ManNAZ 50mM stock (100µM)	Kasumi 2ml $4x10^6$ cell 4µl ManNAZ 50mM stock (100µM)
NB4 2ml $4x10^6$ cell 8µl ManNAZ 50mM stock (200µM)	Kasumi 2ml $4x10^6$ cell 8µl ManNAZ 50mM stock (200µM)

Table18. Investigating of different labelling time periods and concentrations of ManNAZ sugar.

Kasumi and NB4 cell lines were subjected to 24 and 48 hours of labelling with 100µM and 200µM of ManNAZ sugar. After incubation, cells were collected and washed with ice cold PBS and subjected to biotinylation reaction with 0,2 µl DBCO-Peg12-Biotin (50mM stock) in 100 µl PBS incubated for 2 hours on ice. Next, cells were centrifuged down and washed with ice cold PBS. Afterwards, cells were subjected to lysis, SDS-page and Western blot (Method 2.2.1-2.2.4-2.2.7). Biotinylated proteins were detected with streptavidin peroxidase. 48 hours of

labelling time with 100µM ManNAZ concentration yielded the highest signal of biotinyled proteins (Fig.22 A). Average quantification indicated that 48h labelling with 100µM ManNAZ labelling resulted in a 1.6-fold better signal than 24h labelling with 100µM or 200µM ManNAZ. (Fig.22 B) On the other hand, 48h labelling with 200µM ManNAZ labelling showed a similar signal like 48h labelling with 100µM ManNAZ. (Fig22 B). As 200 µM did not improve the signal of biotinylated glycoproteins compared to 100 µM and as increased ManNAZ concentrations pose a risk for increased cellular toxicity, I decided to use 100 µM and 48 hours as labelling conditions for all future experiments.

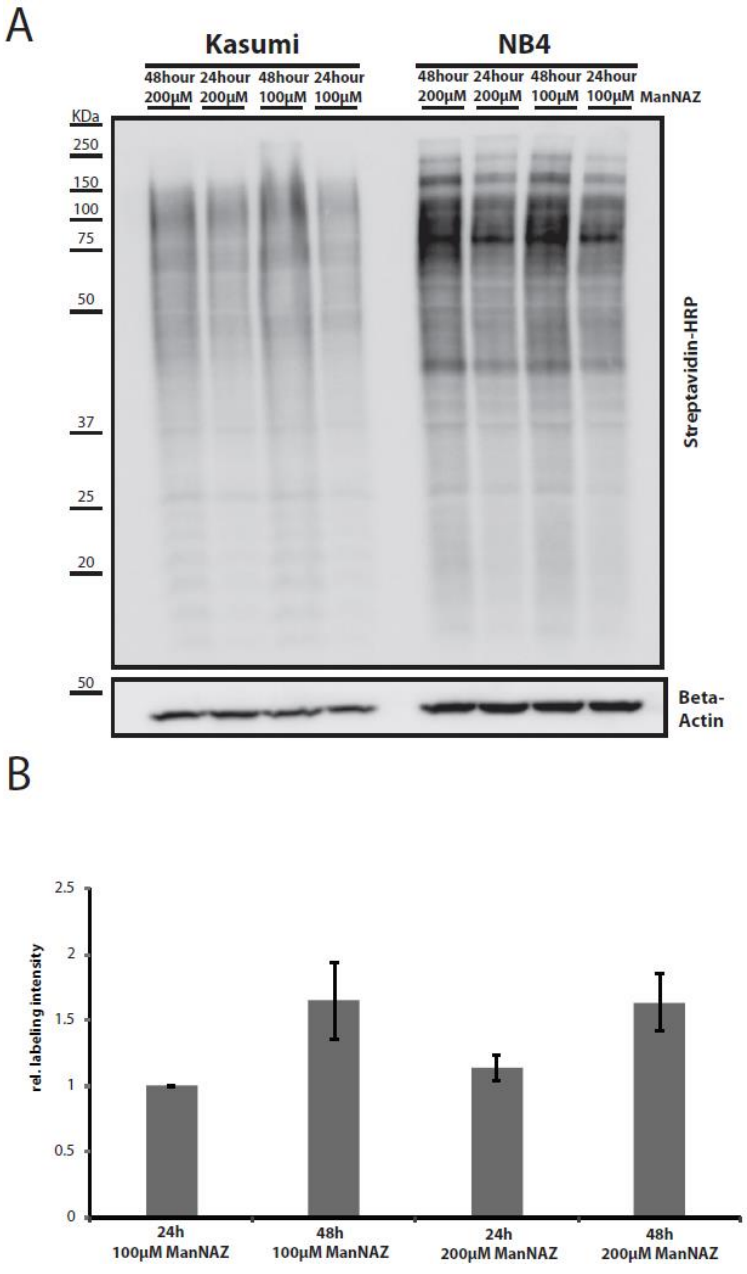

Figure 22. Glycoprotein labelling in AML cell lines as a function of incubation time and ManNAZ concentration. (A) Biotinylated glycoproteins of cell lysates of AML cell lines NB4 and Kasumi incubated with either 100µM or 200µM of ManNAZ for 24 or 48 hours were detected with Streptavidin-peroxidase in WB. Beta-Actin was used as a loading control. (B)Quantification of the average relative intensities of the different incubation periods and ManNAZ concentration (24h-100µM ManNAZ, 48h-100µM ManNAZ, 24h-200µM ManNAZ and 48h-200µM ManNAZ)

3.2.2 Application of different azido sugars on AML cell lines

Next, GalNAZ and ManNAZ sugars were compared with regard to labelling efficiency for SPECS application in AML cell lines. This experiment should give an idea about whether eg. O-glycosylation or N-glycosylation is more abundant in AML cell lines and whether there is a synergetic effect in labelling efficiency using both ManNAZ and GalNAZ. The experimental design was as follows:

48 hour	48 hour
NB4 2ml $4x10^6$ cell 4µl ManNAZ 50mM stock (100µM)	NB4 2ml $4x10^6$ cell 4µl GalNAZ 50mM stock (100µM)
NB4 2ml $4x10^6$ cell DMSO Control	NB4 2ml $4x10^6$ cell 4µl GalNAZ 50mM stock (100µM) + 4µl ManNAZ 50mM stock (100µM)

Table19. Application of different azido sugars.

The AML cell line NB4 was incubated with 100 µM ManNAZ, 100 µM GalNAZ or a combination thereof for 48 hours Conditioned cell culture media were collected and 400µl of the media were subjected to small-scale SPECS application with DBCO-PEG12-Biotin (Method 2.2.10). Afterwards, media were subjected to Western blot and detection of biotinylated proteins with Streptavidin peroxidase (Method 2.2.7). ManNAZ labelling resulted in a 2-fold better signal of biotinylated proteins than GalNAZ. (Fig.23 A-B) Combined labelling with ManNAZ and GalNAZ did not result in a synergistic increase in labelling efficiency. In fact, ManNAZ sugar labelling showed a 1.4-fold better signal than using both sugars. (Fig.23 B). In summary, ManNAZ sugar outperformed GalNAZ in metabolic labelling of AML cell lines.

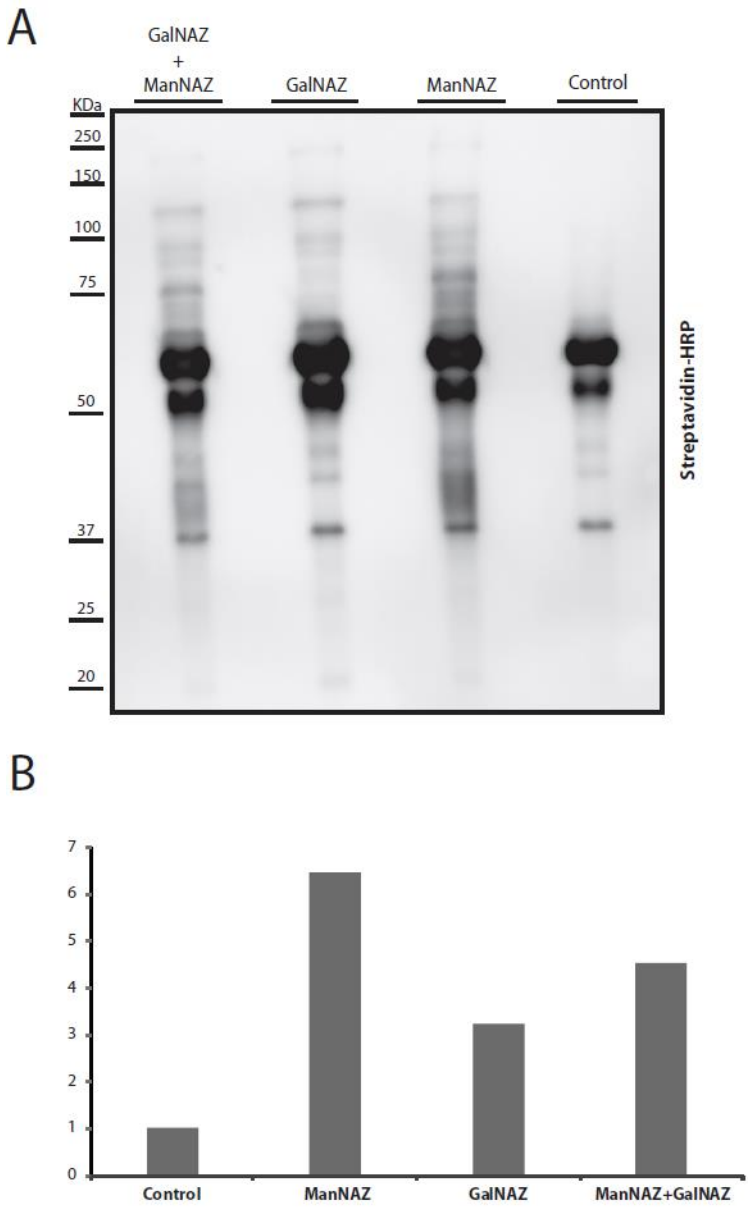

Figure 23. NB4 cell line was metabolically labelled with different azido sugars. (A) Streptavidin-peroxidase detection of biotinylated glycoproteins with WB in conditioned cell culture media supplemented with 100 µM ManNAZ, 100 µM GalNAZ or a combination thereof (B) Quantification of the relative labelling intensity of ManNAZ, GalNAZ and ManNAZ + GalNAZ incubation condition relative to control treated cells.

3.2.3 Application of different buffer and chemicals to reduce unspecific labelling

In the third part of optimization experiment, I tested different buffers and chemicals to reduce non-specific labelling. Tris, IAA and Dimedone were combined as in the table below:

1st	NB4 2ml $4x10^6$ cell 4µl ManNAZ 50mM stock (100µM) + 0.1M Tris pH 7.0 DBCO-Peg12-Biotin	NB4 2ml $4x10^6$ cell DMSO-Control + 0.1 M Tris pH 7.0 DBCO-Peg12-Biotin
2nd	NB4 2ml $4x10^6$ cell 4µl ManNAZ 50mM stock (100µM) + 0.1M IAA + DBCO-Peg12-Biotin	NB4 2ml $4x10^6$ cell DMSO-Control + 0.1M IAA + DBCO-Peg12-Biotin
3rd	NB4 2ml $4x10^6$ cell 4µl ManNAZ 50mM stock (100µM) + 0.1M IAA 0.1MDimedone + DBCO-Peg12-Biotin	NB4 2ml $4x10^6$ cell DMSO-Control + 0.1M IAA 0.1MDimedone + DBCO-Peg12-Biotin

Table 20. Application of different buffer and chemicals to reduce unspecific labelling.

$4x10^6$ NB4 cells were cultured in the presence of 100 µM ManNAZ or DMSO as a solvent control for 48 hours. Afterwards, conditioned media were collected of which 400µl were subjected to small-scale biotinylation with 25 µl of 5 nM DBCO-PEG12-Biotin in the presence of TRIS buffer pH 7.0, after alkylation with IAA or after alkylation with IAA and dimedone (Method 2.2.10). Biotinylated proteins in conditioned media were detected in Western blot with Streptavidin peroxidase (Method 2.2.7). Application of IAA resulted in a slight decrease

of non-specific labelling but for specific labelling, there was a slight decrease as well. Application of dimedone did not reduce non-specific labelling. (Fig.24 A-B). Hence, I decided not to continue with these chemicals in future SPECS experiments for AML cell lines. The old SPECS protocol was used for all AML cell lines (Method 2.2.11).

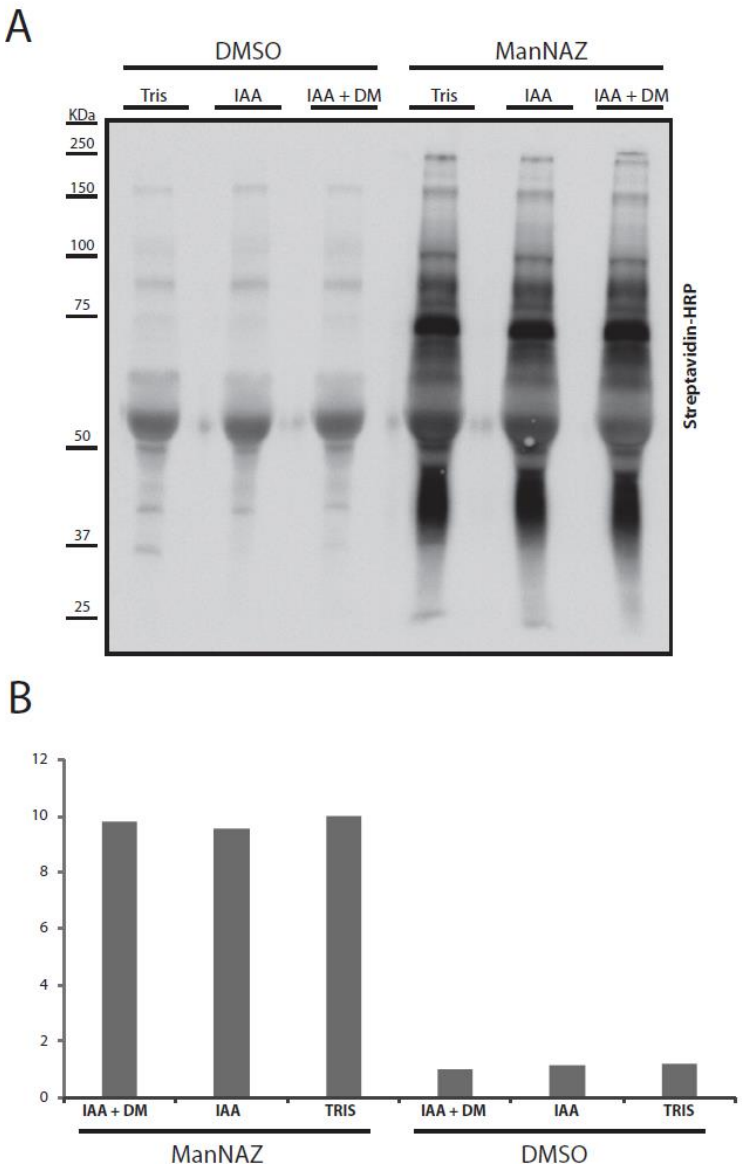

Figure 24. Application of different buffer and chemicals in small scale SPECS experiments. (A) Streptavidin-peroxidase detection of the biotinylated proteins. Conditioned cell culture mediums were supplemented with 100µM of ManNAZ and DMSO as control and cells were incubated for 48 hours. Afterwards cell mediums were collected and treated with 0.1M Tris + DBCO-PEG12-Biotin, 0.1M IAA, 0.1M IAA+ 0.1 Dimedone before the biotinylation reaction. (B) Quantification of the relative labelling intensity of application of Tris, IAA and IAA + Dimedone.

3.2.4 Secretome and Surface Proteome Analysis of different AML cell lines

AML cell lines KG1α, Kasumi, NB4, OCI5, MV4-11 and CMK were cultured in aforementioned conditions (Method 2.1.3) until they reached around $160x10^6$ cells for each cell line in several T75 flasks. Afterwards, cells were collected and $40x10^6$ cells were used for each of the experiments. Three biological replicates were prepared from each AML cell line. These replicates were subjected to the old SPECS (Method 2.2.11) and surface-click protocols (Method 2.2.13). Equal amounts of eluted glycoproteins were loaded on a 10% Tris/Glycine gel according to their protein concentrations and subjected to SDS-page. After Coomassie staining separated proteins and their different distributions became visible (Fig.25).

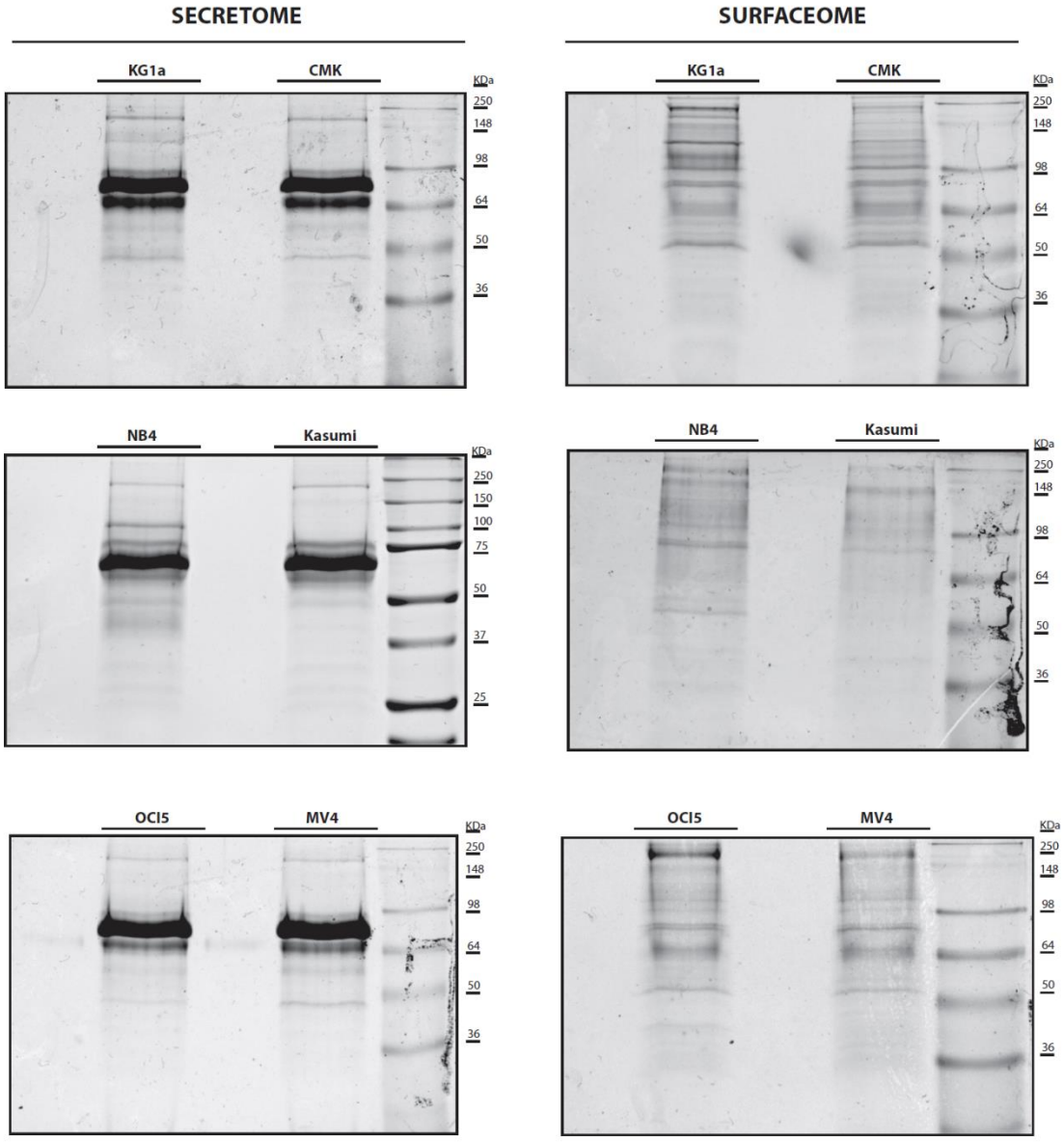

Figure 25. Coomassie staining of the different AML cell line proteomes. $40x10^6$ KG1α, CMK, NB4, Kasumi, OCI5 and MV4-11 cells were cultured in 100µM ManNAZ supplemented conditioned mediums for 48 hours. Afterwards, cell mediums and cells were collected and treated with 100 nmol of DBCO-PEG12-Biotin. After the streptavidin purification of the biotinylated proteins, proteins were loaded on 10% Tris/Glycine gel for SDS-PAGE. Afterwards, gels were subjected to coomassie stainings. Saperated proteins became visible after the distaining step n=3.

Three independent biological replicates for each AML cell lines were analyzed with mass spectrometry (Method 2.2.16) using a LTQ-Velos Orbitrap (14). After MaxQuant analysis, proteins were filtered for potential contaminants and at least two unique peptides (Method 2.2.17). According to UniProt database filter (Glycoprotein, keyword: KW-0325), 699 glycoproteins were identified out of 1078 proteins in the secretome. Topology of the glycoproteins in the secretome were defined as 313 secreted, 227 type-I, 96 type-II, 40 polytopic, 19 GPI and 4 Type-I/GPI (Fig.26 A). Furthermore, secretome data were analysed with Panther and 13% of the hits were assigned to the integrin signalling pathway, 10% to the blood coagulation pathway, 10% to the Wnt signalling pathway, 5 % to the angiogenesis pathway (Fig.27).

Applying the UniProt identifier (Glycoprotein, keyword: KW-0325) as a filter criterion, 949 glycoproteins were identified out of the 5179 proteins in the surface proteome. Topology of glycoproteins in the surface proteome was defined as 449 type I, 195 polytopic, 163 secreted, 97 type II, 38 GPI and 7 TypeI/GPI (Fig.26 B). Glycoproteins of the surface proteome were analysed with the Panther database. 7% of the hits were assigned to the integrin signalling pathway, 6% to the blood coagulation pathway, 5 % to the angiogenesis pathway (Fig.28). Furthermore, different AML cell lines were clustered with Perseus and their relation to each other was depicted in a pedigree chart (Fig29).

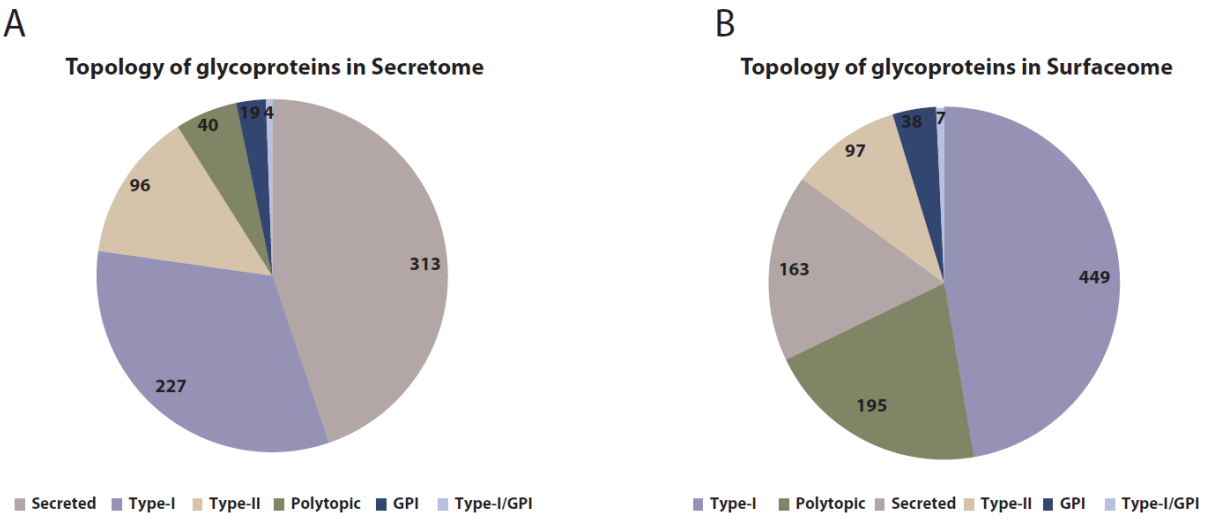

Figure 26. Topology of the glycoproteins in AML cell lines. (A) This graph shows the topology of the glycoproteins in secretome. (B) This graph shows the topology of the glycoproteins in surface proteome.

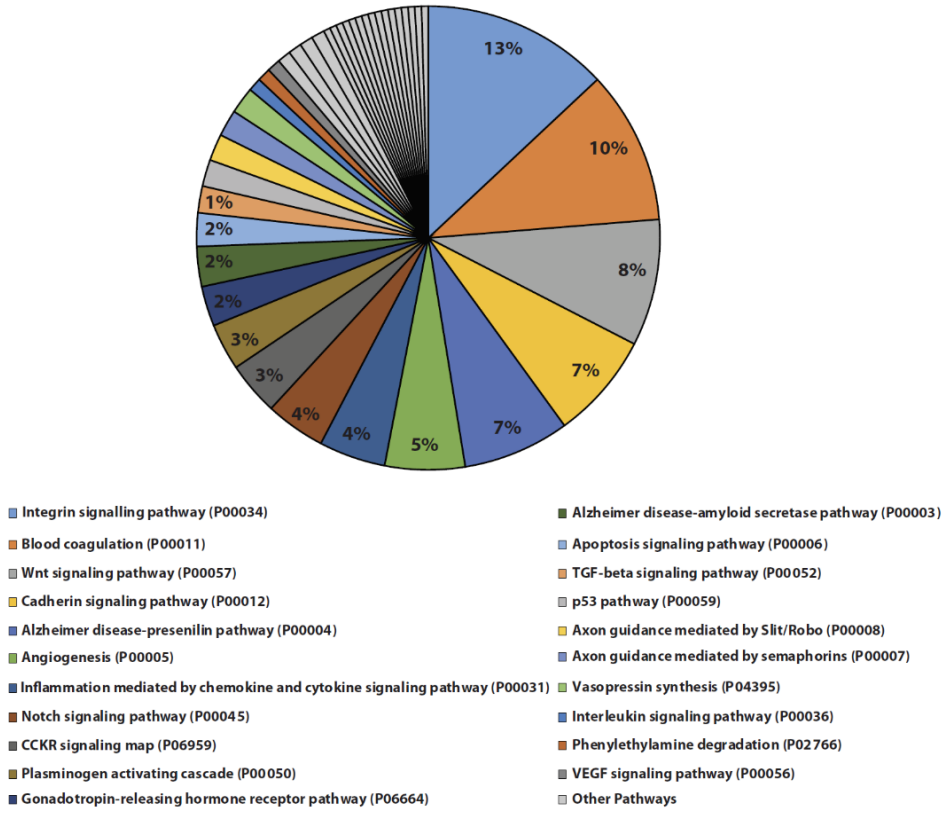

Figure 27. This figure shows GO-Term analysis of glycoproteins to identify pathways covered by secretome analysis of AML cell lines.

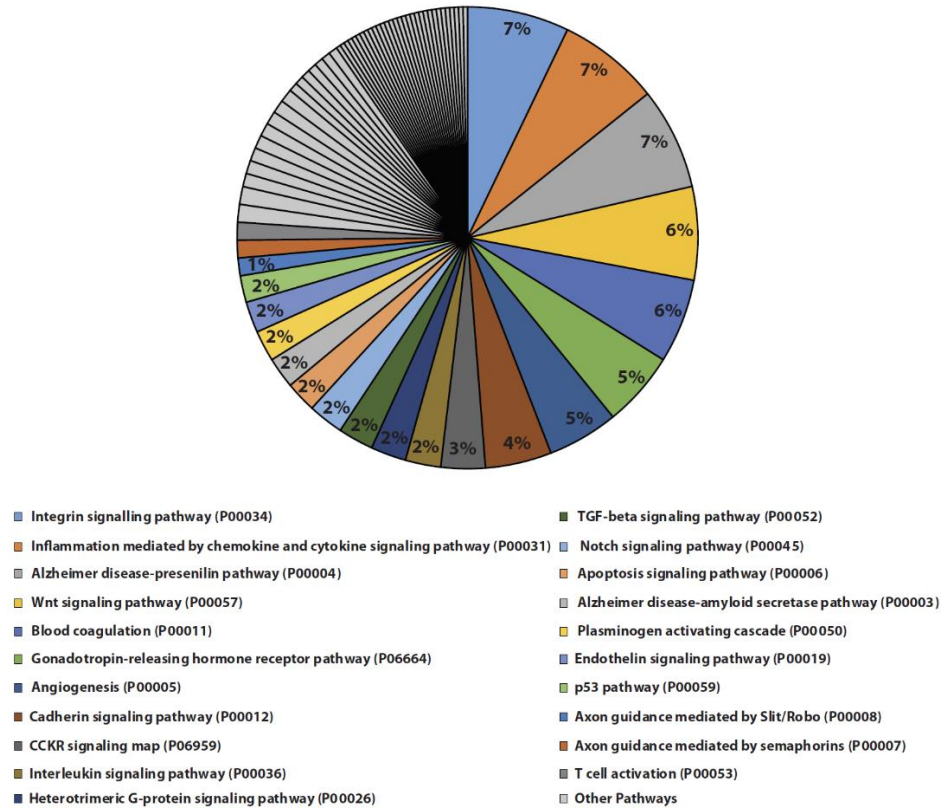

Figure 28. This figure shows GO-Term analysis of glycoproteins to identify pathways covered by surface proteome analysis of AML cell lines.

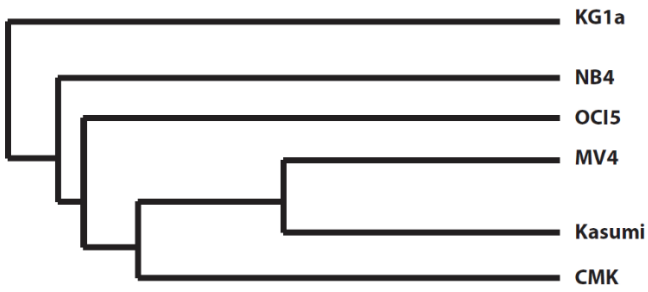

Figure 29. This figure shows cluster analysis of different AML cell lines. (Generated with Perseus)

3.2.5 Receptor Tyrosine Kinase Profiles of different AML cell lines

In particular, I focused on receptor tyrosine kinase profiles of the different AML cell lines. Analysis of the different AML cell lines was performed as mentioned in the method part (Method 2.2.17). Heat maps were created according to highest expression shown in red colour and and less abundant or not detected proteins shown in blue colour. In the surface proteome data 24 different receptor tyrosine kinases were detected. (Fig. 30). NB4 has the generally highest expression of the receptor tyrosine kinases (this might be correlates disease progression and pathology). Insulin growth factor receptor 1-2 were detected in almost every cell lines (Fig. 30, 31) Highest stem cell growth factor receptor (KIT) expression observed in Kasumi and highest Fms like tyrosine kinase (FLT3) expression observed in MV4-11 cell lines. In the secretome data 14 different receptor tyrosine kinases were detected in the medium. (Fig. 31). Highest KIT expression was observed in the Kasumi. Highest expression of Vascular endothelial growth factor receptor 1 (FLT1) was observed in the NB4 cell line but it was not detected in the surface data (Fig. 30, 31) Highest expression of Vascular endothelial growth factor receptor 3 (FLT4) was observed in CMK in both surface and secretome data (Fig. 30, 31). On the other hand, 12 different growth factors were detected in the secretome data (Fig. 32). Growth factor expression was observed mostly in the KG1α cell line (KG1α has stem cell characteristics). Furthermore, these growth factor detections indicated that these cell lines may have an autocrine stimulation. Such as interaction between Angpt1,2-Tie1, CSF1- KIT, VEGFA-FLT1, and HGF-MET interactions (Fig. 30, 31, 32).

RTK profiles of different AML cell lines (Surfaceome)							
Gene names	Peptides	KG1a (M0,M1)	Kasumi (M2)	NB4 (M3)	OCI5 (M4)	MV4 (M5)	CMK (M7)
KIT	30	0.00	1.00	0.00	0.00	0.06	0.00
FLT3	18	0.00	0.34	0.35	0.40	1.00	0.00
FLT4	8	0.00	0.00	0.00	0.00	0.00	1.00
TIE1	10	0.03	0.00	1.00	0.00	0.00	0.43
IGF1R	43	0.00	0.37	1.00	1.00	0.13	0.17
IGF2R	80	0.03	0.36	1.00	0.33	0.53	0.17
RET	27	0.00	0.19	1.00	0.40	0.00	0.01
FGFR1	6	0.00	0.00	0.13	1.00	0.00	0.00
MERTK	14	0.62	0.09	1.00	0.13	0.02	0.06
TYRO3	19	1.00	0.00	0.04	0.40	0.00	0.04
ERBB4	2	0.00	0.00	0.00	0.00	0.00	1.00
EPHA1	4	0.00	0.00	1.00	0.00	0.00	0.00
EPHA4	10	1.00	0.00	0.00	0.00	0.00	0.00
EPHB2	10	0.00	0.00	0.89	0.00	0.00	1.00
EPHB3	11	0.00	0.00	1.00	0.35	0.18	0.00
EPHB4	24	0.01	0.15	1.00	0.01	0.00	0.03
EPHB6	6	0.33	0.00	0.00	1.00	0.00	0.00
INSR	56	0.23	0.65	0.40	0.50	1.00	0.08
CSF1R	14	0.00	0.94	0.74	0.09	1.00	0.00
CSF3R	6	0.03	1.00	0.16	0.00	0.00	0.03
PTK7	39	0.00	0.91	1.00	0.49	0.00	0.48
ROR1	5	1.00	0.00	0.00	0.00	0.00	0.00
ROR2	22	0.00	0.00	1.00	0.00	0.00	0.08
NTRK1	7	0.00	0.00	0.10	0.00	0.00	1.00

Figure 30. This table comprises receptor tyrosine kinase (RTK) profiles of different AML cell lines in surface-proteome. The heat map was generated according to LFQ intensities, highest expression is shown in red colour and lowest expression shown in blue colour.

RTK profiles of different AML cell lines (Secretome)							
Gene names	Peptides	KG1a (M0,M1)	Kasumi (M2)	NB4 (M3)	OCI5 (M4)	MV4 (M5)	CMK (M7)
KIT	9	0.03	1.00	0.12	0.03	0.15	0.31
FLT1	41	0.56	0.00	1.00	0.01	0.00	0.00
FLT4	12	0.00	0.00	0.00	0.00	0.05	1.00
TIE1	15	0.00	0.00	0.11	0.00	0.00	1.00
IGF2R	31	0.24	0.26	1.00	0.34	0.40	0.19
MET	5	0.00	0.00	0.09	0.00	0.00	1.00
MERTK	3	0.00	0.00	1.00	0.00	0.00	0.00
RET	13	0.04	0.00	1.00	0.05	0.00	0.00
FGFRL1	4	0.00	0.00	0.96	1.00	0.00	0.00
MERTK	3	0.00	0.00	1.00	0.00	0.00	0.00
TYRO3	2	0.00	0.00	0.00	0.41	0.00	1.00
CSF1R	5	0.00	0.06	0.06	0.01	1.00	0.00
PTK7	11	0.03	0.28	1.00	0.02	0.09	0.29
NTRK1	3	0.00	0.00	0.00	0.00	0.00	1.00

Figure 31. This table comprises receptor tyrosine kinase (RTK) profiles of different AML cell lines in secretome. According to LFQ intensities heat map was generated, highest expression is shown in red colour and lowest expression shown in blue colour.

Growth Factors profiles of different AML cell lines (Secretome)							
Gene names	Peptides	KG1a (M0,M1)	Kasumi (M2)	NB4 (M3)	OCI5 (M4)	MV4 (M5)	CMK (M7)
VEGFA	3	0.16	0.00	0.06	1.00	0.06	0.00
ANGPT1	24	1.00	0.04	0.02	0.00	0.01	0.17
ANGPT2	35	1.00	0.00	0.00	0.00	0.00	0.00
ANGPTL4	7	0.46	0.00	1.00	0.00	0.00	0.00
HGF	34	1.00	0.00	0.68	0.34	0.00	0.04
CSF1	5	0.03	0.04	0.15	0.00	0.00	1.00
VGF	11	0.00	0.00	1.00	0.00	0.00	0.28
TGFBI	2	1.00	0.00	0.00	0.00	0.00	0.00
PDGFD	15	1.00	0.01	0.10	0.02	0.01	0.16
MEGF8	38	1.00	0.05	0.20	0.16	0.01	0.01
TGFB1	4	0.11	0.53	0.00	0.10	0.00	1.00
PDGFC	6	1.00	0.07	0.29	0.00	0.00	0.13

Figure 32. This table comprises receptor tyrosine kinase ligand (RTKL) profiles of different AML cell lines in secretome. According to LFQ intensities heat map was generated, highest expression is shown in red colour and lowest expression shown in blue colour.

3.2.6 Detection of diagnostic AML reference markers in secretome and surface proteome analysis

Secretome and surface proteome analysis confirmed the immunological expression profile of the AML cell lines provided by DSMZ such as CD33, CD34, CD44, CD7, CD99 (Table 21, Fig. 33, Fig. 34). Furthermore, markers were detected that are already in clinical use for AML diagnostics such as myeloperoxidase (MPO). MPO was detected in the secretome and surface analysis of Kasumi, NB4 and OCI5 (Fig. 33-34). In addition to that, CD34, CD44 are known as leukemia stem cell biomarkers and KG1α which is derived of an AML with M0 subtype with stem cell character showed the highest expression of these proteins (Fig. 33, 34). Therewithal, the Kasumi cell line has the t(8;21) chromosomal translocation,AML1-ETO fusion gene and a described mutant c-KIT (DSMZ No: ACC220). The highest expression of c-KIT was observed in the secretome and surface proteome data of the Kasumi cell line (Fig. 33, 34). On the other hand, MV4-11 cell line has the FLT3-ITD mutation and highest expression of FLT3 was observed in the MV4-11 (Fig. 33, 34).

Cell names	FAB	AML Type	Markers in use
KG1a	(M0,M1)	Acute myeloblastic leukemia with minimal differentiation	CD34,CD44,CD7
Kasumi	(M2)	Acute myeloblastic leukemia with maturation	CD99,KIT
NB4	(M3)	Acute promyelocytic leukemia	FLT1,MPO
OCI5	(M4)	Acute myelomonocytic leukemia	CD33,MPO
MV4	(M5)	Acute monocytic leukemia	FLT3,CD33,MPO-neg
CMK	(M7)	Acute megakaryocytic leukemia	MPO-neg

Table 21. This table comprises biomarkers already established and their correlation with different AML cell lines.

Reference markers on cell surface							
Gene names	Peptides	KG1a (M0,M1)	Kasumi (M2)	NB4 (M3)	OCI5 (M4)	MV4 (M5)	CMK (M7)
CD44	27	1.00	0.37	0.45	0.84	0.69	0.04
CD34	17	1.00	0.12	0.00	0.00	0.01	0.00
MPO	62	0.01	0.40	1.00	0.75	0.00	0.04
CD33	18	0.00	0.64	0.24	0.96	1.00	0.08
CD47	11	0.67	0.17	0.36	1.00	0.24	0.10
CD99	5	0.43	1.00	0.63	0.55	0.73	0.03
KIT	30	0.00	1.00	0.00	0.00	0.06	0.00
CD7	5	1.00	0.00	0.00	0.00	0.00	0.00
FLT3	18	0.00	0.34	0.35	0.40	1.00	0.00
CD166	35	0.71	0.38	0.96	1.00	0.28	0.09
PTPRC	102	0.78	0.21	0.60	1.00	0.54	0.13

Figure 33. This figure shows detected established AML markers on cell surface of AML cell lines. According to LFQ intensities heat map was generated, highest expression is shown in red colour and lowest expression shown in blue colour.

Reference markers in cell media							
Gene names	Peptides	KG1a (M0,M1)	Kasumi (M2)	NB4 (M3)	OCI5 (M4)	MV4 (M5)	CMK (M7)
CD44	15	0.86	0.26	0.53	1.00	0.45	0.06
CD34	8	1.00	0.03	0.00	0.00	0.00	0.00
MPO	81	0.07	0.22	0.44	1.00	0.01	0.09
CD33	4	0.13	0.97	0.83	1.00	0.82	0.00
KIT	9	0.03	1.00	0.12	0.03	0.15	0.31
FLT1	41	0.56	0.00	1.00	0.01	0.00	0.00
FLT3	5	0.08	0.17	0.00	0.00	1.00	0.00
CD166	18	0.30	0.26	1.00	0.45	0.06	0.02
PTPRC	33	1.00	0.08	0.62	0.49	0.20	0.15

Figure 34. This figure shows detected reference markers in the cell media. According to LFQ intensities heat map was generated, highest expression is shown in red colour and lowest expression shown in blue colour.

3.2.7 AML biomarker candidates from secretome and surface proteome data

Confirmation of the differential expression of AML reference markers demonstrated the feasabilitiy of the approach. As the aim of the approach is the identification of soluble biomarkers that allow monitoring disease burden and AML subtype in serum of AML patients we tried to filter for proteins with exclusive expression in the hematopoetic system using proteomicsdb (117). The surface proteome and secretome data of AML cell lines are presented as heat maps (Fig. 35-36). In particular, AML secretome data could provide potential blood-based biomarkers or a novel combination of biomarkers that allow easy monitoring of AML disease load or AML subtype (Fig.35). In the secretome data set, Osteoclast-associated immunoglobulin-like receptor (OSCAR) was identified as the best candidate to be a biomarker for AML irrespective of the AML subtype (Fig. 35). Data of Proteomicsdb show that OSCAR was present in urine, monocytes and proximal fluid (Fig. 37 A). These data show that OSCAR expression is very restricted in the human body and thus may be a good blood-based biomarker candidate to monitor disease burden in AML. Furthermore, CHST14, HS6ST1, COCH, CBLN4, KIT were detected in the secretome of all AML cell lines (Fig. 35-37) and thus may serve as good blood-based biomarkers. Further, I identified some proteins that are highly expressed only in one of the investigated AML cell lines. Hence, these

proteins may serve as blood-based biomarkers to identify and monitor AML subtypes. For example, SLITRK5 is only little expressed in the human body but highly expressed in KG1α cells, a cell line which corresponds to the M0/M1 AML subtype (Fig. 35-36-37B). Further, definition of SLITRK5 as as marker for stem or progenitor cells (US8043803) indicates its applicability for AML. FLT4 shows highest expression in CMK cells, a model cell line for megakaryocytic leukemia and thus may be a potential candidate for identifying and monitoring megakaryocytic leukemia. Further, I identified protein candidates in the surface-proteome data set that are exclusively expressed by only one of the investigated AML cells with minor expression in the rest of the body such as CD200R1 for KG1α, NRXN2 for Kasumi and CHSY1 for NB4 cells (Fig. 36-37). In summary, the secretome and surface proteome data of AML cell lines provide us with a rich source for blood based biomarker candidates to monitor AML. These results need to be validated in primary patient material in the future.

Biomarker Candidates (Secretome)							
Gene names	Peptides	KG1a (M0,M1)	Kasumi (M2)	NB4 (M3)	OCI5 (M4)	MV4 (M5)	CMK (M7)
SLITRK5	23	1.00	0.00	0.01	0.01	0.00	0.16
LRP11	4	1.00	0.00	0.00	0.60	0.00	0.00
CHST14	22	1.00	0.15	0.67	0.53	0.13	0.20
HS6ST1	26	1.00	0.02	0.35	0.14	0.01	0.02
COCH	25	0.29	0.04	1.00	0.01	0.01	0.07
CYTL1	11	0.15	0.01	1.00	0.00	0.00	0.07
PTX4	4	0.00	0.00	1.00	0.54	0.00	0.49
RNASE7	4	0.00	0.00	1.00	0.00	0.00	0.22
PCDH20	11	0.26	0.00	0.00	1.00	0.00	0.00
CHSY1	7	0.67	0.00	0.38	1.00	0.52	0.00
CLSTN2	6	0.00	0.00	0.00	1.00	0.21	0.00
MANEAL	5	0.51	0.00	0.00	1.00	0.00	0.00
CLEC5A	5	0.17	0.00	0.00	1.00	0.00	0.00
OSCAR	7	0.48	0.27	0.40	1.00	0.96	0.13
INHBA	6	0.00	0.00	0.20	0.09	1.00	0.00
CBLN4	2	0.70	0.81	0.42	0.16	1.00	0.34
KIT	9	0.03	1.00	0.12	0.03	0.15	0.31
LRP2	16	0.00	0.00	0.00	0.00	0.00	1.00
TIE1	15	0.00	0.00	0.11	0.00	0.00	1.00
FLT4	12	0.00	0.00	0.00	0.00	0.05	1.00
CSF1	5	0.03	0.04	0.15	0.00	0.00	1.00
HYAL3	4	0.14	0.18	0.62	0.00	0.11	1.00

Figure 35. This figure shows potential AML biomarkers in the secretome that are exclusively expressed by one AML subtypes and are only minor expressed in the body.

Biomarker Candidates (Surfaceome)							
Gene names	Peptides	KG1a (M0,M1)	Kasumi (M2)	NB4 (M3)	OCI5 (M4)	MV4 (M5)	CMK (M7)
SLITRK5	41	1.00	0.01	0.00	0.02	0.00	0.01
SLC8A3	17	1.00	0.00	0.01	0.00	0.00	0.06
TGFBR1	12	1.00	0.05	0.47	0.65	0.28	0.10
IL6R	10	1.00	0.00	0.23	0.14	0.09	0.00
PCDH9	9	1.00	0.00	0.09	0.22	0.00	0.00
STRA6	9	1.00	0.00	0.03	0.00	0.01	0.00
LRRC8B	9	1.00	0.00	0.38	0.41	0.00	0.11
EVI2A	8	1.00	0.23	0.17	0.18	0.51	0.00
FZD5	7	1.00	0.25	0.26	0.18	0.29	0.00
IL2RG	7	1.00	0.02	0.20	0.32	0.00	0.06
HS6ST1	6	1.00	0.00	0.36	0.00	0.00	0.00
CD200R1	4	1.00	0.00	0.00	0.00	0.00	0.00
VSTM1	4	1.00	0.00	0.00	0.00	0.00	0.00
GPR84	12	0.00	0.00	1.00	0.56	0.00	0.01
SLC19A1	12	0.36	0.48	1.00	0.85	0.46	0.18
TIE1	10	0.03	0.00	1.00	0.00	0.00	0.43
CHSY1	9	0.00	0.00	1.00	0.07	0.00	0.00
CD70	8	0.00	0.05	1.00	0.04	0.00	0.20
DSG4	8	0.00	0.00	1.00	0.00	0.00	0.00
SLC5A3	5	0.29	0.18	1.00	0.51	0.39	0.05
CD320	5	0.00	0.00	1.00	0.04	0.04	0.00
IGSF3	25	0.00	0.00	0.20	1.00	0.01	0.21
PLAUR	11	0.59	0.43	0.37	1.00	0.62	0.04
SLC7A11	9	0.44	0.16	0.22	1.00	0.04	0.04
CLEC5A	9	0.00	0.17	0.03	1.00	0.00	0.10
LRFN1	8	0.46	0.33	0.00	1.00	0.00	0.24
TMEM156	7	0.54	0.00	0.88	1.00	0.00	0.00
TRHDE	6	0.00	0.00	0.00	1.00	0.00	0.31
IL31RA	5	0.00	0.00	0.25	1.00	0.00	0.00
LRFN4	11	0.86	0.42	0.51	0.68	1.00	0.00
FCGR1A	9	0.00	0.33	0.14	0.15	1.00	0.00
F2RL3	5	0.00	0.35	0.05	0.00	1.00	0.08
CXCR2	4	0.00	0.63	0.00	0.00	1.00	0.00
KIT	30	0.00	1.00	0.00	0.00	0.06	0.00
SIGLEC12	7	0.00	1.00	0.82	0.00	0.00	0.39
CSF3R	6	0.03	1.00	0.16	0.00	0.00	0.03
NRXN2	4	0.00	1.00	0.00	0.00	0.00	0.00
FLT4	8	0.00	0.00	0.00	0.00	0.00	1.00
CD274	4	0.00	0.00	0.00	0.00	0.00	1.00

Figure 36. This figure shows potential biomarkers in the surface proteome data that individually have minor expression in the body.

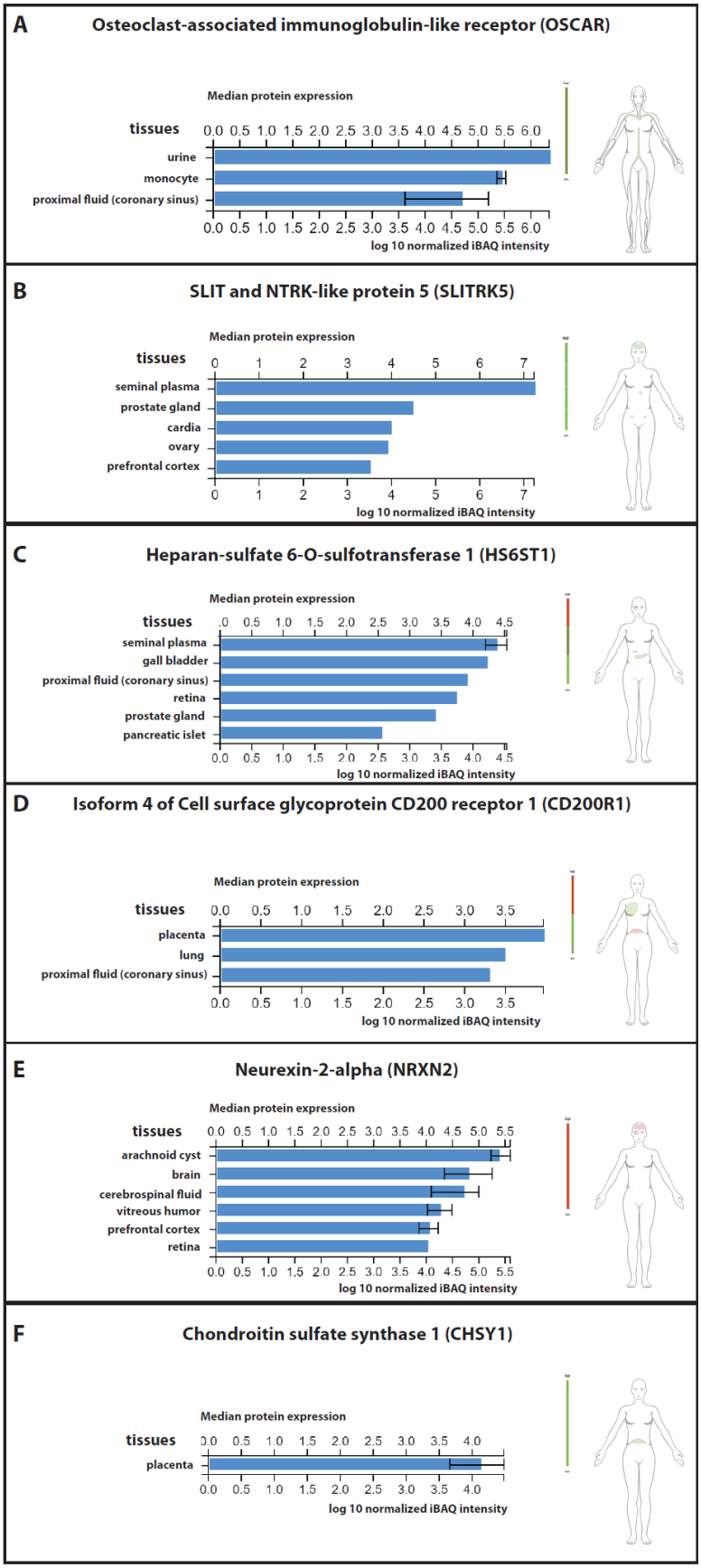

Figure 37. This figure shows some of the biomarker candidates and their expression in the body. (from proteomicsdb (117)).

3.2.8 Biomarker identification in serum of AML patients with MS analysis

Serum is a complex protein mixture with a very high dynamic range that aggravates the analysis with mass spectrometry but may be a source for soluble biomarkers to monitor AML disease burden. Hence, I tried to establish a method that enables the analysis of the AML derived glycoproteome in serum of AML patients. To identify biomarkers that correlate with AML disease load serum of AML patients at diagnosis and after chemotherapy with a complete remission were used for analysis. To reduce dynamic range and complexity of serum samples and enrich for glycoproteins of AML cells, I tried to deplete Immunglobulins and enrich for glycoproteins. To this aim, first Ig fragments were cleaned from serum. 10µl of patient serum were diluted to 500µl with Milli-Q water and incubated with different amounts (0-10-15-30-40-50-70-90-100µl) of G-sepharose as mentioned in the method part (Method 2.2.14). Western blot analysis was performed with Anti-Human IgG. The blot showed that 70µl of G sepharose are required for depletion of immunglobulins in 10 µl serum (Fig.38A). Afterwards, glycoproteins were biotinylated with Alkoxyamine-Peg4-Biotin as mentioned in the method part (Method 2.2.14). Biotinylation efficiency of glycoproteins was checked with Streptavidin-peroxidase (Fig.38B).

After these initial experiments, 75µl of serum samples were used for preparation of mass spectrometry measurements. According to initial experiments G-sepharose was scaled up to 525 µl and the protocol was applied as mentioned in the method part (Method 2.2.14). Patient serum samples at initial diagnosis of AML and complete remission were prepared for MS analysis (Table 22) and measured with an LTQ-Velos Pro Orbitrap. Data were analysed with MaxQuant (Method 2.2.17).

patient 1, sample number	status of the disease	cytogenetics	molecular genetics
69	initial diagnosis AML	*normal karyotype*	RUNX1-, SF3B1-mutation
148	AML, primary refractory,after salvage chemotherapy in complete remission	*normal karyotype*	RUNX1-, SF3B1-mutation

patient 2, sample number	status of the disease	cytogenetics	molecular genetics
84	initial diagnosis AML	47,XY,+8(15)/46,XY(6)	*no known mutations*
159	AML, after consolidation I, complete remission	47,XY,+8(15)/46,XY(6)	*no known mutations*

Table 22. Serum sample numbers, status of the disease, cytogenetics and mutations.

According to UniProt database filter (Glycoprotein, keyword: KW-0325), 190 glycoproteins were identified out of 325 identified proteins in the serum samples demonstrating that glycoprotein enrichment with aminooxybiotin worked. Glycoproteins were classified according their topology as 141 secreted, 34 type-I, 10 polytopic, 3 type-II and 2 GPI-anchored proteins (Fig.39). Furthermore, glycoproteins were classified with the Panther database according their function demonstrating that 37% of identified glycoproteins were involved in the blood coagulation pathway, 10% were involved in the plasminogen activating cascade while 8% of glycoproteins were involved in Wnt and Cadherin signalling pathways (Fig.40). Although the majority of identified glycoproteins originated from the liver, we identified AML biomarkers with differential expression at initial diagnosis of AML and complete remission. For example, myeloperoxidase was decreased 3.5-fold between serum with initial AML diagnosis and serum after chemotherapy with complete remission of the first patient (sample numbers 69-148). In patient 2, myeloperoxidase was decreased 3.6-fold between initial diagnosis of AML and complete remission after chemotherapy (sample numbers 84-159). Furthermore, high fold-changes were observed for CD44 antigen between AML initial

diagnosis and complete remission after chemotherapy, with an 11.7-fold decrease in patient 1 and a 14.5-fold in patient 2 (Table 23).

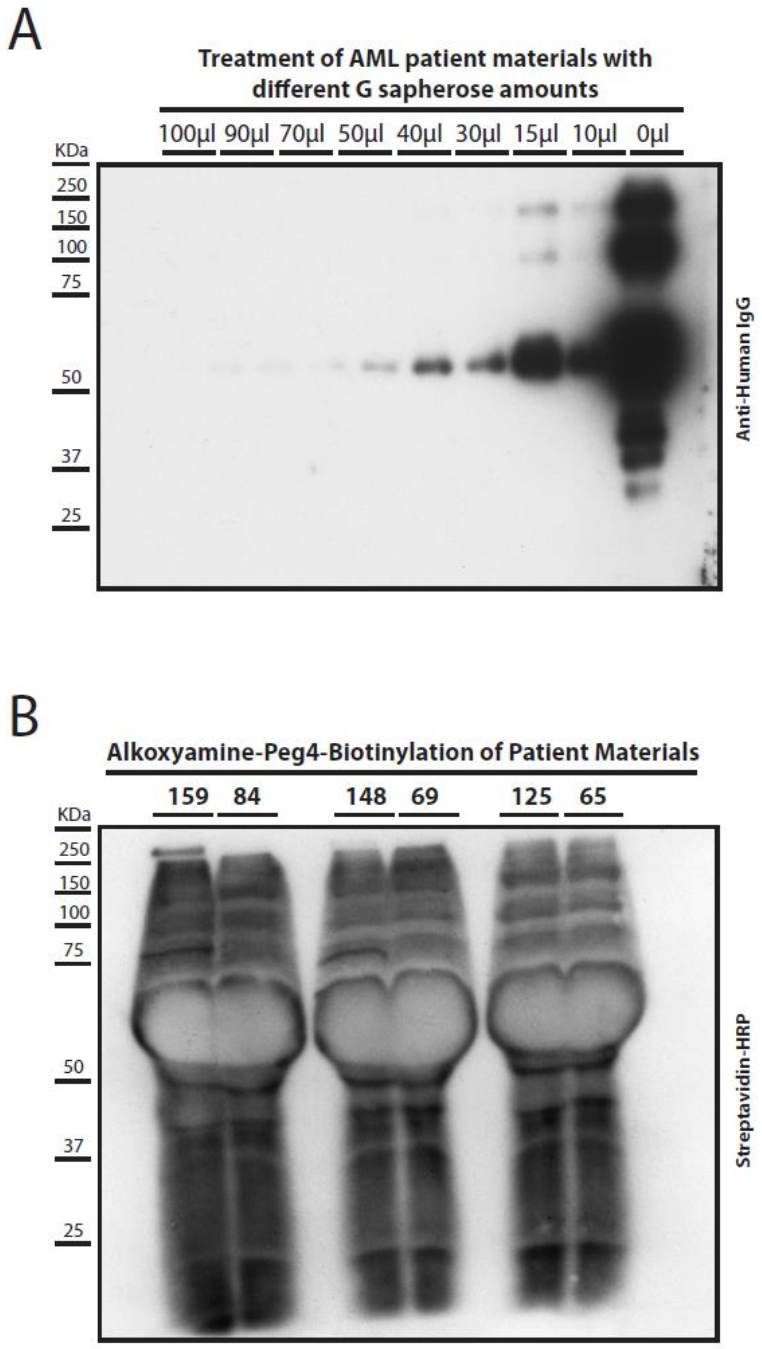

Figure 38. Serum sample preparations steps for MS. A. 10µl of human serum samples were treated with 0µl, 10µl, 15µl,30µl, 40µl, 50µl, 70µl,90µl and 100 µl of G sepharose. Antihuman IgG blot was used to detect remaining IgG in samplesafter treatment. B. After immunglobulin depletion with G sepharose treatment, serum samples were incubated with 250 nmol of aminooxybiotin,20mM phenylenediamine and 1mM sodium periodate in PBS buffer pH 6.7 at 4°C and in the dark for 1 hour. Afterwards biotinylation of glycoproteins was determined with WB-streptavidin-peroxidase. Sample numbers indicate samples of patients at initial diagnosis of AML (65, 69, 84) and corresponding samples after therapy with refactory disease (125) or complete remission (148, 159).

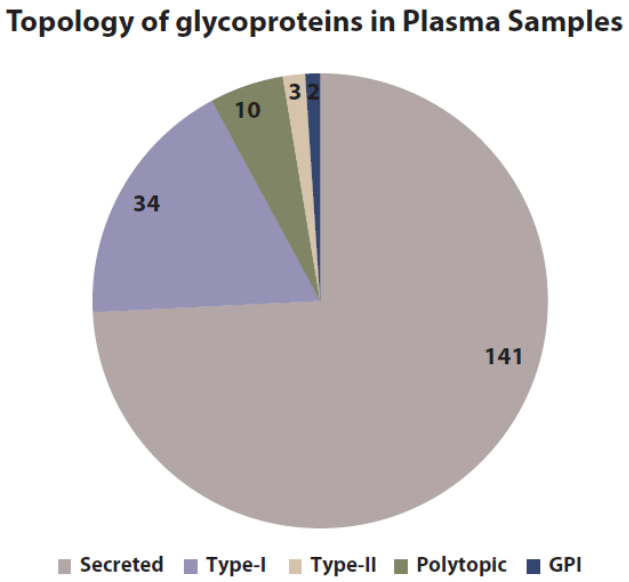

Figure39. This graph shows the topology of identified glycoproteins in the serum samples.

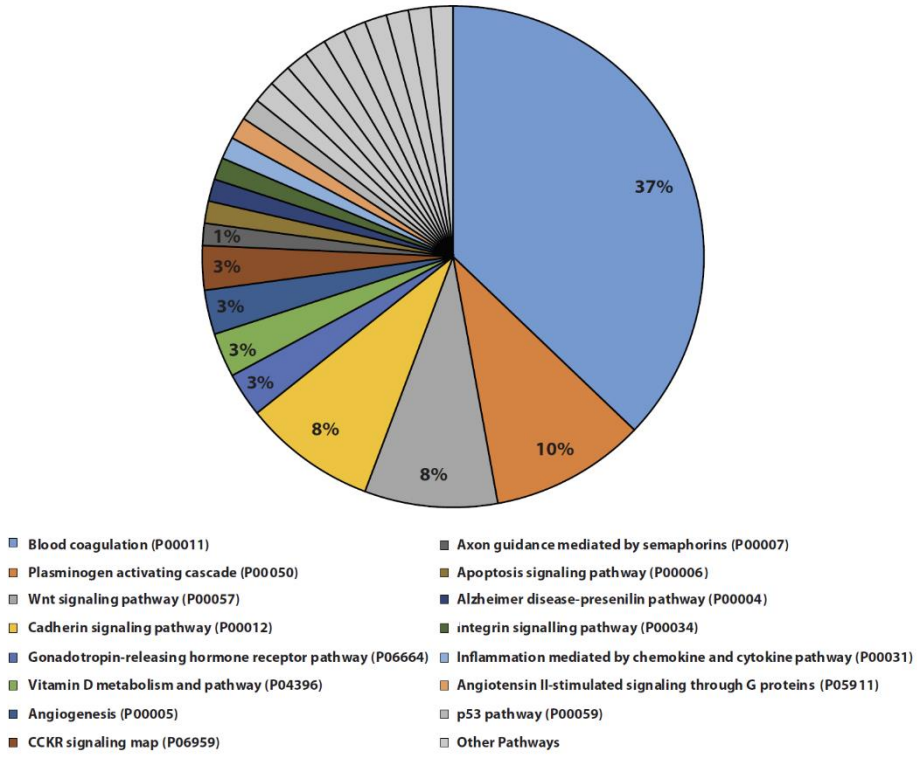

Figure 40. This figure shows the GO-Term analysis with Panther of identified glycoproteins to identify pathways covered by serum sample analysis.

Initial diagnosis (ID) vs complete remission (CR)					
Protein Names	Gene Names	LFQ-ID/CR (69/148)	LFQ-ID/CR (84/153)	Avarage FC	Variance
Myeloperoxidase	MPO	3.59	3.68	3.64	2.27E-05
CD44 antigen	CD44	11.74	14.59	13.17	1.38E-04
Cell surface glycoprotein MUC18	MCAM	1.58	1.53	1.56	2.68E-04
C4b-binding protein beta chain	C4BPB	12.06	22.75	17.40	7.59E-04
Carboxypeptidase N catalytic chain	CPN1	3.83	4.76	4.30	1.31E-03
Coagulation factor XIII A chain	F13A1	1.65	3.61	2.63	5.38E-02
Vitronectin	VTN	1.64	3.72	2.68	5.78E-02
Complement C1q subcomponent subunit A	C1QA	2.20	9.05	5.63	5.90E-02
Secretogranin-3	SCG3	1.87	5.45	3.66	6.16E-02

Table 23. This table shows the fold change of the LFQ values of the specific proteins in between samples with initial diagnosis (ID-69,84) and complete remissions (CR-84,153).

3.3 Identification of resistance mechanism in AML

3.3.1 Sorafenib inhibition experiment in MV4-11 cells in small scale

Sorafenib is a multi-kinase inhibitor that has the potential to stop leukemic blast cell proliferation in AML. However, successful reduction of blast numbers in FLT3-ITD driven AML with Sorafenib is only of short duration as AML blasts develop resistance towards Sorafenib. As resistance of AML blasts towards Sorafenib can be driven by manifold mechanisms, I analyzed the secretome and the surface proteome of the MV4-11 cell line with an FLT3-ITD mutation in response to Sorafenib to test the following hypotheses: (1) Increased expression of alternative receptor tyrosine kinases that are not targeted by Sorafenib or increased expression of other proteins that activate the PI3-Kinase, AKT pathway and MAP-kinase pathway (2), Downregulation of proapoptotic pathways (3) Upregulation of transporters that promote Sorafenib efflux out of the cell, downregulation of transporters that promote Sorafenib influx into the cell. As a first experiment, $2x10^6$ MV4-11 cells each were cultured in RPMI media supplemented with 2.5nM, 5nM, 10nM or20nM of Sorafenib for 2 days and phosphorylation status of FLT3 was checked with FLT3 phosphorylation specific antibodies. Phosphorylation intensity of FLT3 was reduced 13%, 55%, 70% and 88% with 2.5nM, 5nM, 10nM and 20nM Sorafenib treatment respectively (Fig.41 A-B-C). We decided to continue with 5nM and 10nM of Sorafenib treatment in the following SPECS experiments.

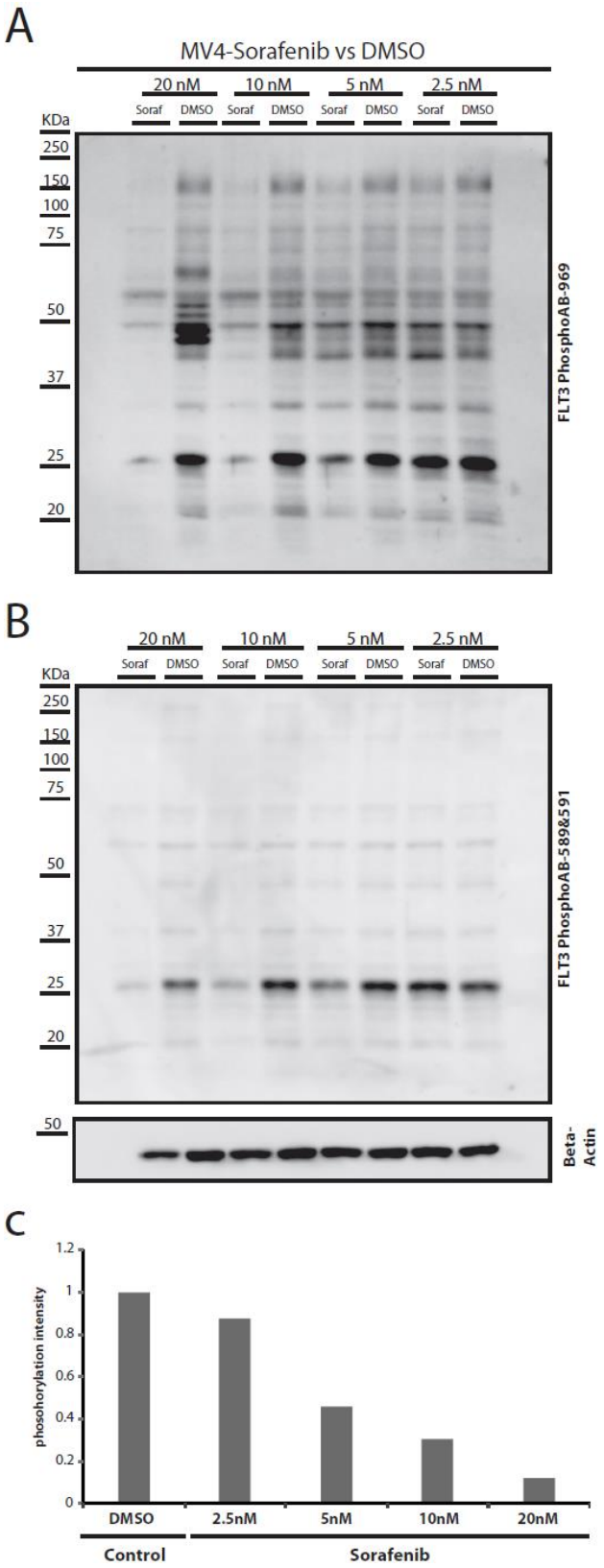

Figure 41. This figure shows preliminary experiment of Sorafenib treatment of MV4-11 cell line. A. $2x10^6$ cells were cultured in cell medium supplemented with 2.5nM, 5nM, 10nM, 20nM of Sorafenib. After two days cells were collected and checked with FLT3-PhosphoAB (969). B. $2x10^6$ cells were cultured in cell medium supplemented with 2.5nM, 5nM, 10nM, 20nM of Sorafenib. After two days cells were collected and checked with FLT3-PhosphoAB (589-591). C. This graph shows the quantification of the average FLT3 phosphorylation

intensity of the all technical replicates from blots A and B with 2.5nM, 5nM, 10nM, 20nM Sorafenib and DMSO control.

3.3.2 Sorafenib inhibition experiment with MV4-11 cell line and SPECS application

Before SPECS experiments, $2x10^6$ MV4-11 cells were cultured in RPMI media supplemented with 5 nM or 10 nM of Sorafenib or DMSO as control and cells were cultured for two weeks chronically until they reached the required numbers for SPECS application (Method 2.2.11) (Fig.42). SPECS and surface-click procedures were performed for three biological replicates of each experiment (Method 2.2.11-2.2.13). 5nM and 10nM-Sorafenib treated MV4-11 cells and resepective control cells were subjected to secretome and surface proteome analysis (Method 2.2.16-2.2.17).

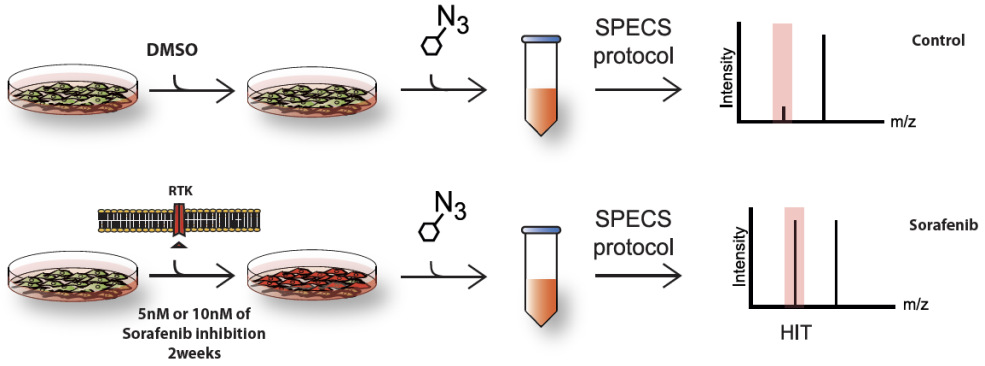

Figure 42. Workflow of the sorafenib and dmso treatments for 2 weeks, metabolic glycan labelling, SPECS protocols and quantification and identification of captured proteins via mass spectrometry.

According to the UniProt database filter (Glycoprotein, keyword: KW-0325), 467 glycoproteins were identified out of overall identified 2331 proteins in the surface proteome analysis of 5nM Sorafenib and respective DMSO treated samples. Comparing LFQ intensities of all glycoproteins between Sorafenib and DMSO treated cells I identified 29 significantly increased and 41 significantly decreased glycoproteins (Fig.43). In the analysis of 10nM Sorafenib and respective DMSO treated MV4-11 cells 314 glycoproteins were identified out of the 910 proteins in surface proteome analysis. In this analysis, considering LFQ intensities show that 11 glycoproteins were significantly increased and 27 glycoproteins were significantly decreased (Fig.44)

Comparison between LFQ intensities of 5nM-Sorafenib replicates versus control replicates show that 6-fold increase for FLT3, 5-fold increase for TNFRSF1B, 2.4-fold increase for ICAM3, 5-fold increase for NCAM2, 3.6-fold increase for SLC38A10, 5.6-fold increase for SLC19A1 and 1.4-fold increase for CD44 (Fig. 43, Table 24). Furthermore, PLXNA1 expression was decreased 4.6 fold, NCAM1 expression was decreased 21 fold, PTPRC expression was decreased 1.5 fold and PTPRJ expression was decreased 1.4 fold (Fig. 43, Table 25). On the other hand, comparison between LFQ intensities of 10nM-Sorafenib replicates versus control replicates show that, NCAM2 expression was increased 8-fold, CD84 expression was increased 14-fold, FLT3 expression was increased 3.6-fold, ICAM3 expression was increased 5.8-fold and CSF1R expression was increased 2.7-fold (Fig. 44, Table 26).

Secretome analysis of 5nM-Sorafenib versus DMSO treated Mv4-11 cells as control led to the identification of344 glycoproteins out of 1071 total identified proteins. LFQ intensities showed that 4 glycoproteins were significantly increased. A 3.4- fold increase was observed for FLT3 (Fig45, Table28). Furthermore, secretome analysis of 10nM-Sorafenib treated Mv4-11 cells versus control cells resulted in the identification of233 glycoproteins out of 860 total identified proteins. According to LFQ intensity change 65 glycoproteins were significantly changed and 5 of them significantly increased. LFQ intensity of FLT3 was increased 3.1-fold but not significant close to border line (Fig46, Table30).

In general, results indicated that increased glycoproteins were mostly related to survival and proliferation pathways or decreased glycoproteins were releated to anti-apoptotic pathways. These results gave a first idea how cells are escaping Sorafenib treatment.

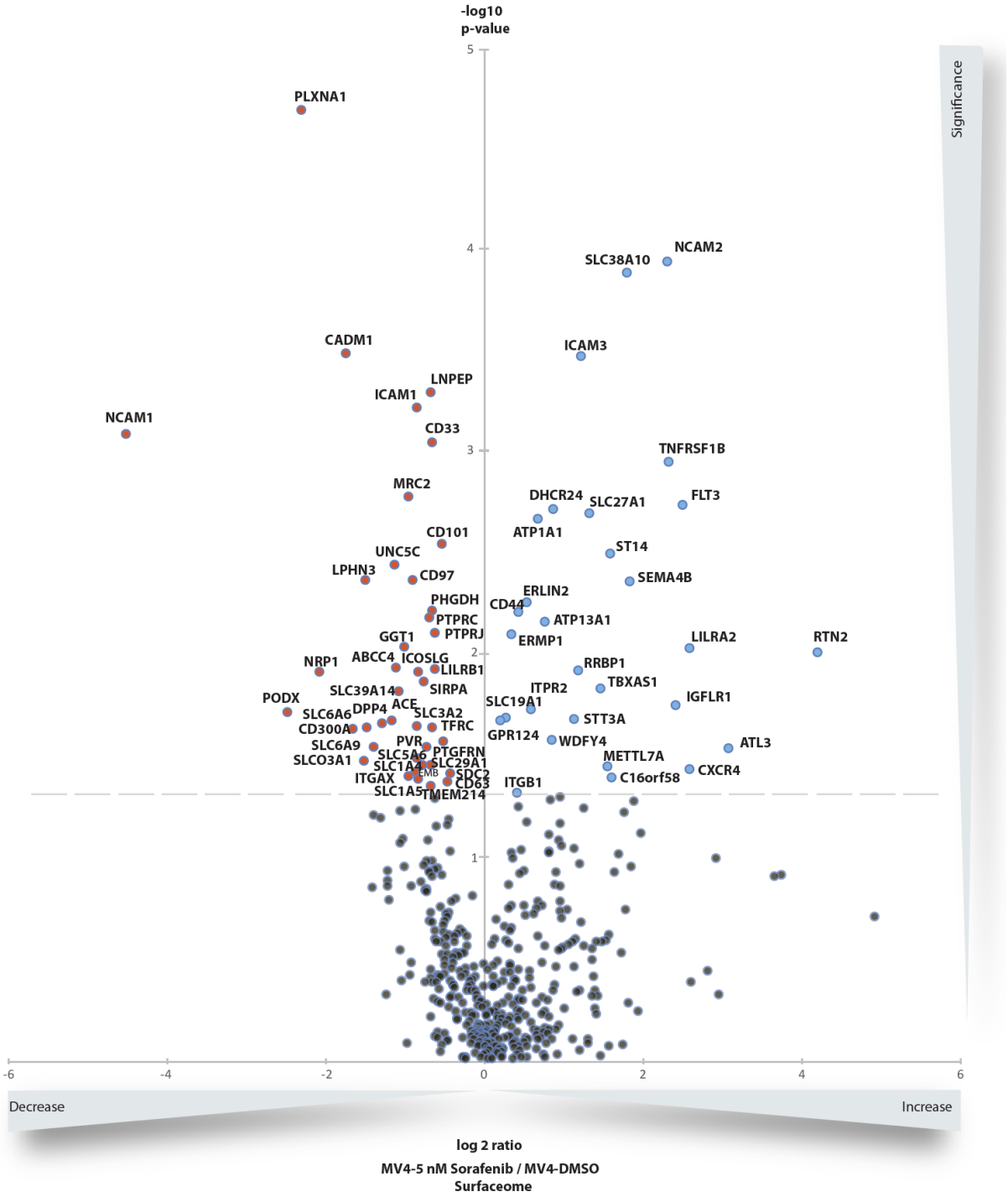

Figure 43. Quantitative surface proteome comparison between 5nM-Sorafenib versus DMSO treated cells with volcano plot. 3 biological replicates were considered for the analysis and p value depicted as negative logarithm while the fold change (MV4-11-5nM Sorafenib/MV4-11-DMSO) is depicted as $\log_2$ value. Significantly changed proteins depicted as: $p \leq 0.05$ ($-\log_{10} \geq 1.3$). Significantly increased glycoproteins according to Uniprot keywords shown in blue and significantly decreased glycoproteins shown in red colour.

Significantly Increased Glycoproteins in Surfaceome (5nM-Sorafenib/Control-DMSO)				
Protein names	**Gene names**	**Peptides**	**Fold change-Sorafenib/Control**	**TTEST**
Neural cell adhesion molecule 2	NCAM2	30	5.22	1.16E-04
Putative sodium-coupled neutral amino acid transporter 10	SLC38A10	13	3.68	1.32E-04
Intercellular adhesion molecule 3	ICAM3	13	2.46	3.39E-04
Tumor necrosis factor receptor superfamily member 1B	TNFRSF1B	5	5.35	1.13E-03
Receptor-type tyrosine-protein kinase FLT3	FLT3	23	6.01	1.85E-03
Delta(24)-sterol reductase	DHCR24	10	1.93	1.94E-03
Long-chain fatty acid transport protein 1	SLC27A1	18	2.65	2.04E-03
Sodium/potassium-transporting ATPase subunit alpha-1	ATP1A1	40	1.70	2.16E-03
Suppressor of tumorigenicity 14 protein	ST14	6	3.18	3.23E-03
Semaphorin-4B	SEMA4B	4	3.80	4.42E-03
Erlin-2	ERLIN2	21	1.55	5.58E-03
CD44 antigen	CD44	20	1.42	6.27E-03
Manganese-transporting ATPase 13A1	ATP13A1	15	1.80	6.98E-03
Endoplasmic reticulum metallopeptidase 1	ERMP1	29	1.35	8.06E-03
Leukocyte immunoglobulin-like receptor subfamily A member 2	LILRA2	5	6.39	9.40E-03
Reticulon-2	RTN2	6	19.56	9.94E-03
Ribosome-binding protein 1	RRBP1	19	2.41	1.21E-02
Thromboxane-A synthase	TBXAS1	6	2.94	1.48E-02
IGF-like family receptor 1	IGFLR1	3	5.63	1.79E-02
Inositol 1,4,5-trisphosphate receptor type 2	ITPR2	17	1.59	1.89E-02
Folate transporter 1	SLC19A1	7	1.29	2.08E-02
Dolichyl-diphosphooligosaccharide-STT3A	STT3A	21	2.32	2.09E-02
G-protein coupled receptor 124	GPR124	25	1.23	2.14E-02
WD repeat- and FYVE domain-containing protein 4	WDFY4	8	1.91	2.69E-02
Atlastin-3	ATL3	9	8.98	2.94E-02
Methyltransferase-like protein 7A	METTL7A	5	3.10	3.58E-02
C-X-C chemokine receptor type 4	CXCR4	3	6.41	3.69E-02
RUS1 family protein C16orf58	C16orf58	11	3.22	4.09E-02
Integrin beta-1	ITGB1	36	1.42	4.85E-02

Table 24. This table shows significantly increased glycoproteins in surface proteome 5nM Sorafenib treated samples versus DMSO as control. LFQ intensities of 3 biological replicates were considered in fold change and $\log_2$ transformed LFQ intensities were considered for ttest. Significantly changed proteins depicted as: $p \leq 0.05$.

Significantly Decreased Glycoproteins in Surfaceome (5nM-sorafenib/Control-DMSO)				
Protein names	Gene names	Peptides	Fold change-Sorafenib/Control	TTEST
Plexin-A1	PLXNA1	31	0.22	2.09E-05
Cell adhesion molecule 1	CADM1	12	0.32	3.29E-04
Leucyl-cystinyl aminopeptidase	LNPEP	24	0.67	5.16E-04
Intercellular adhesion molecule 1	ICAM1	23	0.59	6.07E-04
Neural cell adhesion molecule 1	NCAM1	17	0.05	8.31E-04
Myeloid cell surface antigen CD33	CD33	10	0.67	9.14E-04
C-type mannose receptor 2	MRC2	29	0.55	1.68E-03
Immunoglobulin superfamily member 2	CD101	27	0.73	2.88E-03
Netrin receptor UNC5C	UNC5C	15	0.49	3.65E-03
Latrophilin-3	LPHN3	34	0.37	4.30E-03
CD97 antigen	CD97	17	0.56	4.32E-03
D-3-phosphoglycerate dehydrogenase	PHGDH	23	0.67	6.15E-03
Receptor-type tyrosine-protein phosphatase C	PTPRC	69	0.66	6.65E-03
Receptor-type tyrosine-protein phosphatase eta	PTPRJ	35	0.69	7.91E-03
Gamma-glutamyltranspeptidase 1	GGT1	13	0.52	9.25E-03
Multidrug resistance-associated protein 4	ABCC4	20	0.49	1.18E-02
Leukocyte immunoglobulin-like receptor subfamily B member 1	LILRB1	18	0.69	1.19E-02
ICOS ligand	ICOSLG	4	0.59	1.22E-02
Neuropilin-1	NRP1	9	0.25	1.23E-02
Tyrosine-protein phosphatase non-receptor type substrate 1	SIRPA	23	0.62	1.38E-02
Zinc transporter ZIP14	SLC39A14	4	0.50	1.53E-02
Podocalyxin	PODXL	9	0.19	1.94E-02
Angiotensin-converting enzyme	ACE	3	0.47	2.14E-02
Dipeptidyl peptidase 4	DPP4	6	0.43	2.21E-02
4F2 cell-surface antigen heavy chain	SLC3A2	29	0.59	2.27E-02
Sodium- and chloride-dependent taurine transporter	SLC6A6	4	0.38	2.30E-02
Transferrin receptor protein 1	TFRC	31	0.67	2.32E-02
CMRF35-like molecule 8	CD300A	5	0.34	2.34E-02
Prostaglandin F2 receptor negative regulator	PTGFRN	40	0.74	2.72E-02
Poliovirus receptor	PVR	9	0.64	2.89E-02
Sodium- and chloride-dependent glycine transporter 1	SLC6A9	2	0.40	2.90E-02
Sodium-dependent multivitamin transporter	SLC5A6	7	0.59	3.30E-02
Solute carrier organic anion transporter family member 3A1	SLCO3A1	2	0.37	3.40E-02
Neutral amino acid transporter A	SLC1A4	10	0.62	3.53E-02
Equilibrative nucleoside transporter 1	SLC29A1	9	0.66	3.54E-02
Embigin	EMB	6	0.58	3.82E-02
Syndecan-2	SDC2	12	0.79	3.91E-02
Integrin alpha-X	ITGAX	8	0.55	4.02E-02
CD63 antigen	CD63	2	0.59	4.14E-02
Transmembrane protein 214	TMEM214	10	0.77	4.28E-02
Neutral amino acid transporter B(0)	SLC1A5	15	0.67	4.50E-02

Table 25. This table shows significantly decreased glycoproteins in the surface proteome of 5nM Sorafenib treated MV4-11 cells versus DMSO treated MV4-11 cells as a control. LFQ intensities of 3 biological replicates were considered in fold change and $\log_2$ transformed LFQ intensities were considered for ttest. Significantly changed proteins depicted as: $p \leq 0.05$.

Figure 44. Quantitative surface proteome comparison between 10nM-Sorafenib versus DMSO treated cells with volcano plot. 3 biological replicates were considered for the analysis and p-value depicted as negative decadic logarithm while the fold change (MV4-11-10nM Sorafenib/MV4-11-DMSO) is depicted as $\log_2$ value. Significantly changed proteins depicted as: $p \leq 0.05$ ($-\log_{10} \geq 1.3$). Significantly increased glycoproteins according to Uniprot keywords shown in blue and significantly decreased glycoproteins shown in red colour.

Significantly Increased Glycoproteins in Surfaceome (10nM-sorafenib/Control-DMSO)				
Protein names	**Gene names**	**Peptides**	**Fold change-Sorafenib/Control**	**TTEST**
Neural cell adhesion molecule 2	NCAM2	19	8.36	4.48E-04
Neuroplastin	NPTN	4	2.32	4.04E-03
SLAM family member 5	CD84	5	14.43	6.43E-03
Receptor-type tyrosine-protein kinase FLT3	FLT3	15	3.64	6.93E-03
Leucine-rich repeat-containing protein 25	LRRC25	4	3.13	8.32E-03
Nodal modulator 1	NOMO1	2	2.80	8.36E-03
Platelet glycoprotein 4	CD36	10	2.20	1.10E-02
Intercellular adhesion molecule 3	ICAM3	6	5.87	2.83E-02
Macrophage colony-stimulating factor 1 receptor	CSF1R	7	2.74	4.26E-02
Single Ig IL-1-related receptor	SIGIRR	8	1.68	4.38E-02
Amyloid-like protein 2	APLP2	3	6.93	4.56E-02

Table 26. This table shows significantly increased glycoproteins in surface proteome, 10nM Sorafenib treated samples versus DMSO as control. LFQ intensities of 3 biological replicates were considered in fold change and log_2 transformed LFQ intensities were considered for ttest. Significantly changed proteins depicted as: $p \leq 0.05$.

Significantly Decreased Glycoproteins in Surfaceome (10nM-sorafenib/Control-DMSO)				
Protein names	**Gene names**	**Peptides**	**Fold change-Sorafenib/Control**	**TTEST**
Endothelin-converting enzyme 1	ECE1	5	0.03	3.64E-04
ICOS ligand	ICOSLG	4	0.31	8.17E-04
Tumor necrosis factor receptor superfamily member 6	FAS	5	0.02	1.87E-03
Plexin-D1	PLXND1	16	0.47	4.46E-03
Neural cell adhesion molecule 1	NCAM1	11	0.01	6.90E-03
Interleukin-1 receptor accessory protein	IL1RAP	25	0.59	7.16E-03
Neuropilin-1	NRP1	6	0.03	8.23E-03
Gamma-glutamyltranspeptidase 1	GGT1	11	0.49	1.13E-02
Chloride intracellular channel protein 1	CLIC1	3	0.04	1.25E-02
78 kDa glucose-regulated protein	HSPA5	8	0.06	1.28E-02
Gamma-glutamyltransferase 5	GGT5	7	0.02	1.50E-02
Solute carrier family 43 member 3	SLC43A3	3	0.48	1.53E-02
Integrin alpha-L	ITGAL	38	0.60	2.15E-02
CD209 antigen	CD209	11	0.08	2.30E-02
Carboxypeptidase M	CPM	5	0.13	2.70E-02
Cell adhesion molecule 1	CADM1	10	0.22	2.75E-02
Nectin-2	PVRL2	6	0.44	3.01E-02
Podocalyxin	PODXL	10	0.38	3.44E-02
Endoglin	ENG	9	0.48	3.51E-02
Solute carrier family 2	SLC2A5	3	0.25	3.56E-02
Myeloid cell surface antigen CD33	CD33	8	0.63	3.57E-02
Adenylate cyclase type 3	ADCY3	2	0.28	3.61E-02
Poliovirus receptor	PVR	5	0.43	3.63E-02
Neutral amino acid transporter A	SLC1A4	6	0.68	3.95E-02
Equilibrative nucleoside transporter 1	SLC29A1	8	0.17	4.56E-02
Plexin-A1	PLXNA1	20	0.03	4.83E-02
Neutral amino acid transporter B(0)	SLC1A5	12	0.50	4.99E-02

Table 27. This table shows significantly decreased glycoproteins in surface proteome, 10nM sorafenib treated samples versus DMSO as control. LFQ intensities of 3 biological replicates were considered in fold change and log_2 transformed LFQ intensities were considered for ttest. Significantly changed proteins depicted as: $p \leq 0.05$.

Figure 45. Quantitative secretome comparison between 5nM-Sorafenib versus DMSO treated cells with volcano plot. 3 biological replicates were considered for the analysis and p value depicted as negative logarithm while the fold change (MV4-11-5nM Sorafenib/MV4-11-DMSO) is depicted as $\log_2$ value. Significantly changed proteins depicted as: $p \leq 0.05$ ($-\log_{10} \geq 1.3$). Significantly increased glycoproteins according to Uniprot keywords shown in blue and significantly decreased glycoproteins shown in red colour.

Significantly Increased Glycoproteins in Secretome (5nM-Sorafenib/Control-DMSO)				
Protein names	**Gene names**	**Peptides**	**Fold change-Sorafenib/Control**	**TTEST**
Nardilysin	NRD1	3	3.50	1.32E-03
Receptor-type tyrosine-protein kinase FLT3	FLT3	8	3.42	1.80E-02
Xaa-Pro dipeptidase	PEPD	14	1.45	4.78E-02
Tripeptidyl-peptidase 1	TPP1	8	3.44	5.17E-02

Table 28. This table shows significantly increased glycoproteins in secretome, 5nM Sorafenib treated samples versus DMSO as control. LFQ intensities of 3 biological replicates were considered in fold change and log_2 transformed LFQ intensities were considered for ttest. Significantly changed proteins depicted as: p≤0.05.

Significantly Decreased Glycoproteins in Secretome (5nM-sorafenib/Control-DMSO)				
Protein names	**Gene names**	**Peptides**	**Fold change-Sorafenib/Control**	**TTEST**
Carbohydrate sulfotransferase 14	CHST14	5	0.37	5.47E-07
Testican-1;Testican-3	SPOCK1	2	0.24	5.99E-07
Galectin-3-binding protein	LGALS3BP	13	0.19	1.00E-06
Sulfhydryl oxidase 1	QSOX1	36	0.40	2.24E-06
C-type lectin domain family 11 member A	CLEC11A	33	0.50	3.54E-05
Multiple inositol polyphosphate phosphatase 1	MINPP1	7	0.05	5.10E-05
Amyloid beta A4 proteinsecretase C-terminal fragment 59	APP	6	0.20	5.65E-05
Angiotensin 1-4	AGT	8	0.05	7.78E-05
Clusterin;Clusterin alpha chain;Clusterin beta chain	CLU	11	0.02	1.50E-04
Chitinase-3-like protein 1	CHI3L1	23	0.22	2.48E-04
Ribonuclease T2	RNASET2	10	0.50	4.04E-04
Cell growth regulator with EF hand domain protein 1	CGREF1	8	0.42	5.28E-04
Serglycin	SRGN	8	0.43	9.08E-04
Alpha-dystroglycan;Beta-dystroglycan;Dystroglycan	DAG1	14	0.39	9.86E-04
Calsyntenin-1;CTF1-alpha;Soluble Alc-alpha	CLSTN1	36	0.53	1.07E-03
45 kDa calcium-binding protein	SDF4	19	0.40	1.10E-03
Metalloproteinase inhibitor 1	TIMP1	6	0.39	1.31E-03
Alpha-2-macroglobulin receptor-associated protein	LRPAP1	10	0.67	1.86E-03
EMILIN-2	EMILIN2	25	0.27	1.88E-03
Neutrophil elastase	ELANE	7	0.25	2.46E-03
Pigment epithelium-derived factor	SERPINF1	19	0.51	2.55E-03
Leucine-rich alpha-2-glycoprotein	LRG1	14	0.43	2.77E-03
Azurocidin	AZU1	13	0.67	5.30E-03
Vitamin K-dependent protein S	PROS1	4	0.24	6.03E-03
Carbohydrate sulfotransferase 11	CHST11	12	0.14	8.81E-03
Carbohydrate sulfotransferase 10	CHST10	4	0.29	9.36E-03
Lymphocyte antigen 75	LY75	4	0.24	9.86E-03
Epididymis-specific alpha-mannosidase	MAN2B2	4	0.52	1.09E-02
Melanotransferrin	MFI2	6	0.20	1.15E-02
Nucleobindin-1	NUCB1	31	0.52	1.48E-02
Attractin	ATRN	44	0.56	1.67E-02
Alpha-1,6-mannosylglycoprotein 6-beta-N-acetylglucosaminyltransferase A	MGAT5	11	0.22	1.99E-02
Plexin-B2	PLXNB2	18	0.55	2.06E-02
Receptor-type tyrosine-protein phosphatase gamma	PTPRG	2	0.41	2.61E-02

Table 29. This table shows significantly decreased glycoproteins in secretome, 5nM Sorafenib treated samples versus DMSO as control. LFQ intensities of 3 biological replicates were considered in fold change and log_2 transformed LFQ intensities were considered for ttest. Significantly changed proteins depicted as: p≤0.05.

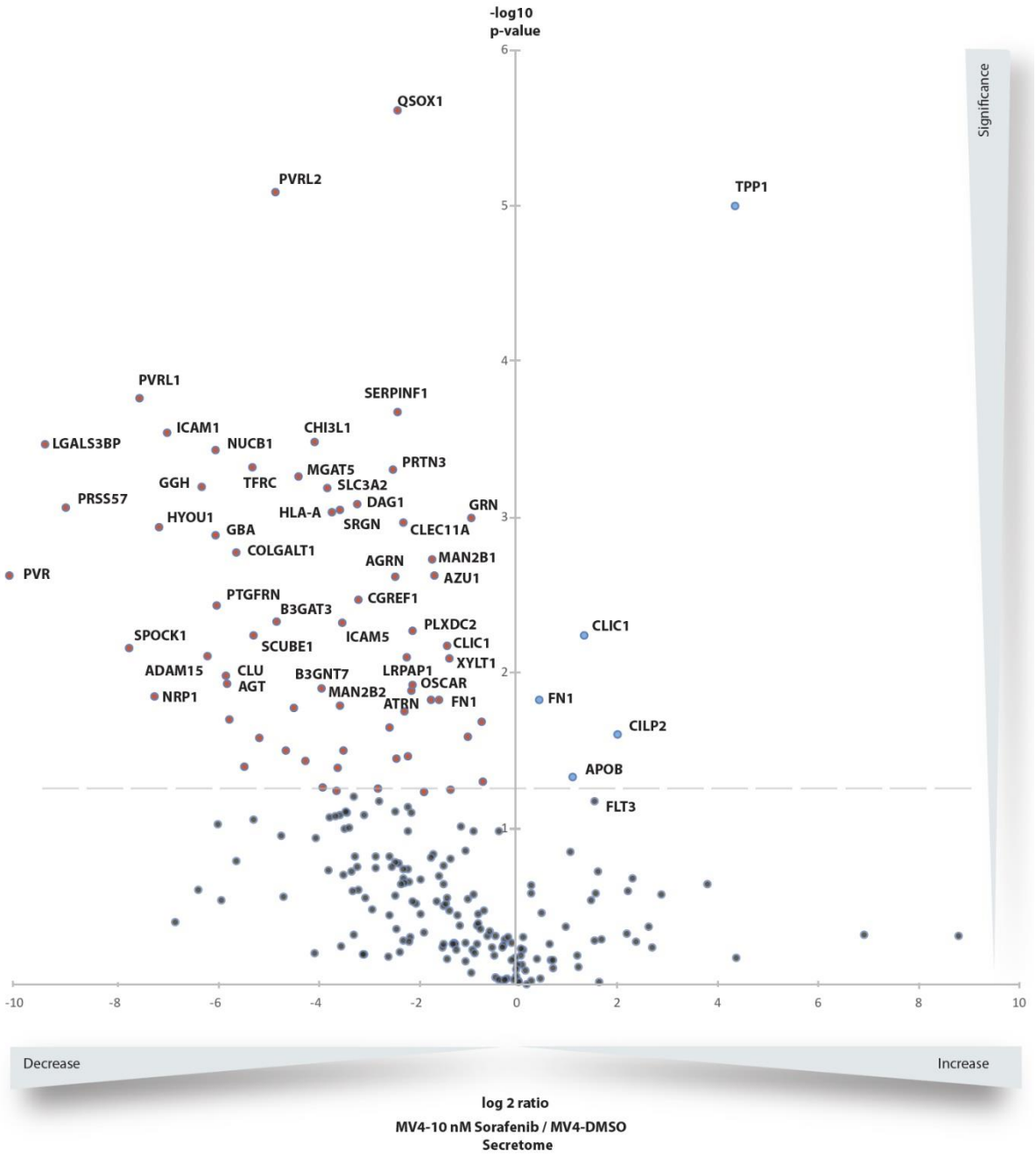

Figure 46. Quantitative secretome comparison between 10nM-Sorafenib versus DMSO treated cells with volcano plot. 3 biological replicates were considered for the analysis and p value depicted as negative logarithm while the fold change (MV4-11-10nM Sorafenib/MV4-11-DMSO) is depicted as $\log_2$ value. Significantly changed proteins depicted as: $p \leq 0.05$ ($-\log_{10} \geq 1.3$). Significantly increased glycoproteins according to Uniprot keywords shown in blue and significantly decreased glycoproteins shown in red colour.

Significantly Increased Glycoproteins in Secretome (10nM-Sorafenib/Control-DMSO)				
Protein names	**Gene names**	**Peptides**	**Fold change-Sorafenib/Control**	**TTEST**
Tripeptidyl-peptidase 1	TPP1	4	21.51	9.93E-06
Chloride intracellular channel protein 1	CLIC1	12	2.69	5.70E-03
Fibronectin;Anastellin	FN1	12	1.45	1.49E-02
Cartilage intermediate layer protein 2	CILP2	2	4.26	2.48E-02
Apolipoprotein B-100;Apolipoprotein B-48	APOB	6	2.31	4.67E-02

Table 30. This table shows significantly increased glycoproteins in secretome, 10nM Sorafenib treated samples versus DMSO as control. LFQ intensities of 3 biological replicates were considered in fold change and log_2 transformed LFQ intensities were considered for ttest. Significantly changed proteins depicted as: p≤0.05.

Significantly Decreased Glycoproteins in Secretome (10nM-Sorafenib/Control-DMSO)				
Protein names	**Gene names**	**Peptides**	**Fold change-Sorafenib/Control**	**TTEST**
Sulfhydryl oxidase 1	QSOX1	32	0.21	2.42E-06
Nectin-2	PVRL2	4	0.04	8.16E-06
Nectin-1	PVRL1	2	0.01	1.72E-04
Pigment epithelium-derived factor	SERPINF1	16	0.21	2.12E-04
Intercellular adhesion molecule 1	ICAM1	6	0.01	2.85E-04
Chitinase-3-like protein 1	CHI3L1	20	0.07	3.31E-04
Galectin-3-binding protein	LGALS3BP	10	0.00	3.39E-04
Nucleobindin-1	NUCB1	24	0.02	3.69E-04
Transferrin receptor protein 1;Transferrin receptor pr	TFRC	10	0.03	4.75E-04
Myeloblastin	PRTN3	6	0.19	4.96E-04
Alpha-1,6-mannosylglycoprotein 6-beta-N-acetylgluc	MGAT5	9	0.05	5.51E-04
Gamma-glutamyl hydrolase	GGH	7	0.01	6.38E-04
4F2 cell-surface antigen heavy chain	SLC3A2	11	0.08	6.51E-04
Dystroglycan;Alpha-dystroglycan;Beta-dystroglycan	DAG1	11	0.12	8.21E-04
Serine protease 57	PRSS57	4	0.00	8.72E-04
Serglycin	SRGN	6	0.09	8.95E-04
HLA class I histocompatibility antigen	HLA-A	5	0.08	9.30E-04
Granulins;Acrogranin	GRN	22	0.57	1.02E-03
C-type lectin domain family 11 member A	CLEC11A	26	0.22	1.08E-03
Hypoxia up-regulated protein 1	HYOU1	9	0.01	1.16E-03
Glucosylceramidase	GBA	5	0.02	1.30E-03
Procollagen galactosyltransferase 1	COLGALT1	4	0.02	1.69E-03
Lysosomal alpha-mannosidase;	MAN2B1	24	0.33	1.85E-03
Azurocidin	AZU1	12	0.34	2.35E-03
Poliovirus receptor	PVR	4	0.00	2.36E-03
Agrin;Agrin N-terminal 110 kDa subunit	AGRN	37	0.20	2.40E-03
Cell growth regulator with EF hand domain protein 1	CGREF1	8	0.12	3.38E-03
Prostaglandin F2 receptor negative regulator	PTGFRN	5	0.02	3.71E-03
Galactosylgalactosylxylosylprotein 3-beta-glucuronos	B3GAT3	5	0.04	4.65E-03
Intercellular adhesion molecule 5	ICAM5	2	0.10	4.80E-03
Plexin domain-containing protein 2	PLXDC2	6	0.25	5.41E-03
Signal peptide, CUB and EGF-like domain-containing p	SCUBE1	5	0.03	5.79E-03
Alpha-2-macroglobulin receptor-associated protein	LRPAP1	7	0.41	6.74E-03
Testican-1	SPOCK1	2	0.01	6.89E-03
Disintegrin and metalloproteinase domain-containing	ADAM15	4	0.01	7.82E-03
Osteoclast-associated immunoglobulin-like receptor	OSCAR	5	0.25	1.20E-02

Table 31. This table shows significantly decreased glycoproteins in secretome, 10nM Sorafenib treated samples versus DMSO as control. LFQ intensities of 3 biological replicates were considered in fold change and log_2 transformed LFQ intensities were considered for ttest. Significantly changed proteins depicted as: p≤0.05.

3.3.3 WB analysis of Sorafenib treated MV4-11 cells versus control

To further corroborate the results of the SPECS analysis and to learn more about the FLT3 phosphorylation status I performed a novel experiment. Three biological replicates of MV4-11 cells were treated with 5nM-Sorafenib or DMSO for 2 weeks (Method 2.1.5). Afterwards, $2x10^6$ cells were treated with 5nM-Sorafenib for three days. Western blot analysis of thereof generated cell lysates with the phospho-specific FLT3 antibody (Tyr589-591) revealed a 30% reduction in FLT3 phosophorylation of Sorafenib treated samples compared to DMSO treated samples. However, FLT3 expression was increased 5-fold in Sorafenib treated samples (Fig. 47, B). TNFR2 expression increased 20% as observed in the mass spectrometry experiment (Fig47. A, C, E, G). Mild reduction of FLT3 phosporylation after three days of incubation with 5 nM Sorafenib revealed that FLT3 phosphorylation was almost at wild type levels. Beta-actin blot was used as loading control (Fig47. G)

To better understand FLT3 expression and phosphorylation status with respect to chronic and acute Sorafenib treatment, MV4-11 cells were either cultured for 2 weeks in the presence of 5nM Sorafenib or DMSO (Method 2.1.5). Afterwards, chronically treated $2x10^6$ MV4-11 cells and wild type $2x10^6$ MV4-11 cells were cultured either in the presence of 5nM sorafenib or DMSO as a control in 6-well format for one day (chronic vs acute Sorafenib effect). After one day of incubation, FLT3 expression and FLT3 phosphorylation status were analysed in chronically and acutely treated MV4-11 cells with Western blot (Fig.48). Western blot results revealed that wild type MV4-11 cells acutely treated with 5 nM Sorafenib showed 14-fold increased FLT3 protein levels compared to DMSO treated wild type MV4-11 cells (Fig.48, A-B). Furthermore, chronicly-Sorafenib treated MV4-11 cells acutely treated with 5 nM Sorafenib and DMSO for one day showed a respective 15-fold and 12-fold increase in FLT3 protein levels compared to DMSO treated wild-type MV4-11 cells. This result revealed that increased FLT3 protein levels in chronically remained high and were only mildly reduced after 24 hours of Sorafenib withdrawal (Fig48. A-B). Analysis of FLT3 phosphorylation status of chronically and wild type MV4-11 cells acutely treated with 5 nM Sorafenib for one day revealed that FLT3 phosporylation was abolished in both situations. However, Sorafenib withdrawal in chronically treated MV4-11 cells led to a 6-fold higher phosphorylation compared to DMSO treated wild type MV4-11 cells (Fig48. C-D). Beta-actin was used as a loading control (Fig48. E)

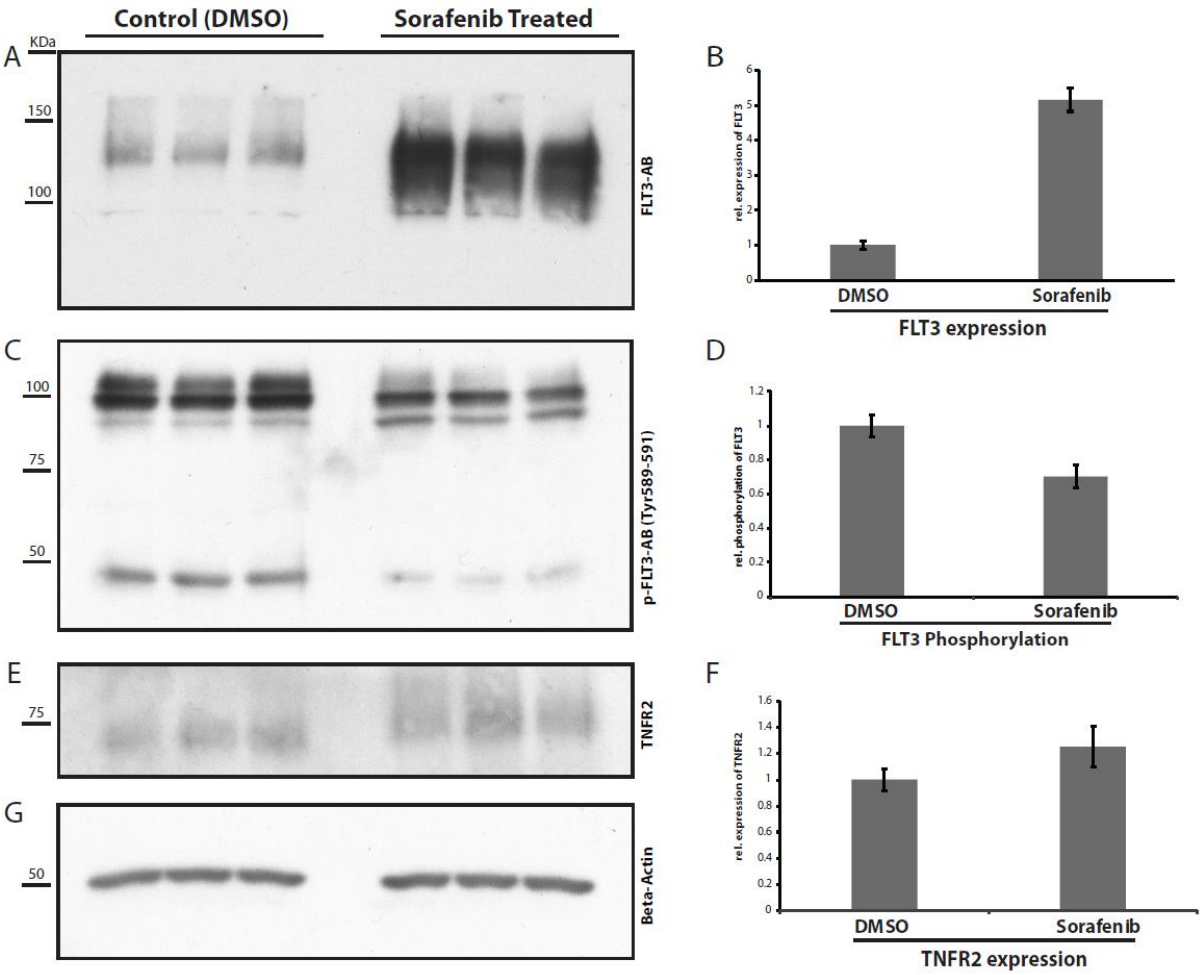

Figure 47. Western Blot analysis of 5nM Sorafenib treated vs control cells. MV4-11 cells were cultured for 2 weeks with 5nM Sorafenib or DMSO. Afterwards, generated resistance cells and control cells were cultured additional 3 days in the RPMI medium supplemented with 5nM Sorafenib in 6 well format. After the treatment, cells were lysate and western blot analysis was done in following. (A) Anti- FLT3 antibody was used for blotting. (C) Phospho-FLT3 antibody (Tyr589-591) was used for blotting. (E) Anti-TNFR2 antibody was used for blotting. (G) Beta-Actin blotting was used as loading control. (B, D, F) These figures shows the quantification of the relative expression intensities of FLT3, pFLT3 and TNFR2. Measurement was done for 3 biological replicates (n=3).

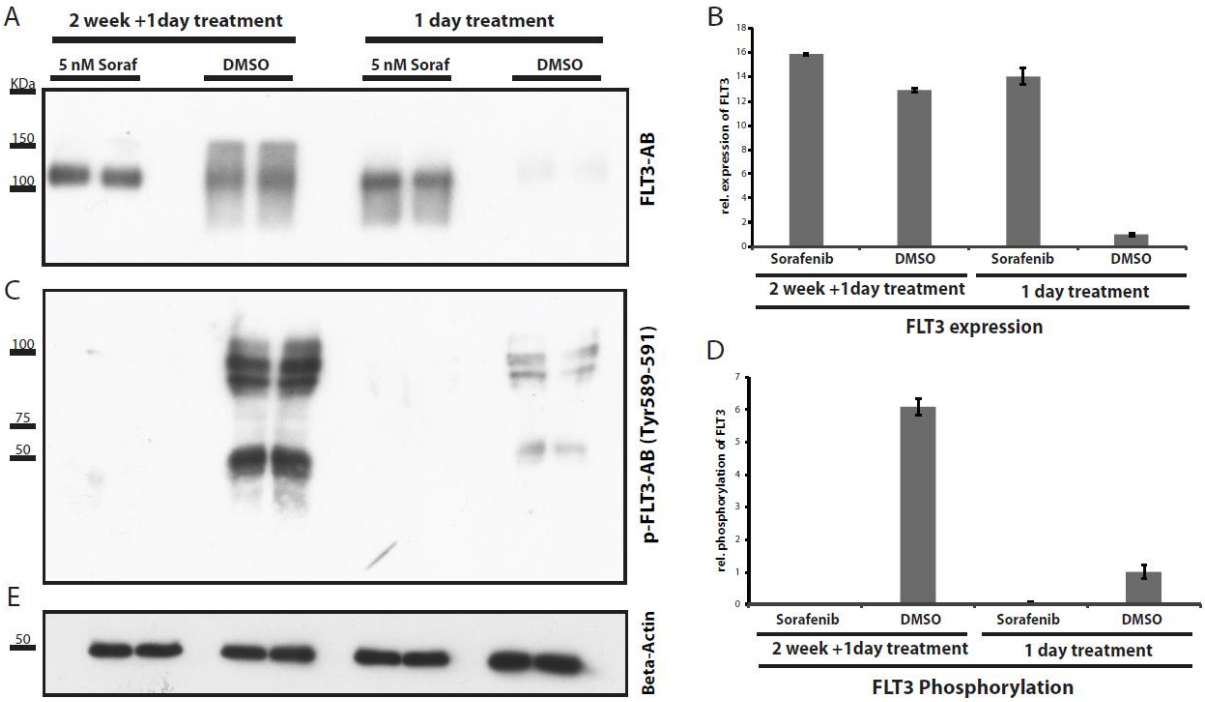

Figure 48. Western Blot analysis of 5nM Sorafenib treated vs control cells. MV4-11 cells were cultured for 2 weeks with 5nM Sorafenib or DMSO. Afterwards, generated resistance cells and control cells were cultured additional 1 day in the RPMI medium supplemented with 5nM Sorafenib in 6 well format. In parallel, wild type Mv4-11 cells were directly cultured for 1 day inside the 5nM Sorafenib and dmso as control. After the treatment, cells were lysed down and western blot analysis was done in following. (A) Anti- FLT3 antibody was used for blotting. (C) Phospho-FLT3 antibody (Tyr589-591) was used for blotting. (E) Beta-Actin blotting was used as loading control. (B, D) These figures shows the quantification of the relative expression intensities of FLT3 and pFLT3. Measurements was done for 2 biological replicates (n=4).

3.4 Identification of RTK biology via specific knock-outs

3.4.1 Establishment of CRISPR-Cas9 gene knock-out on KIT and FLT3

As one part of the project, the CRISPR-Cas9 system should be established to generate knock-outs for receptor tyrosine kinases FLT3 and c-kit in AML cell lines. These experiments were supposed to add additional information on FLT3 and c-Kit kinase biology. As Sorafenib is a multiple tyrosine kinase inhibitor (RTK) and thus targets multiple kinases such as c-raf, B-raf, VEGFR-1,-2,-3, PDGFRβ, FGFR1 and c-kit besides FLT3 we wanted to learn more about the consequences of a specific FLT3/c-kit knockout on the proteomic level in MV4-11/Kasumi cells. C-Kit and FLT3 are frequently mutated receptor tyrosine kinases in AML (42, 118). To this aim, sgRNAs specific for c-Kit and FLT3 exon sites were designed and subcloned into a lentiviral vector (Method 2.4.1). Surface profiling of AML cell lines showed that Kasumi and MV4-11 cells have the highest expressions of KIT and FLT3 (Fig.30).

Firstly, HEK293T, NB4, OCI5, Kasumi and MV4-11 cell lines were transduced with the Cas9-Blasticidine vector and selected with Blasticidine to learn more about expression efficiency of the lentiviral Cas9 vector in the different cell lines (119). After 2 days of transduction, cells were incubated with 10µg/ml of blasticidine for 1 week to select for Cas9 expression. Every two days, medium was exchanged with fresh medium supplemented with 10µg/ml of blasticidine. Afterwards, selected cells were subjected to lysis and western blot analysis of

Cas9 expression with the Cas9 specific antibody (14697, Cell Signaling). Western blot of all cell lines revealed that Cas9 was robustly expressed (Fig.49-50).

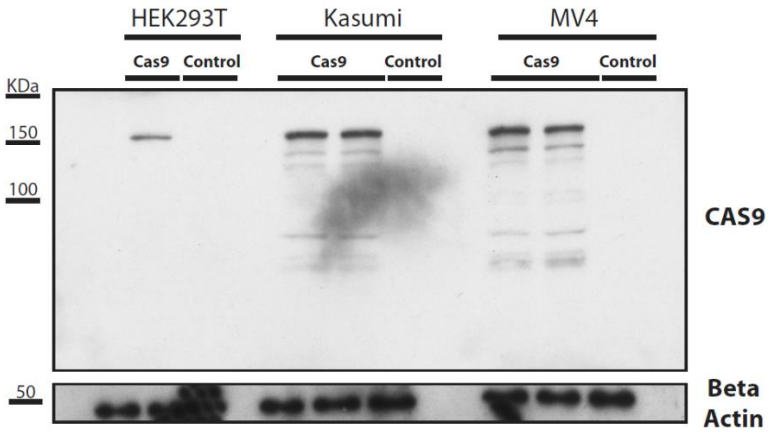

Figure 49. This figure shows the western blot analysis of Cas9 expression in MV4-11, Kasumi and HEK293T cells. Beta-actin was used as loading control. MV4-11, Kasumi and HEK293T cells were transduced with lentiviral-Cas9-blasticidine vector. After 2 days of the transduction, 10µg/ml of blasticidine applied for 1 week. Afterwards, selected cells were subjected to western blot with Cas9 antibody.

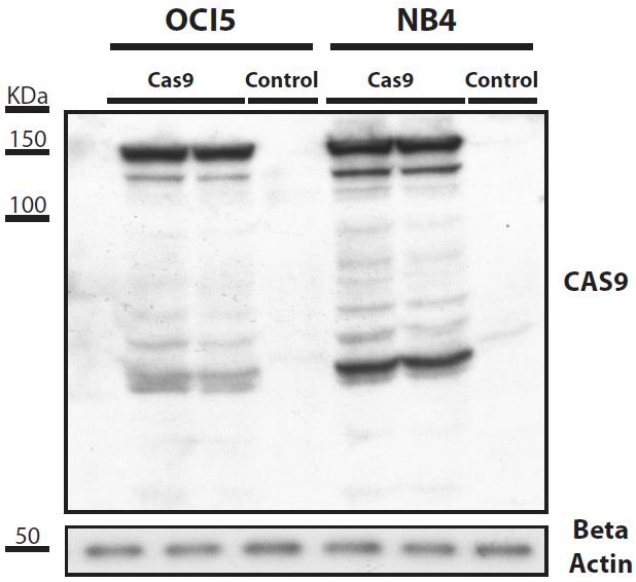

Figure 50. This figure shows the western blot analysis of Cas9 expression. Beta-actin blotting was used as loading control. NB4 and OCI5 cells were transduced with lentiviral-Cas9-blasticidine vector. After 2 days of the transduction, 10µg/ml of blasticidine applied for 1 week. Afterwards, selected cells were subjected to western blot with Cas9 antibody.

Kasumi and MV4-11 cell lines were chosen as a model for c-KIT and FLT3 knockout experiments. First, efficiency of sgRNAs and Cas9 was tested by transient co-transfection of Cas9 and the respective sgRNAs in HEK293T cells (Method 2.4.2-2.4.3). Cleavage lengths perfectly fitted to in silico designs. (Fig. 51-53)

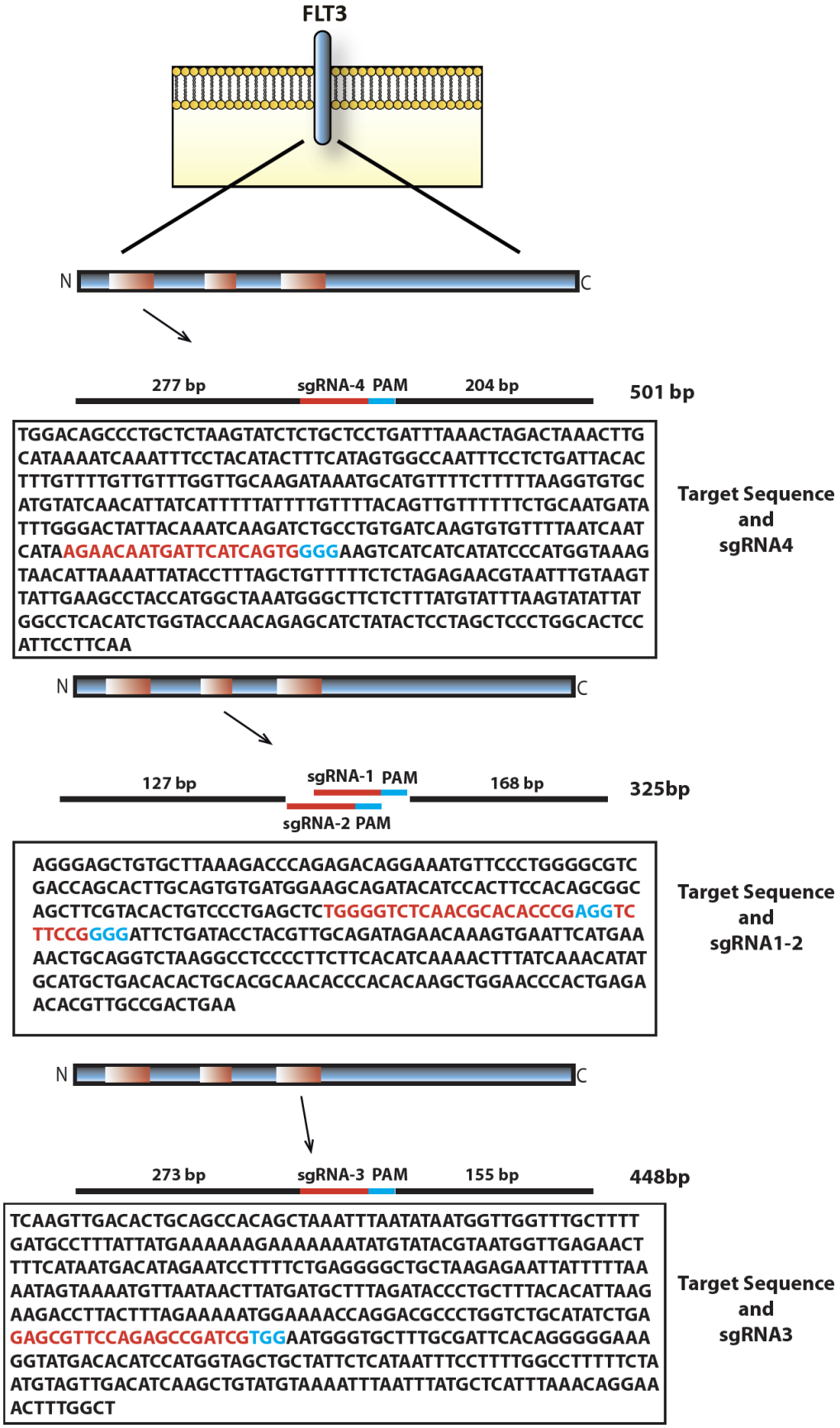

Figure 51. FLT3 receptor and target sequences for CRISPR-Cas9. Guide RNAs shown in red colour and PAM sequence shown in blue colour.

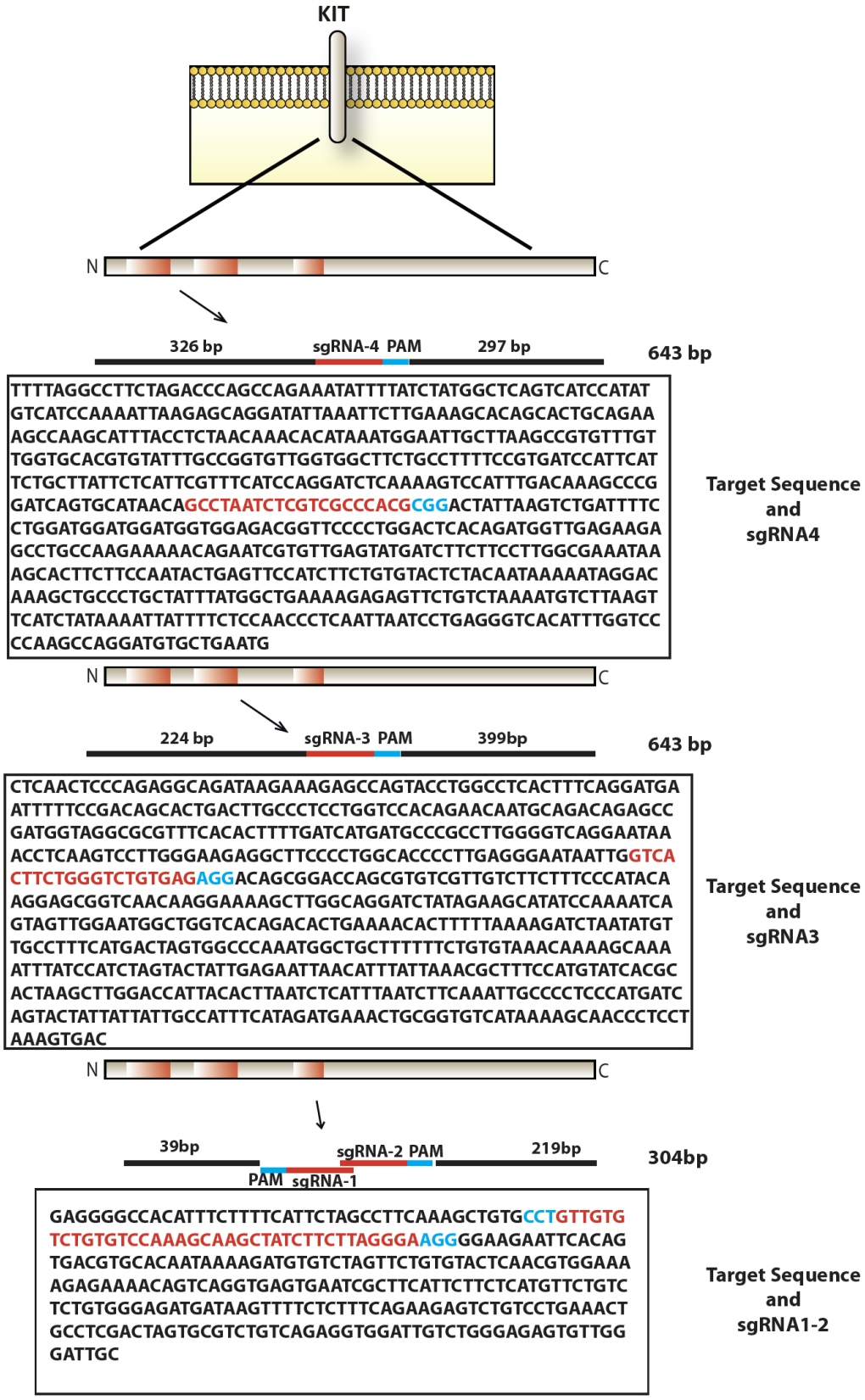

Figure 52. c-KIT receptor and target sequences for CRISPR-Cas9. Guide RNAs shown in red colour and PAM sequence shown in blue colour.

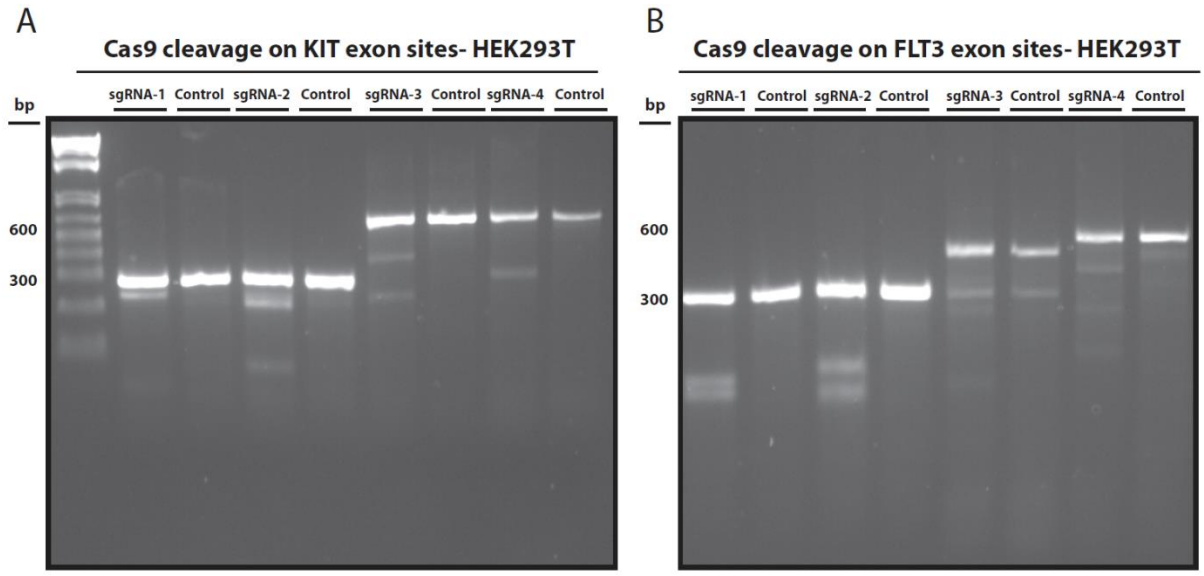

Figure 53. These figures show T7 endonuclease assays of HEK293T cells. (A) HEK293T cells were transduced 4 different sgRNAs specific for KIT exon sites. After the genomic DNA isolations, specific exon sites were amplified with PCR and subjected to T7 endonuclease assay to detect the mutation. (B) HEK293T cells were transduced 4 different sgRNAs specific for FLT3 exon sites. After the genomic DNA isolations, specific exon sites were amplified with PCR and subjected to T7 endonuclease assay to detect the mutation

In constitutively Cas9 expressing cells lines Kasumi and MV4-11, lentiviral vectors coding for sgRNAs targeting c-Kit or FLT3 and GFP as a reporter were transduced via lentiviral gene transfer. Genomic DNA was analysed2-3 days when transduced cells started to express GFP via PCR amplification of sgRNA target sites and a subsequent T7 endonuclease assay. Cleavage bands occurring in CrispR/Cas9 treated MV4-11 and Kasumi cells but not in respective control cells revealed that sgRNA 2-4 for c-Kit and sgRNAs 1,2 and 4 with sgRNA 2 being the best for FLT3 worked in Kasumi and MV4-11 cells respectively (Figure 53-54).

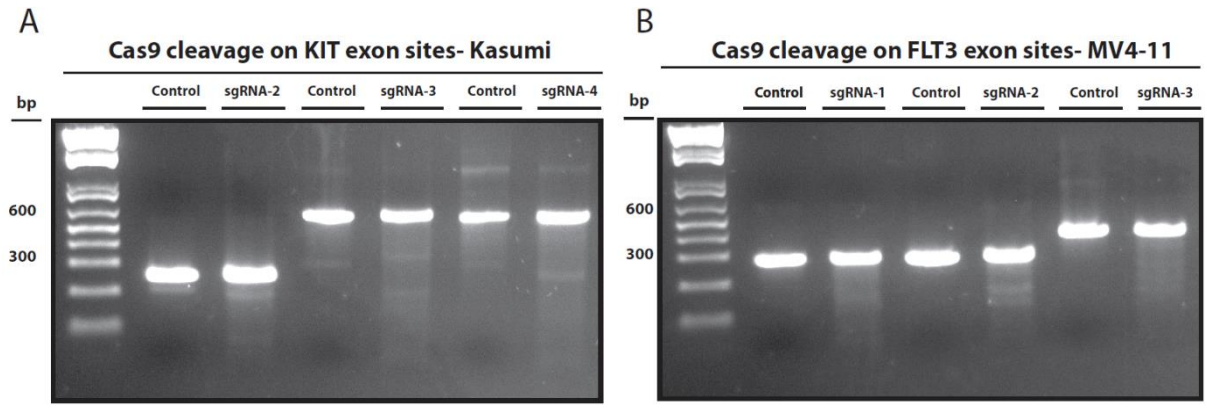

Figure 54. These figures show T7 endonuclease assays of Kasumi and MV4-11 cells. (A) Kasumi cell lines were transduced with KIT-sgRNA2, KIT-sgRNA-3 and KIT-sgRNA-4. After the genomic DNA isolations, specific exon sites were amplified with PCR and subjected to T7 endonuclease assay to detect the mutations. (B) MV4 cell lines were transduced with FLT3-sgRNA1, FLT3-sgRNA-2 and FLT3-sgRNA-3. After the genomic DNA isolations, specific exon sites were amplified with PCR and subjected to T7 endonuclease assay to detect the mutations

Furthermore, CAS9 expressing NB4 and OCI5 cells were used with sgRNA-2 to check if CrispR/Cas9 mediated knockout of FLT3 and c-Kit is working in other AML cell lines. Cleavage bands not present in control cell lines but present in CrispR/Cas9 treated cell lines in the T7 endonuclease assay clearly revealed that CRISPR-CAS9 system is working in different AML cell lines as well (Figure 55).

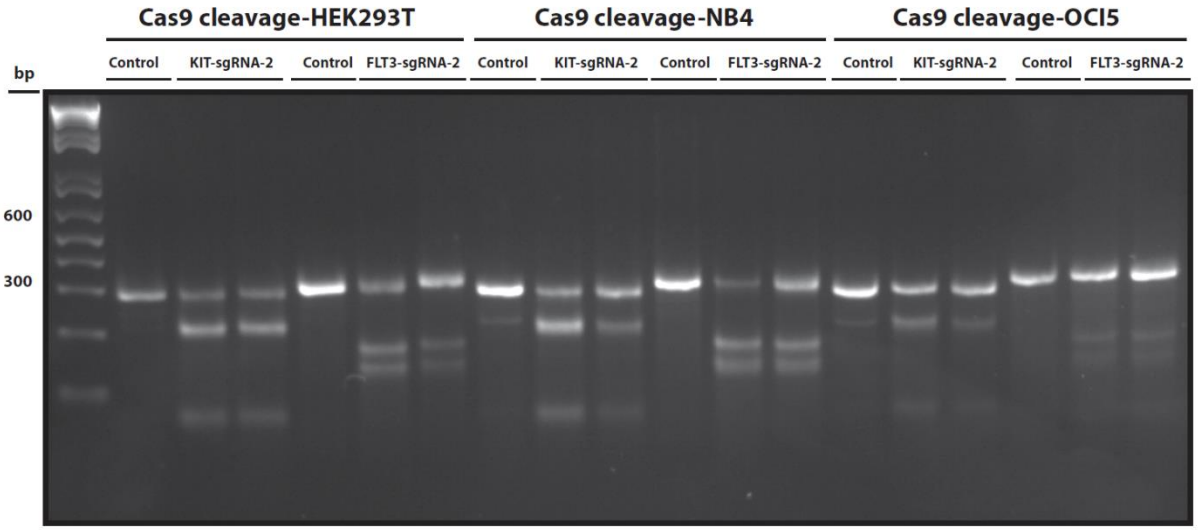

Figure 55. These figures show T7 endonuclease assay of OCI5, NB4 and HEK293T cells. HEK293T, NB4 and OCI5 cells were transduced KIT-sgRNA2 and FLT3-sgRNA-2. After the genomic DNA isolations, specific exon sites were amplified with PCR and subjected to T7 endonuclease assay to detect the mutations.

After I verified that CrispR/Cas9 aided knockout of FLT3 and c-Kit in MV4-11 and Kasumi cells workusing the T7 endonuclease assays, single cells were seeded into 96 well plates to generate single cell clones. GFP^+ single cells were chosen and incubated for 3 weeks. Afterwards cells were collected and subjected to WB analysis. Western blot analysis of MV4-11 single cell clones revealed no clone without FLT3 expresion (Fig.56 A). In contrast, Western blot analysis of Kasumi-single cell clones revealed Kasumi cell line clone sgRNA4-1 as a knockout of c-KIT receptor. Additional western blot analysis with longer exposure times confirmed loss of c-Kit expression (Fig. 56 B-57).

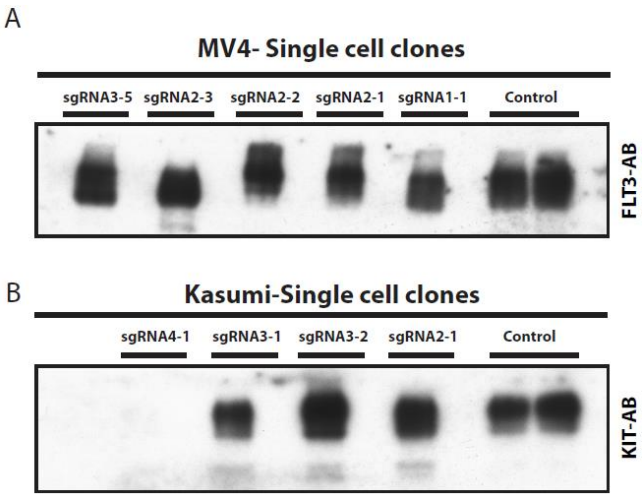

Figure 56. This figures show the western blot analysis of single cell clones of MV4-11 and Kasumi cell lines. (A) Western blot generated with FLT3 antibody and single cell clones were named with their sgRNA names like sgRNA1-1, sgRNA2-1, sgRNA2-2, sgRNA2-3 and sgRNA3-5. (B) Western blot generated with c-KIT antibody and single cell clones were named with their sgRNA names like sgRNA2-1, sgRNA3-2, sgRNA3-1 and sgRNA4-1.

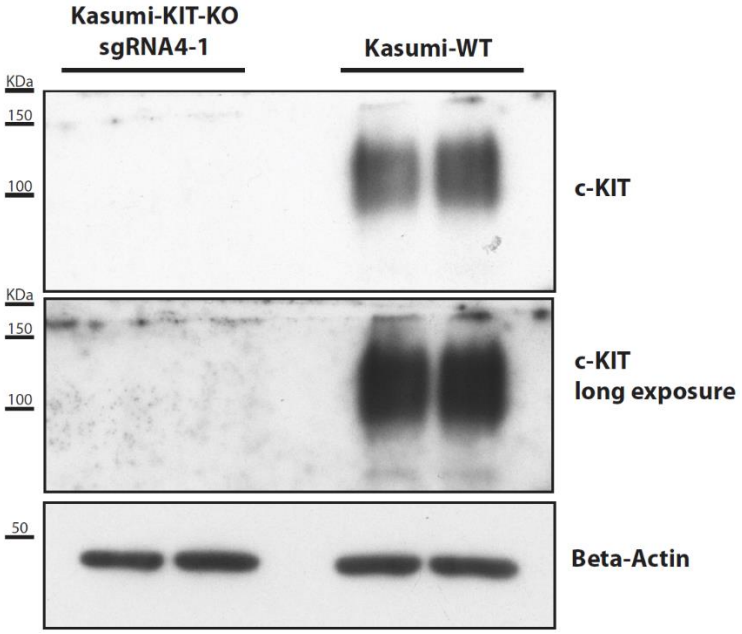

Figure 57. This figures show additional western blot analysis of single cell clone of Kasumi cell lines, KIT-KO vs KIT-WT. These western blots were generated with c-KIT antibody and beta-actin blotting used as loading control.

After Western blot analysis, genomic DNA was extracted from the Kasumi single cell clone sgRNA4-1. The sgRNA target site of c-Kit was amplified with PCR from sgRNA4-1 genomic DNA and subjected to Sanger sequencing. Alignment of Sanger sequencing reads with the reference sequence of c-Kit cDNA in Vector-NTI revealed a 6 nucleotide deletion (Fig.58). Further analysis showed that these mutations were not creating a premature stop codon downstream of the sgRNA target site due to a frameshift but to a 2 amino acid deletion in the c-KIT open reading frame which somehow affected binding of the employed c-Kit antibody that is considered to bind the extracellular domain of c-Kit.

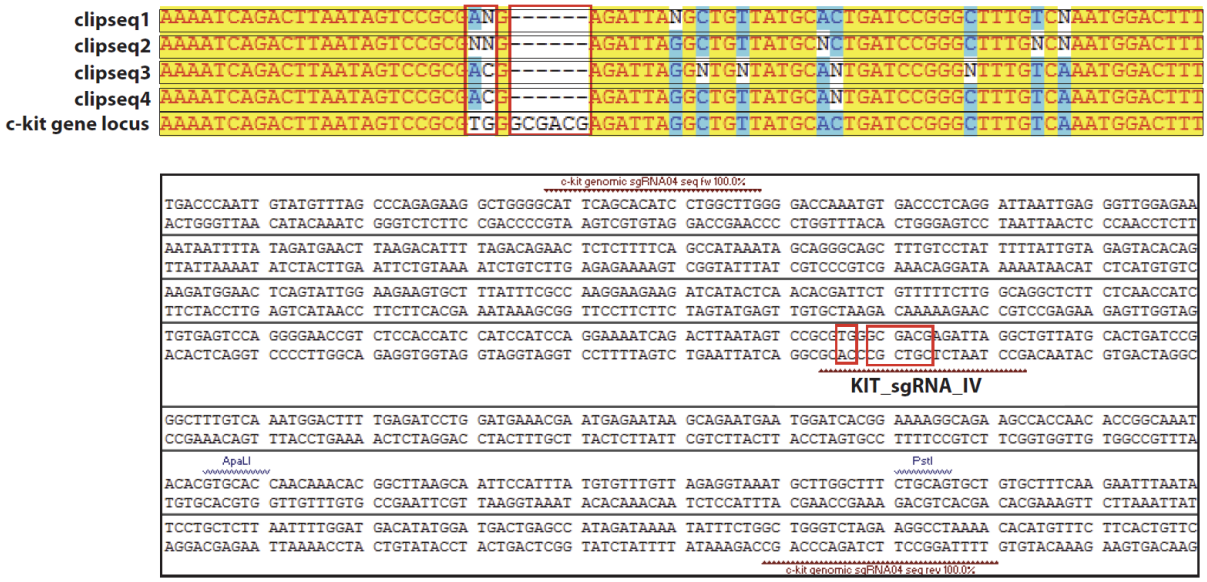

Figure 58. Sequence comparison between single cell clone of Kasumi-sgRNA4-1 cells versus wild type.

3.5 Production of recombinant receptor tyrosine kinase ligands

To study receptor tyrosine kinase activation upon binding of a receptor tyrosine kinase specific ligand (RTKL) such as FLT3 receptor and FLT3 ligand, I produced different receptor tyrosine kinase ligands recombinantly in the mammalian cell line HEK293T. To this aim, I used a bipartite lentiviral vector expression system that is based on the Gal4VP16-UAS system that enables high expression of any kind of target gene (105, 110). One lentivirus expresses the Gal4-VP16 trans-activator while the responder vector contains the genetic information for the RTKL under control of the upstream activating sequence (UAS). Upon Gal4VP16 binding to the UAS sequence the transcription machinery is recruited by the trans-activator domain VP16 of the herpes simplex virus (111). Co-transduction of HEK293T cells with both vectors supported expression of the RTKL in the transduced target cells. All RTKL contained a c-terminal biotin acceptor peptide and a HIS tag. The HIS tag was used for purification of recombinant proteins while the biotinylated BAP tag was used for detection and immobilization on Streptavidin of respective RTKLs. Secreted biotin ligase with an ER retention signal (secBirA-KDEL) was used to biotinylate RTKLs during maturation in the secretory pathway. Therefore, a third lentivirus which coding for secBirA-KDEL was transduced into HEK293T cells. Work flow and check points are demonstrated in Fig.59. FLT3L, KITLG, FGF, EGF, VEGFA, VEGFC, VEGFD, IGF1, and IGF2 coding sequences were cloned under control of the UAS sequence into the responder vector with Gibson assembly (Method 2.3.9). HEK293T cells were transiently transfected with RTKL, BirA, and Gal4VP16 vectors with lipofectamine transfection procedure (Method 2.3.15). After transfection, cells were incubated for 1 day with medium supplemented with 1 µM of biotin. Biotin acceptor proteins were biotinylated so ligands. Analysis of conditioned cell culture media for biotinylated RTK ligands with Western blot demonstrated robust expression of KITLG, FLT3L, FGF, VEGFA, VEGFC and VEGFD between a molecular weight of 25 to 50 KDa (Fig.60 A-B). Schaegger gel was used for detection of the smaller proteins such as IGF1 and IGF2 which were running at

a molecular weight between 15-25KDa. EGF was not detected (Fig.60 C). Next, to create stably expressing cell lines, HEK293T cells were transduced with secBirA, Gal4-Vp16 and responder vector with the respective RTK ligand using a standard lentiviral transduction protocol (Fig. 61, Method 2.3.16-19). Next, transduced cells were incubated for one day in the presence of 1 µM biotin. Western blot analysis of conditioned media revealed robust expression of KITLG, FLT3L and VEGFA (Fig.61). Finally, to obtain pure recombinant receptor tyrosine kinase ligands, large-scale production was applied to HEK293T cells (Method 2.6). After purification, purified proteins were checked analyzed with Coomassie gels for purity and Western Blot for biotinylation efficiency. FLT3L, VEGFA and KITLG were clearly observable again on the blot (Fig62 A). In total, 600µg of VEGFA, 320µg of FLT3 and 50µg of KITLG were produced. Coomassie staining of 1µg of VEGFA and FLT3 demonstrated that both proteins were very cleanshow that clear ligand (Fig.62 B). On the other hand, Coomassie staining of KITLG was not so clear. Therefore, purification steps were applied again on the KITLG two times. This time detection was done with HIS antibody (Fig.63 A) and coomassie staining was applied to KITLG (Fig.63 B). For KITLG, there is a smear form in the western blot analysis (Fig.60-A, Fig.61, Fig62-A and Fig63-A) which we also observed in Coomassie staining. (Fig.63-B)

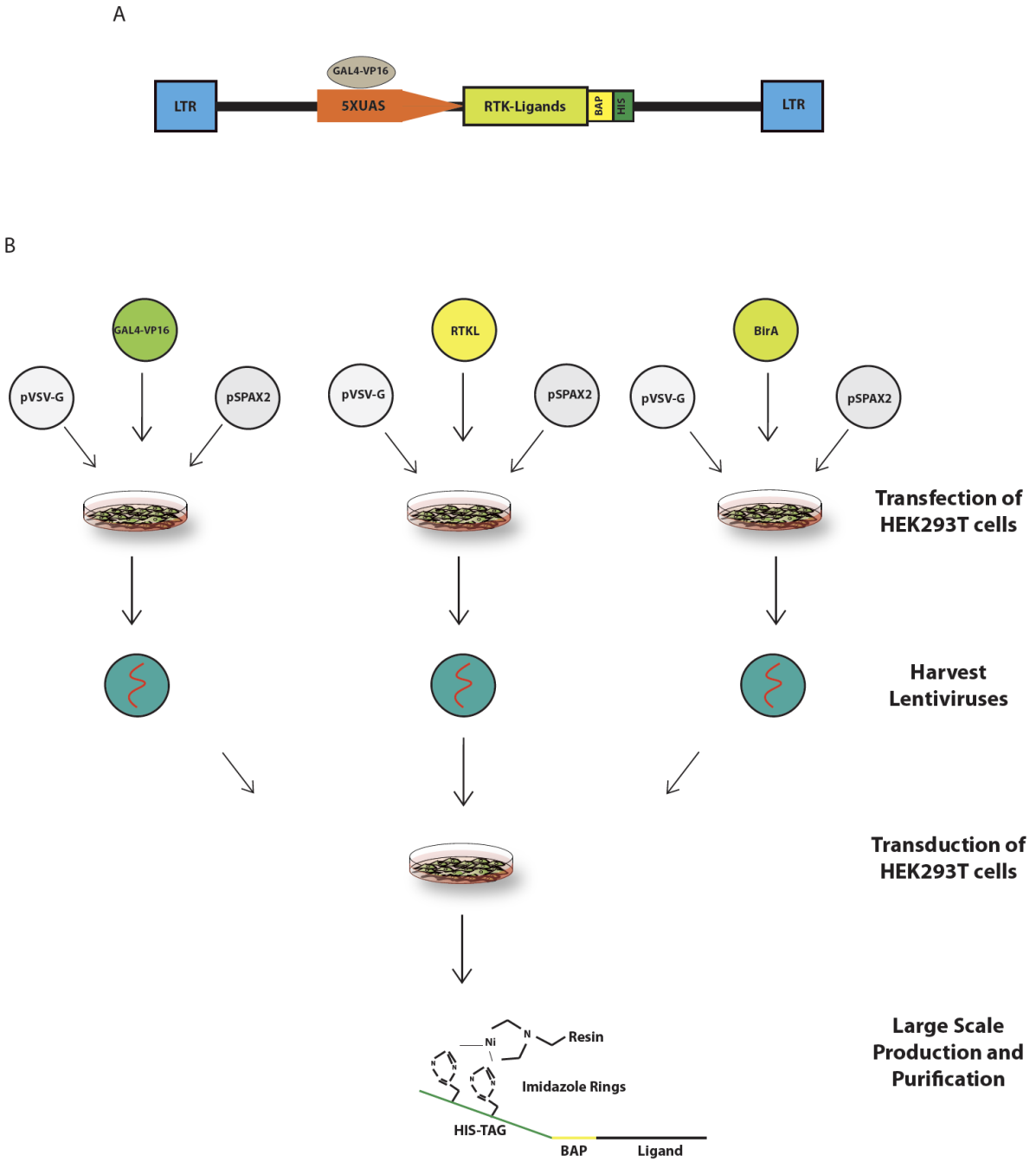

Figure 59. Production of Recombinant Receptor Tyrosine Kinase Ligands. (A) Vector contains upstream activation sequence (UAS). Gal4 binds to UAS. This complex activates gene transcription. The coding sequence of RTKL including a biotin accepting peptide (BAP) and a HIS tag is located downstream of the UAS. (B)Transfection of separate HEK293T cells pools with lentiviral transfer plasmids carrying the genetic information for the RTKL, Gal4-VP16 and the biotin ligase enzyme (BirA). Harvesting lentiviruses. Cotransduction of HEK293T cells with lentiviruses coding for RTKL, Gal4-VP16. Large scale production of RTKL with multilayer flasks and Media collection for HIS tag purification of RTKL

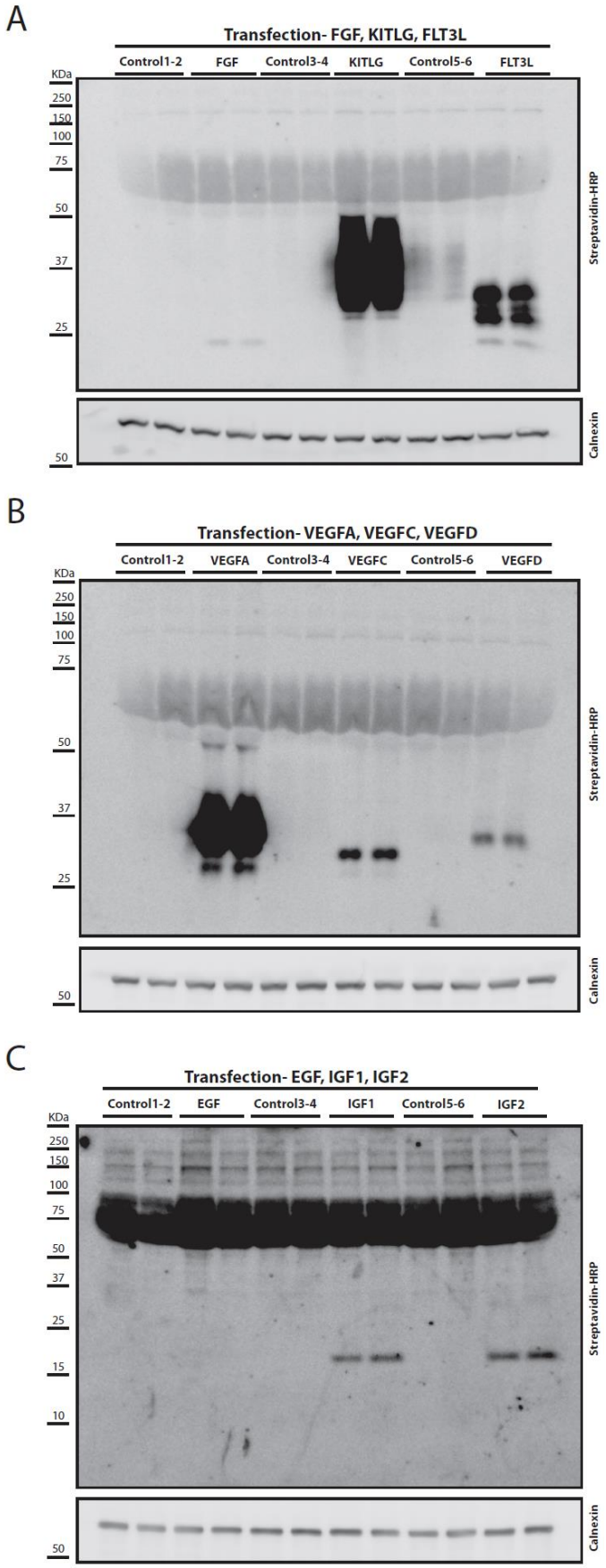

Figure 60. These figures show Western Blot detection of receptor tyrosine kinase ligands with streptavidin peroxidase. Calnexin blottings were used as loading control. HEK293T cells were transfected with corresponding

vectors and cell medium supplemented with 1µM biotin and incubated for one day for biotinylation of ligands. Afterwards, cell mediums were loaded on gels and blotted on nitrocellulose membranes used for blotting. (A) 12% Tris/glycine gel were used to separate the proteins. FGF, KITLG and FLT3L were detected with Strep-HRP blot. (B) 12% Tris/glycine gel were used to separate the proteins. VEGFA, VEGFC and VEGFD were detected with Strep-HRP. (C) Schagger gel was used to separate the proteins. IGF1 and IGF2 were detected with Strep-HRP.

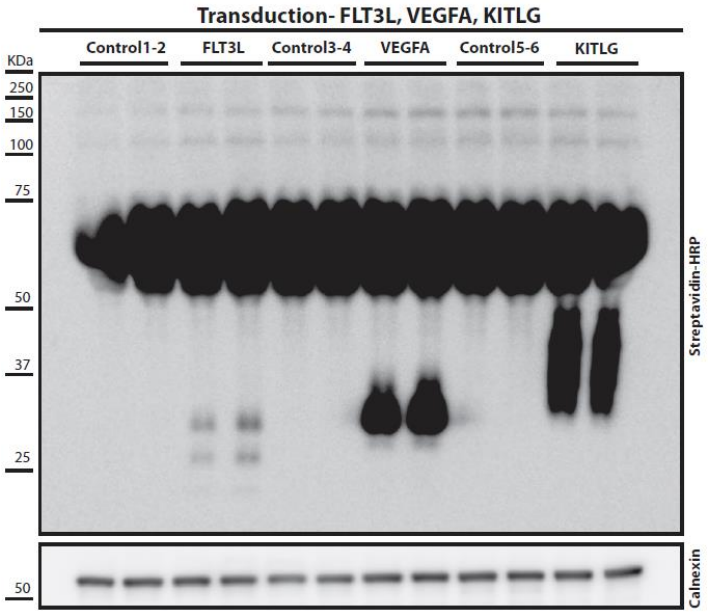

Figure 61. This figure shows Western Blot detection of receptor tyrosine kinase ligands with streptavidin peroxidase. Calnexin blotting were used as loading control. HEK293T cells were transduced with corresponding viruses to generate stable cell lines which produce specific RTKL. Afterwards cell medium supplemented with 1µM biotin and incubated for one day for biotinylation of ligands. Afterwards cell mediums were analysed with streptavidin-HRP (A) 12% Tris/glycine gel were used to separate the proteins. FLT3L, VEGFA and KITLG were detected with Strep-HRP.

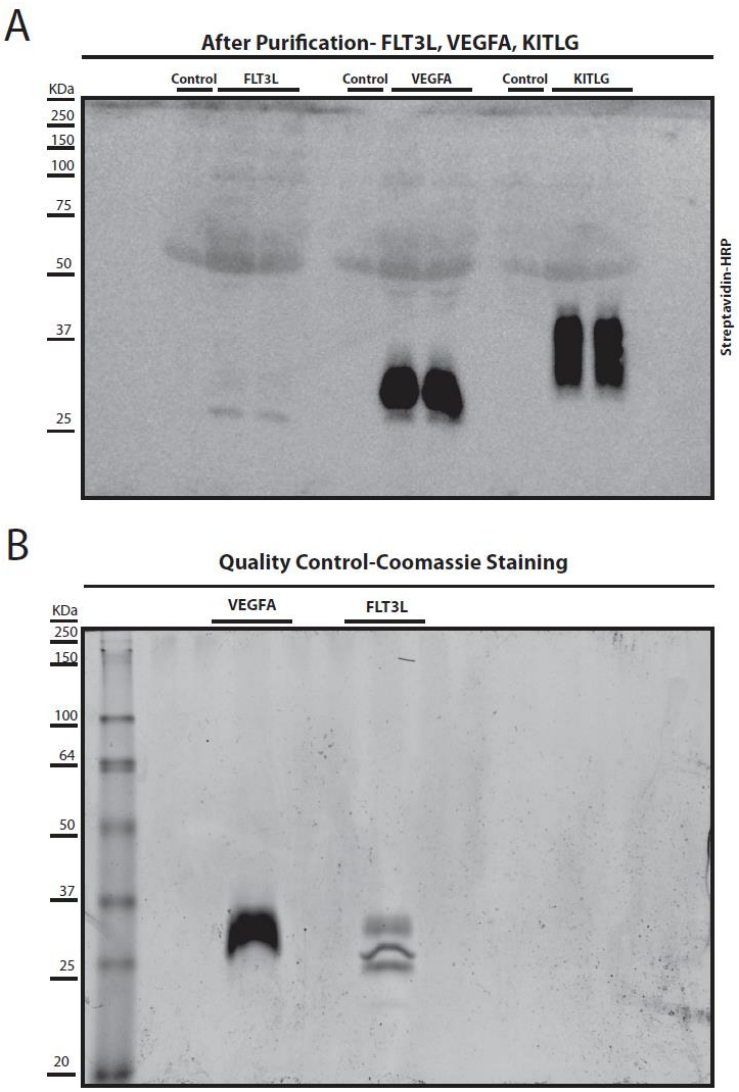

Figure 62. This figure shows ligand quality after the purification step. HEK293T cells were cultured in large scale format for 3-4 days. Afterwards, ligands were purified with HIS-Tag purification. (A) HEK293T cell medium were supplemented with 1µM of biotin. Afterwards, biotinylated FLT3L, VEGFA and KITLG were analysed with streptavidin peroxidase. (B) After the HIS-Tag purification, 1µg of VEGFA and FLT3L were loaded on 12%Tris glycine gel and coomassie staining was applied.

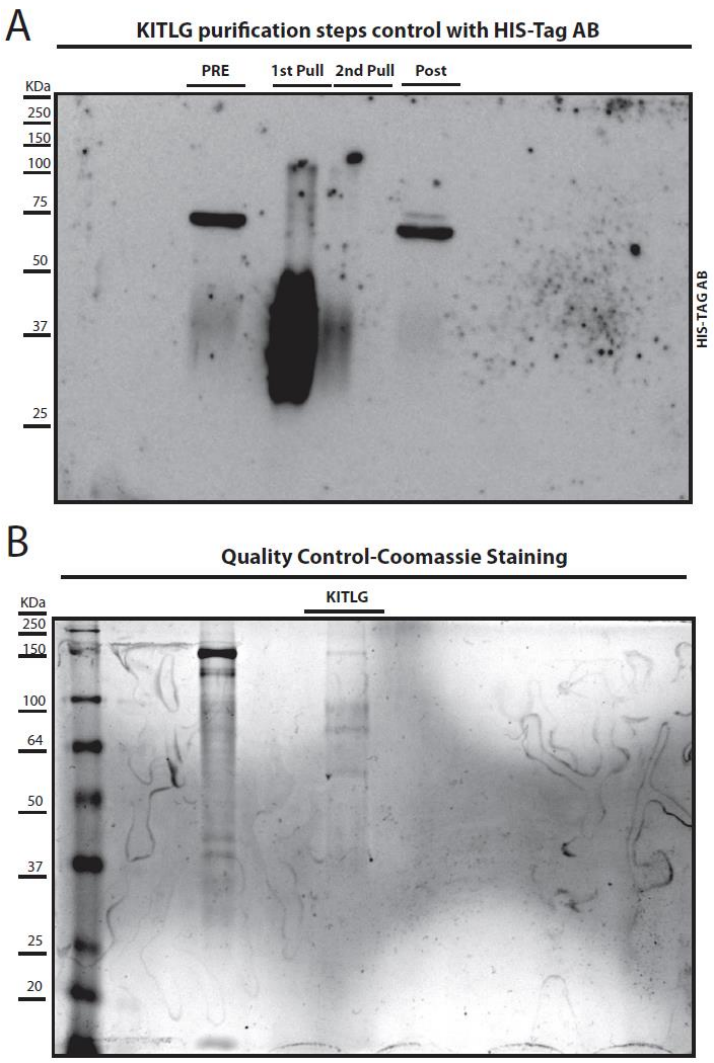

Figure 63. These figures show KITLG purification steps and coomassie stainings. (A) After the large scale production part of the cell medium was loaded as PRE, after 1st attempt of his-tag purification ligands were loaded on as 1st Pull, after 2nd attempt of his-tag purification ligands were loaded as 2nd Pull and flow through loaded as POST. 12% Tris/glycine gel was used for separation of proteins and KITLG were detected with HIS-TAG antibody. (B) After the HIS-Tag purification, 1µg of KITLG was loaded on 12%Tris glycine gel and coomassie staining was applied.

4 Discussion

4.1 Optimization of the SPECS Method

The secretome is a crucial component for intercellular communication in multicellular organisms and comprises secreted and proteolytically released proteins (47). Changes in the secretome composition alter intercellular communication and thus can lead to pathological states such as cancer, neurodegenerative diseases, autoimmune disorders or cardiovascular disease (31-34). Thereby, the secretome is a valuable resource for the identification of biomarkers or investigation of intercellular biology. Due to technical limitations of mass spectrometric analysis, identification of cell-derived glycoproteins is very difficult in the presence of serum or other protein supplements. The recently introduced Secretome Protein

Enrichment with Click Sugar (SPECS) method discriminates cell-derived glycoproteins from exogenously added glycoproteins and all other proteins (27). Hence, using the SPECS method, the secretome of eukaryotic cells can easily be captured from conditioned serum containing media. SPECS combines metabolic labeling of de novo synthesized glycoproteins with azido sugars like ManNAZ in cell culture with subsequent biorthogonal-click chemistry based biotinylation of labeled glycans which works both in vivo and in vitro (120-122). Biorthogonal reaction means chemical reaction that can be happen inside the cell without any toxic effect or any cross react with other native processes (123). For labelling strategies, the best strategy is to use a reaction which does not exist in nature. The first known reaction following this scheme was the Staudinger ligation (124). Following to that, an alternative reaction called 1+3 cycloaddition between an azide group and a terminal alkyne was developed by Huisgen but it was dependent on heat and not suitable for cell based labelling. Afterwards, copper was identified as a catalyst promoting the 1+3 cycloaddition accelerating the reaction to acceptable reaction rates at ambient temperatures suitable for labeling of eukaryotic cells. However, copper is toxic to cells (125). Afterwards, Bertozzi and others took advantages of strained alkynes and consequently the strain promoted, copper-free, 3+2 cycloaddtion was developed (120, 122). Strained alkynes linked to a biotin moiety result in biotinylation of metabolically azide labeled glycoproteins which enables their selective enrichment with streptavidin. As the majority of extracellular proteins is glycosylated, SPECS covers most of the secretome (27). The SPECS method has been successfully applied to primary neurons, murine embryonic fibroblasts, HEK293T cells or Jurkat cells (27, 30, 126, 127). The physiological functions of different proteases such as BACE1 and ADAM10 in neurons, SPPL3 in murine embryonic fibroblasts were studied and their substrates were identified (27, 29, 52). Modulatory roles for ADAM10 and BACE1 in axon guidance and synapse function as well as for SPPL3 in glycosylation have been demonstrated (52, 128).

In this part of the thesis, I optimized the previously published SPECS protocol to increase its sensitivity with respect to the number of identified glycoproteins, number of detected peptides and protein intensity. Furthermore, with the optimization sequence coverage was increased which renders the method more reproducible. Eventually, these improvements will allow a reduction of the required input material. However, this needs to be tested in future experiments, for example by testing different numbers of HEK293T cells with the new and the old protocol. The minimal required or optimum cell number could be determined in these experiments which additionally may reduce the number of required animals if primary cells are investigated.

For optimization experiments, I tested new biotinylation reagents, different buffer compositions and pH for the biotinylation reaction and cysteine alkylation prior to click chemistry aided biotinylation of ManNAZ labelled glycoproteins. Finally, HEK293T cells were subjected to the old and the new optimized SPECS method. Preliminary western blot experiments already revealed that DBCO-Sulfo-Biotin (DSB) outperforms DBCO-PEG12-Biotin in terms of glycoprotein biotinylation efficiency and less unspecific labelling. One reason behind this, DSB has more water soluble property than the DPB. Furthermore, DBCO-PEG12-Biotin has long lipophilic PEG linker that may cause unspecific labelling and decreasing specific labelling due to steric hindrance.

In addition to that, phosphate buffered saline (PBS) increases the biotinylation of ManNAZ labelled proteins compared to distilled water. Different pHs were tested in the strain promoted biotinylation reactions. The optimum pH for biotinylation reaction was determined at pH 7.0 with least unspecific and highest specific labelling. Furthermore, click chemistry aided biotinylation reaction occurs better in the Tris buffer compared to distilled water but PBS shows a better result in terms of sensitivity and specificity. In terms of buffer capacity, distilled water has a poor capacity to resist to pH changes. Hence, the pH of the conditioned cell medium can directly effect the pH of the water and this may lead to big differences in pH and reaction rates. PBS and Tris have a higher buffering capacity resulting in stable pH values after the addition of conditioned cell medium and thus result in better strain promoted biotinylation reactions.

Next, I tried to reduce unspecific labelling of bovine serum albumin by alkylation of unpaired cysteines with iodoacetamide (IAA). Previous studies showed that IAA reduces unspecific thiol-yne reaction between strained alkynes and cysteines (116). However, IAA mediated alkylation did not reduce unspecific labelling of bovine serum albumin. Either strained alkynes react with other functional groups besides cysteines or IAA was not sufficient enough to alkylate the unpaired cysteine residues in BSA which may be the case due to the high levels of albumin. However, despite the high levels of albumin, the method is still specific enough for glycoprotein labelling and enrichment.

In the final experiment, I compared the optimized protocol with the old protocol using an MS-based analysis of the HEK293T cell secretome. According to previous studies for BACE1 and SPPL3 using the old SPECS protocol, the number of quantifiable glycoproteins was increased 1.6 till 2.3-fold respectively to 604 glycoproteins (27, 52, 129). Further, the average sequence coverage of glycoproteins was increased from 4% to 9.7%. Hence, the optimized version of the previously published SPECS method greatly improves the efficiency of strain promoted click chemistry mediated biotinylation of metabolically azide labelled glycoproteins resulting in an almost doubled number of quantifiable glycoproteins.

Overall, the new protocol offers increased protein sequence coverage and a better signal-to-noise ratio. Thus, the higher sensitivity of the optimized SPECS protocol might help to analyse the secretome using a lower number of cells which is interesting for analysis of less abundant primary cell types. For example, for neuronal secretome analysis using the old protocol so far, $40x10^6$ neurons had to be used for one replicate. With the optimized protocol, the number of required cells could be reduced down to $15x10^6$ neurons which finally would lead to a lower number of required animals per experiment.

4.2 Application of SPECS and Surface-Click protocols to AML cell lines

Acute myeloid leukemia (AML) is a myelodysplastic syndrome leading to the production and clonal proliferation of primitive hematopoietic stem cells or immature myeloid progenitor cells. Abnormal proliferation of myeloid progenitor cells could lead to an increase in immature malignant cells (blast) and less healthy blood elements like thrombocytes and erythrocytes in the blood (42, 81). AML is an aggressive and genetically heterogeneous disease which initially is treated with chemotherapy with one exception APL (PML-RARa) (130). However, a specific

feature of AML is recurrence in a chemotherapy resistant form. Statistically 40-60% of patients become resistant to chemotherapy (131). For these reasons, AML requires a more detailed understanding of its molecular biology and an easier ways of disease monitoring. In this thesis, 6 different AML cell lines were used as models for AML subtypes to identify their secretome and surface proteome profiles with SPECS and surface-click protocols.

SPECS and surface-click protocols have been applied to different mammalian cell lines successfully (27, 29, 30, 52, 129). Before using SPECS and surface-click protocols on AML cell lines, I wanted to identify the optimum culturing time, the optimum concentration of ManNAZ, different sugars such as GalNAZ and ManNAZ in terms of labelling efficiency and different chemicals to reduce unspecific labelling and increase the specific labelling in a small-scale format. Testing 100µM and 200µM of ManNAZ sugar in the cell lines NB4 and Kasumi for 24 and 48 hours respectively showed that 48 hours of incubation outperforms the 24 hours of incubation. Previous studies have shown as well that metabolic delivery of ketone groups to sialic acid residues requires at least 15-20 hours. Furthermore, other studies show that high concentrations or long incubation times with aldehyde and thiol group containing sugars lead to apoptosis of treated cells. Hence, part of the observed toxicitiy of applied sugars might be a result of the incorporated functionality. Unpaired thiol groups and aldehyde groups can readily react with a variety of other chemical functional groups and thus are less bioorthogonal than an azide functional group. (132-135) Concentrations of 100µM and 200µM ManNAZ resulted in almost equal glycoprotein labelling. Most likely, the necessary metabolic pathways for sialic acid incorporation are already saturated in the presence of 100µM ManNAZ. Hence in terms of risk of toxicity, I decided to perform the protocol with 48 hours and 100µM of ManNAZ sugar. These concentrations and incubation times correlate with previous SPECS applications (27, 30, 52, 126, 127) and seem to be generally applicable to various cell lines.

In the second part of optimizations, both ManNAZ and GalNAZ sugars were tested in AML cell lines as ManNAZ predominantly labels N-glycosylated extracellular glycoproteins while GalNAZ predominantly labels O-glycosylated extracellular glycoproteins (51, 123). Hence, I wanted to figure out whether GalNAZ results in better glycoprotein labelling than ManNAZ or whether addition of both sugars would improve glycoprotein labelling in a synergistic fashion. NB4 cells were incubated with 100 µM of ManNAZ or GalNAZ and ManNAZ+ GalNAZ and DMSO as control for 48 hours. Consequently, relative labelling intensity of ManNAZ sugar outperforms the other possibilities. Simultaneous labelling with ManNAZ and GalNAZ resulted in higher glycoprotein labelling than exclusive labelling with GalNAZ but still was not as good as exclusive ManNAZ labelling. This could be due to the fact that N-glycosylations are more frequent in glycoproteins than O-glycosylations and that the presence of GalNAZ somehow impairs metabolization of ManNAZ though it is present in the same concentration. Further, labelling intensity of glycoproteins in Western blot is only an indirect read out which measures incorporation of ManNAZ labelled sugars and not the number of labelled glycoproteins. Hence, more intense glycoprotein labelling in the ManNAZ conditions may not directly result in a higher number of identified proteins in a mass spectrometry experiment. However, as GalNAZ can also lead to labelling of intracellular O-GlcNACylated proteins and ManNAZ labelling hits almost all glycoproteins, I decided to pursue exclusive labelling with ManNAZ.

In the third part of optimizations, iodoacetamide and dimedone were used to reduce unspecific labelling of cysteine thiol-yne reactions and Tris buffer was used at strain promoted biotinylation reaction to improve specific glycoprotein labelling. Iodoacetemide and dimedone were used for blocking the free cysteine sulhydryl residues of BSA (116). NB4 cells were used as mode cell line. Conditioned media treated with IAA, dimedone before the biotinylation reaction and Tris was used at strain promoted biotinylation step. At the end, these chemicals did not improve specific glycoprotein labelling or reduce unspecific labelling as well. This may be a result of DBCO-Peg12-Biotin compound reacting with other functional groups besides cysteines. May be dimedone and iodoactemide were not efficient enough to alkylation of unpaired cysteines in bovine serum albumin or other proteins. Furthermore, DBCO-Peg12-Biotin has a very long chain that may lead to higher BSA binding and thus unspecific BSA labelling. On the other hand, unspecific binding can occur between BSA and streptavidin sepharose. So using the streptavidin-hrp also could lead to false positive results. Therefore, after the strain promoted biotinylation, biotinylated glycoproteins can be enriched with streptavidin beads and rather than using the streptavidin-hrp, coomassie staining or specific protein detection (IP) can be applied for the different conditions and detection of the proteins.

After the optimization experiments, AML cell lines KG1α (M0-M1), Kasumi (M2), NB4 (M3), OCI5 (M4), MV4-11 (M5), CMK (M7) were used as a model for the different AML subtypes described in the FAB classification (64). SPECS and surface-click protocols were applied to 3 biological replicates of these AML cell lines. Many glycoproteins were identified in the secretome and surface proteome analysis. A similar differential expression of routine diagnostic AML classification FACS markers in the secretome and surface proteome of the analysed cell lines revealed that the analysed cell lines seem to keep the immune profile of the AML subtype they are derived of. Hence, these results will be a good source for the determination of more specific immune profiles of different AML subtypes, biomarker identification and further mechanistic studies. In the secretome analysis, the most abundant group of glycoproteins were secreted glycoproteins. In the surface analysis the most abundant glycoprotein group were type-I transmembrane proteins. The Go-Term analysis showed that 13% of the identified glycoproteins in secretome and 7% in the surface proteome analysis contributed to integrin signalling pathways. Integrins are a big family of cell surface adhesion proteins that take part in crucial mechanisms such as signal transmission, survival, differentiation and migration of cells (136). Furthermore, 10% of secreted and 6 % of membrane glycoproteins are involved in the blood coagulation pathway. 7% of surface glycoproteins are involved in chemokine and cytokine signalling pathways that are important for basic physiological processes such as immune responses, inflammation and homeostasis in cells (137, 138). Performing a cluster analysis of the analysed cell lines according the quantitites of identified glycoproteins in Perseus revealed that KG1α has different characteristics than the other cell lines such as CD34 expression which is supported by the description of KG1α as a leukemic stem cell model (139).

4.3 Detection of reference markers and biomarker candidates

Further analysis of secretome and surface proteome data revealed reference markers already defined for AML cell lines or used for diagnosis in the clinics. For example, CD34 is defined as a leukemia-stem cell marker and mostly observed on KG1α in our analysis (140). CD44 in

combination with CD34 is used to detect the M0 AML subtype and is expressed in all AML cell lines with highest expression in the KG1α cell line reflecting the M0 subtype. c-KIT is almost exclusively expressed in Kasumi cells while FLT3 is expressed in all AML cell lines except for KG1α with highest expression in MV4-11 cells. Myeloperoxidase (MPO) is routinely used as a diagnostic clinical marker for AML which was detected in the secretome and surface analysis of Kasumi, NB4 and OCI5 cell lines. Furthermore, CD99 and FLT1 as well as CD33 and CD7 immunological markers were detected in the secretome and surface proteome analysis of which the latter two are linked to a bad prognosis for survival in AML (141).

Appropriate detection of AML reference markers shows the feasibility of our SPECS and surface-click applications. As we planned to find soluble biomarkers, we analysed the identified glycoprotein hits with proteomicsdb (117) and filtered them for minor expression in the body apart from the hematopoietic system, in particular not liver-based proteins. Consequently, OSCAR, CHST14, HS6ST1, COCH, CBLN4 were detected in the secretome of all AML cell lines and minor expression in the body. Especially, Osteoclast-associated immunoglobulin-like receptor (OSCAR) is an important biomarker candidate which is expressed in urine, monocytes and proximal fluid, the latter being blood from the heart (117). OSCAR modulates the innate and adaptive immune system and takes part in cell activation and maturation (142). Hence, levels of OSCAR should be analysed in AML patient sera before and after chemotherapy. If the OSCAR level is significantly reduced between initial diagnosis and after complete remission, this would be a new biomarker candidate for AML. Furthermore, persistently increased levels of OSCAR of resistant forms AML during therapy could be used as an indicator for therapy failure and help clinicians to rapidly switch the therapy regimen without a bone marrow biopsy. These applications could be done for other biomarker candidates as well. Therewithal, many of the identified glycoproteins are exclusively expressed in one type of the AML cell lines. For instance, FLT4 has the highest expression in CMK but is not expressed in the other investigated cell lines. Hence, FLT4 would be a potential immunophenotyping marker for defining megakaryocytic leukemia. Furthermore, in the surface data there are many candidates exclusively expressed in one of the cell lines. These could be tested for their capability to identify AML subtypes. However, this needs to be further validated with other techniques and patient material.

4.4 Receptor tyrosine kinase profiles of different AML cell lines

Receptor tyrosine kinases (RTK) are playing key roles in diverse biological processes such as signalling, proliferation, differentiation, metabolic pathways and apoptosis (69). The main mechanism of receptor tyrosine kinase activation is binding of specific receptor tyrosine kinase ligands to the RTK extracellular domain triggering dimerization and a conformational change of the RTK which leads to activation of its intracellular tyrosine kinase domain (TKD) and subsequently downstream signalling pathways (69). RTK activity is part of the physiological cellular metabolism and tightly controlled. However, receptor tyrosine kinases can obtain activating mutations or be overexpressed leading to abnormal signalling which is one step to cancerogenesis (69). In clinics, various receptor tyrosine kinase inhibitors are in use for suppressing cancer cell growth (42, 73, 81). In this regard, I considered the receptor tyrosine kinase profile analysis of different AML cell lines as a useful approach to learn more about aberrant receptor tyrosine kinase activation in AML. The translocation t(8;21) generating the AML1-ETO fusion gene is one of the most frequent genetic abnormalities in

AML patients. 13%-22% of c-kit mutation are correlated with the t(8;21) chromosomal translocation and c-kit expression is highly upregulated in AML1/ETO positive AML (39-41). A closer look to the generated RTK data revealed highest c-kit expression in the Kasumi cell line compared to the other investigated AML cell lines. This fits well as Kasumi cells bear an AML1-ETO fusion gene generating t(8;21) chromosomal translocation (DSMZ No: ACC220). For these reasons, Kasumi cells are a good model for studying c-KIT related biology of leukemic blasts upon c-KIT inhibition or KITLG stimulation. On the other hand, FMS-like tyrosine kinase-3 (CD135) is an important receptor tyrosine kinase involved in the development of the hematopoietic system (143). FLT3 mutations are the most common mutations (30%) in acute myeloid leukemia and linked to a poor survival prognosis of AML patients. Thus, FLT3 expression and its therapeutic inhibition is one of the main concerns in current developments of AML therapeutic intervention (42, 81, 118). FLT3-ITD (internal tandem duplication) mutations are found in approximately 25% of patients with de novo AML. Patients with FLT3-ITD mutation often have a more aggressive form of AML and have a higher probability of relapse after remission (42, 81, 144). Hence, I used the MV4-11 cell line defined as carrying the FLT3-ITD mutation (DSMZ No: ACC102) while the analysis of RTK revealed that the MV4-11 cell line has the highest FLT3 expression compared to other cell lines. For these reasons, MV4-11 is a good model to study FLT3-ITD related biology upon FLT3 inhibition or FLT3 stimulation experiments. Furthermore, Vascular endothelial growth factor receptor-1 (FLT1) is a receptor tyrosine kinase that is involved in control of cell proliferation. It has been reported to interact with the factors VEGFA, PIGF and VEGFB is a therapeutic target for various cancer including AML (145, 146). In the RTK results, the highest FLT1 expression was observed in the secretome of the NB4 cell line but was not detected in the surface data. May be the reason most of the FLT1 ectodomains are shedded to media as signalling factor and present in soluble form. The highest expression of Vascular endothelial growth factor receptor-3 (FLT4) is observed on CMK in both secretome and surface proteome data. FLT4 exclusively express in megakaryocytic leukemia that may be a potential biomarker but this needs to be validated with patient materials. NB4 generally has the highest expression of various types of receptor tyrosine kinases, this might be correlated with disease progression and pathology but requires further validation with patient survival statistics. Further analysis of secretome data showed that 12 different growth factors (GF) are present in the cell culture medium of AML cells. Growth factor expression is mostly observed in the KG1α and KG1α is already defined as a model for leukemic-stem cell (139). Furthermore, many of the investigated cell lines express growth factors and GF related receptor tyrosine kinases that may interact with each other such as Angpt1,2-Tie1 (147, 148), CSF1-CSF1R (149, 150), VEGFA-FLT1 (151), and HGF-MET interactions (152, 153). However, these interactions need to be validated with protein-protein interaction methods such as FRET in specific AML cell line and their downstream signalling pathways.

4.5 Sorafenib inhibition experiments lead to increase in survival receptor

Sorafenib is a multi-kinase inhibitor that inhibits FLT3, c-KIT, VEGFR, RAF and PDGFR. Initial applications in AML showed a transient suppression of blast formation for an average time period of 72 days (71, 74-77). However, recurrence occurred fast with occurrence of Sorafenib resistant blasts (71, 78-80).

In cancer, two main classes of mutations are defined. Class-I mutations comprises mutations that activates signal transduction pathways and result in increased proliferation. This comprises RTK activation related mutations. In AML, these are FLT3-ITD, FLT3-TKD, c-KIT, CBL, JAK2, and NRAS mutations (154, 155). Class-II mutations comprises mutations in transcription factors that affect differentiation of hematopoietic cells. In AML, fusion transcripts such as PML-RARa, RUNX1-ETO, CBFb-MYH11 and MLL rearrangements are considered as class-II mutations (154, 155). Furthermore, there are still different mutations that are not classified yet such as TET2, IDH1, IDH2, DNMT3A, ASXL1 and EZH2 (154, 155). Widely accepted classification and prognostic schemes for AML include mutation status of FLT3, NPM1 and CEBPA. Furthermore, TP53, SRSF2, ASXL1, DNMT3A and IDH2 mutations have also strong influence on clinical outcomes (156-158).

In AML, targeted therapy application are focussed on the FLT3-ITD mutation (42, 71). Patients with FLT3-ITD mutation have a high risk of relapse (42, 81, 144). Hence, the MV4-11 cell line is a good model to study Sorafenib application and development of Sorafenib resistance as it has the FLT3-ITD mutation (DSMZ No: ACC102). My main hypothesis was that RTK inhibitor resistance upon its chronic application may be a result of overexpression of FLT3 or alternative receptor tyrosine kinases that may thus compensate lack of survival and growth promoting FLT3 signalling. Another hypothesis was that overexpression of chemokines or other growth factors increase in the autocrine signalling such as increase in the FLT3L level or other chemokines promote resistance towards Sorafenib. Testing different Sorafenib concentrations in MV4-11 cells and phosphorylation intensity with phosphorylation specific antibodies, FLT3 phosphorylation was reduced by 55%, 70% with 5nM, 10nM Sorafenib treatment respectively. Sorafenib treatment stopped proliferation of MV4-11 cells for nearly one weak with cells reinitiating proliferation in the second week. This may be due to a switch in metabolism of the cell and alternative expression of other receptors compensating loss of survival and proliferation promoting FLT3 signalling due to Sorafenib. Secretome analysis of 2-2.5 weeks chronically Sorafenib treated MV4-11 cells demonstrated that some survival and proliferation related receptors were significantly increased after chronic Sorafenib treatment such as FLT3, CD84, ICAM3, TNFRSF1B, CD44, CSF1R and IGFLR1. In particular, FLT3 activates PI3K and RAS pathways that are connected to survival and proliferation (84). FLT3 itself was a target for Sorafenib treatment (42, 71) and showed a strong significant increase of FLT3 upon acute and chronic Sorafenib treatment. Furthermore, CD84 was significantly increased upon Sorafenib treatment which has been described as a survival promoting receptor in Chronic Lymphocytic Leukemia (159). CD84 belongs to the SLAM immunoglobulin super family which has been described to interact and activate the BCL2 pathway leading to survival (159). It has been reported that ICAM3 activates PI3K/Akt pathway and thus can stimulate cancer cell proliferations (160). ICAM3 expression has been described to be increased in radio resistant cervical cancer cells as well (161). After Sorafenib treatment, ICAM3 was significantly increased as well. Furthermore, TNFRSF1B induces anti-apoptotic signals (162), CSF1R was significantly increased at higher Sorafenib concentration and has been described to play a role in cell growth and cell survival (163, 164). These results revealed that Sorafenib treatment leads to increased expression of alternative survival and proliferation promoting receptors in AML cell lines (Figure 64). This may render cells sensitive to alternative extrinsic growth or survival promoting molecules such as chemokines or interleukins leading to FLT3 independent activation of survival and growth promoting downstream signalling pathways. However, identification of interleukins maybe hampered by the fact that the SPECS protocol

uses a 30 kDa filter to remove unreacted DBCO reagent or ManNAZ sugars (27). Furthermore, NCAM2 showed robust significantly increased expression while NCAM1 expression was almost abolished. After 2 weeks of Sorafenib treatment, partial cells started to attach to the flask surface. This may be related to altered expression of cell adhesion molecules such as changes in NCAM receptor expression and needs to be further validated. On the other hand, FAS, PTPRC and PTPRJ were significantly decreased after Sorafenib application. As PTPRC has been defined as a negative regulator of cytokine receptor signalling (165) and PTPRJ has been described as negative regulator of FLT3 signalling and suppressor of AKT and ERK pathways (166, 167) this may be a mechanism for AML cells to improve the phosphorylation state of FLT3 receptor and other receptor tyrosine kinases. The FAS receptor is a member of the tumour necrosis factor receptor family that initiate apoptosis via the extrinsic pathway (168-170). In Sorafenib treated cells FAS was significantly decreased which may be a mechanism to protect cells from apoptosis.

Further analysis showed that, solute carriers were also increased with Sorafenib treatment such as SLC38A10, SLC19A1. These transporters may promote Sorafenib drug efflux out of the cell. In addition to these analysis, FLT3 and FLT3-phosphorylation were checked with Western blot analysis. In these analysis, we observed that already after 1 day of Sorafenib treatment, FLT3 phosphorylation is abolished in Sorafenib treated cells with upregulated FLT3 expression and wild type cells. However, reduced Sorafenib concentrations in chronically treated MV4-11 cells led to a mucher stronger increase in phosphorylation which is a consequently a strong proliferation signal. This result shows that the regular usage and dosage of Sorafenib are important parameters to bear in mind for a successful treatment of AML with Sorafenib and RTK inhibitor application in general. Furthermore, contribution of significantly increased and decreased receptors to Sorafenib resistance could be checked via further analysis. For example, sensitivity of MV4-11 cells towards Sorafenib could be tested upon CRISPR or siRNA mediated knock-outs of significantly increased receptors. Additionally, to validate these in vitro findings bone primary AML blasts of Sorafenib treated patients should be analysed as well.

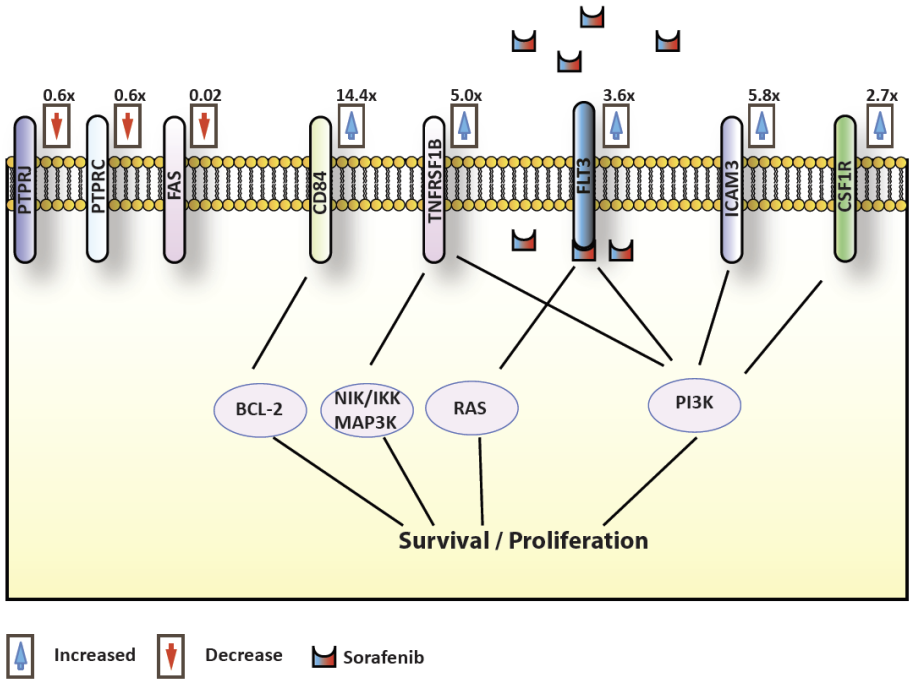

Figure 64. Overall possible resistance mechanism due to Sorafenib treatment. Significantly increased receptors are shown with blue arrow and significantly decreased receptors shown in red colour. Fold changes are calculated according to LFQ values Sorafenib/DMSO.

4.6 Establishment of CRISPR-CAS9 gene knock-out on FLT3 and KIT

Clustered regularly interspaced short palindromic repeats (CRISPR) in combination with the bacterial nuclease Cas9 are a state-of-the-art technology for genome editing which aids the generation of targeted gene knockouts (97). This part of thesis comprises CRISPR system set up for gene KO on AML cell lines. RTK inhibitors generally interact with multiple receptors and I would like to understand the specific receptor effect on the AML cell lines. So, Kasumi and MV4-11 cell lines were chosen as a model for KIT and FLT3 KO experiments. Lentiviral-Cas9-Blasticidine vector and lentiviral-sgRNA carrying vectors were used for the knock-out experiments. While designing the sgRNA, specificity of target exon and not effecting the crucial pathways taken into account. So I take the best candidates from the mit designing server (Zhang lab) and sgRNAs cloned under the U6 promoter vectors. After the Cas9 expression on the HEK293T, Kasumi and Mv4-11 cell lines, sgRNAs were applied as next step. CRISPR cleavages were achieved and proved with T7 endonuclease assays. Afterwards, single cell clones were generated and analysed with WB. We achieved knock-out on KIT receptor on Kasumi cell but not in the FLT3 on MV4-11 cell. As AML have less transduction capacity FACS-sorting should be applied directly after the transduction and cell with knock-out should be sorted and prepare for MS analysis. Furthermore, different sgRNAs can be design for FLT3 and c-Kit for knock-out. On the other hand, KIT knockout was seeming to be achieve, 6 nucleotides were removed in the target sequence but there is not any pre-stop codon form on the sequence so this needs to be validated with further experiments and afterwards proteome analysis follow up.

4.7 MS Analysis of AML serum samples

A step towards the analysis of soluble biomarkers in AML is the analysis of human serum with mass spectrometry. Human serum contains 7-22mg/ml of immunoglobulins and 35-50 mg/ml of albumin while other proteins are low abundant and thus has a very high dynamic range (171, 172). Due to technical limitations of mass spectrometry (MS), these highly abundant proteins prevent detection of low abundant proteins such as glycoproteins released from AML blasts in a mass spectrometry read out. Hence, I designed a protocol to remove these highly abundant proteins in serum samples. To this aim, G sepharose was used to get rid of immunoglobulins. Afterwards, a glycoprotein enrichment step is necessary to get rid of albumin. Therefore, aminooxybiotin, sodium periodate and m-phenylenediamine are used for oxidation and biotinylation of glycoproteins. This step was adapted from a previous study (173). Afterwards, biotinylation quality is checked with streptavidin-peroxidase. These preliminary experiments showed that these steps are necessary to get rid of immunoglobulins and albumin. After these experiments, samples with initial diagnosis and sample with complete remission were taken into account for a biomarker study. Consequently, MS analysis revealed that 190 glycoproteins were identified out of total 325 identified proteins in the serum samples. Of 190 identified glycoproteins, 141 were secreted proteins. Further GO-Term analysis indicated that 37% of the hits were involved in the blood coagulation pathway, 10% of the hits were involved in the plasminogen-activating cascade while 8% of identified glycoproteins were involved in Wnt and Cadherin signalling. Despite, I could remove most the immunoglobulins and albumin, results showed that the sample contained a lot of other abundant liver-originating proteins such as Haptoglobulin, Alpha-2 macroglobulin, Apolipoprotein A-B, transferrin and so on. Hence, the protocol needs to be further improved by for example clearing of these abundant proteins with depletion spin columns or other suitable techniques. However, I still was able to detect AML biomarkers in our MS analysis samples such as myeloperoxidase which was decreased 3.5-fold in between samples with initial diagnosis and complete remission. Furthermore, high changes were detected in the CD44 antigen level with a 11.7- and 14.5-fold decrease between samples with initial diagnosis and complete remission. These promising results indicated that after the improvement, this method can provide further interesting biomarker possibilities for confirmation of our in vitro data and as a tool for clinical diagnostics.

5. Summary and Future Aspect

The secretome is a crucial component for intercellular communication in multicellular organisms and comprises secreted and proteolytically released proteins (47). Changes in the secretome composition alter intercellular communication and thus can lead to pathological states such as cancer, neurodegenerative disease, autoimmune disorders or cardiovascular disease (31-34). Thereby, the secretome is a valuable resource for the identification of biomarkers or investigation of intercellular biology. Secretome protein enrichment with click sugars (SPECS) enables the identification of cell derived glycoproteins comprising the secretome in fetal calf serum containing conditioned media. Previous applications of the SPECS method to various scientific questions already demonstrated its feasibility and gave deep insights into protease biology (27, 29, 30, 52). As proposed before, SPECS is applicable to most of mammalian cell types. In this thesis, I established an optimized version of the SPECS method, applied SPECS to identify the secretome and surface proteome of different AML cell

lines, and studied the impact of Sorafenib on the surface proteome and secretome to identify Sorafenib resistance mechanisms in AML. Further I established CRISPR in AML cell lines and established the recombinant production of receptor tyrosine kinase ligands.

Testing different buffers with various pHs, more water soluble strained alkynes I established an optimized version of the SPECS protocol that allows the detection of nearly 1.6-fold more glycoproteins with higher sequence coverages and higher signal intensities (129). Future experiments will demonstrate how much the required input material can be reduced and whether less abundant primary cell types can be investigated with the optimized method. Furthermore, alternative strained alkynes attached to biotin moieties such as DBCO-S-S-PEG3-Biotin or DBCO-PEG4-Biotin conjugates could be tested for improving the efficiency and specificity of the protocol. Furthermore, the amount of streptavidin bead and the elution step could be adjusted for an even more optimized protocol. Next, these optimizations should be applied to the surface-click protocol to improve the glycoprotein detection on cellular lysates.

Acute myeloid leukemia (AML) is a myelodysplastic syndrome leading to the production and proliferation of immature myeloid progenitor cells. Abnormal proliferation of myeloid progenitor cells could lead to increase in immature malignant cells (blast) and less healthy blood elements like thrombocytes and erythrocytes in the blood (42, 81) Because of the aggressive and heterogeneous characteristics of AML survival rates are really low (82, 83). So in this manner, AML requires a more detailed understanding of its molecular biology. Using SPECS and surface-click, the secretome and surface proteome of different AML cell lines were successfully analysed. Analysing the data revealed that all reference markers established in flow cytometry aided diagnostic of AML were detected in the secretome and surface-proteome data. Further, I identified a lot of proteins such as receptor tyrosine kinases, solute carriers, different pathway related proteins that allow differentiation of the investigated AML cell lines and their respective AML subtypes. In the future, these protein hits could be evaluated in patient derived AML cells for their potential as biomarkers that allow easier disease monitoring and classification of AML. Especially, identified proteins that have a high expression in the myelopoietic system and low or lacking expression in other tissues of the body (such as OSCAR) should be taken into account. Furthermore, AML cell line profiles could be useful for further mechanistic studies and specific drug applications. On the other hand, I established a method for analysing the serum samples from the AML patients. In the future, AML patient material analysis should be improved with the cleaning the liver based most abundant proteins but still we detected the biomarkers that related to AML such as MPO and CD44.

In AML, one of the main concern of targeted therapy application is FLT3-ITD mutation (42, 71). Patients with FLT3-ITD mutation has a high risk of relapse (42, 81, 144). So, the main goal of this thesis was to identify Sorafenib resistance mechanisms of AML blasts analysing the secretome and the surface proteome. This underlying hypothesis is that treatment with receptor tyrosine kinase inhibitors can lead to activation of compensation mechanisms such as overexpression of the targeted receptor tyrosine kinase, overexpression of alternative RTKs, downregulation of pro-apoptotic pathways or increased autocrine stimulation by expression of respective ligands. Investigating the surface proteome and secretome of the

FLT3-ITD carrying cell line MV4-11 revealed that Sorafenib treatment resulted in increased expression of survival and proliferation related proteins while apoptosis inducing receptors were significantly decreased. In the future, proteins with alternative expression upon Sorafenib should be validated via Western blot or FACS analysis. Furthermore, downstream signalling pathways should be analysed and direct survival pathways should be enlightened in regard to sorafenib application. To verify whether these resistance mechanisms hold true in vivo, samples before and with recurrence under Sorafenib treatment should be comparatively analysed as well. To obtain a better mechanistic understanding how dysregulated expression of certain proteins contributes to Sorafenib resistance, increased receptors such as receptor tyrosine kinases should be knocked-out/knocked down with CRISPR/shRNA or inhibition experiments should be done with additional inhibitors and cell proliferation and sensitivity should be observed. Additionally, c-KIT inhibition and different drug applications could be studied with regard to compensation mechanisms in the Kasumi cell line. Solute carriers might be one of the interesting topic to proceed in the future. Different drugs can be applied on different cells and common solute career expression change can be enlightened and drug related solute careers can be identified with further mechanistic studies.

I established the letiviral based CRISPR-CAS9 knock-out system for KIT and FLT3 receptors. CRISPR-Cas9 operations were proved with t7 endonuclease assay. Furthermore, c-KIT Knockout proved with sequencing and WB analysis. So in the future steps, c-KIT-KO and FLT3-KO validations should be finished with additional experiments with different antibodies and sequencing. On the other hand, integration deficient psPAX2 (174) could be used for short term expression of Cas9 and this application could minimize the off-target possibilities. After the KO of specific RTKs, secretome and surface proteome should be analysed and this may enlighten the mechanism and connections of the target receptor.

In the last part of the thesis, recombinant receptor tyrosine kinase ligand production system successfully established and FLT3L, VEGFA and KITLG have synthesized already. These ligands should be applied to corresponding cell lines (MV4-11, NB4 and Kasumi) and their secretome and surface proteome analysis should be finished. These analyses would give an idea about how AML cells change their proteome with growth factors stimulations.

6. References

1. Aebersold R, Mann M. Mass-spectrometric exploration of proteome structure and function. Nature. 2016;537(7620):347-55.
2. Larance M, Lamond AI. Multidimensional proteomics for cell biology. Nat Rev Mol Cell Biol. 2015;16(5):269-80.
3. Fenn JB, Mann M, Meng CK, Wong SF, Whitehouse CM. Electrospray ionization for mass spectrometry of large biomolecules. Science. 1989;246(4926):64-71.
4. Karas M, Hillenkamp F. Laser desorption ionization of proteins with molecular masses exceeding 10,000 daltons. Anal Chem. 1988;60(20):2299-301.
5. Domon B, Aebersold R. Mass spectrometry and protein analysis. Science. 2006;312(5771):212-7.
6. Makarov A. Electrostatic axially harmonic orbital trapping: a high-performance technique of mass analysis. Anal Chem. 2000;72(6):1156-62.
7. Savaryn JP, Toby TK, Kelleher NL. A researcher's guide to mass spectrometry-based proteomics. Proteomics. 2016;16(18):2435-43.
8. Shukla AK, Futrell JH. Tandem mass spectrometry: dissociation of ions by collisional activation. J Mass Spectrom. 2000;35(9):1069-90.
9. Zubarev R. Protein primary structure using orthogonal fragmentation techniques in Fourier transform mass spectrometry. Expert Rev Proteomics. 2006;3(2):251-61.
10. Zubarev RA, Horn DM, Fridriksson EK, Kelleher NL, Kruger NA, Lewis MA, et al. Electron capture dissociation for structural characterization of multiply charged protein cations. Anal Chem. 2000;72(3):563-73.
11. Pitteri SJ, Chrisman PA, Hogan JM, McLuckey SA. Electron transfer ion/ion reactions in a three-dimensional quadrupole ion trap: reactions of doubly and triply protonated peptides with SO2*. Anal Chem. 2005;77(6):1831-9.
12. Syka JE, Coon JJ, Schroeder MJ, Shabanowitz J, Hunt DF. Peptide and protein sequence analysis by electron transfer dissociation mass spectrometry. Proc Natl Acad Sci U S A. 2004;101(26):9528-33.
13. Olsen JV, Macek B, Lange O, Makarov A, Horning S, Mann M. Higher-energy C-trap dissociation for peptide modification analysis. Nat Methods. 2007;4(9):709-12.
14. Makarov A, Denisov E, Kholomeev A, Balschun W, Lange O, Strupat K, et al. Performance evaluation of a hybrid linear ion trap/orbitrap mass spectrometer. Anal Chem. 2006;78(7):2113-20.
15. McDonald WH, Yates JR, 3rd. Shotgun proteomics: integrating technologies to answer biological questions. Curr Opin Mol Ther. 2003;5(3):302-9.
16. McLafferty FW, Breuker K, Jin M, Han X, Infusini G, Jiang H, et al. Top-down MS, a powerful complement to the high capabilities of proteolysis proteomics. FEBS J. 2007;274(24):6256-68.
17. Gygi SP, Rist B, Gerber SA, Turecek F, Gelb MH, Aebersold R. Quantitative analysis of complex protein mixtures using isotope-coded affinity tags. Nat Biotechnol. 1999;17(10):994-9.
18. Ong SE, Blagoev B, Kratchmarova I, Kristensen DB, Steen H, Pandey A, et al. Stable isotope labeling by amino acids in cell culture, SILAC, as a simple and accurate approach to expression proteomics. Mol Cell Proteomics. 2002;1(5):376-86.
19. Bantscheff M, Schirle M, Sweetman G, Rick J, Kuster B. Quantitative mass spectrometry in proteomics: a critical review. Anal Bioanal Chem. 2007;389(4):1017-31.
20. Hyung SW, Lee MY, Yu JH, Shin B, Jung HJ, Park JM, et al. A serum protein profile predictive of the resistance to neoadjuvant chemotherapy in advanced breast cancers. Mol Cell Proteomics. 2011;10(10):M111 011023.
21. Krishnamurthy D, Levin Y, Harris LW, Umrania Y, Bahn S, Guest PC. Analysis of the human pituitary proteome by data independent label-free liquid chromatography tandem mass spectrometry. Proteomics. 2011;11(3):495-500.

22. Eng JK, McCormack AL, Yates JR. An approach to correlate tandem mass spectral data of peptides with amino acid sequences in a protein database. J Am Soc Mass Spectrom. 1994;5(11):976-89.
23. Perkins DN, Pappin DJ, Creasy DM, Cottrell JS. Probability-based protein identification by searching sequence databases using mass spectrometry data. Electrophoresis. 1999;20(18):3551-67.
24. Cox J, Mann M. MaxQuant enables high peptide identification rates, individualized p.p.b.-range mass accuracies and proteome-wide protein quantification. Nat Biotechnol. 2008;26(12):1367-72.
25. Hughes CS, Foehr S, Garfield DA, Furlong EE, Steinmetz LM, Krijgsveld J. Ultrasensitive proteome analysis using paramagnetic bead technology. Mol Syst Biol. 2014;10:757.
26. Kleifeld O, Doucet A, auf dem Keller U, Prudova A, Schilling O, Kainthan RK, et al. Isotopic labeling of terminal amines in complex samples identifies protein N-termini and protease cleavage products. Nat Biotechnol. 2010;28(3):281-8.
27. Kuhn PH, Koroniak K, Hogl S, Colombo A, Zeitschel U, Willem M, et al. Secretome protein enrichment identifies physiological BACE1 protease substrates in neurons. EMBO J. 2012;31(14):3157-68.
28. Loo D, Jones A, Hill MM. Lectin magnetic bead array for biomarker discovery. J Proteome Res. 2010;9(10):5496-500.
29. Kuhn PH, Wang H, Dislich B, Colombo A, Zeitschel U, Ellwart JW, et al. ADAM10 is the physiologically relevant, constitutive alpha-secretase of the amyloid precursor protein in primary neurons. EMBO J. 2010;29(17):3020-32.
30. Schwenk BM, Hartmann H, Serdaroglu A, Schludi MH, Hornburg D, Meissner F, et al. TDP-43 loss of function inhibits endosomal trafficking and alters trophic signaling in neurons. EMBO J. 2016;35(21):2350-70.
31. Gloghini A, Bongarzone I. Cell-secreted signals shape lymphoma identity. Semin Cancer Biol. 2015;34:81-91.
32. Li X, Jiang J, Zhao X, Zhao Y, Cao Q, Zhao Q, et al. In-depth analysis of secretome and N-glycosecretome of human hepatocellular carcinoma metastatic cell lines shed light on metastasis correlated proteins. Oncotarget. 2016;7(16):22031-49.
33. Lin Q, Lim HS, Lin HL, Tan HT, Lim TK, Cheong WK, et al. Analysis of colorectal cancer glyco-secretome identifies laminin beta-1 (LAMB1) as a potential serological biomarker for colorectal cancer. Proteomics. 2015;15(22):3905-20.
34. Sharma A, Bender S, Zimmermann M, Riesterer O, Broggini-Tenzer A, Pruschy MN. Secretome Signature Identifies ADAM17 as Novel Target for Radiosensitization of Non-Small Cell Lung Cancer. Clin Cancer Res. 2016;22(17):4428-39.
35. Nami B, Wang Z. HER2 in Breast Cancer Stemness: A Negative Feedback Loop towards Trastuzumab Resistance. Cancers (Basel). 2017;9(5).
36. Yaziji H, Goldstein LC, Barry TS, Werling R, Hwang H, Ellis GK, et al. HER-2 testing in breast cancer using parallel tissue-based methods. JAMA. 2004;291(16):1972-7.
37. Owens MA, Horten BC, Da Silva MM. HER2 amplification ratios by fluorescence in situ hybridization and correlation with immunohistochemistry in a cohort of 6556 breast cancer tissues. Clin Breast Cancer. 2004;5(1):63-9.
38. Slamon DJ, Clark GM, Wong SG, Levin WJ, Ullrich A, McGuire WL. Human breast cancer: correlation of relapse and survival with amplification of the HER-2/neu oncogene. Science. 1987;235(4785):177-82.
39. Kuchenbauer F, Schnittger S, Look T, Gilliland G, Tenen D, Haferlach T, et al. Identification of additional cytogenetic and molecular genetic abnormalities in acute myeloid leukaemia with t(8;21)/AML1-ETO. Br J Haematol. 2006;134(6):616-9.
40. Paschka P, Marcucci G, Ruppert AS, Mrozek K, Chen H, Kittles RA, et al. Adverse prognostic significance of KIT mutations in adult acute myeloid leukemia with inv(16) and t(8;21): a Cancer and Leukemia Group B Study. J Clin Oncol. 2006;24(24):3904-11.

41. Gao X, Lin J, Gao L, Deng A, Lu X, Li Y, et al. High expression of c-kit mRNA predicts unfavorable outcome in adult patients with t(8;21) acute myeloid leukemia. PLoS One. 2015;10(4):e0124241.
42. De Kouchkovsky I, Abdul-Hay M. 'Acute myeloid leukemia: a comprehensive review and 2016 update'. Blood Cancer J. 2016;6(7):e441.
43. Patel JP, Gonen M, Figueroa ME, Fernandez H, Sun Z, Racevskis J, et al. Prognostic relevance of integrated genetic profiling in acute myeloid leukemia. N Engl J Med. 2012;366(12):1079-89.
44. Stirewalt DL, Radich JP. The role of FLT3 in haematopoietic malignancies. Nat Rev Cancer. 2003;3(9):650-65.
45. Gilliland DG, Griffin JD. The roles of FLT3 in hematopoiesis and leukemia. Blood. 2002;100(5):1532-42.
46. Price PJ, Brewer GJ. Serum-Free Media for Neural Cell Cultures. In: Fedoroff S, Richardson A, editors. Protocols for Neural Cell Culture. Totowa, NJ: Humana Press; 2001. p. 255-64.
47. Meissner F, Scheltema RA, Mollenkopf HJ, Mann M. Direct proteomic quantification of the secretome of activated immune cells. Science. 2013;340(6131):475-8.
48. Huse JT, Liu K, Pijak DS, Carlin D, Lee VM, Doms RW. Beta-secretase processing in the trans-Golgi network preferentially generates truncated amyloid species that accumulate in Alzheimer's disease brain. J Biol Chem. 2002;277(18):16278-84.
49. Sletten EM, Bertozzi CR. From mechanism to mouse: a tale of two bioorthogonal reactions. Acc Chem Res. 2011;44(9):666-76.
50. Sletten EM, Bertozzi CR. Bioorthogonal chemistry: fishing for selectivity in a sea of functionality. Angew Chem Int Ed Engl. 2009;48(38):6974-98.
51. Teo CF, Wells L. Monitoring protein O-linked beta-N-acetylglucosamine status via metabolic labeling and copper-free click chemistry. Anal Biochem. 2014;464:70-2.
52. Kuhn PH, Voss M, Haug-Kroper M, Schroder B, Schepers U, Brase S, et al. Secretome analysis identifies novel signal Peptide peptidase-like 3 (Sppl3) substrates and reveals a role of Sppl3 in multiple Golgi glycosylation pathways. Mol Cell Proteomics. 2015;14(6):1584-98.
53. Luis TC, Killmann NM, Staal FJ. Signal transduction pathways regulating hematopoietic stem cell biology: introduction to a series of Spotlight Reviews. Leukemia. 2012;26(1):86-90.
54. Doulatov S, Notta F, Laurenti E, Dick JE. Hematopoiesis: a human perspective. Cell Stem Cell. 2012;10(2):120-36.
55. Hjelle SM, Forthun RB, Haaland I, Reikvam H, Sjoholt G, Bruserud O, et al. Clinical proteomics of myeloid leukemia. Genome Med. 2010;2(6):41.
56. Corces-Zimmerman MR, Majeti R. Pre-leukemic evolution of hematopoietic stem cells: the importance of early mutations in leukemogenesis. Leukemia. 2014;28(12):2276-82.
57. Arber DA, Orazi A, Hasserjian R, Thiele J, Borowitz MJ, Le Beau MM, et al. The 2016 revision to the World Health Organization classification of myeloid neoplasms and acute leukemia. Blood. 2016;127(20):2391-405.
58. Grove CS, Vassiliou GS. Acute myeloid leukaemia: a paradigm for the clonal evolution of cancer? Dis Model Mech. 2014;7(8):941-51.
59. Siegel RL, Miller KD, Jemal A. Cancer statistics, 2016. CA Cancer J Clin. 2016;66(1):7-30.
60. Ishii K, Young NS. Anemia of Central Origin. Semin Hematol. 2015;52(4):321-38.
61. Gonzalez-Porras JR, Cordoba I, Such E, Nomdedeu B, Vallespi T, Carbonell F, et al. Prognostic impact of severe thrombocytopenia in low-risk myelodysplastic syndrome. Cancer. 2011;117(24):5529-37.
62. Kumar CC. Genetic abnormalities and challenges in the treatment of acute myeloid leukemia. Genes Cancer. 2011;2(2):95-107.
63. Dohner H, Estey E, Grimwade D, Amadori S, Appelbaum FR, Buchner T, et al. Diagnosis and management of AML in adults: 2017 ELN recommendations from an international expert panel. Blood. 2017;129(4):424-47.

64. Bennett JM, Catovsky D, Daniel MT, Flandrin G, Galton DA, Gralnick HR, et al. Proposals for the classification of the acute leukaemias. French-American-British (FAB) co-operative group. Br J Haematol. 1976;33(4):451-8.
65. Graham FL, Whitmore GF. The effect of-beta-D-arabinofuranosylcytosine on growth, viability, and DNA synthesis of mouse L-cells. Cancer Res. 1970;30(11):2627-35.
66. Wang LM, White JC, Capizzi RL. The effect of ara-C-induced inhibition of DNA synthesis on its cellular pharmacology. Cancer Chemother Pharmacol. 1990;25(6):418-24.
67. Lehmann M, Vilar Kde S, Franco A, Reguly ML, Rodrigues de Andrade HH. Activity of topoisomerase inhibitors daunorubicin, idarubicin, and aclarubicin in the Drosophila Somatic Mutation and Recombination Test. Environ Mol Mutagen. 2004;43(4):250-7.
68. Gill H, Leung AY, Kwong YL. Molecularly targeted therapy in acute myeloid leukemia. Future Oncol. 2016;12(6):827-38.
69. Lemmon MA, Schlessinger J. Cell signaling by receptor tyrosine kinases. Cell. 2010;141(7):1117-34.
70. Hojjat-Farsangi M. Small-molecule inhibitors of the receptor tyrosine kinases: promising tools for targeted cancer therapies. Int J Mol Sci. 2014;15(8):13768-801.
71. Fathi AT, Chen YB. The role of FLT3 inhibitors in the treatment of FLT3-mutated acute myeloid leukemia. Eur J Haematol. 2017;98(4):330-6.
72. Levis M. FLT3 mutations in acute myeloid leukemia: what is the best approach in 2013? Hematology Am Soc Hematol Educ Program. 2013;2013:220-6.
73. Palumbo MO, Kavan P, Miller WH, Jr., Panasci L, Assouline S, Johnson N, et al. Systemic cancer therapy: achievements and challenges that lie ahead. Front Pharmacol. 2013;4:57.
74. Borthakur G, Kantarjian H, Ravandi F, Zhang W, Konopleva M, Wright JJ, et al. Phase I study of sorafenib in patients with refractory or relapsed acute leukemias. Haematologica. 2011;96(1):62-8.
75. Pratz KW, Cho E, Levis MJ, Karp JE, Gore SD, McDevitt M, et al. A pharmacodynamic study of sorafenib in patients with relapsed and refractory acute leukemias. Leukemia. 2010;24(8):1437-44.
76. Crump M, Hedley D, Kamel-Reid S, Leber B, Wells R, Brandwein J, et al. A randomized phase I clinical and biologic study of two schedules of sorafenib in patients with myelodysplastic syndrome or acute myeloid leukemia: a NCIC (National Cancer Institute of Canada) Clinical Trials Group Study. Leuk Lymphoma. 2010;51(2):252-60.
77. Zhang W, Konopleva M, Shi YX, McQueen T, Harris D, Ling X, et al. Mutant FLT3: a direct target of sorafenib in acute myelogenous leukemia. J Natl Cancer Inst. 2008;100(3):184-98.
78. Man CH, Fung TK, Ho C, Han HH, Chow HC, Ma AC, et al. Sorafenib treatment of FLT3-ITD(+) acute myeloid leukemia: favorable initial outcome and mechanisms of subsequent nonresponsiveness associated with the emergence of a D835 mutation. Blood. 2012;119(22):5133-43.
79. Al-Kali A, Cortes J, Faderl S, Jones D, Abril C, Pierce S, et al. Patterns of molecular response to and relapse after combination of sorafenib, idarubicin, and cytarabine in patients with FLT3 mutant acute myeloid leukemia. Clin Lymphoma Myeloma Leuk. 2011;11(4):361-6.
80. Ravandi F, Cortes JE, Jones D, Faderl S, Garcia-Manero G, Konopleva MY, et al. Phase I/II study of combination therapy with sorafenib, idarubicin, and cytarabine in younger patients with acute myeloid leukemia. J Clin Oncol. 2010;28(11):1856-62.
81. Saultz JN, Garzon R. Acute Myeloid Leukemia: A Concise Review. J Clin Med. 2016;5(3).
82. Mrozek K, Marcucci G, Nicolet D, Maharry KS, Becker H, Whitman SP, et al. Prognostic significance of the European LeukemiaNet standardized system for reporting cytogenetic and molecular alterations in adults with acute myeloid leukemia. J Clin Oncol. 2012;30(36):4515-23.
83. Tallman MS, Gilliland DG, Rowe JM. Drug therapy for acute myeloid leukemia. Blood. 2005;106(4):1154-63.
84. Takahashi S. Downstream molecular pathways of FLT3 in the pathogenesis of acute myeloid leukemia: biology and therapeutic implications. J Hematol Oncol. 2011;4:13.

85. de Necochea-Campion R, Shouse GP, Zhou Q, Mirshahidi S, Chen CS. Aberrant splicing and drug resistance in AML. J Hematol Oncol. 2016;9(1):85.
86. Mali P, Yang L, Esvelt KM, Aach J, Guell M, DiCarlo JE, et al. RNA-guided human genome engineering via Cas9. Science. 2013;339(6121):823-6.
87. Cong L, Ran FA, Cox D, Lin S, Barretto R, Habib N, et al. Multiplex genome engineering using CRISPR/Cas systems. Science. 2013;339(6121):819-23.
88. Zhang F, Cong L, Lodato S, Kosuri S, Church GM, Arlotta P. Efficient construction of sequence-specific TAL effectors for modulating mammalian transcription. Nat Biotechnol. 2011;29(2):149-53.
89. Wood AJ, Lo TW, Zeitler B, Pickle CS, Ralston EJ, Lee AH, et al. Targeted genome editing across species using ZFNs and TALENs. Science. 2011;333(6040):307.
90. Sander JD, Dahlborg EJ, Goodwin MJ, Cade L, Zhang F, Cifuentes D, et al. Selection-free zinc-finger-nuclease engineering by context-dependent assembly (CoDA). Nat Methods. 2011;8(1):67-9.
91. Makarova KS, Haft DH, Barrangou R, Brouns SJ, Charpentier E, Horvath P, et al. Evolution and classification of the CRISPR-Cas systems. Nat Rev Microbiol. 2011;9(6):467-77.
92. Deveau H, Garneau JE, Moineau S. CRISPR/Cas system and its role in phage-bacteria interactions. Annu Rev Microbiol. 2010;64:475-93.
93. Christian M, Cermak T, Doyle EL, Schmidt C, Zhang F, Hummel A, et al. Targeting DNA double-strand breaks with TAL effector nucleases. Genetics. 2010;186(2):757-61.
94. Miller JC, Holmes MC, Wang J, Guschin DY, Lee YL, Rupniewski I, et al. An improved zinc-finger nuclease architecture for highly specific genome editing. Nat Biotechnol. 2007;25(7):778-85.
95. Porteus MH, Baltimore D. Chimeric nucleases stimulate gene targeting in human cells. Science. 2003;300(5620):763.
96. Sander JD, Joung JK. CRISPR-Cas systems for editing, regulating and targeting genomes. Nat Biotechnol. 2014;32(4):347-55.
97. Ran FA, Hsu PD, Wright J, Agarwala V, Scott DA, Zhang F. Genome engineering using the CRISPR-Cas9 system. Nat Protoc. 2013;8(11):2281-308.
98. Jinek M, Chylinski K, Fonfara I, Hauer M, Doudna JA, Charpentier E. A programmable dual-RNA-guided DNA endonuclease in adaptive bacterial immunity. Science. 2012;337(6096):816-21.
99. Zhang Y, Heidrich N, Ampattu BJ, Gunderson CW, Seifert HS, Schoen C, et al. Processing-independent CRISPR RNAs limit natural transformation in Neisseria meningitidis. Mol Cell. 2013;50(4):488-503.
100. Garneau JE, Dupuis ME, Villion M, Romero DA, Barrangou R, Boyaval P, et al. The CRISPR/Cas bacterial immune system cleaves bacteriophage and plasmid DNA. Nature. 2010;468(7320):67-71.
101. Haeussler M, Schonig K, Eckert H, Eschstruth A, Mianne J, Renaud JB, et al. Evaluation of off-target and on-target scoring algorithms and integration into the guide RNA selection tool CRISPOR. Genome Biol. 2016;17(1):148.
102. Perez EE, Wang J, Miller JC, Jouvenot Y, Kim KA, Liu O, et al. Establishment of HIV-1 resistance in CD4+ T cells by genome editing using zinc-finger nucleases. Nat Biotechnol. 2008;26(7):808-16.
103. Chen F, Pruett-Miller SM, Huang Y, Gjoka M, Duda K, Taunton J, et al. High-frequency genome editing using ssDNA oligonucleotides with zinc-finger nucleases. Nat Methods. 2011;8(9):753-5.
104. Saleh-Gohari N, Helleday T. Conservative homologous recombination preferentially repairs DNA double-strand breaks in the S phase of the cell cycle in human cells. Nucleic Acids Res. 2004;32(12):3683-8.
105. Keegan L, Gill G, Ptashne M. Separation of DNA binding from the transcription-activating function of a eukaryotic regulatory protein. Science. 1986;231(4739):699-704.
106. Hartley KO, Nutt SL, Amaya E. Targeted gene expression in transgenic Xenopus using the binary Gal4-UAS system. Proc Natl Acad Sci U S A. 2002;99(3):1377-82.

107. Scheer N, Campos-Ortega JA. Use of the Gal4-UAS technique for targeted gene expression in the zebrafish. Mech Dev. 1999;80(2):153-8.
108. Ornitz DM, Moreadith RW, Leder P. Binary system for regulating transgene expression in mice: targeting int-2 gene expression with yeast GAL4/UAS control elements. Proc Natl Acad Sci U S A. 1991;88(3):698-702.
109. Fischer JA, Giniger E, Maniatis T, Ptashne M. GAL4 activates transcription in Drosophila. Nature. 1988;332(6167):853-6.
110. Koster RW, Fraser SE. Tracing transgene expression in living zebrafish embryos. Dev Biol. 2001;233(2):329-46.
111. Sadowski I, Ma J, Triezenberg S, Ptashne M. GAL4-VP16 is an unusually potent transcriptional activator. Nature. 1988;335(6190):563-4.
112. Beckett D, Kovaleva E, Schatz PJ. A minimal peptide substrate in biotin holoenzyme synthetase-catalyzed biotinylation. Protein Sci. 1999;8(4):921-9.
113. Barker DF, Campbell AM. The birA gene of Escherichia coli encodes a biotin holoenzyme synthetase. J Mol Biol. 1981;146(4):451-67.
114. Bornhorst BJ, Falke JJ. Reprint of: Purification of Proteins Using Polyhistidine Affinity Tags. Protein Expr Purif. 2011.
115. Hengen P. Purification of His-Tag fusion proteins from Escherichia coli. Trends Biochem Sci. 1995;20(7):285-6.
116. van Geel R, Pruijn GJ, van Delft FL, Boelens WC. Preventing thiol-yne addition improves the specificity of strain-promoted azide-alkyne cycloaddition. Bioconjug Chem. 2012;23(3):392-8.
117. Wilhelm M, Schlegl J, Hahne H, Gholami AM, Lieberenz M, Savitski MM, et al. Mass-spectrometry-based draft of the human proteome. Nature. 2014;509(7502):582-7.
118. Cancer Genome Atlas Research N, Ley TJ, Miller C, Ding L, Raphael BJ, Mungall AJ, et al. Genomic and epigenomic landscapes of adult de novo acute myeloid leukemia. N Engl J Med. 2013;368(22):2059-74.
119. Sanjana NE, Shalem O, Zhang F. Improved vectors and genome-wide libraries for CRISPR screening. Nat Methods. 2014;11(8):783-4.
120. Baskin JM, Prescher JA, Laughlin ST, Agard NJ, Chang PV, Miller IA, et al. Copper-free click chemistry for dynamic in vivo imaging. Proc Natl Acad Sci U S A. 2007;104(43):16793-7.
121. Laughlin ST, Baskin JM, Amacher SL, Bertozzi CR. In vivo imaging of membrane-associated glycans in developing zebrafish. Science. 2008;320(5876):664-7.
122. Luchansky SJ, Argade S, Hayes BK, Bertozzi CR. Metabolic functionalization of recombinant glycoproteins. Biochemistry. 2004;43(38):12358-66.
123. Jewett JC, Bertozzi CR. Cu-free click cycloaddition reactions in chemical biology. Chem Soc Rev. 2010;39(4):1272-9.
124. Prescher JA, Dube DH, Bertozzi CR. Chemical remodelling of cell surfaces in living animals. Nature. 2004;430(7002):873-7.
125. Rostovtsev VV, Green LG, Fokin VV, Sharpless KB. A stepwise huisgen cycloaddition process: copper(I)-catalyzed regioselective "ligation" of azides and terminal alkynes. Angew Chem Int Ed Engl. 2002;41(14):2596-9.
126. Kuhn PH, Colombo AV, Schusser B, Dreymueller D, Wetzel S, Schepers U, et al. Systematic substrate identification indicates a central role for the metalloprotease ADAM10 in axon targeting and synapse function. Elife. 2016;5.
127. Wagner M, Oelsner M, Moore A, Gotte F, Kuhn PH, Haferlach T, et al. Integration of innate into adaptive immune responses in ZAP-70-positive chronic lymphocytic leukemia. Blood. 2016;127(4):436-48.
128. Voss M, Kunzel U, Higel F, Kuhn PH, Colombo A, Fukumori A, et al. Shedding of glycan-modifying enzymes by signal peptide peptidase-like 3 (SPPL3) regulates cellular N-glycosylation. EMBO J. 2014;33(24):2890-905.

129. Serdaroglu A, Muller SA, Schepers U, Brase S, Weichert W, Lichtenthaler SF, et al. An optimised version of the secretome protein enrichment with click sugars (SPECS) method leads to enhanced coverage of the secretome. Proteomics. 2017;17(5).
130. de The H, Chen Z. Acute promyelocytic leukaemia: novel insights into the mechanisms of cure. Nat Rev Cancer. 2010;10(11):775-83.
131. Estey EH. Acute myeloid leukemia: 2013 update on risk-stratification and management. Am J Hematol. 2013;88(4):318-27.
132. Aich U, Meledeo MA, Sampathkumar SG, Fu J, Jones MB, Weier CA, et al. Development of delivery methods for carbohydrate-based drugs: controlled release of biologically-active short chain fatty acid-hexosamine analogs. Glycoconj J. 2010;27(4):445-59.
133. Kim EJ, Sampathkumar SG, Jones MB, Rhee JK, Baskaran G, Goon S, et al. Characterization of the metabolic flux and apoptotic effects of O-hydroxyl- and N-acyl-modified N-acetylmannosamine analogs in Jurkat cells. J Biol Chem. 2004;279(18):18342-52.
134. Sampathkumar SG, Li AV, Jones MB, Sun Z, Yarema KJ. Metabolic installation of thiols into sialic acid modulates adhesion and stem cell biology. Nat Chem Biol. 2006;2(3):149-52.
135. Yarema KJ, Mahal LK, Bruehl RE, Rodriguez EC, Bertozzi CR. Metabolic delivery of ketone groups to sialic acid residues. Application To cell surface glycoform engineering. J Biol Chem. 1998;273(47):31168-79.
136. Campbell ID, Humphries MJ. Integrin structure, activation, and interactions. Cold Spring Harb Perspect Biol. 2011;3(3).
137. Turner MD, Nedjai B, Hurst T, Pennington DJ. Cytokines and chemokines: At the crossroads of cell signalling and inflammatory disease. Biochim Biophys Acta. 2014;1843(11):2563-82.
138. Borish LC, Steinke JW. 2. Cytokines and chemokines. J Allergy Clin Immunol. 2003;111(2 Suppl):S460-75.
139. She M, Niu X, Chen X, Li J, Zhou M, He Y, et al. Resistance of leukemic stem-like cells in AML cell line KG1a to natural killer cell-mediated cytotoxicity. Cancer Lett. 2012;318(2):173-9.
140. Costello R, Mallet F, Chambost H, Sainty D, Arnoulet C, Gastaut JA, et al. The immunophenotype of minimally differentiated acute myeloid leukemia (AML-M0): reduced immunogenicity and high frequency of CD34+/CD38- leukemic progenitors. Leukemia. 1999;13(10):1513-8.
141. Webber BA, Cushing MM, Li S. Prognostic significance of flow cytometric immunophenotyping in acute myeloid leukemia. Int J Clin Exp Pathol. 2008;1(2):124-33.
142. Nemeth K, Schoppet M, Al-Fakhri N, Helas S, Jessberger R, Hofbauer LC, et al. The role of osteoclast-associated receptor in osteoimmunology. J Immunol. 2011;186(1):13-8.
143. Boyer SW, Schroeder AV, Smith-Berdan S, Forsberg EC. All hematopoietic cells develop from hematopoietic stem cells through Flk2/Flt3-positive progenitor cells. Cell Stem Cell. 2011;9(1):64-73.
144. Gale RE, Green C, Allen C, Mead AJ, Burnett AK, Hills RK, et al. The impact of FLT3 internal tandem duplication mutant level, number, size, and interaction with NPM1 mutations in a large cohort of young adult patients with acute myeloid leukemia. Blood. 2008;111(5):2776-84.
145. Qian BZ, Zhang H, Li J, He T, Yeo EJ, Soong DY, et al. FLT1 signaling in metastasis-associated macrophages activates an inflammatory signature that promotes breast cancer metastasis. J Exp Med. 2015;212(9):1433-48.
146. Zhang SD, McCrudden CM, Meng C, Lin Y, Kwok HF. The significance of combining VEGFA, FLT1, and KDR expressions in colon cancer patient prognosis and predicting response to bevacizumab. Onco Targets Ther. 2015;8:835-43.
147. Eklund L, Kangas J, Saharinen P. Angiopoietin-Tie signalling in the cardiovascular and lymphatic systems. Clin Sci (Lond). 2017;131(1):87-103.
148. Wakabayashi M, Miwa H, Shikami M, Hiramatsu A, Ikai T, Tajima E, et al. Autocrine pathway of angiopoietins-Tie2 system in AML cells: association with phosphatidyl-inositol 3 kinase. Hematol J. 2004;5(4):353-60.

149. Patsialou A, Wyckoff J, Wang Y, Goswami S, Stanley ER, Condeelis JS. Invasion of human breast cancer cells in vivo requires both paracrine and autocrine loops involving the colony-stimulating factor-1 receptor. Cancer Res. 2009;69(24):9498-506.
150. Richardsen E, Uglehus RD, Johnsen SH, Busund LT. Macrophage-colony stimulating factor (CSF1) predicts breast cancer progression and mortality. Anticancer Res. 2015;35(2):865-74.
151. Kampen KR, Ter Elst A, de Bont ES. Vascular endothelial growth factor signaling in acute myeloid leukemia. Cell Mol Life Sci. 2013;70(8):1307-17.
152. Frohling S. Ligand-induced MET signaling as targetable codependence in acute myeloid leukemia. Haematologica. 2012;97(8):1118.
153. Organ SL, Tsao MS. An overview of the c-MET signaling pathway. Ther Adv Med Oncol. 2011;3(1 Suppl):S7-S19.
154. Dombret H. Gene mutation and AML pathogenesis. Blood. 2011;118(20):5366-7.
155. Takahashi S. Current findings for recurring mutations in acute myeloid leukemia. J Hematol Oncol. 2011;4:36.
156. Dohner H, Estey EH, Amadori S, Appelbaum FR, Buchner T, Burnett AK, et al. Diagnosis and management of acute myeloid leukemia in adults: recommendations from an international expert panel, on behalf of the European LeukemiaNet. Blood. 2010;115(3):453-74.
157. Vardiman JW, Thiele J, Arber DA, Brunning RD, Borowitz MJ, Porwit A, et al. The 2008 revision of the World Health Organization (WHO) classification of myeloid neoplasms and acute leukemia: rationale and important changes. Blood. 2009;114(5):937-51.
158. Papaemmanuil E, Gerstung M, Bullinger L, Gaidzik VI, Paschka P, Roberts ND, et al. Genomic Classification and Prognosis in Acute Myeloid Leukemia. N Engl J Med. 2016;374(23):2209-21.
159. Binsky-Ehrenreich I, Marom A, Sobotta MC, Shvidel L, Berrebi A, Hazan-Halevy I, et al. CD84 is a survival receptor for CLL cells. Oncogene. 2014;33(8):1006-16.
160. Kim YG, Kim MJ, Lim JS, Lee MS, Kim JS, Yoo YD. ICAM-3-induced cancer cell proliferation through the PI3K/Akt pathway. Cancer Lett. 2006;239(1):103-10.
161. Chung YM, Kim BG, Park CS, Huh SJ, Kim J, Park JK, et al. Increased expression of ICAM-3 is associated with radiation resistance in cervical cancer. Int J Cancer. 2005;117(2):194-201.
162. Torrey H, Butterworth J, Mera T, Okubo Y, Wang L, Baum D, et al. Targeting TNFR2 with antagonistic antibodies inhibits proliferation of ovarian cancer cells and tumor-associated Tregs. Sci Signal. 2017;10(462).
163. Casas S, Nagy B, Elonen E, Aventin A, Larramendy ML, Sierra J, et al. Aberrant expression of HOXA9, DEK, CBL and CSF1R in acute myeloid leukemia. Leuk Lymphoma. 2003;44(11):1935-41.
164. Stanley ER, Chitu V. CSF-1 receptor signaling in myeloid cells. Cold Spring Harb Perspect Biol. 2014;6(6).
165. Irie-Sasaki J, Sasaki T, Matsumoto W, Opavsky A, Cheng M, Welstead G, et al. CD45 is a JAK phosphatase and negatively regulates cytokine receptor signalling. Nature. 2001;409(6818):349-54.
166. Yan CM, Zhao YL, Cai HY, Miao GY, Ma W. Blockage of PTPRJ promotes cell growth and resistance to 5-FU through activation of JAK1/STAT3 in the cervical carcinoma cell line C33A. Oncol Rep. 2015;33(4):1737-44.
167. Godfrey R, Arora D, Bauer R, Stopp S, Muller JP, Heinrich T, et al. Cell transformation by FLT3 ITD in acute myeloid leukemia involves oxidative inactivation of the tumor suppressor protein-tyrosine phosphatase DEP-1/ PTPRJ. Blood. 2012;119(19):4499-511.
168. Lavrik IN, Krammer PH. Regulation of CD95/Fas signaling at the DISC. Cell Death Differ. 2012;19(1):36-41.
169. Kaufmann T, Strasser A, Jost PJ. Fas death receptor signalling: roles of Bid and XIAP. Cell Death Differ. 2012;19(1):42-50.
170. Kober AM, Legewie S, Pforr C, Fricker N, Eils R, Krammer PH, et al. Caspase-8 activity has an essential role in CD95/Fas-mediated MAPK activation. Cell Death Dis. 2011;2:e212.
171. Jin Y, Zhao L, Peng F. Prognostic impact of serum albumin levels on the recurrence of stage I non-small cell lung cancer. Clinics (Sao Paulo). 2013;68(5):686-93.

172. Gonzalez-Quintela A, Alende R, Gude F, Campos J, Rey J, Meijide LM, et al. Serum levels of immunoglobulins (IgG, IgA, IgM) in a general adult population and their relationship with alcohol consumption, smoking and common metabolic abnormalities. Clin Exp Immunol. 2008;151(1):42-50.
173. Zeng Y, Ramya TN, Dirksen A, Dawson PE, Paulson JC. High-efficiency labeling of sialylated glycoproteins on living cells. Nat Methods. 2009;6(3):207-9.
174. Wanisch K, Yanez-Munoz RJ. Integration-deficient lentiviral vectors: a slow coming of age. Mol Ther. 2009;17(8):1316-32.

7. Abbreviations

ACS	American Cancer Society
ALL	Acute Lymphocytic Leukemia
AML	Acute Myeloid Leukemia
BirA	Bifunctional Ligase
BSA	Bovine Serum Albumin
c-KIT	Mast/Stem cell Growth Factor Receptor KIT
CBC	Complete Blood Count
CD84	SLAM Family Member 5
CID	Collision Induced Dissociation
CLL	Chronic Lymphocytic Leukemia
CML	Chronic Myeloid Leukemia
CRISPR	Clustered Regularly Interspaced Short Palindromic Repeats
CSF1R	Colony Stimulating Factor 1 Receptor
DMSO	Dimethyl Sulfoxide
DPB	DBCO-Peg12-Biotin
DSB	DBCO-Sulfo-Biotin
DTT	Dithiothreitol
ECD	Electron Capture Dissociation
EGF	Epidermal Growth Factor
ESI	Electrospray Ionization

ETD	Electro Transfer dissociation
FAB	French-American-British
FAS	Tumor Necrosis Factor Receptor Superfamily Member 6
FACS	Fluorescent-Activated Cell Sorting
FCS	Fetal Calf Serum
FGF	Fibroblast Growth Factor
FLT3	Fms like Tyrosine Kinase 3
FLT3-ITD	Internal Tandem Duplication of FLT3
FLT3-TKD	Tyrosine Kinase Domain of FLT3
FLT3L	Fms like Tyrosine Kinase 3 Ligand
FLT4	Vascular Endothelial Growth Factor Receptor 3
FTICR	Fourier-Transform Ion Cyclotron Resonance
GalNAZ	N-azidoacetylgalactosamine tetraacylated
GlcNAZ	N-azidoacetylglucosamine tetraacylated
GFP	Green Fluorescent Protein
HCD	High-energy Collisional Dissociation
HDR	Homology Directed Repair
HIS-tag	Histidine Tag
IAA	Iodoacetemide
iBAQ	Intensity Based Absolute Quantification
ICAM3	Intercellular Adhesion Molecule 3
ICAT	Isotope-Coded Affinity Tags
IGF1	Insulin like Growth Factor-1
IGF2	Insulin like Growth Factor-2
IGFLR1	IGF-like Family Receptor 1
INDEL	Insertion/Deletion
KITLG	Mast/Stem cell Growth Factor Receptor KIT Ligand
LFQ	Label-Free Quantification
LIT	Linear Ion Traps

ManNAZ	Tetraacetyl-N-azidoacetyl-mannosamine
MALDI	Matrix-assisted Laser Desorption/Ionization
MPO	Myeloperoxidase
MS	Mass Spectrometry
m/z	Mass to Charge Ratio
NEAA	Non-Essential Amino Acids
NHEJ	Non-Homologous End Joining
OSCAR	Osteoclast-associated Immunoglobulin-like Receptor
PAM	Protospacer Adjacent Motif
PBS	Phosphate Buffer Saline
PI3K	Phosphatidylinositol 3-Kinase Regulatory Subunit Alpha
PTPRC	Protein Tyrosine Phosphatase Receptor Type C
PTPRJ	Protein Tyrosine Phosphatase Receptor Type ETA
Q	Quadrupole
RTK	Receptor Tyrosine Kinase
RTKL	Receptor Tyrosine Kinase Ligand
sgRNA	Single Guide RNA
SILAC	Stable Isotope Labelling of Amino Acids in Cell Culture
SPECS	Secretome Protein Enrichment with Click Sugar
TALENs	Transcription Activator-like Effector Nucleases
TNFRSF1B	Tumor Necrosis Factor 2
TOF	Time of Flight
UAS	Upstream Activating Sequence
WHO	World Health Organization
VEGFA	Vascular Endothelial Growth Factor A
ZFNs	Zinc Finger Nucleases

Acknowledgements

Every hero story comprises way, guide and companions.

For the guide- I would like to express my gratitude to my thesis supervisor Dr. med. Peer-Hendrik Kuhn for his inspirational comments and supports. I would like to thank Prof. Stefan Lichtenthaler and Prof. Kathrin Lang for their generous supports.

For the companions- I am grateful to my wife, my son and my family for their patience and everlasting support. I wish to thank to my friends, Stephan Müller, Alessio Colombo, Martina Pigoni, Katrin Moschke and Jasenka Njavro for their moral supports.

For the way- Way never ends…

München, 08.05.2017 Alperen Cagatay Serdaroglu